

DISSERTATION

SYSTEMS AND OPERATIONAL MODELING AND SIMULATION TO ADDRESS
RESEARCH GAPS IN TRANSPORTATION ELECTRIFICATION

Submitted by

Aaron I. Rabinowitz

Department of Systems Engineering

In partial fulfillment of the requirements

For the Degree of Doctor of Philosophy

Colorado State University

Fort Collins, Colorado

Summer 2023

Doctoral Committee:

Advisor: Thomas Bradley

Jeremy Daily

Sudeep Pasricha

Chris Weinberger

Copyright by Aaron I. Rabinowitz 2023

All Rights Reserved

ABSTRACT

SYSTEMS AND OPERATIONAL MODELING AND SIMULATION TO ADDRESS RESEARCH GAPS IN TRANSPORTATION ELECTRIFICATION

Transportation electrification is increasingly thought of as a necessity in order to mitigate the negative effects of climate change and this has recently resulted in large investments, within the US and globally, into green transportation technology. In order to ensure that the electrification transition of the transportation sector is carried out in an efficient and effective manner, it is important to address key research gaps. The proposed research involves addressing 4 important research gaps related to electrification in the transportation sector. The four research gaps addressed are quantifying the energetic benefits which may be achieved via the use of Connected Autonomous Vehicle (CAV) technology to enable optimal operational and dynamic control in Electric Vehicles (EVs), the quantification of the operational inconvenience experienced by Battery Electric Vehicle (BEV) users compared to Internal Combustion Vehicle (ICV) users for given infrastructural parameters, and quantification of the potential economic competitiveness of BEVs for Heavy Duty (HD) Less Than Truckload (LTL) fleets. The identified research gaps are addressed via quantitative, data-based, and transparent modeling and simulation. In the first two cases, comprehensive simulation experiments are conducted which show both the potential energetic improvements available as well as the best methods to achieve these improvements. In the second case, a novel method is developed for the quantification of operational inconvenience due to energizing a vehicle and an empirical equation is derived for estimating said inconvenience based on vehicular and infrastructural parameters. The empirical equation can be deployed on a geo-spatial basis in order to provide quantitative measures of BEV inequity of experience. In the last case a novel, data-driven simulation based Total Cost of Ownership (TCO) model for class 8 BEV tractors is developed and used to project economic competitiveness in the near and medium term

future. Findings from the proposed research will provide critical information for industry and policy-makers in their mission to enable an efficient and equitable transportation future.

ACKNOWLEDGEMENTS

This material is based upon work supported by the U.S. Department of Energy's Office of Energy Efficiency and Renewable Energy (EERE). The specific organization overseeing this report is the Vehicle Technologies Office under award number DE-EE0008468. Additional funding and support were provided by the Advanced Vehicle Technology Competitions group at Argonne National Laboratory, Idaho National Laboratory and the Electric Power Research Institute. Invaluable support was provided by collaborators at the aforementioned institutions and faculty and students at Colorado State University, Western Michigan University, and the University of Michigan.

DEDICATION

I dedicate this work to my parents, my partner, my adviser, and the many others I have had the pleasure of working with along the way. Also Teddy (good boy).

TABLE OF CONTENTS

ABSTRACT	ii
ACKNOWLEDGEMENTS	iv
DEDICATION	v
LIST OF TABLES	x
LIST OF FIGURES	xii
Chapter 1	Introduction 1
1.1	Motivation 1
1.2	Identification of Research Gaps 2
1.2.1	Research Gap 1 2
1.2.2	Research Gap 2 3
1.2.3	Research Gap 3 5
1.2.4	Research Gap 4 6
1.3	Research Questions and Tasks 8
1.3.1	Research Question 1 8
1.3.2	Research Question 2 9
1.3.3	Research Question 3 11
1.4	Organization of Chapters 12
Chapter 2	Development and Evaluation of Velocity Predictive Optimal Energy Management Strategies in and Connected Hybrid Electric Vehicles 14
2.1	Preface 14
2.2	Overview 14
2.3	Introduction 15
2.4	Predictive Optimal Energy Management Strategies (POEMS) Methodology 18
2.4.1	Overall System 18
2.4.2	System Inputs 20
2.4.3	Subsystem 1: Perception 25
2.4.4	Subsystem 2: Planning 27
2.4.5	Subsystem 3: Vehicle Plant 33
2.4.6	System Outputs 35
2.5	Results 38
2.5.1	Direct Analysis of Velocity Prediction Accuracy using MAE 38
2.5.2	Overall System Fuel Economy (FE) Output 42
2.5.3	Results Summary 43
2.6	Conclusions 45
2.7	Summary 46
Chapter 3	Real Time Implementation Comparison of Urban Eco-Driving Controls . . . 47
3.1	Preface 47
3.2	Overview 47

3.3	Introduction	48
3.4	Literature Review	49
3.4.1	Rules-Based Eco-Driving (RBED)	50
3.4.2	Discretized Control Optimization (DCO)	51
3.4.3	Polynomial Trajectory Optimization (PTO)	53
3.4.4	Summary	55
3.5	System Definition	56
3.6	Subsystem 1: Perception	57
3.6.1	Path Constraints	58
3.7	Subsystem 2: Planning	61
3.7.1	Baseline Control	61
3.7.2	Optimal Control	64
3.8	Subsystem 3: Plant	71
3.9	Results	72
3.9.1	Optimal Solver Results	73
3.9.2	Eco-Driving Traces	78
3.9.3	Summary	82
3.10	Discussion	84
3.10.1	Problem Complexity	84
3.10.2	Ineffectiveness of Brute Force Solver Methods	85
3.10.3	Difficulties Experienced by Gradient Descent Methods	86
3.11	Conclusions	89
3.12	Summary	90
Chapter 4	Assessment of Factors in the Reduction of BEV operational Inconvenience . .	91
4.1	Preface	91
4.2	Overview	91
4.3	Introduction	92
4.3.1	Quantifying Inconvenience	94
4.3.2	BEV Operational Inconvenience	95
4.4	Data	97
4.5	Methods	101
4.5.1	Definition of Inconvenience	101
4.5.2	Models	103
4.5.3	Optimal Charge Scheduling	108
4.6	Results	111
4.6.1	Experiment and Regression Analysis	114
4.7	Discussion	119
4.8	Conclusions	121
4.9	Summary	122
Chapter 5	A Geo-Spatial Method for Calculating BEV Charging Inconvenience using Publicly Available Data	123
5.1	Preface	123
5.2	Overview	123

5.3	Introduction	124
5.4	BEV Operational Inconvenience	127
5.4.1	Definition of Inconvenience Score	127
5.4.2	Itinerary Data	130
5.5	Calculating Inconvenience Score	130
5.6	Models	131
5.6.1	Vehicle Model	132
5.6.2	Infrastructure Model	133
5.7	Individual Trace Results	134
5.8	Inconvenience Formulae	136
5.9	Geographical Calculation	141
5.9.1	Geographies	142
5.9.2	Locations of Electric Vehicle Support Infrastructure (EVSE) Infrastructure	143
5.9.3	Geographic Computation of DCL	144
5.9.4	Geographic Computation of ERCP	146
5.9.5	Geographic Computation of HC	147
5.9.6	Assumed Values	151
5.10	Results	151
5.11	Discussion	153
5.12	Conclusions	157
5.13	Summary	157
Chapter 6	Class 8 BEV Tractor Economic Modeling	159
6.1	Preface	159
6.2	Introduction	159
6.3	Literature Review	161
6.3.1	HD BEV TCO	161
6.3.2	Battery Pricing	162
6.4	Baseline TCO Model	163
6.4.1	Vehicle Cash Flow	165
6.4.2	Energy Cash Flow	170
6.4.3	Insurance Cash Flow	172
6.4.4	Maintenance Cash Flow	172
6.4.5	Taxes and Fees Cash Flow	173
6.4.6	Labor Cash Flow	173
6.4.7	Payload Cash Flow	173
6.4.8	Summary	176
6.5	Modified TCO Model	177
6.5.1	Modified Vehicle Cash Flow	177
6.5.2	Modified Energy Cash Flow	179
6.5.3	Time Loss Cash Flow	188
6.5.4	Summary	189
6.6	Results	191
6.6.1	Model Results	191

6.6.2	Sensitivity Analysis	196
6.7	Discussion	200
6.8	Conclusions	204
6.9	Summary	206
Chapter 7	Conclusion	207
7.1	Summary	207
7.2	Research Contributions	212
7.3	Future Work	213
References		215
Appendix A	Regression Results	247
A.1	Normalized TCO for Class 8 ICV Tractors	247
A.2	Normalized TCO for Class 8 BEV Tractors	248
A.3	Relative TCO for Class 8 BEV and ICV Tractors	249
Appendix B	INRIX Data Weighting	251
List of Abbreviations		256

LIST OF TABLES

2.1	Data sources and associated signals	22
2.2	Drive-cycle characteristics for data drive-cycle and EPA drive cycles	24
2.3	Relative similarities between EPA dynamometer drive-cycles and the data drive-cycle	24
2.4	Candidate Prediction Methods	25
2.5	The candidate prediction methods results organized from best performing to worst performing.	26
2.6	Parameters and values for Autonomie 2010 Toyota Prius Model	34
2.7	EPA dynamometer drive-cycle FE (km/L) results from Autonomie 2010 Toyota Prius model and ANL D ³	35
2.8	Fuel Economy <i>km/L</i> for 2010 Toyota Prius model with Dynamic Programming (DP) derived methods and Autonomie baseline on EPA dynamometer drive cycles (Time Horizon only effects the Perfect Prediction Model Predictive Control (PP-MPC) and Constant Velocity Model Predictive Control (CV-MPC) methods)	37
2.9	Structure of Optimal Long Short-Term Memory (LSTM)Deep Neural Network (DNN)	39
2.10	Data Groups for LSTMDNN	39
2.11	FE (<i>km/L</i>) simulation results based on cross-validation study predictions	42
3.1	Publications Reviewed by Method Type	56
3.2	Data Available to CAVs	58
3.3	Variables and Parameters for IDM	62
3.4	Energy Economy (EE) Regression Results for Intelligent Driver Model (IDM) Parameters	63
3.5	Kia Soul EV Future Automotive Systems Technology Simulator (FASTSim) Model Parameters	72
3.6	Performance of Random Seeding Method	86
4.1	Dataset Fields	97
4.2	Values of multipliers based on energizing event type	103
4.3	Vehicle Parameters	104
4.4	Base vehicle energy consumption rates	105
4.5	Experiment Parameters and Levels	114
4.6	Model summary	115
4.7	ANOVA	115
4.8	Significant terms in empirical equation ($\alpha = 0.01$)	116
4.9	Experiment Parameters and Levels	118
4.10	Model Summary	118
4.11	ANOVA	119
4.12	Significant terms in empirical equation	119
4.13	Parameters for example localities	120
4.14	S_{IC} [min/km] for ICV and BEV with and without home charging in example localities	120

5.1	Total US population in housing units by density and tenure per 2021 American Community Survey (ACS) table B25033 [205]	125
5.2	Values of multipliers based on charging event type	129
5.3	Vehicle Parameters	132
5.4	Base vehicle energy consumption rates	133
5.5	Experiment Parameters and Levels	137
5.6	Model Summary	138
5.7	ANOVA	138
5.8	Significant Coefficients	139
5.9	Estimations for home charging availability	149
6.1	TCO Model Cash Flows	164
6.2	ICV component costs	165
6.3	ICV Vehicle cash flow components (2020 USD)	166
6.4	BEV Vehicle cash flow components (2020 USD)	170
6.5	Class 8 sleeper tractor loaded fuel economy and range from TEMPO	171
6.6	Parameters in sensitivity analysis	197
A.1	ICV Normalized TCO model summary	247
A.2	ICV Normalized TCO ANOVA	247
A.3	ICV Normalized TCO significant terms in empirical equation ($\alpha = 0.05$)	248
A.4	BEV Normalized TCO model summary	248
A.5	BEV Normalized TCO ANOVA	248
A.6	BEV Normalized TCO Significant terms in empirical equation ($\alpha = 0.05$)	249
A.7	Relative TCO model summary	249
A.8	Relative TCO ANOVA	249
A.9	Relative TCO Significant terms in empirical equation ($\alpha = 0.05$)	250

LIST OF FIGURES

2.1	POEMS logic flow schematic	19
2.2	Example brake specific fuel consumption plot with Ideal Operating Line (IOL) and operating points with and without POEMS	20
2.3	Selected data drive-cycle; drive order was purple, yellow, blue, then green, red circles represent traffic signals	23
2.4	Schematic of DP Method	28
2.5	Schematic comparison between Full Cycle Dynamic Programming (FC-DP) and Model Predictive Control (MPC) methods	33
2.6	Comparison of DP derived methods and Autonomie baseline control on sample drive cycle	36
2.7	Mean Absolute Errors (MAEs) for LSTMDNN trained on data groups A, B, and C for 10, 15, and 20 second horizons	40
2.8	Predicted (black) vs. actual vehicle velocity (blue) for LSTMDNN trained on all data groups at 10 and 20 seconds prediction horizon	41
2.9	Percentage FE improvements for DP derived methods for all data groups and time horizons	43
2.10	FE simulation data trace for all methods	44
3.1	Eco-Driving System Schematic	56
3.2	Example upper and lower boundaries "corridor"	60
3.3	Comparison of cost function values for 2015 Kia Soul EV. Red polygon outlines the operational envelope of the UDDS, US06, and HWFET Environmental Protection Agency (EPA) dynamometer drive cycles and is shown as reference for common driving conditions.	67
3.4	Mean and standard deviation of EE improvement over baseline results for all methods and cost functions	74
3.5	Mean and standard deviation of cost function reduction over baseline results for all methods and cost functions	74
3.6	Correlation between cost function reduction and EE improvement for all cost functions	76
3.7	Significance of comparative results (P-values), purple indicates that the column significantly outperformed the row, blue indicates that the row significantly outperformed the column, green indicates the difference between the row and column was insignificant at 95% confidence	76
3.8	Mean and standard deviations of run-times for all methods and cost functions	78
3.9	Example position vs. time traces for all methods and cost functions	79
3.10	Example velocity vs. time traces for all methods and cost functions	80
3.11	comparison of run-time and EE improvement means for all methods and cost functions	82
3.12	Example polynomial trajectory defined by knots	84
3.13	Knot location vs. trajectory cost for non-fixed knots	87
3.14	Progress of Genetic Algorithm (GA) solution	88

4.1	Distribution of Itinerary Lengths in the Dataset	98
4.2	Distribution of Daily and Yearly Mean Driving Distances in the Dataset	98
4.3	Home locations in dataset	100
4.4	Parking event locations in dataset	100
4.5	3 hour State of Energy (SOE) charging traces at various charging rates for a vehicle with an 80 kWh battery	107
4.6	Top-down DP schematic	109
4.7	Optimal charging traces for BEVs with no home charging and identical vehicle and infrastructure parameters	111
4.8	Optimal charging trace for BEV with home charging	112
4.9	Optimal fueling trace for ICV	113
4.10	Significant ($\alpha = 0.01$) terms of empirical equation and standard error	117
5.1	Charging activity pyramid. Modified composite of original graphic by T. Bohn, Argonne National Laboratory. From [207]	126
5.2	Simulation traces for a BEV (vehicle #118,211) with no home or work charging and identical parameters	135
5.3	Simulation traces for a BEV (vehicle #118,211) with home or work charging available and identical parameters	136
5.4	Significant Regression Coefficients and Error Bars	140
5.5	Significant Regression Coefficients and Error Bars for national, Colorado, and Denver Metropolitan Statistical Area (MSA) itinerary subsets	141
5.6	Geometries in Denver Colorado urbanized area	142
5.7	Distribution of census tract areas compared to mean level 8 H3 hex cell area for Denver Colorado urbanized area	143
5.8	Locations of charging stations in Denver Colorado urbanized area	144
5.9	Destination Charger Likelihood (DCL) for hex cells in Denver Colorado urbanized area	145
5.10	DCL distribution for hex cells in Denver Colorado urbanized area	146
5.11	En-Route Charging Penalty (ERCP) for hex cells in Denver Colorado urbanized area .	147
5.12	ERCP distribution for hex cells in Denver Colorado urbanized area	147
5.13	Census tract level residence type and tenure patterns	148
5.14	Home Charging (HC) for H3 hex cells in Denver Colorado urbanized area	150
5.15	HC PDF comparison for H3 hex cells in Denver Colorado urbanized area	151
5.16	S_{IC} for H3 hex cells in Denver Colorado urbanized area	152
5.17	S_{IC} PDF comparison for H3 hex cells in Denver Colorado urbanized area	153
5.18	Demographic data for H3 hex cells in Denver Colorado urbanized area	155
5.19	Demographic data for H3 hex cells in Denver Colorado urbanized area	156
6.1	Battery pack cost scenarios	167
6.2	Battery pack cost scenario contours	168
6.3	Battery pack mass by capacity and year of manufacture	168
6.4	Motor, inverter, and auxiliary systems cost by capacity and year of manufacture	169
6.5	Distribution of miles driven by load for class 8 sleeper tractors (2002 Vehicle Inventory and Use Survey (VIUS))	171

6.6	Distribution of annual Vehicle Miles Traveled (VMT) for class 8 sleeper tractors (2002 VIUS)	172
6.7	Maintenance cost per km driven for class 8 sleeper tractors	173
6.8	CDF of miles driven by load for class 8 sleeper tractors (2002 VIUS)	175
6.9	Net Present Value (NPV) of Payload cash flow by battery capacity and model year	175
6.10	TCO for ICV and BEV model year 2025 class 8 sleeper tractors from TEMPO and CSU model with TEMPO assumptions	176
6.11	CSU battery pack cost scenarios	178
6.12	CSU battery pack cost scenario contours	178
6.13	Historical diesel prices in 2020 USD	179
6.14	Historical commercial electricity prices in 2020 USD	180
6.15	Time of Use (TOU) tariffs in 4 US states	182
6.16	Electricity pricing in continental US by level 3 H3 Hex cell	183
6.17	Optimal charge schedule for an INRIX HD itinerary with a long range battery	185
6.18	Optimal charge schedule for an INRIX HD itinerary with a short range battery	186
6.19	Price paid per kWh by battery pack size and daily driving distance for class 8 BEV tractor	187
6.20	Time spent en-route charging per day by battery pack size and daily driving distance for class 8 BEV tractor	189
6.21	TCO for ICV and BEV model year 2025 class 8 sleeper tractors from TEMPO and CSU models with realistic costs of electricity and cost of en-route charging and average annual VMT	190
6.22	TCO for ICV and BEV model year 2025 class 8 sleeper tractors from TEMPO and CSU models with realistic costs of electricity and cost of en-route charging and double average annual VMT	191
6.23	Projected TCO for class 8 BEV tractors by model year, battery pack capacity, and daily driving distance with CSU baseline assumptions	192
6.24	Projected TCO for class 8 BEV tractors as a percentage of equivalent ICV TCO by model year, battery pack capacity, and daily driving distance with CSU baseline assumptions	193
6.25	Projected TCO for class 8 BEV tractors as a percentage of equivalent ICV TCO by model year, battery pack capacity, and daily driving distance with CSU optimistic assumptions	194
6.26	Projected maximum competitive distance-matched vehicle range for class 8 BEV tractors by model year using CSU's battery pack price projections	195
6.27	Projected maximum competitive distance-matched vehicle range for class 8 BEV tractors by model year using CSU's battery pack price projections with increased diesel price	196
6.28	Significant coefficients ($\alpha = 0.05$) from normalized TCO regression	198
6.29	Significant coefficients ($\alpha = 0.05$) from Levelized Cost of Driving (LCOD) regression	200
6.30	TCO comparison for model year 2025 class 8 BEV tractors with various ranges and 500 km daily driving requirements	201
6.31	TCO comparison for model year 2025 class 8 BEV tractors with various ranges and 1000 km daily driving requirements	202

6.32	TCO comparison for model year 2035 class 8 BEV tractors with various ranges and 1000 km daily driving requirements	203
B.1	Total tracked vehicles in INRIX data by day	252
B.2	Average tracked vehicles in INRIX data by geometry	253
B.3	Transportation job densities by geometry from LODES WAC (NAICS 48/49)	253
B.4	INRIX data geo-spatial weights	254
B.5	Comparison between weighted and un-weighted INRIX geo-spatial densities	254

Chapter 1

Introduction

1.1 Motivation

Electrification in the transportation sector is an increasing priority in the US and across the globe. In the US, 27% of Green-House Gas (GHG) emissions originate from the transportation sector [1] and these GHGs contribute to global climate change and various human health impacts [2]. Simply reducing the output of the transportation sector is not an economically viable option. The transportation sector is the backbone of the modern economy and thus it is critical to develop a high capacity, sustainable, and equitable transportation sector for the future.

Vehicular electrification contributes a potential solution to this problem (in cooperation with de-carbonization in power generation) but, as of yet, the vast majority of vehicles on the roads in the US and the vast majority of new vehicle sales remain Internal Combustion Vehicles (ICVs) [3]. Recently, the US government and prominent US Original Equipment Manufacturers (OEMs) have announced ambitious plans to see 50% of new Light Duty (LD) vehicle sales be Electric Vehicles (EVs) by 2030 [4]. The US government plan includes \$174 billion of investment in vehicle electrification as well as \$7.5 billion in direct and indirect investment into Electric Vehicle Support Infrastructure (EVSE) infrastructure [5]. These funds will have a positive impact, but significant research gaps remain in the field of vehicular electrification, and until these are addressed, planners can only work with incomplete information.

A second potential solution is presented by connected autonomy. Modern and near future technologies in the areas of sensing, communications, and processing increasingly enable the practical deployment of highly optimized intelligent transportation components. Connected Autonomous Vehicles (CAVs), intelligent infrastructure, and optimal logistics provide the potential for significant reductions in energy consumption and emissions while maintaining or improving

system capacity [6–8]. Questions remain as to how best leverage the opportunities given by connected autonomy in order to meet broader transportation system goals.

Knowledge gaps that exist at the intersection of electrification, connectivity, and automation provide roadblocks towards continued progress. Fortunately, much can be learned through application of modeling and simulation and data analysis in order help fill the gaps. To maximize the benefits of electrified transportation, this dissertation research improves the efficiency of individual vehicles using optimal control, accelerates adoption of Battery Electric Vehicles (BEVs) by improving the ownership experience, and demonstrating the improved economics of Medium Duty (MD) fleet vehicle ownership.

1.2 Identification of Research Gaps

The following research gaps were identified as critical for the mission of this research.

1.2.1 Research Gap 1

Hybrid Electric Vehicle (HEV) Optimal Operational Control with Real Velocity Predictions

Connected vehicular autonomy may play an important role in increasing vehicular efficiency, especially in the context of urban driving. Advanced Driver Assistance System (ADAS) technology has seen rapid market penetration due to its potential to bring safety and convenience benefits to customers [9–11]. Further developments in connectivity and autonomy may lead to the commercialization of CAVs which will, in turn, enable the application of optimal control on a real-time basis. Vehicular optimal control is a well studied subject but generally treated in a scholastic manner as an application case for optimal control theory. Information on the effectiveness and practicality of vehicular optimal operational (relating to the operation of the powertrain for a given motion trace) and dynamic (relating to the motion of the vehicle) control remains at a shortage. CAV technology can be used to improve the efficiency of an individual vehicle in two principle ways.

One way in which CAV technology can improve vehicular efficiency is through the optimal operational control of HEVs and Plug-in Hybrid Electric Vehicles (PHEVs) through the application of Velocity Prediction enabled Optimal Energy Management Strategies (VP-OEMS). VP-OEMSs use predictions of future vehicle velocity to inform an optimal solver which generates an optimal operational strategy. This process has been the subject of active research since the first publication in 2001 [12]. Note that in the current transportation environment, perfect future velocity prediction is not possible. To address this issue, researchers have used Model Predictive Control (MPC) which, in this context, is the application of Dynamic Programming (DP) optimization to fixed length prediction windows. Research on this topic has demonstrated that perfect velocity prediction is not required [13], and that even heuristic approaches which rely on acceleration event prediction can be used [14, 15] to achieve improvements in FE. High-fidelity prediction of future vehicle velocity is presently achievable through the employment of Machine Learning (ML) and Artificial Neural Network (ANN) methods and CAV technology [16–24]. In order to facilitate real world implementation, certain specific research gaps must be addressed. One such research gap, as defined in [25] is the quantification of the performance of VP-OEMS with actual velocity predictions. To the author’s knowledge, no comprehensive study addressing this research gap exists to date. This research gap will be addressed by collecting a real-world Advanced Driver Assistance System (ADAS) and Vehicle to Everything (V2X) dataset for an urban CAV, using this dataset to evaluate methods of generating velocity predictions, using these velocity predictions to define optimal operational controls, and, finally, evaluating the efficiency gains attained using Autonomie simulations.

1.2.2 Research Gap 2

Comprehensive Comparative Study of Eco-Driving Trace Solver Methodology

The second way in which CAV technology can be used to improve vehicular efficiency is via optimal dynamic control. Eco-Driving, which is a strategy designed to reduce fuel consumption by minimizing accelerations has been well known and has been shown to be effective when employed

by human drivers [26]. Eco-Driving is taught as a part of drivers' education in Singapore and has resulted in a Energy Economy (EE) improvement of 11% to 15% there [27]. Differences in culture, infrastructure, and available technology will play a major role in determining the effectiveness of efforts to promote Eco-Driving. For example, vehicular autonomy and CAV technology provide an increased opportunity for the application of Eco-Driving strategies because they circumvent driver acceptance/training issues. When compared to a human driver (i.e. manual Eco-Driving), a CAV has the ability to follow optimal trajectories more precisely and can take into account information which is beyond line-of-sight.

Compared to manual Eco-Driving, autonomous Eco-Driving yields the following potential benefits:

- Ability to precisely follow optimal energy traces;
- Ability to account for traffic information which is beyond line-of-sight;
- Ease and scalability of implementation;

When developing and applying an autonomous Eco-Driving system, the manner in which an Eco-Driving algorithm generates the trace for the vehicle to follow will have a major impact on the effectiveness of the algorithm. Much research has been conducted in this space in recent years and a great variety of solutions have been put forward in the literature. The reason for this diversity is the complicated nature of the problem and the many dimensional design space which results from it. To the author's knowledge, no comprehensive, comparative study exists. This research gap will be addressed by summarizing and subdividing Eco-Driving Control (EDC) strategies, defining a framework for practical implementation of solver methods, implementing a selection of common methods, and evaluating these methods in terms of performance and practicality using real-world data [28].

1.2.3 Research Gap 3

Quantification of BEV Operational Inconvenience and Sensitivity Analysis for Contributing Factors

The US government and US OEMs have recently set ambitious goals for BEV market penetration [4]. These targeted efforts should help accelerate the growth of the BEV market share which remains small [3]. Although economic factors are important in individual car buying decisions, evidence suggests that consumers also strongly weight inconvenience in their decision making process. Several studies from around the world [29–31] have found that inconvenience, or perception of inconvenience, related to BEV range and charging play a large part in individuals deciding whether or not to purchase BEVs. Concerns about BEV operational inconvenience are founded in several realities related to vehicular energizing (charging or fueling) namely BEV range and charging times.

Historically, low BEV adoption rates have rendered the energizing inconvenience issue a low priority as most BEV owners primarily charged at home [32]. Public and private supercharging networks have also made long distance BEV travel increasingly feasible in recent years [33]. However, as adoption increases, and BEVs penetrate non-luxury car markets, the model of BEV owners living in single unit dwellings will become less relevant and public infrastructure will become increasingly important.

The importance of public infrastructure for various potential BEV market segments has been recognized and funding for rapid development of said infrastructure has been approved [34] but several key questions remain to be answered:

1. What are the ultimate relative operational inconveniences for BEVs vs ICVs for those who can charge at home and those who cannot?
2. What are the relative merits of DC Fast Charging (DCFC) infrastructure vs DC Level 2 (LVL 2) charging infrastructure help reduce the inconvenience of BEV operation, especially for vehicle operators who cannot charge at home?

3. What level of EVSE infrastructure rollout, if any, is sufficient to achieve convenience parity for BEV operators?
4. What are the implications of EVSE infrastructure on BEV equity and energy justice?

In order to answer these questions, a fundamental research gap must be addressed, namely how to evaluate the inconvenience associated with BEV operation. This gap is addressed via a flexible data-based method for evaluating energizing inconvenience which is applicable to any vehicle regardless of powertrain type and thus allows for direct comparisons between different vehicles and different conditions of operation. The method uses longitudinal itinerary data and DP energizing scheduling to produce optimal (least inconvenient) energizing traces for a set of vehicles given assumptions about energizing infrastructure. Using national datasets, an empirical equation is then fitted which relates contributing factors such as vehicle design and EVSE infrastructure access to inconvenience experienced. Finally this equation is applied on a geo-spatial basis using publicly available data in a scalable manner. The resulting information is used to answer the enumerated questions.

1.2.4 Research Gap 4

Class 8 Less Than Truckload (LTL) Fleet BEV Replacement Potential Assessment and Sensitivity Analysis

Our modern economy could not exist without the heavy LTL trucking sector. The US economy relies on a fleet of nearly 40 million commercial trucks which move more than 70% of the nation's freight tonnage [35] and are responsible for 17.2% of US GHG emissions [36]. About 4 million of these trucks are class 8 tractors [37] which haul the most freight per vehicle and have the highest energy consumption rates. In order to mitigate the impact that this sector has on the global environment, new technologies and infrastructure investments must be explored. One possible solution is the partial or full electrification of the sector.

As EV technology progresses, the opportunity to electrify larger and heavier duty vehicles has and will continue to grow. Compared to LD electrification, Heavy Duty (HD) electrification

presents many additional difficulties. The additional difficulties relate to battery technology and economics. Although LD BEVs often have shorter ranges, higher purchase prices, and weigh more than equivalent ICVs the differences are comparatively small. BEV range, purchase price, and weight are driven by battery capacity. Battery technology has progressed majorly in the past 15 years which has resulted in greater specific energies and lower prices on the cell and pack level. There is evidence that Lithium-Ion (Li-Ion) battery technology may be approaching maturity and that further gains will be achieved more in manufacturing and recycling than fundamental technological advancements. At the same time, raw materials needed for battery production may become more scarce as production increases. Benefits of high scale manufacturing will accrue for high volume production battery packs such as those used in LD vehicles to a greater degree than for low volume battery packs such as those used in HD vehicles. Economic factors of production indicate that purchase prices for HD BEVs will remain high compared to equivalent ICVs.

However, BEVs are cheaper to operate than ICV and thus are more competitive in Total Cost of Ownership (TCO) than in purchase price. For class 8 tractors, around 90% of TCO is from operational costs. Because LTL fleets are large businesses they will be more sensitive to periodical costs and TCO than to purchase price. The opportunity, thus, exists for BEVs to become competitive in certain market niches. It is not trivial to predict what or how numerous these niches will be, comprehensive modeling is needed in order to identify them.

Existing analysis is overly simplistic in the evaluation of BEV manufacturing and operational costs in several ways. First, existing research often bases battery cost modeling for HD vehicles on pricing data for LD vehicles [38–42]. Battery packs for HD vehicles are specialist equipment and will be produced in much lower volume. Thus it is not reasonable to assume that price per unit storage will scale linearly. Second, current analysis fails to model charging dynamics with sufficient detail [38]. BEV operations are more heavily impacted by energizing than ICV operations due to the longer times required for charging and the incentives to charge at low rates. The cost of charging will also be effected by the time-of-day in which the charge occurs. It is common for BEV replacement literature to assume that all charging must occur during long dwells

and that certain long itineraries are infeasible [43–45]. However, fast charging is increasingly available and thus these long itineraries are feasible if more expensive and time consuming. More detailed modeling and data driven analysis is required to address these gaps.

1.3 Research Questions and Tasks

The thrust of this research is to gain a greater understanding of the potential for future EVs in terms of capabilities of the individual vehicles, the market for said vehicles, and the equity impacts of an electric transition. EV technology presents a solution to many issues in relation to the transportation sector but also potential drawbacks. Dissertation research will advance the state of the art by answering the following research questions.

1.3.1 Research Question 1

What energetic benefits can be attained for CAV EVs through the application of infrastructure communication-enabled real-time optimal control?

The future vehicle fleet is expected to be characterized by both an increasing proportion of EVs and of CAVs. The presence of automotive connectivity and increasing on-board computational capabilities allow for dynamic (relating to the motion of the vehicle) as well as operational (relating to the operation of the powertrain for a given motion trace) optimization to be carried out and applied in real-time. Dynamic and operational optimal control present the opportunity to meaningfully improve the efficiency of EVs if these can be carried out in real-time. The following are research tasks associated with RQ1:

- **RQ1.T1 - Assessment of performance and real-time control feasibility of operational optimal control for HEVs using experimentally derived (real-world) driving data**
Operational optimal control of HEV has been well studied in academia as a case study for various optimal control methods. Implementation of prediction-enabled Optimal Energy Management Strategies (OEMS) require high fidelity prediction of vehicle motion and the efficient evaluation of the control. Research gaps towards implementation identified

in [25] include evaluating the performance of Predictive Optimal Energy Management Strategies (POEMS) with real velocity predictions. Identifying methods which allow for the performance and run-time of prediction enabled OEMS for HEVs with real predictions to meet acceptable levels for real-time implementation will allow for development to progress to the prototype phase.

- **RQ1.T2 - Assessment of performance and real-time control feasibility of dynamic optimal control for EVs.** Like operational control of HEVs, dynamic optimal control has been extensively studied as an optimal control problem with a variety of optimal controls, heuristics, and metaheuristics applied to the problem. The diversity of approaches is combined with a corresponding diversity in problem framing. In order to evaluate which way to proceed for prototyping and, ultimately, implementation, a comprehensive framing of the problem must be realized and, along with real-world data, used to evaluate the various controls proposed in literature.

The results of these tasks will define the optimal cost functions, real time capabilities and optimal performance of all of the proposed algorithms available in literature. These types of results will have value to the research community and industry in guiding their implementation of POEMS in the novel application of CAV EVs.

1.3.2 Research Question 2

What effects do factors such as vehicle range and the availability of various charging options have on BEV *operational inconvenience*?

Short, medium, and long terms goals to increase BEV sales in the US face the issue of the inconvenience, or perception of inconvenience, associated with operating a BEV. Underlying realities of energy storage and the physics of charging batteries dictate that BEVs will have less range and require longer to energize than equivalent ICVs. As the US government embarks on an ambitious program to increase the penetration of EV charging networks, questions remain as to

how best invest the capital in terms of increasing BEV market share and minimizing inequity of experience. The following research tasks are associated with RQ2:

- **RQ2.T1 - Definition of a quantitative metric for inconvenience associated with operating a BEV.** Deriving an applicable definition of inconvenience is the first step in quantifying and calculating it. Much research has been conducted in the transportation field into minimizing inconvenience for large groups down to individual agents. A survey of literature must be conducted and a quantitative metric for inconvenience defined.
- **RQ2.T2 - Definition of a method for calculating the inconvenience associate with operating a BEV.** A method must be derived for calculating inconvenience experienced given vehicular itinerary information for an individual BEV operator. Such a method should be sufficiently flexible as to allow for evaluation of theoretical inconvenience values for the same itinerary with different vehicular and energizing conditions. Should a robust and flexible method be derived, experiments on the effects of various vehicular and infrastructural parameters can be performed.
- **RQ2.T3 - Determination of the effects of vehicular parameters and the availability or unavailability of various charging options on BEV operational inconvenience.** Variations in vehicle particulars and charging availability will dictate that different people will experience different levels of inconvenience for the same driving behavior. BEVs will have various full-charge ranges and certain people will have the ability to charge at home reliably while others will not. Additionally, the availability of LVL 2 chargers at common destinations such as shopping centers, supermarkets, gyms, large workplaces, and others and proximity to dedicated DCFC stations will vary geographically. Geographic and socio-economic differences may lead to significant inequity of experience for BEV operators and it is imperative to understand what the effects of underlying factors are in order to be able to effectively minimize the issue.

- **RQ2.T4 - Scalable application of quantitative inconvenience metric on a geo-spatial basis.** In order to understand the impacts of vehicular technology and EVSE infrastructure on BEV operational inconvenience a method of quickly computing expected inconvenience score for geometric units should be developed. This geo-spatial application will allow individuals to understand how home location will impact their experience, planners to directly evaluate proposed EVSE infrastructure, and interest groups to identify and understand resulting inequities.

Having completed this research, a significantly greater understanding of the experiences of BEV operators in the present and future and what factors underlie these experiences will be gained. The knowledge gained can be used in order to gain a quantitative understanding of infrastructural impacts on BEV equity and energy justice and make way for a green and equitable transportation future.

1.3.3 Research Question 3

In what market niches will future class 8 BEV semi-tractors be competitive with ICV equivalents and what impacts will design and operational factors have?

The Medium Duty / Heavy Duty (MD/HD) fleet represents only 4% of US vehicle registrations but accounts for a quarter of yearly fuel use [46] . Within this group, the most efficient on a per-ton-mile basis are class 8 tractors. Class 8 tractors are also consider to be relatively difficult to electrify due to energy and power requirements. This research asks the question: what are potential market niches in which class 8 BEV tractors can be competitive and what factors underlie this.

- **RQ3.T1 - Development and validation of class 8 tractor BEV and ICV TCO model.** In order to perform comparative evaluations validated models for class 8 tractors with combustion and electric powertrains must be developed. The current state-of-the-art model for vehicle TCO is National Renewable Energy Laboratory (NREL)'s TEMPO. TEMPO contains flawed assumptions but provides a good comparison point. The developed model's results should match TEMPO results when the same assumptions are used.

- **RQ3.T2 - Development of realistic battery pricing models for class 8 BEV tractors.** Rather than relying on LD pricing data alternative sources of pricing information will be found. These sources which may derive from fundamental modeling, OEM data, or a combination of the two will inform a realistic battery pricing model for the low volume class 8 battery packs.
- **RQ3.T3 - Development of data-based, intelligent charging pricing and timing model for class 8 BEV tractors.** In order to truly understand what BEV operators will pay for electricity it is necessary to perform data-based modeling. Prices of electricity vary by location, time, and rate. A flat price will not sufficiently capture the dynamics and may under or over state BEV competitiveness. The developed model will use real-world class 8 truck itineraries and optimal charging simulation to understand the real prices paid for electricity.
- **RQ3.T4 - Identification of competitive market niches for future class 8 BEV tractors and analysis of contributing factors.** With the new models developed in the previous research tasks an analysis will be performed to identify where future class 8 BEV tractors may become competitive with ICV equivalents. Because the cost modeling developed will necessarily be subject to assumptions a sensitivity analysis with respect to these will be conducted.

The results of the outlined research tasks will be a novel and comprehensive new understanding of the potential for electrification which exists in the HD fleet. This new knowledge can be used to inform fleet operators, OEMs, and utilities on directions for future development.

1.4 Organization of Chapters

The research conducted towards this dissertation is presented in 5 chapters. Chapter 2 describes work conducted towards addressing Research Gap 1 and contains research task RQ1.T1. Chapter 3 describes work conducted towards addressing Research Gap 2 and includes research task RQ1.T2.

Chapters 4 and 5 describe work conducted towards addressing Research Gap 3 and comprise of research tasks RQ2.T1, RQ2.T2, RQ2.T3, and RQ2.T4. Chapter 6 describes work conducted towards addressing Research Gap 4 and in made up of research tasks RQ3.T1, RQ3.T2, RQ3.T3, and RQ3.T4. These chapters are followed by a summary conclusion in Chapter 7.

Chapter 2

Development and Evaluation of Velocity Predictive Optimal Energy Management Strategies in and Connected Hybrid Electric Vehicles

2.1 Preface

This chapter is derived from [47] which was primarily authored by this dissertation's author. Significant contribution was provided by Tushar Gaikwad in the prediction method analysis [48] and by Dr. Zach Asher in conceptualization and presentation. Important material support for data collection was provided by the EcoCAR Mobility Challenge. The content of the paper addresses RQ1.T1. RQ1 focuses on determining what energetic benefits can be attained for Connected Autonomous Vehicles (CAVs) through the application of infrastructure connected optimal control. In this chapter the focus is on velocity-prediction enabled optimal energy management strategies for Hybrid Electric Vehicles (HEVs). Predictive optimal control has been long studied but recent advances in machine learning have made the framework more feasible as high fidelity predictions have become increasingly possible. The work in this chapter is a comprehensive study which serves to evaluate how high-fidelity velocity predictions can best be attained and what information is needed to attain them and follows with what energetic benefits can be attained by using these predictions for optimal control.

2.2 Overview

In this study, a thorough and definitive evaluation of Predictive Optimal Energy Management Strategies (POEMS) applications in connected vehicles using 10 to 20-second predicted velocity is conducted for a HEV. The presented methodology includes synchronous data-sets gathered in Fort Collins, Colorado using a test vehicle equipped with sensors to measure ego vehicle position

and motion and that of surrounding objects as well as receive Infrastructure to Vehicle (I2V) information. These data-sets are utilized to compare the effect of different signal categories on prediction fidelity for different prediction horizons within a POEMS framework. Multiple Artificial Intelligence (AI) and Machine Learning (ML) algorithms use the collected data to output future vehicle velocity prediction models. The effects of different combinations of signals and different models on prediction fidelity in various prediction windows are explored. All of these combinations are ultimately addressed where the rubber meets the road: Fuel Economy (FE) enabled from POEMS. FE optimization is done using Model Predictive Control (MPC) with a Dynamic Programming (DP) optimizer. FE improvements from MPC control at various prediction time horizons are compared to that of Full Cycle Dynamic Programming (FC-DP). All FE results are determined using high-fidelity simulations of an Autonomie 2010 Toyota Prius model. The FC-DP POEMS provides the theoretical upper limit on FE improvement achievable with POEMS but is not currently practical for real world implementation. Perfect Prediction Model Predictive Control (PP-MPC) represents the upper limit of FE improvement practically achievable with POEMS. Real Prediction Model Predictive Control (RP-MPC) can provide nearly equivalent FE improvement when used with high-fidelity predictions. Constant Velocity Model Predictive Control (CV-MPC) uses a constant speed prediction and serves as a "null" POEMS. Results showed that RP-MPC, enabled by high-fidelity ego future speed prediction, led to significant FE improvement over baseline nearly matching that of PP-MPC.

2.3 Introduction

Improving FE is a critical goal to reducing climate change and air pollution. The transportation sector is responsible for 27% of all greenhouse gas emissions produced globally and more than 50% of nitrogen oxide emissions [1]. Recent studies show that greenhouse gas emissions are a significant contributor to global climate change [2] and lowered life expectancy in many countries [49]. Greenhouse gas emission levels are directly related to the FE of vehicles; reducing total

miles driven is a difficult-to-implement and politically controversial goal, thus much research into methods to improve vehicle FE has been performed [50].

A critical component of improving FE is vehicle electrification. Recently, HEV and Plug-in Hybrid Electric Vehicle (PHEV) have been widely researched because of their greater potential to increase FE and emissions over that of conventional Internal Combustion Engine (ICE) vehicles [51]. However, currently available HEVs do not operate optimally [52].

In addition to advancements in powertrain technology, recent developments in the automotive industry have led to huge advancements in CAV technology. Advanced Driver Assistance System (ADAS) technology has seen rapid market penetration due to its potential to bring safety and convenience benefits to customers [9–11]. Automation (i.e. ADAS) and connectivity (i.e. CAV) technology are critical technologies not only for safety and commercialization of autonomous vehicles but also for energy efficiency through implementation of POEMS on HEVs and PHEVs which can increase their FE and reduce their emissions [12, 15, 53–55].

POEMS use predicted vehicle velocity (enabled through ADAS [56] and connectivity) as an input to optimal control. The optimal solution output is then used as an input to the vehicle plant, ideally an HEV or PHEV due to the additional operational degrees of freedom [25]. This process has been the subject of active research since the first publication in 2001 [12]. Note that in the current transportation environment, perfect future velocity prediction is not possible. To address this issue, researchers have used MPC which, in this context, is the application of DP optimization to fixed length prediction windows. Research in this space has demonstrated that perfect velocity prediction is not required [13], and that even heuristic approaches which rely on acceleration event prediction can be used [14, 15] to achieve improvements in FE. Although it is worth noting that these FE improvements are modest compared to those theoretically achievable with perfect prediction of vehicle velocity. High-fidelity prediction of future vehicle velocity is presently achievable through the employment of ML and Artificial Neural Network (ANN) methods and CAV technology [16–24]. Despite all of this research, a thorough investigation of the datasets and prediction models' effect on vehicle FE (the full system) has not been conducted. The latest

research has explored the effect on velocity prediction error metrics rather than resultant vehicle FE [24, 48]. In order to facilitate real world implementation, certain specific research gaps must be addressed; these research gaps are defined in [25] as:

1. Performance of Optimal EMS with Actual Velocity Predictions
2. Performance of Optimal EMS when Subjected to Disturbances
3. Performance of Optimal EMS in Real Vehicles

To the author's knowledge, this paper represents the first comprehensive study fully addressing Research Gap 1. Previous research in the area of POEMS has focused on select aspects of Research Gap 1 but no comprehensive study has been performed which concerns the use of real-world data and real-time prediction methods in POEMS. This study, being such a comprehensive analysis, allows for research to progress towards other aspects of implementation namely Research Gaps 2 and 3. Previous research in this area is summarized as follows. The efficacy of predictive Optimal EMS for improving efficiency in HEVs was first shown in 2001 in [12] utilizing perfect prediction. In 2008 velocity prediction was introduced to the literature in [57] which used an analytical traffic based velocity prediction model. In 2015, the advantages of ANN prediction were shown in [18, 19]. In 2017 and 2018 a series of studies [13, 56, 58, 59] experimented with different data streams to optimize prediction with a shallow ANN. In 2019 more modern machine learning techniques were introduced into the field in [60] where reinforcement learning was used along with traffic data to train an ANN to produce optimal controls for a power-split hybrid. Also in 2019, [24, 61] showed that high fidelity predictions were possible through the use of deep Long Short-Term Memory (LSTM) ANNs. Finally, in 2020, a thorough analysis of various combinations of real world data streams and machine learning techniques [24, 48, 62] showed that the highest degree of prediction fidelity could be attained through the use of LSTM ANNs with the use of Signal Phase and Timing (SPaT) and Lead Vehicle data.

Thus, in order to close the gap, this paper outlines a comprehensive system-level study addressing the interactions between groups of available real-world data, velocity prediction methods, and Optimal EMS methods with respect to the overall system output: FE.

This paper rigorously evaluates the dataset and perception model for POEMS and evaluates performance using the FE for a validated HEV to enable full system performance insight, which to-date is missing from the literature. Cutting-edge AI technology is leveraged to generate high-fidelity future vehicle velocity predictions in 10 to 20 second windows. The predictions are fed into an MPC control method in order to determine the optimal instantaneous torque split for a power-split HEV. The FE achievable with the proposed POEMS will be compared to that achievable with perfect prediction Full drive-Cycle DP (FC-DP), Perfect Prediction MPC (PP-MPC), Constant Velocity-prediction MPC (CV-MPC), and Autonomie baseline control. This paper will further show that the proposed method is implementable on current vehicles with current technology and has the potential to provide significant FE improvements within the HEV fleet if implemented.

2.4 POEMS Methodology

2.4.1 Overall System

HEV POEMS uses predictions of future vehicle velocity to inform an optimal powertrain control strategy, thus achieving greater energy efficiency. Powertrain controls include torque split and gear shifting based on powertrain states such as battery State of Charge (SOC) and current gear in the case of a parallel power-train configuration or only torque split in the case of a paralleled configuration.

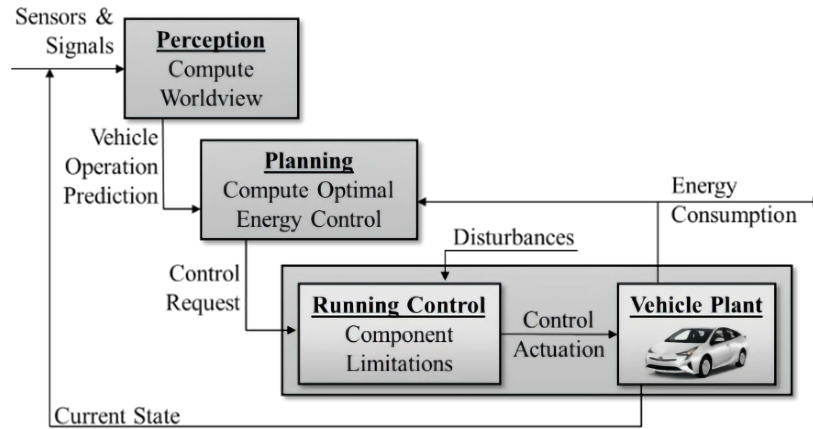


Figure 2.1: POEMS logic flow schematic

As shown in Figure 2.1, a POEMS consists of three major subsystems. The first is the perception system which predicts vehicle motion using information about previous and current vehicle motion, powertrain states, driver inputs, ADAS, and Vehicle to Everything (V2X) data as inputs. The second is the planning subsystem which computes optimal controls based on the predicted vehicle velocity. And finally the third subsystem is the vehicle plant which can be either the physical vehicle or high-fidelity simulation model of the vehicle. The final system outputs are the actual vehicle velocity and powertrain states.

POEMS achieve greater FE by ensuring that the engine is used in regions of maximum efficiency as often as possible. This concept is shown in Figure 2.2 which includes a brake specific fuel consumption map for an example engine and different combinations of engine speed and torque which produce different engine efficiencies. Thus, most engine controllers attempt to operate the engine along its Ideal Operating Line (IOL) [63] which contains the most efficient torque for a given engine speed. POEMS use information about future vehicle velocity to ensure that the engine only operates in the most efficient segment of the IOL, what can be thought of as an IOL Segment.

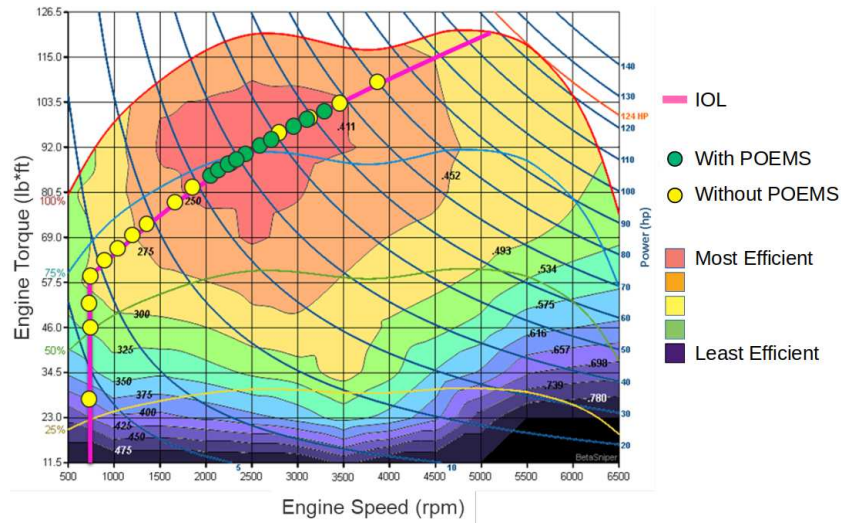


Figure 2.2: Example brake specific fuel consumption plot with IOL and operating points with and without POEMS

As shown in Figure 2.2, simply operating along the IOL (yellow dots) does not guarantee efficient operation. POEMS increase FE by guaranteeing operation within the IOL Segment (green dots).

Although this paper only concerns vehicle motion, the POEMS method can be extended to account for additional exogenous inputs such as cabin heating and cooling requirements [64–66] without fundamentally changing the method.

2.4.2 System Inputs

Data-Set Development

The first step in the development of practical and high-fidelity real world future vehicle speed prediction was to collect a sample generic data-set which would represent all data sources potentially available to a given CAV. All data sources selected are currently available to CAVs or will be available in the near future [67]. In this section a taxonomy for such a data-set is defined. This taxonomy defines data both in terms of its source form and its processed form and defines the process of transformation.

The first step in defining the data-set is to define the sources of the data. Three distinct source categories are proposed:

1. VEH: Vehicle operational data such as vehicle motion, performance, and driver inputs. This data concerns only the ego vehicle itself and its driver.
2. ADAS: Advanced Driver Assistance System (ADAS) data [68]. This consists of the data generated by external object sensors on the vehicle and concerns objects within the vehicle's line of sight.
3. V2I: Data which the vehicle receives through connectivity to infrastructure and other vehicles.

In order to be considered an CAV, a vehicle must receive information from all three of the above sources. Most modern vehicles receive data from the VEH and ADAS sources [69] and V2I is available in some regions [70]. These signals were obtained from the ego vehicle CAN bus and the City of Fort Collins, Colorado.

Within these source categories, signals of use in vehicle future velocity prediction are shown in Table 2.1.

Table 2.1: Data sources and associated signals

Data Source	Signal	Description
VEH	General Vehicle Signals	Signals such as speed, acceleration, throttle position, and steered angle which can be found via CAN on any vehicle
VEH	Historical Speeds (HS)	Historical speed data for the vehicle at the current location
ADAS	Lead Vehicle Track (LV)	Relative location of confirmed lead vehicle from ADAS system
V2I	Signal Phase and Timing (SPaT)	Signal phase and timing of next traffic signal
V2I	Segment Speed (SS)	Traffic speed through current road segment

All VEH signals should be available on all modern vehicle CAN networks while ADAS enabled vehicles will produce a lead vehicle track for safety and autonomous cruise control purposes. The information for SPaT and SS comes from the SAE J2735 SPaT/Map message. Thus all signals used in this study are available to a generic CAV while traveling on a connected infrastructure. Most modern vehicles will have access to the VEH and ADAS sourced signals. A total of 13 drive-cycles worth of data were collected along the data drive-cycle by one driver over two days. Details about data collection and availability can be found in the team's previous work [62].

Data Drive-Cycle Selection

In order to gauge the effects of real-world data-based predictions on the performance of POEMS, a real-world dataset was required. It was desired to gather data in conditions which would allow for optimal POEMS performance such that the relative differences between various POEMS methods would be as great as possible. A secondary consideration was that, in order to

allow for optimal ML and ANN prediction performance, the data collection should be conducted along a repeating drive-cycle and that this cycle should be short enough that more than 10 cycles could be collected in a single day. The drive cycle which was selected was a 4 mile long drive-cycle along urban arterial roads in downtown Fort Collins, Colorado which is shown in Figure 2.3.



Figure 2.3: Selected data drive-cycle; drive order was purple, yellow, blue, then green, red circles represent traffic signals

In order to assess the characteristics of the data drive-cycle, it was determined that the data drive-cycle and the EPA dynamometer drive cycles should be characterized by their distributions of speeds and accelerations. These basic statistical measures were chosen in order to allow for easy comparison between the drive-cycles. The drive cycle characteristics data is shown in Table 2.2.

Table 2.2: Drive-cycle characteristics for data drive-cycle and EPA drive cycles

Drive-Cycle	Mean Non-Zero Speed (MNZS)	Standard Deviation of Non-Zero Speeds (SNZS)	Mean Absolute Acceleration (MAA)	Standard Deviation of Absolute Accelerations (SAA)
Data	18.6988	8.5699	1.1557	1.1432
UDDS	10.7923	5.5850	0.4723	0.4859
US06	23.1791	9.5014	0.6538	0.7851
HWFET	21.7191	4.1752	0.1713	0.2443

Based on these characteristics, the similarity of the data drive-cycle and the EPA dynamometer drive-cycles was calculated using the multivariate normal distribution. The relative similarities between the EPA cycles and the data drive-cycle are shown in Table 2.3.

Table 2.3: Relative similarities between EPA dynamometer drive-cycles and the data drive-cycle

UDDS	US06	HWFET
0.5885	0.2394	0.1721

It must be stressed that the comparison between a data drive-cycle and the EPA dynamometer drive cycles could only be calculated after data collection was done and the data drive-cycle was known. Of the candidate data drive-cycles tried, the drive-cycle shown in Figure 2.3 resulted in the most favorable comparison to EPA dynamometer drive cycles.

The selected data drive-cycle was most similar to the UDDS EPA dynamometer drive-cycle because higher numbers imply that the real-world drive cycle from Figure 3 is more similar.

2.4.3 Subsystem 1: Perception

Having collected an extensive real-world CAV dataset, a comprehensive study on prediction methods was conducted. The initial analysis of the prediction study can be found in [24] and is summarized below:

A wide field of potential prediction algorithms including classical ML and ANN methods were considered. The candidate methods are listed in Table 2.4

Table 2.4: Candidate Prediction Methods

Method	Method Type
Long Short Term Memory (LSTM) Deep Neural Network (DNN)	ANN
Convolutional Neural Network (CNN)	ANN
CNN-LSTM	ANN
Decision Trees	ML
Bagged Trees	ML
Random Forest	ML
Extra Trees	ML
Ridge	ML
K-Nearest-Neighbors (KNN)	ML
Linear Regression without Interactions (LR)	Statistical
Linear Regression with Interactions (LRI)	Statistical

All methods were trained, tested, and validated on a 9/2/2 data-split basis respectively. The training and evaluation metric was Mean Absolute Error (MAE), where X is the predicted velocity value, Y is the actual velocity value, and n is the total number of timesteps.

$$MAE(X, Y) = \frac{\sum_{i=1}^n |X_i - Y_i|}{n} \quad (2.1)$$

An extensive study was conducted on different combinations of the signals in Table 2.1 as well as different combinations of macro-parameters for the methods. From this general study, the best results for each method for 10, 15, and 30 second time horizon speed predictions in terms of MAE are listed in Table 2.5.

Table 2.5: The candidate prediction methods results organized from best performing to worst performing.

Method	MAE - 10s	MAE - 15s	MAE - 20s
LSTM	1.78	2.55	3.09
CNN	1.84	2.77	3.50
CNN-LSTM	1.97	2.7	3.26
Decision Trees	2.69	3.60	4.12
Bagged Trees	2.23	3.09	3.67
Random Forest	2.30	3.15	3.72
Extra Trees	1.99	2.73	3.30
Ridge	2.67	3.84	4.67
KNN	2.67	3.84	4.67
LR	2.65	3.82	4.65
LRI	2.57	3.60	4.28

The results of the general study showed that the LSTM had the best performance at 10, 15, and 20 seconds.

Based on this collected evidence, it was concluded that an LSTM should be used with the POEMS system. For further discussions and details, the reader is referred to the team's previous publications [24, 48].

2.4.4 Subsystem 2: Planning

HEV POEMS planning subsystems generally fall into two groups: (1) those based on Pontryagin's Maximum Principle such as ECMS [71], a-ECMS [53], as well as their derivatives, and (2) those based on DP. The advantages of Minimum Principle methods is that these are "real-time" strategies since they are relatively computationally cheap. But this method is typically non-optimal and recent research suggests that the equivalence factor prediction is analogous to velocity prediction [72]. The advantages of DP based methods is that they guarantee discovery of the globally optimal solutions assuming that the vehicle velocity prediction is accurate. The research team discovered the critical importance of this aspect through documenting that even if significant and real world velocity mispredictions are present, the solution is still near optimal [73] which has led to new method of real world practical implementation [14, 15]. Additionally, the rise in the use of AI within the CAV space has led to deployments of vehicles with high-performance GPUs on-board the vehicle which potentially enables real-time computation of DP [74], which has been a common criticism for eventual DP implementation. For these reasons, DP methods were selected for this study.

DP is a numerical method based on Bellman's principle of Optimality, which solves multistage decision-making problems and finds the global optimal solution by operating recursively backwards through time and storing only the optimal controls at each step [75, 76]. DP and its derivative strategies have been applied to the problem of FE optimization for HEVs previously [12, 52, 77, 78] for full and partial drive cycles as well as for perfect and real predictions.

DP can be thought of as a recursive equation solver with memory. A recursive solution to a problem is to evaluate all possible paths by evaluating every possible combination of decisions independently. While a recursive solution will find a global optimum it will require an exponentially increasing number of function evaluations for each additional time-step. DP solves this run-time problem by iterating backwards through time and storing the optimal controls for each discrete state value at each time-step then evaluating the same controls from the same discrete state values until the first time-step. The result of the backward iteration is an optimal control matrix which can be used to find optimal controls at each time-step based on the current state values when iterating forwards. The backwards iteration step is referred to as the optimization step while the forward iteration step is referred to as the evaluation step. The DP method is shown schematically in Figure 2.4.

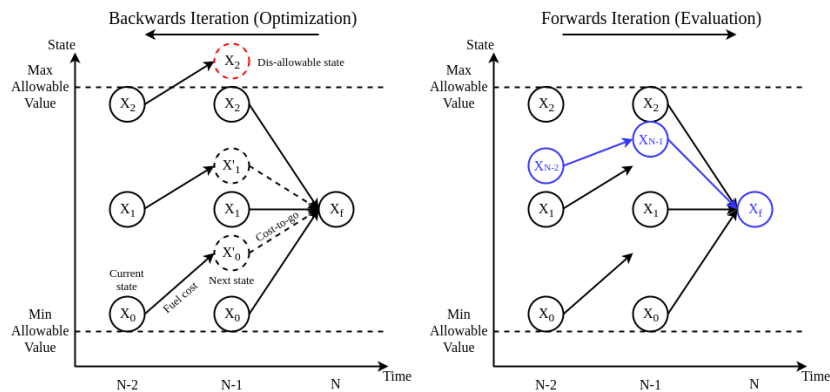


Figure 2.4: Schematic of DP Method

The optimization step of the DP method, as shown in Figure 2.4, creates an optimal matrix which can be used to compute optimal controls at each step by combining current and "remembered" costs. The optimization step iterates backwards from the last time-step (N) to the first which is not shown. The state values (represented by solid-outlined circles) show discrete state values. At time-step $N - 1$, the model is evaluated for each of the discrete state values at each discrete control value which results in a series of new "intermediate" state values (represented by dashed-outlined circles) and associated control costs. Following this, the lowest cost (optimal)

control is selected for each discrete state value. At time-step $N - 2$ the same process is repeated but in addition to the control cost, the cost-to-go is calculated and added. The cost-to-go from a given intermediate state value is calculated by interpolating from the stored optimal control costs from state $N - 1$. This process repeats itself until the first time-step is reached. The DP method shown in Figure 2.4 is constrained in two ways: (1) a large penalty is applied for distance from the desired end state value at time-step N which forces the optimal controls for all state values at time-step $N - 1$ to produce the same state value at time-step N and (2) controls which lead to intermediate states which are above or below the maximum and minimum value lines (represented by red dashed-outlined circles) respectively are not considered. The output of the Optimization step is an optimal control matrix which stores the optimal controls for each discrete starting state value at each time-step.

The evaluation step of the DP method, also shown in Figure 2.4, iterates forward from the first time-step through the last time-step from a given starting state value. At each time-step, interpolation is done using the starting state value (represented by blue solid-outlined circles) and the optimal control matrix values for the current time-step to determine the optimal control for the current time-step. The optimal control is then applied and the starting state value for the subsequent time-step is calculated. This process is repeated until the penultimate time-step is reached.

High-Fidelity DP Solution for the HEV Optimization Problem

The formulation of the DP problem for the 2010 Toyota Prius is as follows:

- The powertrain state x is the battery SOC
- The powertrain control u is the engine power
- The exogenous input for the powertrain w is the vehicle speed
- The time index k denotes the current time-step

The general form of the dynamic equation is shown below. It uses a high-fidelity model of the vehicle to generate the SOC at time-step $k + 1$ based on the SOC at time-step k , the engine power at time-step k , and the vehicle speed at time-step k as:

$$x(k+1) = x(k) + f(x(k), u(k), w(k))\Delta(t) \quad (2.2)$$

Where $f(x(k), u(k), w(k))$ is the charging/discharging rate for the battery $dSOC/dt$. The charging/discharging rate function $f(x(k), u(k), w(k))$ can be written out as:

$$\frac{dSOC}{dt} = \frac{P_{batt}\epsilon_{chg}}{V_{oc}C} = \frac{(P_{batt,mot} + P_{batt,gen})\epsilon_{chg}}{V_{oc}C} \quad (2.3)$$

Where V_{oc} and C are the battery open-circuit voltage and charge capacity respectively. The charging/discharging efficiency is defined as:

$$\epsilon_{chg} = \begin{cases} C_{chg} & P_{batt} \geq 0 \\ C_{dchg} & P_{batt} < 0 \end{cases} \quad (2.4)$$

Where C_{chg} and C_{dchg} are constants reflecting the battery's efficiency in charging and discharging respectively. The powers $P_{batt,mot}$ and $P_{batt,gen}$ are calculated as follows:

$$P_{batt,mot} = \frac{T_{mot}\omega_{mot}}{\epsilon_{mot}} \quad (2.5)$$

$$P_{batt,gen} = \frac{T_{gen}\omega_{gen}}{\epsilon_{gen}} \quad (2.6)$$

The efficiencies ϵ_{mot} and ϵ_{gen} are the efficiencies of the motor and generator respectively. Note that the efficiencies are in the denominator as the terms $P_{batt,mot}$ and $P_{batt,gen}$ are the power that the battery must provide to each to produce the required output powers $P_{mot} = T_{mot}\omega_{mot}$ and $P_{gen} = T_{gen}\omega_{gen}$. The following process is followed:

Starting with the current vehicle speed $w(k)$ and acceleration $\dot{w}(k)$ the vehicle power can be calculated using the road loads power equation.

$$P_{veh} = (m\dot{w}(k) + A + Bw(k) + Cw(k)^2)w(k) \quad (2.7)$$

Where m is the vehicle mass and A , B , and C are vehicle specific constants. For a given engine power u_i , the electric power required is:

$$P_{elec} = P_{veh} - u_i \quad (2.8)$$

For the given u_i , the engine torque and speed can be interpolated from the engine IOL and the combination of engine speed (ω_{eng}) and torque (T_{eng}) along with electric power can be used to determine the torques and speeds of the motor and generator from the planetary gearset dimensions.

The torques are calculated as follows:

$$T_{whl} = \frac{P_{veh}R_{whl}}{w(k)} \quad (2.9)$$

$$T_{pt} = \frac{T_{whl}}{\rho_{fd}} \quad (2.10)$$

$$T_{gen} = \frac{-\rho}{1 + \rho} T_{eng} \quad (2.11)$$

$$T_{ring} = -\rho(T_{gen} - T_{eng}) \quad (2.12)$$

$$T_{mot} = T_{pt} - T_{ring} \quad (2.13)$$

Where T_{whl} and R_{whl} are the torque applied at and the radius of the driven wheels respectively, T_{pt} is the output torque of the power-train (before the differential) and ρ_{fd} is the final drive ratio, ρ is the gear ratio of the sun gear to the ring gear for the planetary gearset, T_{ring} is the torque of the ring gear, T_{gen} is the torque of the generator, T_{eng} is the torque of the engine, and T_{mot} is the torque of the motor.

And the speeds are calculated as follows:

$$\omega_{whl} = \frac{w(k)}{R_{whl}} \quad (2.14)$$

$$\omega_{mot} = \omega_{ring} = \rho_{fd} \omega_{whl} \quad (2.15)$$

$$\omega_{gen} = \frac{\rho + 1}{\rho} \omega_{eng} - \frac{\omega_{ring}}{\rho} \quad (2.16)$$

Where R_{whl} , R_{sun} , and R_{ring} are the radii of the wheel, sun gear, and ring gear respectively, T_{pt} is the torque produced by the powertrain before the differential, and ρ_{fd} is the final drive ratio.

The cost function for the DP problem for control u_i at time-step k can be formulated as either a FE maximization or a fuel consumption minimization. Since fuel consumption minimization is more intuitive and widely used in previous studies and, thus, will be utilized in this study.

$$J_i(k) = J_{im} + \begin{cases} J_{ctg} & k > N \\ J_{pen} = (x_f - x(k+1))^2 C_{pen} & k = N \end{cases} \quad (2.17)$$

Where $J_{im,i}$ is the cost of fuel consumed to reach the intermediate state value which is calculated using the engine speed and torque and the engine FC map, J_{ctg} is the cost-to-go to the next state which is calculated through integration, and J_{pen} is the manually assigned penalty function associated with not arriving at the desired final SOC at the final time-step $k = N$.

Model Predictive Control (MPC) Methods

MPC is a framework to implement prediction-based optimal control. It utilizes a model of the system and a fixed time horizon to generate operational decisions. The DP model discussed in the previous section can be directly utilized in a fixed-horizon MPC framework with a few modifications.

The FC-DP and a generic MPC method are shown schematically in Figure 2.5.

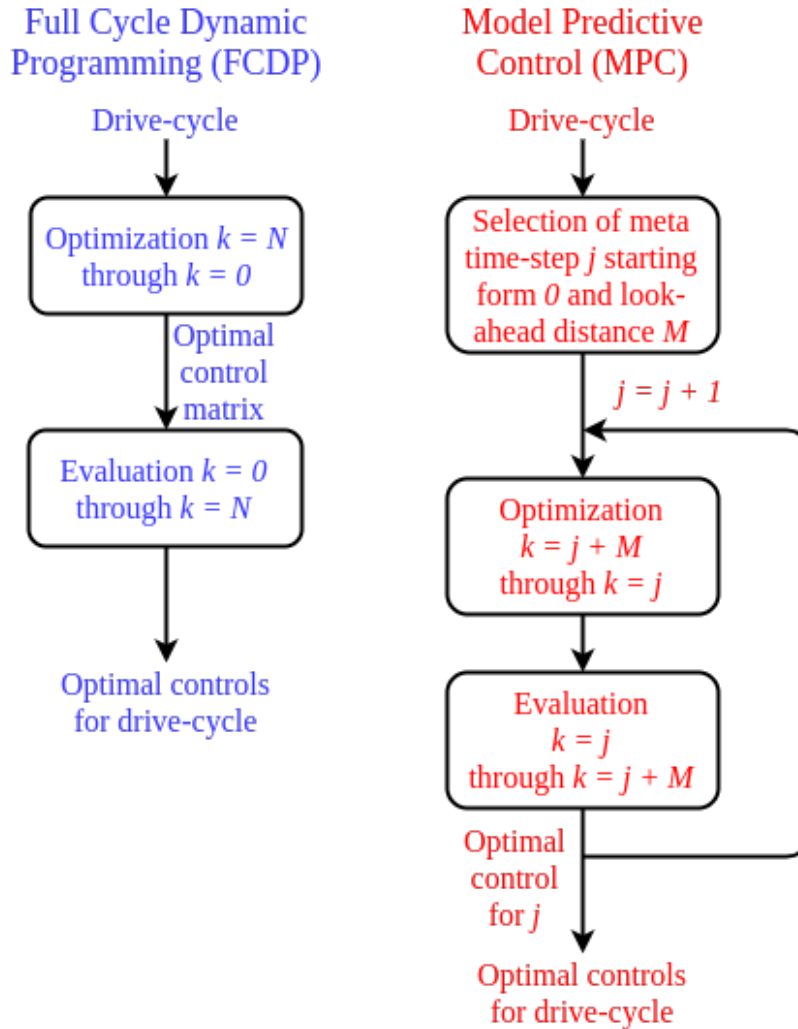


Figure 2.5: Schematic comparison between FC-DP and MPC methods

In effect, MPC performs the DP method on a shortened drive-cycle at each step of the actual drive-cycle. Naturally, MPC should take significantly longer to run on a per time-step basis as full drive-cycle DP. A more detailed explanation can be found in [24].

2.4.5 Subsystem 3: Vehicle Plant

This study was conducted using a validated Autonomie model of a 2010 Toyota Prius. The 2010 Prius is equipped with a Toyota e-CVT gearbox which utilizes two electric motors (motor and generator) connected to the engine and the differential through a planetary gearset to create

a Continuously Variable Transmission (CVT) [79]. Because of the e-CVT architecture, the Prius driveline is controlled entirely by torque commands without having distinct gear states, thus the only powertrain control for the Prius is torque split and the only powertrain state is battery SOC.

Due to the lack of a publicly available FE model specific to the 2010 Toyota Prius, the model used was a generic Autonomie power-split HEV model which was modified to represent a 2010 Toyota Prius by setting the following parameters to the publicly available values shown in Table 2.6.

Table 2.6: Parameters and values for Autonomie 2010 Toyota Prius Model

Parameter	Value
Overall Vehicle Mass	1530.87 kg
Frontal Area	2.6005 m ²
Coefficient of Drag	0.259
Coefficient of Rolling Resistance	0.008
Wheel Radius	0.317 m
Final Drive Ratio	3.267
Sun Gear Number of Teeth	30
Ring Gear Number of Teeth	78
Battery Open-Circuit Voltage	219.7 V
Battery Internal Resistance	0.373 Ω
Battery Charge Capacity	6.5 Ah

Validation of the Autonomie 2010 Prius model was conducted based on publicly available test results from Argonne National Laboratory's (ANL) Downloadable Dynamometer Database (D³)

[80]. The FE results obtained via the model for three EPA dynamometer drive-cycles are compared to those found in D³ in Table 2.7.

Table 2.7: EPA dynamometer drive-cycle FE (km/L) results from Autonomie 2010 Toyota Prius model and ANL D³

Drive-Cycle	Data	Model	Percentage Difference
UDDS	32.14	31.79	1.09 %
US06	29.72	30.30	1.95 %
HWFET	19.26	18.98	1.45 %

With all modeled FE values within 2% of those found in the ANL D³ database, the Autonomie 2010 Toyota Prius model was considered validated for further research. It should be noted that, in accordance with physical testing procedure, the initial SOC for the vehicle model was set to fully charged for validation purposes but was set to 50% for further research. Thus, FE results for the same EPA dynamometer drive-cycles later in the paper with baseline control will be slightly lower than those listed in table 2.7.

2.4.6 System Outputs

In addition to FC-DP and PP-MPC, the CV-MPC method was implemented. The CV-MPC method is functionally identical to PP-MPC except that the prediction vector is replaced with a speed vector where all speeds are the current vehicle speed. The CV-MPC method acts as a "null" predictive method which can serve as a point of comparison. The value of a given level of prediction fidelity can be gauged by its performance relative to PP-MPC and CV-MPC. A comparison of the DP derived methods for a sample drive cycle is shown in Figure 2.6.

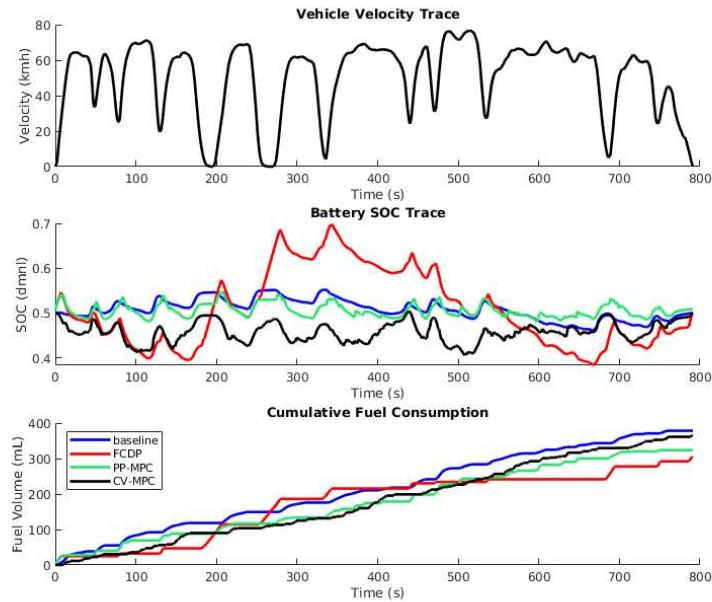


Figure 2.6: Comparison of DP derived methods and Autonomie baseline control on sample drive cycle

For the sample drive cycle in Figure 2.6, the FC-DP method outperformed the PP-MPC method which outperformed the CV-MPC method and all outperformed the Autonomie baseline control method. Because of the double-sided charge-sustaining penalty, all SOC traces started and ended at exactly 50% which means that fuel consumption can be compared directly without electrical equivalence. For the sample drive-cycle, FC-DP was able to outperform PP-MPC because it has more freedom to deviate from the start and finish SOC constraints. Generally, the longer the time horizon, the more effective PP-MPC should become. A study was conducted on the UDDS, US06, and HWFET EPA dynamometer drive-cycles to demonstrate this. Results for the study are shown in Table 2.8.

Table 2.8: Fuel Economy *km/L* for 2010 Toyota Prius model with DP derived methods and Autonomie baseline on EPA dynamometer drive cycles (Time Horizon only effects the PP-MPC and CV-MPC methods)

Drive-Cycle	Time Horizon	Baseline	FC-DP	PP-MPC	CV-MPC
UDDS	10	28.28	40.32	39.11	35.10
UDDS	15	28.28	40.32	39.45	35.13
UDDS	20	28.28	40.32	39.71	35.00
US06	10	17.57	20.05	18.20	17.50
US06	15	17.57	20.05	18.44	17.20
US06	20	17.57	20.05	18.76	17.21
HWFET	10	28.13	28.59	26.30	24.24
HWFET	15	28.13	28.59	26.56	24.90
HWFET	20	28.13	28.59	26.64	24.37

An immediately noticeable trend is that increases in time horizon resulted in better FE for PP-MPC which allowed the PP-MPC FE to approach but not reach the FE produced by the FC-DP method. Another noticeable effect is that the relative efficacy of the methods varied between the drive-cycles with the DP derived methods showing massive improvement over baseline in the stop-and-go UDDS drive-cycle, while the PP-MPC and CV-MPC methods did not result in FE improvements for the relatively static HWFET drive cycle.

That DP derived methods present the greatest potential for FE improvement in low speed stop-and-go conditions is not a surprise. Low speed stop-and-go conditions are where traditional control methods perform worst as they are unable to operate the IC engine in its most efficient areas. DP methods use knowledge of the future speeds of the vehicle to continue to operate the IC engine efficiently in stop-and-go conditions. An interesting result is that, even with inaccurate information

about future vehicle velocity, the CV-MPC method significantly outperformed Autonomie baseline by a significant amount on the UDDS drive-cycle.

2.5 Results

2.5.1 Direct Analysis of Velocity Prediction Accuracy using MAE

Based on the results of the general study documented in Section 2.4.3, a second, specific, study was carried out in order to optimize prediction fidelity from LSTMDeep Neural Network (DNN)s.

Long Short-Term Memory (LSTM) ANNs are a special case of Recurrent Neural Network (RNN)s developed by Hochreiter and Schmidhuber [81] which utilize LSTM neurons in hidden layers. While classical recurrent neurons use a single gate to establish the relationship between inputs and outputs, LSTM neurons contain multiple gates which determine how much information should be remembered and forgotten within the neuron as well as the weighting of old and new information. The presence of the remember and forget gates allows LSTM neurons to utilize information from multiple time steps in the past [82]. For this reason, LSTM networks are ideally suited for problems where immediate and relayed reactions to inputs are present.

Because of its demonstrated feasibility, the LSTM is the prediction model which will be focused on. The following optimal architecture was arrived at:

Table 2.9: Structure of Optimal LSTM DNN

Layer	Composition
1	Input layer - n_{inputs} fully connected
2	64 LSTM neurons
3	Dropout - 10%
4	Batch normalization
5	32 LSTM neurons
6	12 LSTM neurons
7	Output layer - $n_{outputs}$ fully connected

The LSTM DNN described in Table 2.9 was selected for its high performance and reasonable training time. Adding more complexity to the network past the optimal network failed to generate significant performance gains. The LSTM DNN was trained on the following groups of signals:

Table 2.10: Data Groups for LSTM DNN

Group Label	Composition
A	Speed, Acceleration, Engine Speed, Gear, Steered Angle, Throttle Position, Brake Pressure
B	A + HS + LV
C	A + HS + LV + SPaT + SS

The data groups were selected to reflect the data available to different categories of vehicle. A vehicle with neither ADAS nor connectivity only has access to A. Vehicles with ADAS and GPS

navigation but no infrastructure connectivity have access to A and B. CAVs have access to all data groups. For groups A, B, and C a cross-validation study was run wherein the LSTMDDNN was trained on 9 random laps, validated on 2 random laps, and tested on 2 random laps 30 times. The average MAEs for the cross-validation study are shown in Figure 2.7. The standard deviations of MAEs were all less than 5% of the mean values.

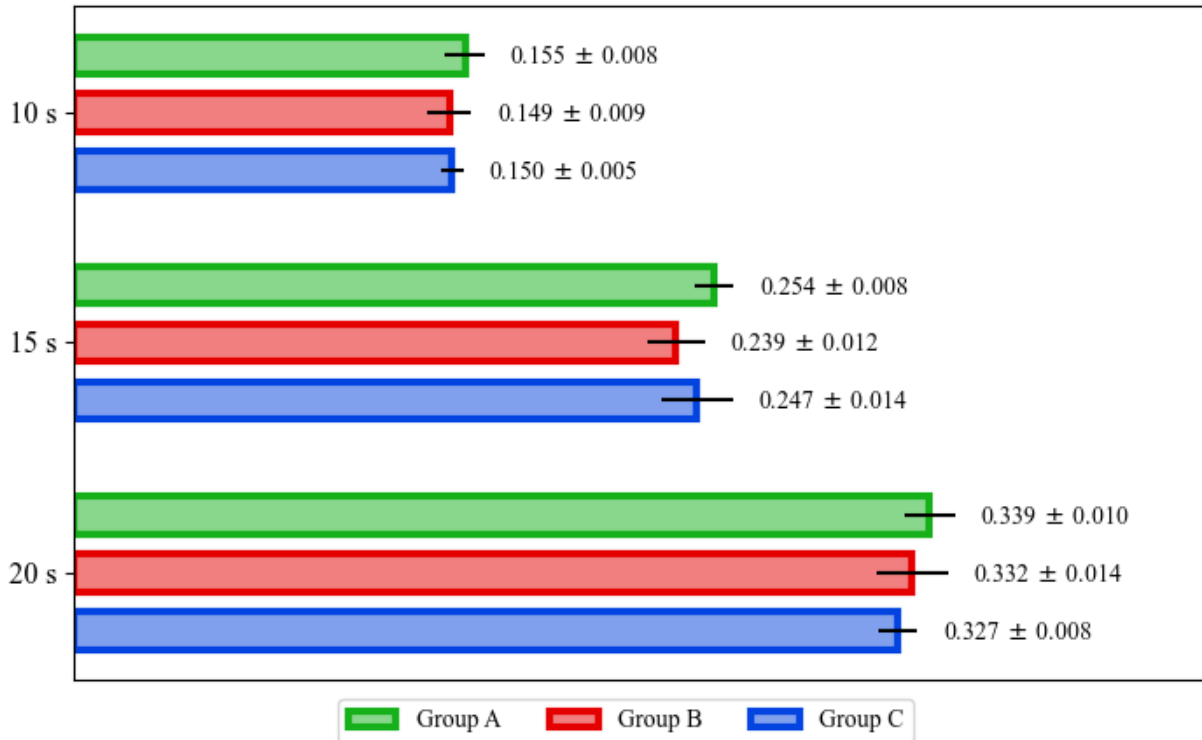


Figure 2.7: MAEs for LSTMDDNN trained on data groups A, B, and C for 10, 15, and 20 second horizons

As is evident in Figure 2.7, the difference in prediction performance between LSTMDDNNs trained on the different data groups was minimal if slightly favoring group B over A and C. A visual comparison of the predictions for all groups at 10 and 20 seconds is shown in Figure 2.8.

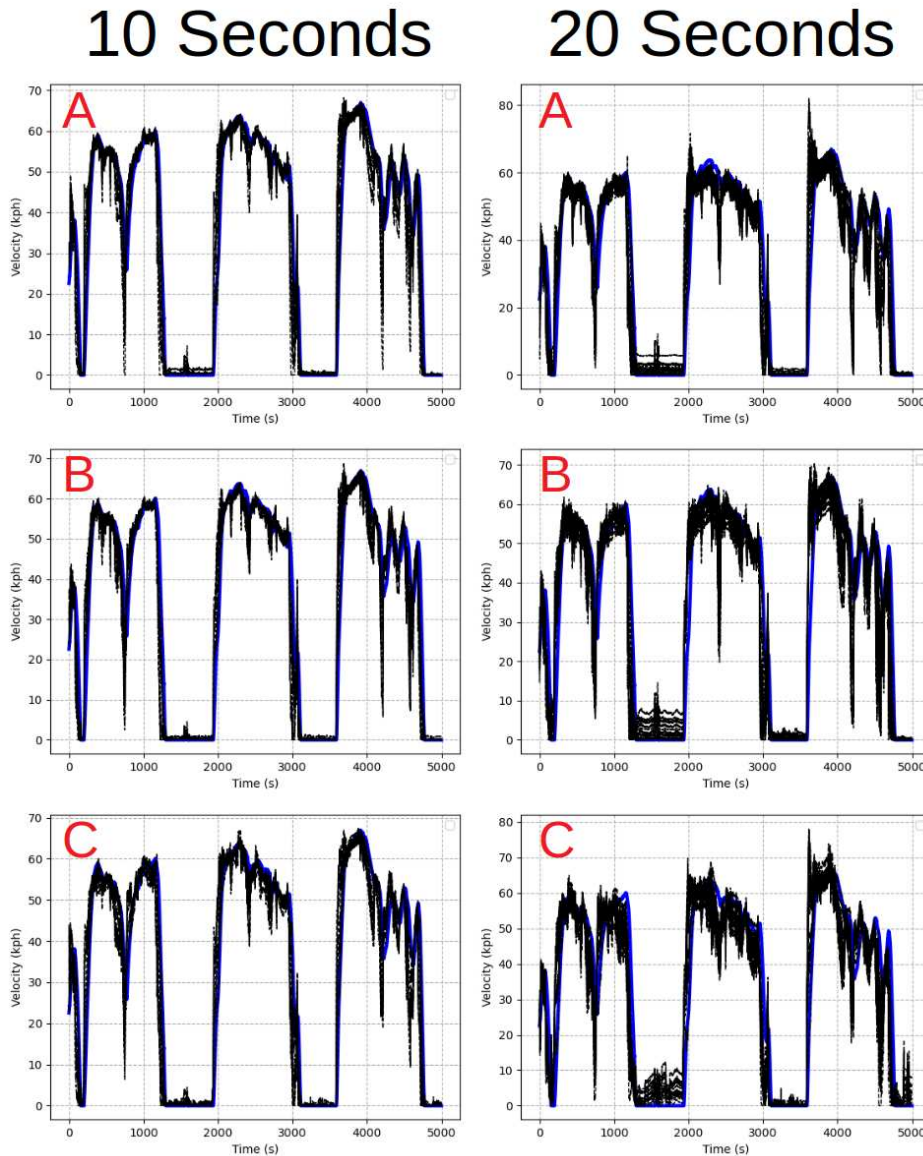


Figure 2.8: Predicted (black) vs. actual vehicle velocity (blue) for LSTM-DNN trained on all data groups at 10 and 20 seconds prediction horizon

As the prediction window increases, the LSTM-DNN predictions are still able to roughly hold the shape of the velocity trace but produce a greater volume of mis-predictions. The predictions generated using LSTM-DNNs trained on the different groups look slightly differently and produce slightly different MAEs but the time horizon length has, by far, the greater impact.

2.5.2 Overall System FE Output

Using the predictions from the cross validation study mentioned in Section 2.5.1, FE simulations were conducted using the DP derived methods and Autonomie baseline controls. The mean FE results for the study are listed in Table 2.11 and percentage improvements over baseline for the DP derived methods with all data groups and at 10, 15, and 20 seconds are shown in Figure 2.9.

Table 2.11: FE (*km/L*) simulation results based on cross-validation study predictions

Group Label	Prediction Horizon (s)	Baseline	FC-DP	PP-MPC	RP-MPC	CV-MPC
A	10	18.33	24.10	21.78	20.73	20.07
B	10	18.33	24.10	21.78	20.85	20.07
C	10	18.33	24.10	21.78	20.83	20.07
A	15	18.33	24.10	21.87	21.24	20.01
B	15	18.33	24.10	21.87	20.45	20.01
C	15	18.33	24.10	21.87	20.15	20.01
A	20	18.33	24.10	22.22	20.80	20.00
B	20	18.33	24.10	22.22	20.75	20.00
C	20	18.33	24.10	22.22	21.05	20.00

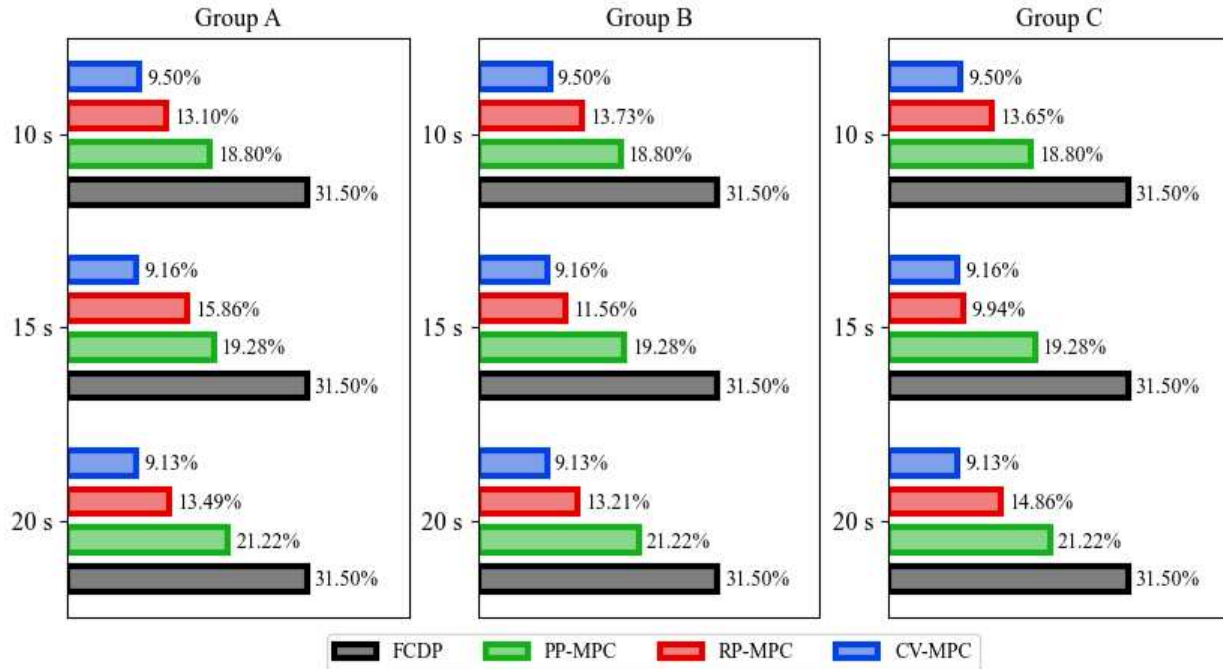


Figure 2.9: Percentage FE improvements for DP derived methods for all data groups and time horizons

2.5.3 Results Summary

The FE results for the DP derived methods, when taken in conjunction with the results of the LSTM prediction illustrate several trends:

1. With perfect predictions MPC methods will produce better FE results for longer prediction horizons.
2. A greater volume of mis-predictions will result in worse FE results for MPC methods
3. The small differences in prediction MAE observed between the data groups at all three time horizons are insufficient to explain the large differences observed in FE percentage improvement over baseline for the RP-MPC method between the data groups for the 15 and 20 second horizons.

It is illustrative that, for all cases, the average performance of the RP-MPC method came in between that of the CV-MPC and PP-MPC methods. The PP-MPC method, by definition, produces

no mis-predictions while the CV-MPC method, by definition, produces only mis-predictions when the vehicle is moving. It would be logical for the RP-MPC method which produces some degree of mis-prediction to produce FE improvements which are somewhere between those produced by the CV-MPC and RP-MPC methods. The differences in vehicle future velocity prediction MAE between the data groups shown in Figure 2.7 were relatively small where the differences in FE improvement performance based on those predictions shown in Figure 2.9 were significant. Furthermore, no consistent trend links the prediction MAE with the percentage FE improvement which leads to the conclusion that MAE is an insufficient metric to describe mis-prediction levels with respect to the RP-MPC method. Further research should be conducted to investigate whether other metrics serve better in this role.

The robustness of DP to velocity prediction error is directly demonstrated in the CV-MPC method which uses a "null" prediction of constant current speed over the entire prediction horizon. It showed significant improvements over baseline while the RP-MPC method showed significant improvements over CV-MPC. An examination of the data trace for all methods using predictions based on group A data for a 10 second prediction horizon are shown in Figure 2.10.

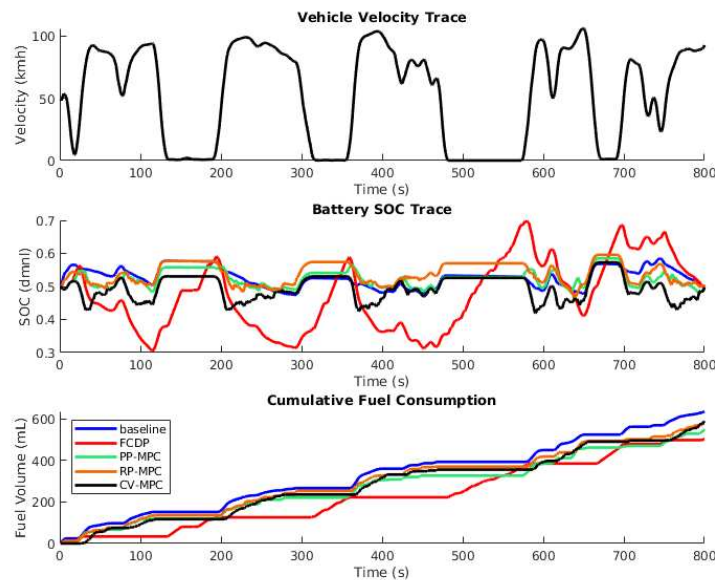


Figure 2.10: FE simulation data trace for all methods

It can be clearly seen that the MPC methods discover similar local optima, and produce similar optimal state trajectories while the FC-DP method, with much more freedom to deviate from the final SOC constraint, takes a substantially different path and ends up using less fuel.

2.6 Conclusions

In order to demonstrate the function of various implementations, the data available to different types of vehicle were classified, an extensive real-world driving dataset was collected which incorporated said data, ML and ANN methods were used to predict the ego vehicle future speed using different groups of data, and the best predictions were used in FE simulation to determine the effectiveness of practically implementable POEMS. The results of the velocity prediction study showed that when using a LSTMDNN, high-fidelity velocity prediction was possible using only data which is available to conventional vehicles without ADAS or V2X connectivity and that the addition of ADAS and V2X connectivity resulted in modest fidelity gains. The results of the FE study showed the following:

- FE improvement achievable with RP-MPC approaches that achievable with PP-MPC.
- RP-MPC consistently outperformed CV-MPC.
- Predictions made with ADAS and V2X resulted in greater FE improvement in the 20 second window.

An unavoidable conclusion is that the relationship between prediction fidelity and FE improvement using DP-derived methods cannot be explained by differences in prediction MAE.

This study shows that POEMS implementation on HEVs and PHEVs is feasible with causal and implementable prediction and control technologies and would lead to significant improvements in HEV and PHEV fleet efficiency if implemented. The same system architecture as autonomous vehicles (perception, planning, control, plant) can be applied to energy efficiency through the deployment of POEMS enabled vehicles. The FE improvement which would result is significant

and the technology can be implemented currently. The results of this study thus serve as a step towards real world implementation and commercialization.

2.7 Summary

The purpose of research directed towards RQ1 was to determine what energetic benefits could be attained through connected vehicle optimal control. The work in this chapter focused on POEMS for HEVs. There are two main questions surrounding POEMS. The first of which is what effect prediction accuracy has on control effectiveness and the second is how to produce sufficiently accurate predictions. The study on which this chapter was based built on previous work by the author [48, 62] which used real world data to perform an investigation into velocity prediction methods. The results of the previous work showed that LSTM DNNs were well suited to the velocity prediction task and were able to produce high fidelity results with various combinations of signals. This work was extended to include an analysis of what energetic benefits could be attained when using the LSTM velocity predictions to inform optimal energy management strategies. Results indicated that gains in the 10% to 15% range could be attained in urban driving conditions and that predictions could be made with sufficient accuracy without the benefit of infrastructure communication. Overall the results of the study indicated that large benefits could be expected from commercial implementation.

Chapter 3

Real Time Implementation Comparison of Urban Eco-Driving Controls

3.1 Preface

This chapter is derived from [83] which was primarily authored by this dissertation's author. Important help was provided by Chon Chia Ang in code development, Dr. Zach Asher, Dr. Richard Meyer, and Dr. Ilya Kolmanovsky in conceptualization and presentation. The content of the paper addresses RQ1.T2. RQ1 focuses on determining what energetic benefits can be attained for Connected Autonomous Vehicles (CAVs) through the application of infrastructure connected optimal control. In this chapter the focus is on using optimal Eco-Driving control to improve the energy efficiency of Battery Electric Vehicles (BEVs) in urban driving conditions. Urban driving provides a highly complex set of constraints which define possible trajectories for individual vehicles deriving from traffic and, ultimately, traffic signals. With knowledge of future traffic signals it is possible to implement optimal control and attain substantial energy savings without reducing average speed. This chapter summarizes and categorizes the existing literature on the subject then implements selected methods to evaluate their potential energy savings and feasibility as real-time controls.

3.2 Overview

CAV technology has the potential to enable significant gains in Energy Economy (EE). Much research attention has been focused on autonomous Eco-Driving control enabled by various methods. In this study, the state of the literature on autonomous Eco-Driving control is reviewed, an overall systems description of Eco-Driving control for a CAV is provided, and representative methods are evaluated comparatively against each-other in simulation. Simulations are conducted

using real-world traffic signal data and a validated Future Automotive Systems Technology Simulator (FASTSim) model. Results indicate that an EE improvement in the range of 5% to 15% is attainable depending on the method and cost function used. In this paper it is shown that Dynamic Programming (DP) methods are most effective in improving EE but are significantly more computationally expensive than other methods. Genetic Algorithm (GA) methods are shown to present the most potential in terms of EE improvement and run-time. Results also indicate that velocity sensitive cost functions allow all methods to perform better than pure acceleration minimization.

3.3 Introduction

In response to rising concerns over climate change and energy costs, a significant portion of automotive development effort has gone into the reduction of energy use and Green-House Gas (GHG) emissions from road vehicles. Over time, vehicles have become significantly more efficient in terms of both EE and GHG emissions per mile [84, 85] under pressure from environmental regulations from the U.S. Environmental Protection Agency (EPA) and its global equivalents which exert ongoing pressure on Original Equipment Manufacturers (OEMs) to continue this effort [86]. In order to improve vehicular energy efficiency, traditional Internal Combustion Engine (ICE) powertrains have incorporated electric motors and evolved into hybrid electric vehicles and BEVs [87] which promise further greenhouse gas reductions per vehicle [88]. Regardless of powertrain technology and regardless of methods of power generation, the pressure to reduce vehicular energy consumption will continue to be present.

Vehicle energy efficiency is also subject to modes of operation. Eco-Driving is a strategy designed to reduce fuel consumption by minimizing accelerations and unnecessary braking events. Eco-Driving is well known and has been shown to be effective when employed by human drivers [26]. As an example, Eco-Driving is taught as a part of drivers' education in Singapore and has resulted in a EE improvement of 11% to 15% there [27]. Differences in culture, infrastructure, and available technology will play a major role in determining the effectiveness

of efforts to promote manual Eco-Driving. Vehicular autonomy and CAV technology provide a more general opportunity for the application of Eco-Driving strategies because they circumvent driver acceptance/training issues. When compared to a human driver (i.e. manual Eco-Driving), a CAV has the ability to follow optimal trajectories precisely and can take into account information which is beyond line-of-sight.

Compared to manual Eco-Driving, autonomous Eco-Driving yields the following potential benefits:

- Ability to precisely follow optimal energy traces;
- Ability to account for traffic information which is beyond line-of-sight;
- Ease and scalability of implementation;
- Improved driver/passenger acceptance.

A great variety of solutions for autonomous Eco-Driving control have been put forward in the literature. This diversity is due to the complicated nature of the problem and the many dimensional design space which results from it. To the author's knowledge, no comprehensive, comparative study exists. This study attempts to address this research gap by summarizing and subdividing Eco-Driving control strategies, defining a framework for comparative implementation of solver methods, implementing a selection of common methods, and evaluating these methods in terms of performance and practicality using real-world data [28]. The current state of the literature is discussed in Section 3.4, a system and subsystems overview for an assumed Eco-Driving CAV is provided in Sections 3.5, 3.6, 3.7, and 3.8, results are presented in Section 3.9, and conclusions are presented in Section 3.11.

3.4 Literature Review

Much research exists in the area of autonomous Eco-Driving controls. In conducting the literature review, the authors were particularly interested in publications which proposed methods

which might be implemented in real-time. A real-time control was defined as a control which was explicitly or could be implemented in a receding horizon context. Such a control should be able to execute multiple times per second.

The authors propose that the methods reviewed may be categorized by purpose and structure as follows. First, a division can be made into the categories of rules-based and optimal. Rules-based methods serve the purpose of providing simple and computationally light algorithms for computing target speed on an instantaneous basis. Rules-based methods often mimic the heuristics that human drivers follow when attempting to minimize energy consumption such as lighter accelerations and longer following distances. By contrast optimal methods attempt to find a minimum energy consumption trace for a given time or distance horizon. Optimal methods, thus, require information about future conditions even if this is done purely with assumptions. Within the set of optimal methods one can further subdivide into globally optimal methods and locally optimal methods. Globally optimal methods serve the purpose of finding the control which results in the global minimum energy consumption. For globally optimal methods function dictates form and all methods proposed are variations of DP. Locally optimal methods serve the purpose of finding a control trace which is more efficient than one which could be attained by a rules-based method but require less computational time than globally-optimal methods. Locally optimal methods often involve transcribing the problem into the time domain and performing trajectory optimization. As will be seen in Section 3.9, local optima will often resemble the global optimum far more closely than they do a rules-based method's solution. The authors propose a taxonomy based on groupings in form and function which divides methods into the following categories: Rules-Based Eco-Driving (RBED), Discretized Control Optimization (DCO), and Polynomial Trajectory Optimization (PTO).

3.4.1 Rules-Based Eco-Driving (RBED)

RBED is a subset of autonomous Eco-Driving control wherein a vehicle reduces its energy consumption through a set of predefined rules which are functions of vehicle states. Due to

their feed-forward nature, RBED methods are relatively simple to implement. Compared to normal human driving behavior, RBED methods capable of yielding considerable fuel economy improvement [89, 90]. A common RBED algorithm is Intelligent Driver Model (IDM) [91] with several works presenting modified versions of the method in Eco-Driving simulations [92–95]. Although non-IDM RBED methods appear in the literature [96–98], IDM and its derivatives dominate RBED literature and are often used as a comparison point in optimal Eco-Driving literature. When implemented on a sufficient percentage of vehicles, RBED methods have shown promise in traffic calming [92, 99]. RBED control has also been extended to cooperative and centralized fleet control schemes [93, 94].

3.4.2 Discretized Control Optimization (DCO)

The purpose of a DCO method is to compute optimal controls for a vehicle at a set of discrete points in time or distance. DCO methods require a state transition model and information about future exogenous inputs. The DCO category consists, primarily, of DP and Reinforcement Learning (RL) methods.

DP [76, 100], is a well known mathematical optimization method which will produce globally optimal solutions to control problems subject to a chosen discretization. A realization of the DP derived optimal solution depends on whether the chosen discretization and the model appropriately matches the real world application. In order to account for constraints in position and speed inherent to autonomous Eco-Driving control, both must be problem states. The control in the autonomous Eco-Driving problem is acceleration or a related control such as throttle. Such a 2 state 1 control DP algorithm is presented in [101, 102] which minimizes fuel consumption while navigating around traffic signals. [103] presents a 2 state 1 control DP algorithm for heavy duty trucks in highway conditions. Both methods must execute at a low rate and serve to set targets for a lower level controller. The primary issue with DP methods for real-time implementation is that run-times scale exponentially with the number of states and controls. This scaling issue is often referred to as the "curse of dimensionality". In the autonomous Eco-Driving literature DP

solutions proposed as real-time controls use sub-optimal implementations of DP to avoid the issue. DP methods are also often proposed as a high level control algorithm, executing at low frequency, which serves to set targets for low a level controller. It is most common to see DP implemented as a comparison point for the performance of another proposed solution with the caveat that the DP solution is not a candidate for real-time implementation.

Sub-optimal implementations of DP are found in [104–107]. [104, 105] overcome the run-time scaling issues by removing position as a problem state. This is accomplished by adding a tunable constant cost to the running cost to ensure that the correct final distance is reached at the correct time. This tunable parameter must be found via numerical root-finding. Overall this method, which can be thought of as a pseudo 2 state DP method. The pseudo 2 state method was found to execute in less time than an equivalent 2 state DP method which emphasizes the importance of the run-time scaling effects inherent to DP. A major limitation with [104, 105] is that, having removed the position state, it is not possible for the optimization to account for traffic signals in fixed positions making the method less applicable for urban Eco-Driving. [106], proposes an Approximate Dynamic Programming (ADP) solver for traffic-signal constrained driving which uses a non-optimal rollout method to approximate the cost-to-go. [106] accounts for traffic signals by determining if it is feasible to pass in a "go" phase or, if not, implementing eco-approach and eco-departure. [107] proposes a method by which pre-computed DP solutions may be adjusted to account for perturbations in external inputs without having to re-compute the DP solution thus reducing the required frequency of DP method evaluations for real-time control. In all cases, global optimality is traded for reductions in run-time.

[108–113] propose DP based method where the DP solution is computed at a low frequency and is used as a target by a lower level controller. Exemplary of the type is [114] which uses Vehicle to Infrastructure (V2I) information and DP to set velocity targets for a cruise control system for urban driving. This method was tested both in Hardware In Loop (HIL) simulation and on-road and was shown to produce a 30% EE improvement at a cost of an 8% increase to travel time.

RL based methods are proposed in [115–117]. [115] uses RL for optimizing motor power control for an electric vehicle subject to road grade but not traffic. The RL control was found to perform nearly as well as DP for the same problem. The algorithms seen in [116] and [117] are focused on comfort (reduction of jerk) and collision avoidance rather than Eco-Driving and also found similar performance to equivalent DP solutions with lower run-time. Ultimately reinforcement learning suffers from the same disadvantages that DP does for the application, namely the long run-time required to compute the strategy but not to the same extent.

3.4.3 Polynomial Trajectory Optimization (PTO)

The optimal Eco-Driving optimal control problem can also be solved as a trajectory optimization problem by transcribing into the time domain. Direct transcription transforms the problem into a n dimensional optimization with the number of dimensions set by the level of discretization. but at lower levels of discretization. Run-time for the trajectory optimization will scale with dimensionality depending on the solver used. At very high levels of discretization linear interpolation can be used between trajectory points. In order to reduce run-time a lower discretization may be used but this will necessitate polynomial interpolation between the optimization points. Because every segment of an interpolation polynomial is a function of multiple knot points, using an interpolation polynomial comes at the cost of introducing nonlinearity into the problem. PTO methods may use bounded nonlinear solvers such as Interior-Point Optimization (IPOPT) or Sequential Least Squares Programming (SLSQP) or metaheuristics.

PTO is commonly used for motion planning in robotics [118]. Nonlinear bounded solvers are used to perform PTO for autonomous Eco-Driving in [119–121]. A comparison to DP is provided in [122] for the related optimal energy management problem where the PTO method, using a nonlinear bounded solver was shown to be able to approximate the globally optimal solution and to produce a solution in orders of magnitude less time than DP. The particularities of the optimal Eco-Driving problem are difficult for bounded nonlinear solvers to deal with. The issue is that

vehicle motion is subject to time varying constraints in position caused by other vehicles and by traffic signals as well as in speed by other vehicles and speed limits. These constraints will be discussed in Section 3.6. The combination of nonlinearity caused by interpolation polynomials and the complexity of the constraints make the computation of meaningful gradients difficult and thus gradient descent solvers should struggle. [119–121] do not consider distance and speed constraints simultaneously. The issues that gradient descent solvers experience are somewhat mitigated in [123] in which best interpolation splines [124, 125] are used rather than interpolation polynomials. Best interpolation splines consider each segment separately and can be used to guarantee that constraints will not be violated but come at the cost of additional run-time.

Metaheuristics are also commonly used as solvers for PTO methods with GA and Particle Swarm Optimization (PSO) methods being the most often proposed. GA and PSO both take inspiration from nature. PSO [126] takes inspiration from animals which exhibit schooling or swarming behaviors. PSO works by generating a field of candidate solutions (particles) and then computing gradients for each particle based on individual and global best discovered solutions. GA [127–129] mimics natural selection by encoding decision variables for a discretized problem into phenotypes then mating the highest fitness phenotypes over many successive iterations. GA can be modified in many ways including by introducing random mutation, elitist selection, and others to change the breadth of the search. Where PSO is still at its core a gradient descent method, GA is not and is, thus, not subject to the difficulties that gradient descent methods face with the optimal Eco-Driving problem.

GA was utilized in [130] to generate optimal driving operations from real-world data with final results yielding an improved fuel economy of 22% compared to the initial population. Similarly, [131] used GA to group vehicles in compatible streams to provide a smoother traffic flow with the algorithm scaling favorably in comparison to DP. In recent studies [132–134], GA PTO methods were applied to both conventional and electric vehicles with results showing favorable fuel economy improvement for both types of vehicles. PSO was employed in various studies to optimize energy consumption for individual vehicles [131, 135–137] and to streamline vehicle

platoon behavior at intersections [138]. A comparison of PSO a based PTO method with DP [137] found that PSO significantly under-performed DP in terms of efficiency but executed in significantly less time. PSO and GA have also been used in conjunction and the combined method was shown to be more effective than either individually [131, 136].

The general consensus in the literature would be that PTO methods provide the opportunity to compute locally optimal solutions in meaningfully less time than a globally optimal solution could be computed using DP. The constraints used in much of the PTO literature were simplifications of what the authors would consider the minimum constraints for optimal Eco-Driving in urban conditions. The complex boundaries inherent to the optimal Eco-Driving problem are difficult for gradient based solvers to account for and are, perhaps, easier for metaheuristics to account for. However, the use of GA or PSO comes at the cost of introducing randomness to the problem.

3.4.4 Summary

The publications reviewed are listed by category and method type in Table 3.1. The literature contains a variety of approaches to the optimal Eco-Driving problem. There is significant variation in the constraints used in the studies surveyed. The distinction in constraints more or less reflects a division in focus between urban driving and other types of driving. Urban driving is constrained by the positions and velocities of surrounding vehicles as well as traffic signal locations and states. The constraints present in urban driving are time-varying. Inevitably, the constraints used will need to be approximate as precise knowledge of future values is not possible. Because all optimal Eco-Driving methods proposed are intended to be used in a receding horizon manner some simplification is acceptable. However, in order to make direct comparisons between methods, a standard and sufficiently representative set of constraints must be applied to all.

Table 3.1: Publications Reviewed by Method Type

Category	Method Type	Publications
Rules-Based Eco-Driving (RBED)	Intelligent Driver Model (IDM)	[89], [90], [91], [92], [99], [93], [94], [95]
	Rule-Set	[96], [97], [98]
Discretized Control Optimization (DCO)	Dynamic Programming (DP)	[101], [102], [104], [105], [106], [107] [108], [109], [110], [111], [112], [113], [114]
	Reinforcement Learning (RL)	[115], [116], [117]
Polynomial Trajectory Optimization (PTO)	Bounded Nonlinear Solvers	[119], [120], [121], [123]
	Metaheuristics	[130], [131], [132], [133], [134] [131],[135], [136], [137]

3.5 System Definition

The Eco-Driving system can be broken down into three subsystems as shown in Figure 3.1. This systems-level diagram is consistent with advanced vehicle control applications such as autonomous vehicles [139] and with energy efficiency improvement strategies such as optimal energy management [25]. The Eco-Driving subsystems are, respectively, the Perception subsystem, the Planning subsystem, and the Plant subsystem.

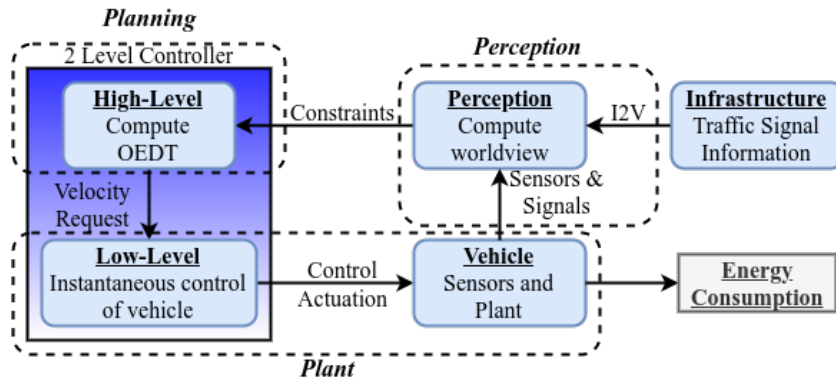


Figure 3.1: Eco-Driving System Schematic

The Perception subsystem uses the sensors and connectivity capabilities of the ego vehicle and computes motion boundaries based on a detected lead vehicle (with on-board sensors and V2V) and upcoming traffic signal information (V2I). The proliferation of new vehicles equipped with a forward object detection system will soon reach 100% per an agreement between the National Highway Traffic Safety Administration (NHTSA) and automakers which mandates the inclusion of said systems in order to enable automatic emergency braking as a standard feature [140]. These systems often comprise a radar and a visual object detection system which work in concert to determine the location, motion, and type of objects in the ego vehicle's forward vision cone. In addition to enabling safety oriented features such as collision avoidance systems, the forward object detection system also enables convenience oriented features such as adaptive cruise control. In the future, most vehicles may also be equipped with V2I technology in the form of a transponder which communicates with infrastructure transponders according to the Society of Automotive Engineers (SAE) specification J2735 [67]. Among the messages contained in the SAE J2735 specification are the SPaT and MAP messages which provide the signal phase and timing and locations of upcoming traffic signals.

The vehicle is assumed to contain a two-level controller with a high-level controller computing an optimal Eco-Driving trace and the low-level controller being responsible for carrying out the optimal Eco-Driving trace in a safe manner. The Planning subsystem, which is composed of the high-level controller, takes the information about lead vehicle motion, speed limit, as well as future traffic signal information and uses it to compute the optimal Eco-Driving trace.

The final subsystem, the Plant, is the ego vehicle (physical or simulated) which executes the optimal Eco-Driving trace and outputs the resultant energy consumption. The subsystems and the manner in which they are treated in this study are explained in the following subsections.

3.6 Subsystem 1: Perception

In order for Eco-Driving control to be evaluated in a real-world context, the algorithms which generate the optimal Eco-Driving trace must be able to function using only information which is

currently, or will soon be available to CAVs. The information which is available to CAVs comes from the Advanced Driver Assistance System (ADAS) system of the CAV as well as from V2I communication where available. The data which is available to CAVs via their ADAS systems and V2I communication is listed in Table 3.2 and is further elaborated in [47].

Table 3.2: Data Available to CAVs

Signal	Description	Source
Lead Vehicle	Relative location of confirmed lead vehicle	ADAS
Signal Phase and Timing (SPAT)	Phase and timing for subsequent traffic signals	V2I
Positions of Subsequent Traffic Lights (MAP)	Latitude and longitude coordinates for subsequent traffic signals	V2I
Speed Limit	Currently active speed limit for the ego vehicle	V2I

With this information, a CAV can generate path constraints for the optimal Eco-Driving problem. For this study, path constraints consist of allowable locations (distances along the vehicle path) for the vehicle at specific times and allowable speeds for the vehicle at specific locations.

3.6.1 Path Constraints

The ego vehicle should not be deliberately programmed to violate traffic laws even if this provides efficiency and/or travel-time benefits. This means that the vehicle should neither exceed the speed limit, disobey traffic signals, nor collide with any other vehicle. If the ego vehicle is the first vehicle in a queue then an upper boundary can be generated from SPaT knowledge as an inequality constraint,

$$x(t) < B_U(t), t \in [0, T] \quad (3.1)$$

where x is the vehicle distance along its route, B_U is the upper boundary which is a function of time, and T is the final time of the drive cycle. There are many ways to generate this upper boundary based on lead vehicle and traffic signal positions. A general approach would be to formulate the upper boundary based on a piecewise function wherein the boundary is generated by the closer of the nearest stop phase and the immediate lead vehicle. For the purposes of this study, only vehicles with no immediate lead vehicle are considered (i.e. there are vehicles in front of the ego vehicle but always at least one signal away) as in such a case, a long-term optimal trajectory can be generated.

An assumption made here is that waiting out a go phase while not moving, although potentially optimal for a single vehicle, will cause congestion and will not be fleet optimal. Thus, a lower bound on distance as a function of time is also defined as an inequality constraint,

$$x(t) > B_L(t), t \in [0, T] \quad (3.2)$$

where B_L is a piecewise function of time based on the positions and phases of leading traffic signals. The upper bound and lower bound combine to form a "corridor" on a phase map as shown in Figure 3.2.

In limiting possible paths to those entirely within the boundaries corridor, the ego vehicle is limited to largely following traffic norms and is far less likely to radically affect normal traffic patterns. The selection of stop phases to define the boundaries is done using the IDM model further described in Section 3.7. The IDM simulation is carried out for a given amount of time and the upper bound is defined by the preceding phases of the traffic signals passed by the model vehicle and the lower bound is defined by succeeding phases of the same signals. As the IDM model represents a baseline driver, the corridor created this way is one which must reflect normal driving and, thus, is useful for this purpose. It should be noted that the boundaries created in this manner are non-convex.

Traffic signals are generally adaptive and were in this specific case. In this study full knowledge for traffic signal timing in the future is assumed. The effects of adaptive traffic signal timing may

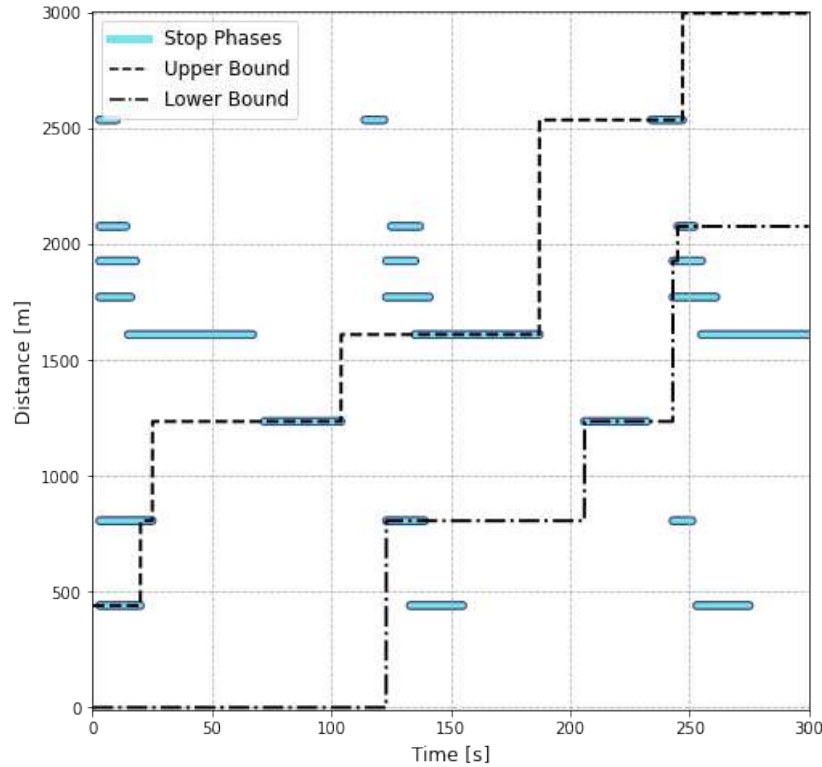


Figure 3.2: Example upper and lower boundaries "corridor"

be dealt with through the implementation of stochastic constraints as in [113]. Uncertainty on the timing of traffic signals will have the effect of extending the stop phases as used in optimization and thus tightening the corridor.

An element of reality is added to this study through the use of real-world SPAT data in the generation of path boundaries. This data was collected in 2019 and consists of traffic light phase and timing data from 19 traffic signals along a 4 mile route in downtown Fort Collins, CO. This data was collected by the authors and its collection is described in [62]. Several hours of SPAT data for each of the traffic signals was collected in collaboration with the Fort Collins Traffic Operations center. From this data and the distances of the traffic signals along the route, a phase map was constructed.

In order to conform to traffic norms and regulations the ego vehicle velocity is required to satisfy the inequality,

$$0 \leq v(t) \leq S_L(t), t \in [0, T] \quad (3.3)$$

where $S_L(t)$ is the road speed limit at time t . For the Fort Collins drive cycle used in this study, the speed limit for all roads at all times was 35 mph (15.65 m/s).

3.7 Subsystem 2: Planning

The Planning subsystem is responsible for calculating an optimal Eco-Driving trace based on the constraints computed by the Perception subsystem. As described in Section 3.5, the planning system is assumed to contain a high-level controller which computes optimal velocities and a low-level controller which implements them. This study is only concerned with the high-level controller. It is also assumed that the high-level controller will operate in a Model Predictive Control (MPC) framework for all methods. The optimal methods selected for implementation were DP DCO, and PTO using IPOPT, GA, and PSO as solvers. IDM was used as the baseline control to compare against. These methods are defined in the following subsections.

3.7.1 Baseline Control

Intelligent Driver Model (IDM)

IDM, developed by Trieber, Hennecke, and Helbing in 2000 [91] is an RBED method intended to enable agent based traffic modeling. This model represented a step improvement on previous car-following models as it was meta-stable, prevented collisions, and all parameters had physical interpretations. The IDM is formulated as follows:

$$\dot{x}_i = \frac{dx_i}{dt} = v_i \quad (3.4)$$

$$\eta = \left(1 - \left(\frac{v_i}{v_0} \right)^\delta - \left(\frac{s^*(v_i, v_{i-1})}{s_i} \right)^2 \right) \quad (3.5)$$

$$\dot{v}_i = \frac{dv_i}{dt} = \begin{cases} a\eta & \eta \geq 0 \\ b\eta & \eta < 0 \end{cases} \quad (3.6)$$

$$s_i = x_{i-1} - x_i - l_{i-1} \quad (3.7)$$

$$s^*(v_i, v_{i-1}) = s_0 + v_i T + \frac{v_i(v_{i-1} - v_i)}{2\sqrt{ab}} \quad (3.8)$$

Table 3.3: Variables and Parameters for IDM

Parameter	Description	Representative Value
i	Ego vehicle (lead vehicle is vehicle $i-1$)	N/A
x	Distance	N/A
v	Velocity	N/A
s	Distance headway (space between lead and follow vehicle)	N/A
s^*	Desired distance headway	N/A
η	Proportion of maximum acceleration used	N/A
s_0	Minimum distance headway	15 m
T	Desired time headway	4 s
δ	Velocity exponent	4
l	Vehicle length	2 m
a	Maximum forward acceleration	5 m/s ²
b	Maximum deceleration	5 m/s ²

In this study, as mentioned previously, only the optimal trace for the lead vehicle is considered. Thus the upper bound of the traffic light constraints is used in place of a lead vehicle with varying distances but always zero speed.

IDM can represent a spectrum of drivers in terms of aggression in acceleration and follow distance. Parameter selection for IDM is important as it effects the efficiency of the generated trace. Those parameters which have the greatest effect on EE are a , b , and δ . An experiment was run on said parameters using 100 different constraint sets per case and a FASTSim [141] 2015 Kia Soul EV model. This experiment was a full-factorial design with the levels for a and b being 1, 5, and 9 m/s² (this range encompassing virtually all passenger vehicle accelerations [142, 143]), and the levels for δ being 2, 4, and 6. The EE results of this experiment were regressed onto the values for a , b , and δ and interaction terms and the results are presented in Table 3.4.

Table 3.4: EE Regression Results for IDM Parameters

coef	value	std err	t	$P > t $
Intercept	143.6204	0.664	216.293	0.000
a	-1.6560	0.514	-3.220	0.005
b	-1.6921	0.514	-3.290	0.004
$a : b$	0.3316	0.398	0.832	0.416
δ	-1.6026	0.514	-3.116	0.006
$a : \delta$	-0.4282	0.398	-1.075	0.296
$b : \delta$	-0.0932	0.398	-0.234	0.817
$a : b : \delta$	0.0664	0.309	0.215	0.832

The results of the regression analysis indicated that a , b , and δ were significant terms which negatively effected EE while none of the interaction terms were significant. Thus, values for a , b , and δ can be set independently. Several papers propose methods for setting these values or the values themselves. In literature the default value for δ is given as 4 [91, 144–146] and there is reason to hold this assumption as valid. NREL produced a report in 2021 [147] which extracted 39,000 individual driving features (acceleration-from-stop, deceleration-to-stop, and cruise events) from collected driving data and fit IDM parameters to the data. Although the IDM model used by NREL is slightly differently formulated than in this paper, the results are, nevertheless, informative. NREL found clusters for δ at .88, 1.40, 1.75, 2.13, and 4.78, ultimately the paper recommends a

value of 4 for δ . Setting values for a and b was also based on literature where default values are generally given as 5 m/s² for both. The authors did not see any reason to deviate from these established values.

3.7.2 Optimal Control

All optimal control solver methods address the following problem,

$$\min_{\bar{U}} J(S_0, \bar{U}) \quad (3.9)$$

where

$$J(S_0, \bar{U}) = \Phi(S_N) + \sum_{k=1}^N \Psi(S_k, U_k) \quad (3.10)$$

s.t.

$$S_{k+1} = f(S_k, U_k), \quad k = 0, \dots, N-1 \quad (3.11)$$

$$B_L(t) \leq S(t) \leq B_U(t) \quad (3.12)$$

where $\Psi(\bar{S}, \bar{U})$ is the running cost, $\Phi(\bar{S})$ is the final state cost, $\bar{S} = [x, v]^\top$ is the state vector containing the problem states position and velocity, $\bar{S}_0 = [x_0, v_0]^\top$ is the initial values of the state vector, $\bar{U} = [a]$ is the control vector containing the control acceleration, J is the cost for S and U , and B_L and B_U are vectors containing the constraints as described in section 3.6. The overline indicates an array containing values at multiple discrete time intervals. The goal of the optimization is to find the optimal Eco-Driving trace (\bar{U}^*) such that J^* is equal to the global minimum value for J .

The cost J is evaluated one of three ways. It is common in literature for the cost function for an Eco-Driving optimization to be entirely based on acceleration. The case for using an acceleration based cost function is made in several articles [148–150]. Nevertheless, the authors determined to consider progressively less abstracted cost functions as well. The cost functions were also designed to be able to compute quickly and to be calculable for both long traces and for single

time steps. The cost functions used are specified below.

Cost Functions

Acceleration l^2 Norm (AL2N) Cost Function

The Acceleration l^2 Norm (AL2N) cost function is simply the square of the l^2 Norm of acceleration sequence. It is given by

$$J_{AL2N}(\bar{U}) = \sum_{k=1}^N a_k^2 \quad (3.13)$$

Note that minimizing the l^2 Norm squared is equivalent (gives the same acceleration sequence) as minimizing the l^2 Norm but is computationally advantageous as it does not require the computation of square roots.

Road Power Cost (RPC) Cost Function

The Road Power Cost (RPC) cost function is based on the road loads ABC formula [151] multiplied by velocity to return power. This cost function takes into account the impacts of viscous and aerodynamic drag in addition to acceleration, and is given by

$$J_{RPC}(\bar{S}, \bar{U}) = \sum_{k=1}^N [Av_k + Bv_k^2 + Cv_k^3 + ma_k v_k] \quad (3.14)$$

where A , B , and C are the coefficients of the road loads equation and m is the vehicle mass. For FASTSim vehicles, the road loads coefficients are not provided and hence were chosen as $A = 0$, $B = C_{RR}$, and $C = \rho F C_D$ with C_{RR} being the coefficient of rolling resistance, ρ being the density of air, F being the vehicle frontal area, and C_D being the vehicle coefficient of aerodynamic drag.

One of important aspects of AL2N and RPC cost functions is their independence of powertrain model. An approach related to RPC has been studied in [152] under the name wheel power minimization.

Battery Power Cost (BPC) Cost Function

The Battery Power Cost (BPC) cost function is an extension of the RPC cost function which accounts for the efficiency of the motor/inverter based on power requirements. This calculation is a simplified facsimile of the FASTSim model and requires powertrain modeling details. The BPC cost is calculated as follows:

$$J_{BPC}(\bar{S}, \bar{U}) = \sum_{k=1}^N \eta_k(v_k, a_k) P_R(v_k, a_k) \quad (3.15)$$

$$P_R(v_k, a_k) = Av_k + Bv_k^2 + Cv_k^3 + ma_k v_k \quad (3.16)$$

$$\eta_k(v_k, a_k) = \begin{cases} \eta_T^{-1} \eta_{M/I}^{-1}(P_R(v_k, a_k)) & P_R \geq 0 \\ \eta_T \eta_{M/I}(P_R(v_k, a_k)) & P_R < 0 \end{cases} \quad (3.17)$$

The transmission efficiency term η_T is a constant and the motor/inverter efficiency term $\eta_{M/I}$ is calculated by interpolating using the FASTSim motor efficiency curve. It should be noted that BPC requires more component specific information as well as interpolation and, thus, may be more difficult to implement and will require more computational time.

Summary

The three different cost functions reflect three different approaches to optimizing EE. A comparison of the cost function values for a 2015 Kia Soul EV is shown in Figure 3.3.

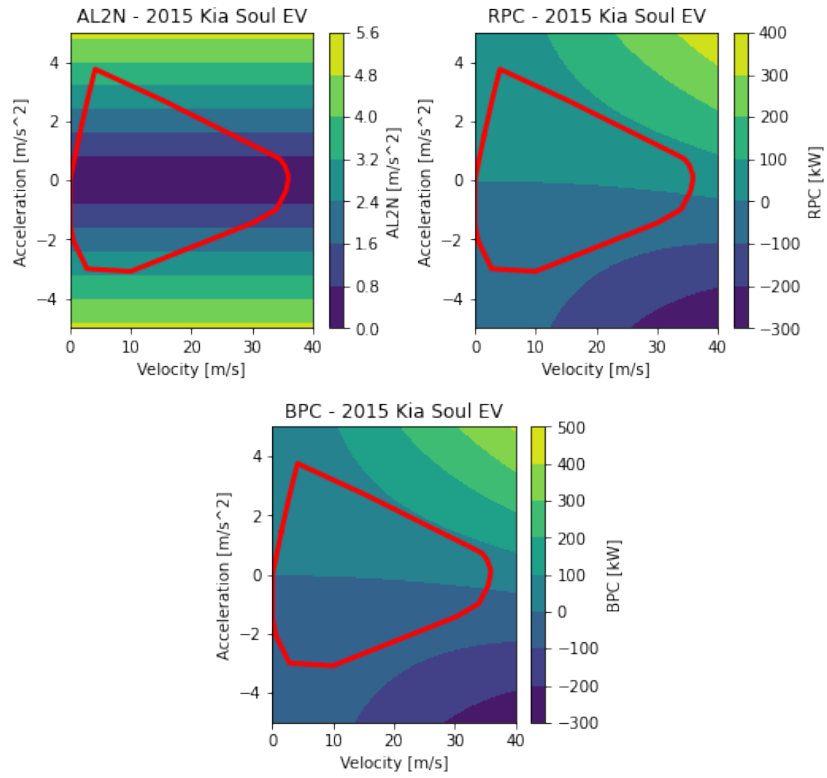


Figure 3.3: Comparison of cost function values for 2015 Kia Soul EV. Red polygon outlines the operational envelope of the UDDS, US06, and HWFET EPA dynamometer drive cycles and is shown as reference for common driving conditions.

Note that the velocity sensitive cost functions RPC and BPC have similar contour plots but both differ significantly from the AL2N cost function.

Optimizers

2 State Dynamic Programming (2SDP)

DP is a well known and commonly used optimal control method. The principle advantage of DP is that it guarantees a globally optimal solution subject to the chosen discretization. The primary disadvantage of DP is that it will generally require significantly greater computational time and effort than other methods and heuristics. In the case of Eco-Driving control, which is a 2 state 1 control non-linear optimization problem with time varying constraints, 2 State Dynamic Programming (2SDP) is a natural choice and it appears in literature in multiple forms as described in Section 3.4. The dynamics of the problem in discrete-time are represented by

$$v_{k+1} = v_k + u_k \Delta t \quad (3.18)$$

$$x_{k+1} = x_k + v_k \Delta t \quad (3.19)$$

The boundary violation cost function J_{PC} is shown in equation (3.20), where the path constraints in x were enforced by a squared error penalty function. The boundary violation cost is added to the running cost $\Psi(S_k, U_k)$ at each time-step.

$$J_{PC}(S_k, U_k) + \begin{cases} \beta_x(x_k - B_{L,k})^2 & x_k < B_{L,k} \\ 0 & B_{L,k} \leq x_k \leq B_{U,k} \\ \beta_x(x_k - B_{U,k})^2 & x_k > B_{U,k} \end{cases} + \begin{cases} \beta_v(v_k - 0)^2 & v_k < 0 \\ 0 & 0 \leq v_k \leq S_{L,k} \\ \beta_v(v_k - S_{L,k})^2 & v_k > S_{L,k} \end{cases} \quad (3.20)$$

where $B_{L,k} = B_L(t_k)$, $B_{U,k} = B_U(t_k)$, and $S_{L,k} = S_L(t_k)$. The final state cost function is

$$\Phi(S_N) = \beta_{FS}(x_N - x_{target})^2 \quad (3.21)$$

where x_{target} is the desired ending position and β_{FS} is a tuned parameter.

Spline Non-Linear Programming (SNLP)

A second common method to solve time-varying controls problems is via direct transcription [153] wherein a problem in continuous time is transcribed to the time domain and solved at discrete times. Direct Transcription (DT) significantly increases the dimensionality of a control problem but allows the use of efficient methods such as IPOPT and SLSQP for linear and non-linear problems [154–156]. The dynamics of the problem are represented by

$$\bar{v}_{k+1} = \bar{v}_k + \bar{u}_k \Delta t \quad (3.22)$$

$$\bar{x}_{k+1} = \bar{x}_k + \bar{v}_k \Delta t \quad (3.23)$$

The running cost and final state cost functions are the same as that for 2SDP and are shown in equations (3.20) and (3.21) respectively.

An issue with using IPOPT to solve discrete-time optimal control problems is that the run-time required scales exponentially with the length of the state vector [157]. In order to avoid using extremely high levels of discretization it is common to use polynomial interpolation between more distant optimization points. The authors chose to define trajectories using Piecewise Cubic Hermitic Interpolation Polynomial (PCHIP) splines with knots placed at those points in time where the upper or lower boundaries change. The trajectories are defined as

$$\bar{S} = PCHIP(\bar{\epsilon}, \bar{t}_{knots}, \bar{B}_{L,knots}, \bar{B}_{U,knots}, \bar{t}) \quad (3.24)$$

where $\bar{\epsilon}$ are the locations of the vehicle at the knot times (\bar{t}_{knots}) relative to the boundaries at the knot times ($\bar{B}_{L,knots}$ and $\bar{B}_{U,knots}$), and \bar{t} is the discrete time vector for the problem.

Spline Genetic Algorithm (SGA)

The first metaheuristic method discussed is the Spline Genetic Algorithm (SGA). For this study, the phenotypes optimized are ϵ vectors. The initial population is generated randomly with an initial guess inserted in place of one randomly generated phenotype. The GA method used employs sorted selection wherein the best phenotypes are selected for crossover and random mutation wherein a certain percentage of the total chromosomes from all phenotypes are changed to a random number each step. The method also employs elitist carry-over wherein the best phenotype is kept for the next step un-changed. The dynamics and cost function for SGA are identical to those for Spline Non-Linear Programming (SNLP). GA is inherently parallelizable and scalable meaning that it is well suited to modern parallel computing and may benefit significantly in terms of run-time from such an implementation.

Spline Partical Swarm Optimization (SPSO)

The second heuristic method used is Spline Particle Swarm Optimization (SPSO) which uses the PSO heuristic to optimize a positional spline trajectory. In this study, the particles used are ϵ vectors for a given set of boundaries and the trace in distance and velocity is computed as in equation (3.24). PSO is a quasi-Newton method as it applies a modified gradient search but does so with many particles simultaneously. The particle position and velocity update equations for PSO are given as

$$\bar{\epsilon}_{k+1} = \bar{\epsilon}_k + \bar{V}_k \quad (3.25)$$

$$\bar{V}_{k+1} = w\bar{V}_k + c_1r_1(\bar{\epsilon}_{best,p,k} - \bar{\epsilon}_k) + c_2r_2(\epsilon_{best,g,k} - \bar{\epsilon}_k) \quad (3.26)$$

where \bar{V} is the vector of particle n-dimensional velocities, w is the momentum term which sets the weight of the current velocity, c_1 and c_2 are the local and global position weights, r_1 and r_2 are random weights assigned to the local and global terms, $\bar{\epsilon}_{best,p}$ is a vector of the best solutions found by each particle, and $\epsilon_{best,g}$ is the global best solution found by any of the particles. In this study a mutation step was added to the PSO solver in order to enable faster convergence [135] with the mutation step functioning similarly to how it functions in the SGA method. Like the GA, PSO is inherently parallelizable and scalable making it well suited for a parallel implementation.

3.8 Subsystem 3: Plant

For this study a 2015 Kia Soul EV was selected as the vehicle of interest. This particular EV was selected because dynamometer data for it is available from ANL's Downloadable Dynamometer Database (D³) [80] and because the research group owns a drive-by-wire capable physical vehicle for future studies. For vehicle simulation NREL's FASTSim [141] was selected. FASTSim is an efficient, accurate, and robust 1-dimensional vehicle simulation which is commonly

used in research. Construction of the FASTSim Kia Soul EV model was done using a combination of publicly available data, common FASTSim validated model parameters [158], and tuned model parameters. The model parameters are shown in Table 3.5.

Table 3.5: Kia Soul EV FASTSim Model Parameters

Parameter	Value	Units	Source
Mass	1664	kg	ANL D ³ test data sheet [80]
Frontal Area	2.87	m	Public information [159]
Coefficient of Drag (C_D)	.35	N/A	Public information [159]
Coefficient of Rolling Resistance (C_{RR})	.0188	N/A	Tuned parameter
Maximum Battery Storage	25.5	kWh	Tuned Parameter
Wheelbase	2.57	m	Public information [159]
Max Motor Power	81	kW	Public information [159]

The two tuned parameters, C_{RR} and Maximum Battery Storage, were tuned from assumed values in order to best match the battery State of Charge (SOC) and battery power traces from the D³ data. After tuning the data, the 2015 Kia Soul EV FASTSim model was able to match the D³ data to within 0.2% in terms of energy consumption while closely matching the SOC and battery power traces with mean absolute percentage error values of 0.763% and 1.552%¹. The vehicle plant will add uncertainty to the optimization in the forms of sensor noise and actuator error. Neither of these is modeled in FASTSim. However the FASTSim vehicles have a limited ability to follow traces subject to powertrain parameters. Thus, the robustness of the solvers, in terms of ability to produce feasible traces was reflected in the results.

3.9 Results

Each optimal Eco-Driving trace generation method was evaluated in terms of the following two criteria:

¹Zero-valued points omitted

1. Ability to produce energy efficient solution traces
2. Ability to produce solutions within acceptable levels of run-time

The authors evaluated the performance of the methods in generating optimal Eco-Driving traces for 5 minute driving trajectories. Longer time horizons allow for the solvers to improve over baseline to a greater degree but also increase the optimization space for the solvers leading to rapid growth in run-times. The 5 minute time horizon was picked as a sufficient compromise. Although ultimately, any on-board implementation must be receding horizon based to account for changing information in real-time, this paper is only concerned with the efficacy of solver methods for single evaluations.

The purpose of this study was, specifically, to compare the relative merits of several optimal Eco-Driving trace methods found in literature. Consequently, the scope was limited. The authors assumed that optimal Eco-Driving trace generation is one step in an optimal Eco-Driving control algorithm which operates in a receding-horizon manner and that this algorithm comprises the upper level of a two level controller with the lower level being responsible for the instantaneous control of the vehicle. This conception of an optimal Eco-Driving control framework is consistent with the literature as described in Section 3.4.

3.9.1 Optimal Solver Results

EE Improvement

A standard experiment was run for evaluation of the methods with respect to the solver and cost function. This experiment was a full-factorial design in which each solver was evaluated for 100 pre-defined boundaries cases and with each cost function. These pre-defined cases were defined by a selection of random starting times and locations on the phase map as shown in 3.6. The decision to run 100 cases per combination was made in order to allow for the use of large sample statistics.

The results of the experiment in terms of EE improvement over baseline and in terms of cost function reduction over baseline are shown in Figures 3.4 and 3.5.

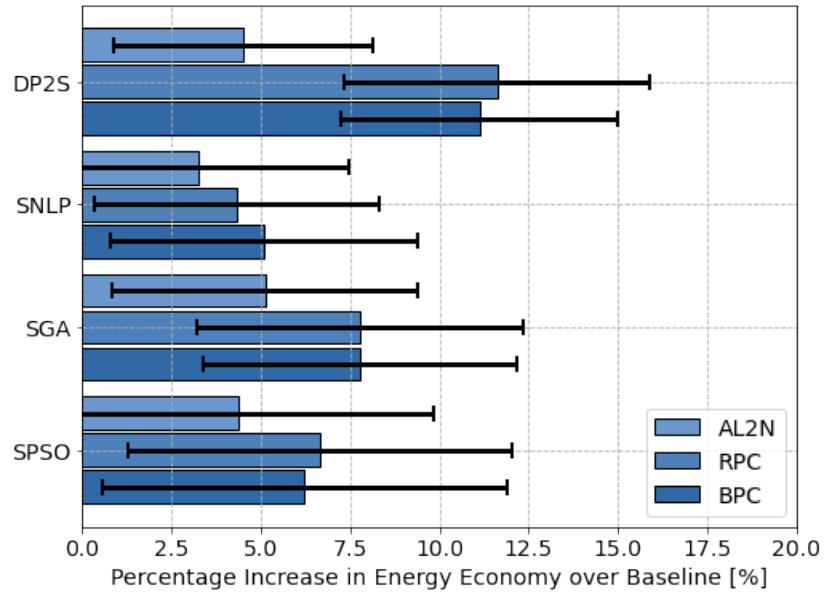


Figure 3.4: Mean and standard deviation of EE improvement over baseline results for all methods and cost functions

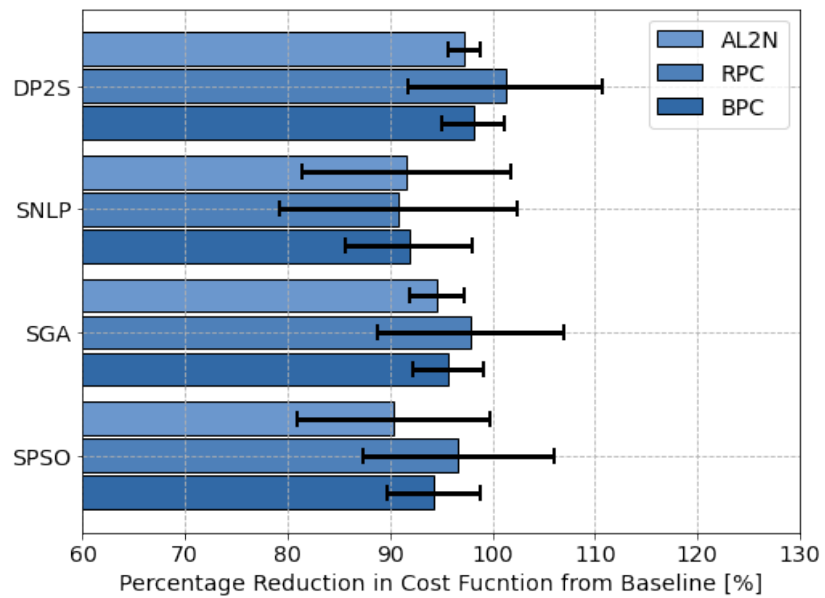


Figure 3.5: Mean and standard deviation of cost function reduction over baseline results for all methods and cost functions

From Figures 3.4 and 3.5 a definitive order is visible in the relative performances of the methods in relation to EE improvement and cost function reduction. Readers will observe that the cost function reduction exceeded 100% on a recurring basis for the RPC and BPC cost functions. The ability of the RPC and BPC cost functions to be reduced by greater than 100% is reflective of the regeneration potential over a given drive cycle for those cost functions and is an artifact of the particular boundary conditions used in the experiments. All optimal Eco-Driving traces in the experiment start at 15.65 m/s (35 mph) which is the speed limit of the 4 streets used for data collection but optimal Eco-Driving traces were not required to match this speed at the end of the drive cycle. Thus, it was possible for the energy regenerated over the course of the drive cycle to exceed the energy spent. Generally, the ranges seen for EE improvement as a percentage of the mean were quite large in comparison to the same for cost function improvement and this is the result of the low correlations between cost function improvement and EE improvement for all methods and cost functions. Correlations between cost function improvement and EE improvement are shown for all cost functions in Figure 3.6.

Correlation between cost function improvement and EE improvement was shown to be best for BPC then RPC; in both cases the correlation was significantly better than for AL2N. This is attributed to models in BPC and RPC providing closer match to the model in FASTSim. Due to the large uncertainties regarding the EE improvement results, the significance of the observed differences in effectiveness could not be assumed and thus T-tests were conducted between all combinations of method and cost function and the results are presented in Figure 3.7.

Results shown in Figures 3.4 and 3.7 indicate that the best performing method in terms of improving EE was 2SDP followed by the heuristic methods and finally SNLP. The same results indicate that the velocity sensitive cost functions enable better solutions to be found than AL2N. Neither result is surprising, only DP should be able to find globally optimal solutions and more information should lead to a better solution.

Finally, it should be added that by reducing the acceleration and braking limits by a factor of 10 to 0.5 m/s², the IDM method was able to produce a mean improvement of 5.51% with a standard

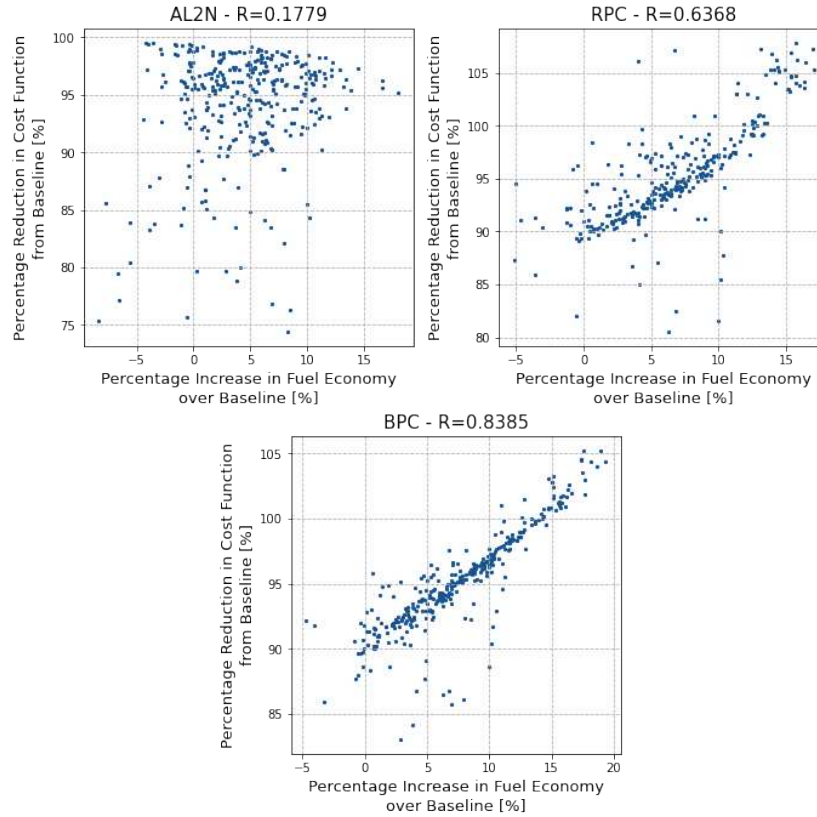


Figure 3.6: Correlation between cost function reduction and EE improvement for all cost functions

Method		2SDP	SNLP	SGA	SPSO	2SDP	SNLP	SGA	SPSO	2SDP	SNLP	SGA	SPSO
	Cost Function	AL2N	AL2N	AL2N	AL2N	RPC	RPC	RPC	RPC	BPC	BPC	BPC	BPC
2SDP	AL2N		0.039	0.159	0.925	0.000	0.995	0.000	0.000	0.000	0.148	0.000	0.005
SNLP	AL2N	0.039		0.001	0.104	0.000	0.053	0.000	0.000	0.000	0.001	0.000	0.000
SGA	AL2N	0.159	0.001		0.214	0.000	0.193	0.000	0.019	0.000	0.897	0.000	0.104
SPSO	AL2N	0.925	0.104	0.214		0.000	0.925	0.000	0.002	0.000	0.195	0.000	0.012
2SDP	RPC	0.000	0.000	0.000	0.000		0.000	0.000	0.000	0.428	0.000	0.000	0.000
SNLP	RPC	0.995	0.053	0.193	0.925	0.000		0.000	0.001	0.000	0.177	0.000	0.008
SGA	RPC	0.000	0.000	0.000	0.000	0.000	0.000		0.046	0.000	0.000	0.963	0.011
SPSO	RPC	0.000	0.000	0.019	0.002	0.000	0.001	0.046		0.000	0.033	0.040	0.559
2SDP	BPC	0.000	0.000	0.000	0.000	0.428	0.000	0.000	0.000		0.000	0.000	0.000
SNLP	BPC	0.148	0.001	0.897	0.195	0.000	0.177	0.000	0.033	0.000		0.000	0.149
SGA	BPC	0.000	0.000	0.000	0.000	0.000	0.000	0.963	0.040	0.000	0.000		0.009
SPSO	BPC	0.005	0.000	0.104	0.012	0.000	0.008	0.011	0.559	0.000	0.149	0.009	

Figure 3.7: Significance of comparative results (P-values), purple indicates that the column significantly outperformed the row, blue indicates that the row significantly outperformed the column, green indicates the difference between the row and column was insignificant at 95% confidence

deviation of 2.79%, comparable to the results from the SPSO method. The IDM method was omitted from the comparison as it cannot be made to meet the end position constraint and, thus, achieved better EE by reducing average speed thus rendering the results not directly comparable.

Computational Load

All methods for this study were implemented in Python 3 with the NumPy and Scipy libraries. All solvers were run-time optimized in Python and all are vectorized to the highest degree possible in order to minimize run-time [160]. Nevertheless, a specific outcome of the Python implementation is that Python has very limited parallel processing capability [161] which means that the authors were not able to experiment on the impacts of parallel processing on run-time for the SGA and SPSO methods. The computer used for simulation contained an AMD Ryzen 7 3700x 8-core multi-threading capable CPU with 16 gigabytes of RAM running the 64 bit Ubuntu 18.04 LTS operating system with Python 3.8. All simulations were conducted on the same computer to ensure the integrity of relative run-times. Even though Python is unlikely to be used for onboard implementation, the computational time results are of interest for the relative comparison of different methods in terms of computational time required. Figure 3.8 shows the relative run-times for each method and cost function.

An immediate conclusion is that the 2SDP method is not competitive with the other methods as a real-time control due to its large run-time requirement. Implementation specifics play a huge part in determining run-time and it is possible to significantly reduce the run-time requirements for the 2SDP method by changing hardware and language but these changes would also benefit the other methods and the relative gap should remain on the same order of magnitude. The authors did not find a single paper in the literature which implemented a 2SDP method in real time. The closest examples would be [112, 114], in which a DP solver is used as the higher level in a 2 level receding-horizon controller but the DP algorithm takes multiple seconds to produce a novel solution, and [106] which implements a real-time ADP solver.

It is also evident that the SGA method is the quickest to execute and could be made to execute in even less time with the use of parallel processing, with the same being true for SPSO. Current

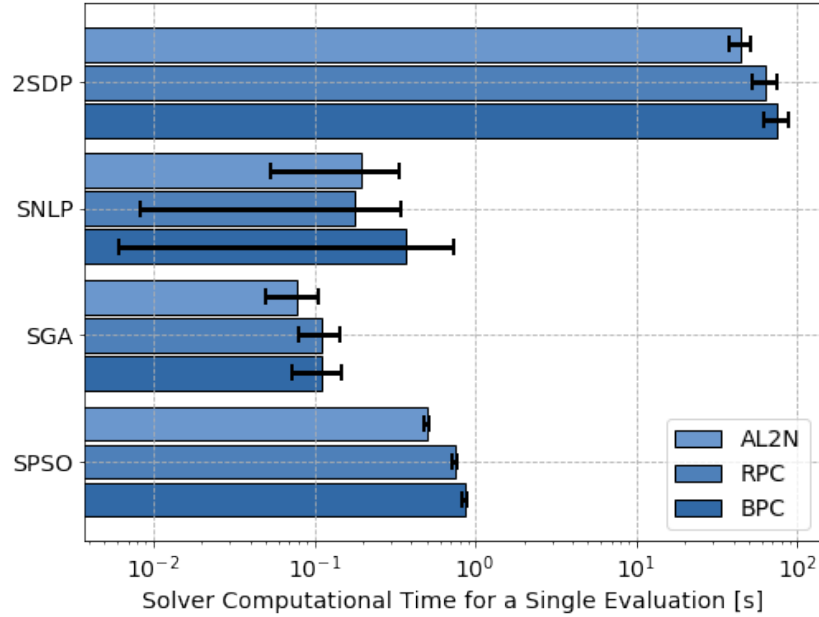


Figure 3.8: Mean and standard deviations of run-times for all methods and cost functions

vehicular compute systems differ in architecture from desktop computers although this may soon change [162]. Implementation on automotive controllers may result in different relative run-times but these differences should not be enough to overcome the orders of magnitude run-time differences seen in this study.

3.9.2 Eco-Driving Traces

The differences in EE improvement reflect visual differences in optimal Eco-Driving trace traces. A representative example is shown in Figure 3.9 and 3.10 for all methods and cost functions with one set of constraints.

In general, the optimal Eco-Driving traces improve over the baseline traces primarily by minimizing the speed reduction due to traffic signals. There are many local optima in the results space and many are very similar to the global optimum thus the non-DP methods are most likely to settle on a local optimum. However these local optima clearly approximate the global optimum. The optimal traces for the AL2N cost function are visually distinct from those generated using the speed sensitive cost functions. While the AL2N cost function is only sensitive to absolute

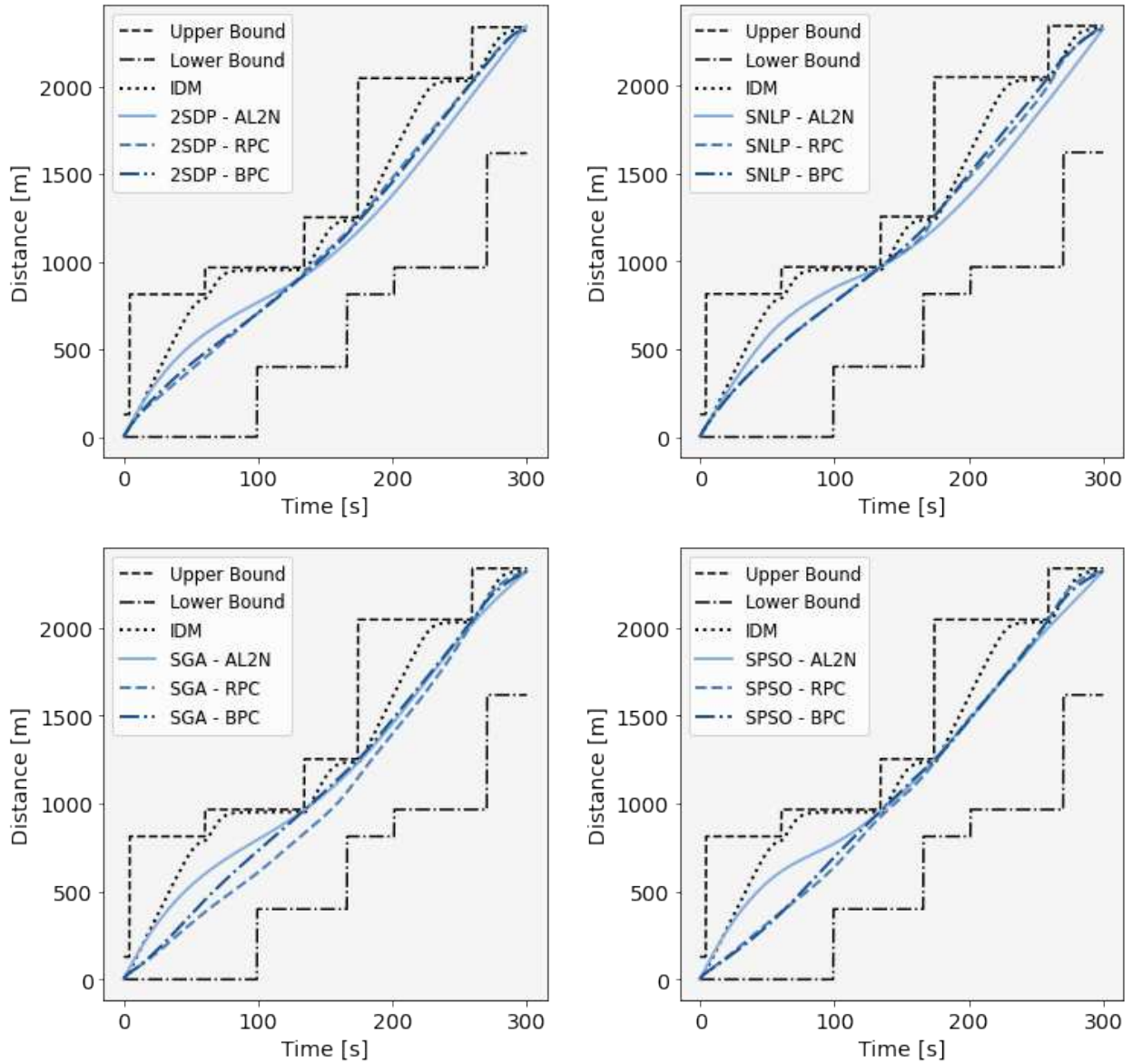


Figure 3.9: Example position vs. time traces for all methods and cost functions

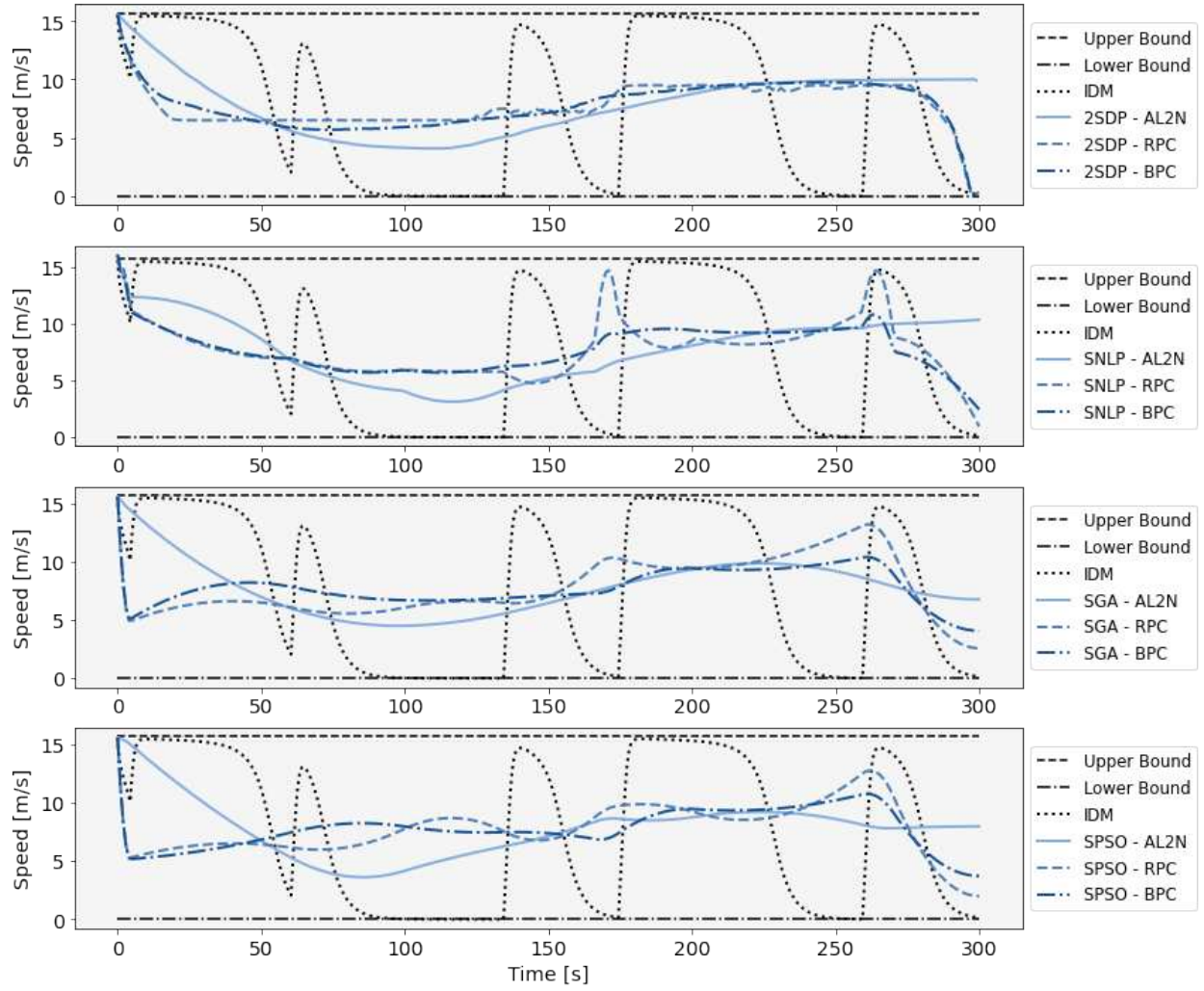


Figure 3.10: Example velocity vs. time traces for all methods and cost functions

acceleration, the speed sensitive cost functions are sensitive to directional acceleration as well as proportional to speed, speed squared and speed cubed. The result is that the speed sensitive cost functions will tend to reduce maximum speed and encourage deceleration to a greater degree than AL2N. When compared to the literature, traces seen in this study, are more jerky. There are two reasons for this. First, the constraints used in this study are more complex than those used in most of the literature being time-varying and in distance and speed. The second is that no explicit proxy for passenger comfort was added to the cost function. The velocity sensitive cost functions resulted in traces with lower speeds and higher decelerations which would, no doubt, be less comfortable for passengers.

Non-optimal methods may also be used to generate Eco-Driving traces. Four optimal methods for generating optimal Eco-Driving traces were compared to IDM where IDM parameters used were chosen to be representative of normal driving behavior. IDM parameters can also be chosen to result in improved EE. The IDM acceleration parameters and aggression parameter were shown to have large and significant effects on EE in Section 3.7. By reducing the allowed accelerations by a factor of 10 to 0.5 m/s^2 , a mean EE improvement of around 5% was attained. An EE improvement of 5% is on the low end of what was attained with the optimal methods. IDM is a low cost algorithm which requires no look-ahead information making it much easier to implement than the optimal methods. There are, however, advantages of the optimal methods over non-optimal methods regardless how the non-optimal methods are applied. Optimal control allows for a degree of performance and flexibility that non-optimal control does not. The boundary conditions used for all optimal methods used in this study required that the vehicle arrive at a given distance at a given time thus maintaining a precise average speed. The solvers were able to still produce significantly more efficient traces than baseline. Low acceleration IDM, by contrast, cannot meet the same final condition and was able to improve over baseline principally by traveling at a lower mean speed. In generating optimal Eco-Driving traces there is a balance between maximizing EE and limiting travel time. In this study the travel-time aspect was removed from consideration by applying a strict final condition but all optimal control methods presented could be modified to allow for a

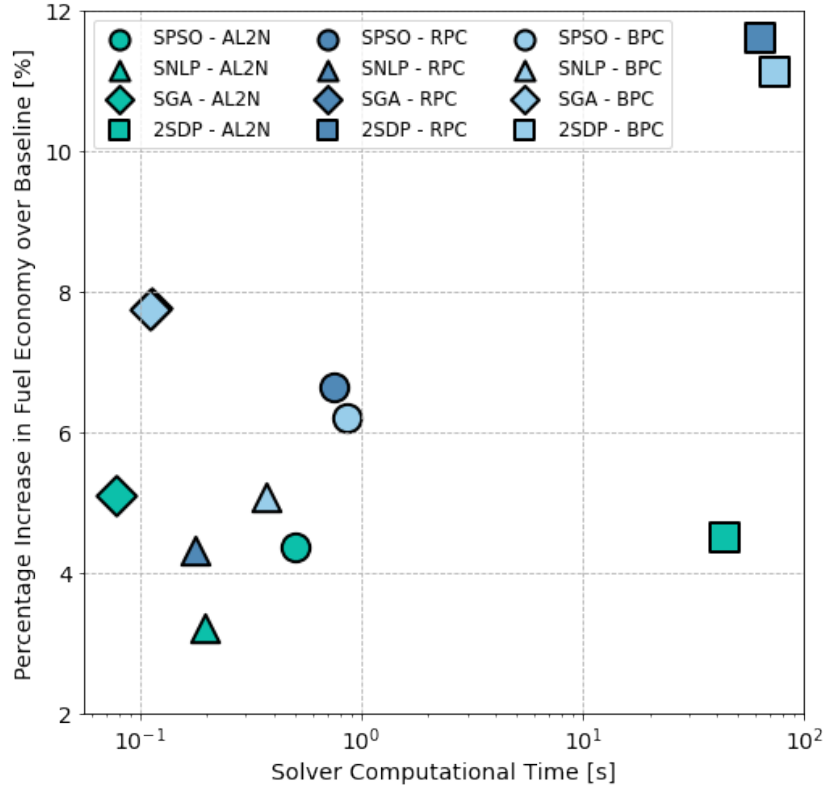


Figure 3.11: comparison of run-time and EE improvement means for all methods and cost functions

precise trade-off between EE and travel time. Thus, while requiring more in terms of increased computational load and look-ahead information, optimal control does enable more precision and flexibility than non-optimal control.

3.9.3 Summary

The mean results for the methods and cost functions are presented for run-time and EE improvement in Figure 3.11. Several observations can be made. The first is that the globally optimal solution produced by 2SDP is usually significantly more efficient than the locally optimal solutions but requires much more run-time. DP can be made to run quicker with partial parallelization [163] but this would not be enough to reduce the run-times to the level of the PTO methods. The literature contains several papers describing the practical implementation of multi-state DP based Eco-Driving control algorithms but these either evaluate the problem on a less than 1 Hz basis or use sub-optimal approximations of the cost-to-go function. DP based optimal

Eco-Driving trace solvers seem unlikely to become the basis of widely available commercial Eco-Driving systems due to the computational cost unless they rely on cloud computing.

Of the PTO solvers implemented, it is clear that the GA based method was most effective in both criteria of evaluation. Visually, the SGA method with the RPC and BPC cost functions occupies a position up and to the right of the general trend line seen in Figure 3.11 indicating a favorable performance in both criteria. One reason for this is that the specifics of the optimal Eco-Driving trace generation problem, as defined in this study, lend to the strengths of the GA which can explore complex optimization spaces quickly and efficiently by exploring many directions simultaneously and removing poor solutions from the selection pool. PSO also explores many solutions simultaneously but those particles which are seeded in low reward regions have to gradually approach better solutions.

The specifics of the optimal Eco-Driving trace problem as posed in this study did not favor the SNLP or SPSO methods. At their cores IPOPT and PSO are gradient search algorithms, extensions of Newton's method, and require the computation of a gradient at each optimization step. With nonlinearity caused by the interpolation polynomials and the non-convexity of the constraints, such gradient search methods were less effective. It is not surprising that the SGA method was found to be the best of the type.

Another observation from Figure 3.11 is the benefit of additional information to solvers in generating the optimal Eco-Driving trace. In literature it is common to see minimization of acceleration used as a proxy for maximization of EE. This trend of acceleration minimization is also very common in robotics control literature and, as many concepts in CAV control arise from robotics it is easy to see the origins of the assumption. The assumption that acceleration minimization is a valid proxy for EE optimization is stated explicitly in several well cited papers [148, 149]. A main reason for the use the l^2 norm of acceleration for a cost function is that it is independent of vehicle and powertrain parameters and the optimization can be reduced to a conventional quadratic programming problem. The outcomes of this study indicate that cost functions which incorporated more information about the vehicle such as velocity, aerodynamic

characteristics, rolling resistance, and powertrain efficiencies enabled optimizers to achieve higher EE for electric vehicles assuming perfect preview of the constraints. Note that the velocity sensitive cost functions in this study require minimal additional time to compute compared to the l^2 norm of acceleration.

3.10 Discussion

3.10.1 Problem Complexity

One solution not considered thus far for the optimal Eco-Driving problem is a brute force solution. It would be logical to assume that random seeding could provide a possible method for solving PTO problems. As will be demonstrated, the non-linearity and non-convexity of the PTO optimal Eco-Driving problem render brute force methods infeasible as solvers. Consider the polynomial trajectory shown in Figure 3.12.

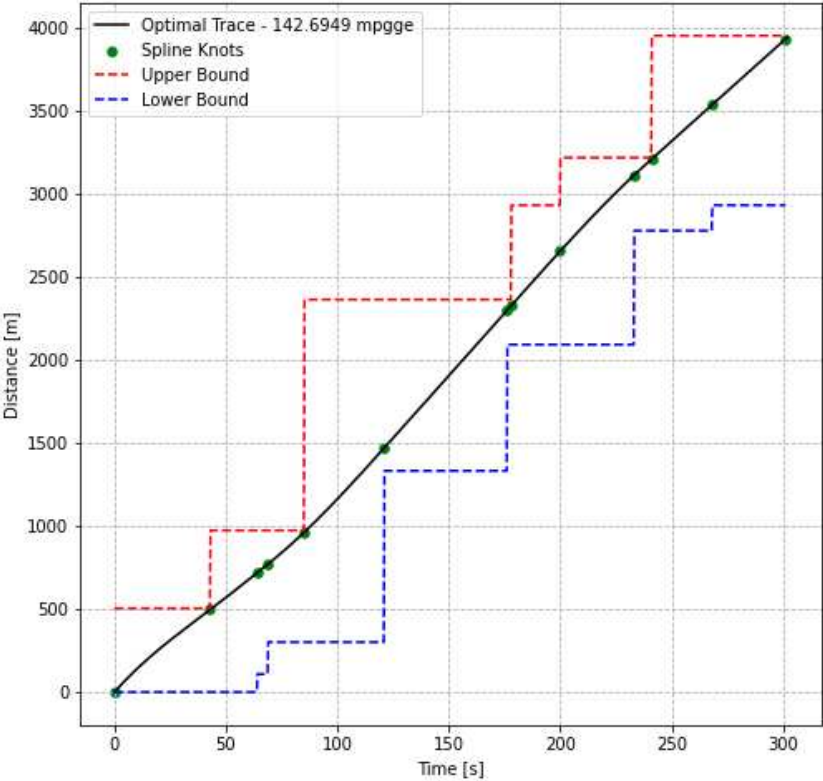


Figure 3.12: Example polynomial trajectory defined by knots

The trajectory in Figure 3.12 runs for 300 seconds but is defined by only 13 knot points. The optimization space is further reduced to 11 dimensions because the first and last knots are fixed in distance by the problem initial and final conditions. The knots are located at points where the upper or lower bounds change allowing for the spline to be defined by the minimum number of knots. Lower numbers of knots means lower problem dimensionality and faster solutions. The use of polynomial trajectories introduces nonlinearity. Because the problem states (position, velocity, and acceleration) at the boundaries of each segment (the knot points) must be equal for cubic splines, the shape of each segment is a function of all knot locations in the spline. Each segment is most influenced by the knots which terminate and those knots closest to the segment have greater influence but all knots have some influence. The reason that the optimal Eco-Driving problem is so complex has to do with how the spline interacts with the non-convex boundary conditions. Moving the knot points in distance can easily result in a trajectory that violates the boundary conditions even if the knot point remains within the position boundaries. The likelihood of intermediate points violating bounds decreases with knot frequency but violations remain possible. For optimal Eco-Driving with PTO methods finding a feasible solution is non-trivial.

3.10.2 Ineffectiveness of Brute Force Solver Methods

Using the boundaries from Figure 3.12 once again as an example, brute force solver methods can be trialed. The brute force concept would be to seed the space with a large number of possible solutions and then evaluate all of the solutions and pick the lowest cost solution. Using random seeding, a given number of random traces can be generated. One should note that this is how the initial populations for GA and PSO are created. If a good solution can be found by simply generating a huge initial population the metaheuristics may be unnecessary. The performance of the random seeding method is summarized in Table 3.6.

Table 3.6: Performance of Random Seeding Method

Number of Traces	Best Trace Cost	Number of Allowable Traces	Run-time
5,000	2.757e53	0	0.058
10,000	1.701e53	0	0.127
50,000	1.121e53	0	0.691
500,000	4.117e52	0	8.365

The main issue presented is that there is no guarantee of even a single valid trace being generated by the random seeding, in fact it is often the case that not a single valid trace is generated even among 500,000 traces. The size of the population must be 5,000 and 10,000 in order to execute in a comparable amount of time as the SGA method which will produce a valid trace in more than 99% of instances. It can be concluded that brute force methods are not viable solvers for the optimal Eco-Driving Trace generation problem.

3.10.3 Difficulties Experienced by Gradient Descent Methods

One of the salient findings of this study is the relative performance between the PTO methods with GA having performed best. As mentioned previously, gradient descent solvers which include IPOPT and PSO struggle due to the difficulty of computing gradients which derives from the nonlinearity of the polynomial and the non-convexity of the boundaries. this difficulty is illustrated in Figure 3.13.

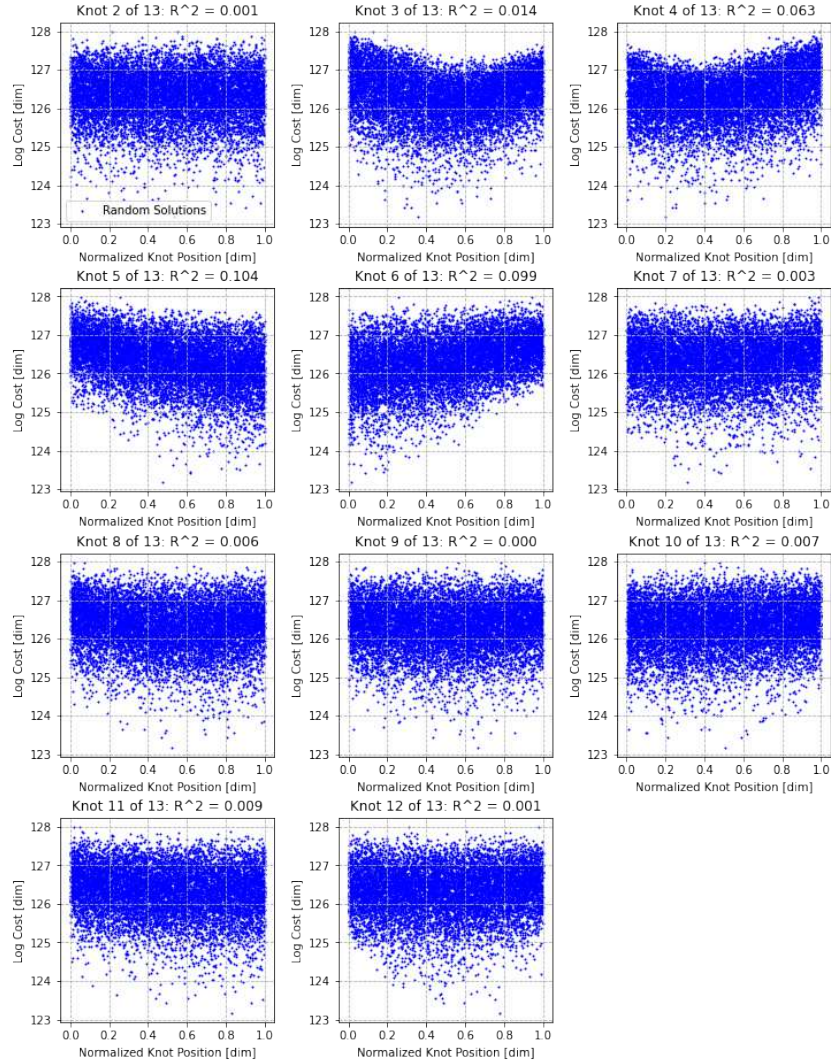


Figure 3.13: Knot location vs. trajectory cost for non-fixed knots

As can be seen in Figure 3.13, there is no strong determinative relationship between knot location and trace cost for any of the knots. This reflects the complexity of the problem. Because the locations of all knots interact so heavily to determine trajectory cost, it is quite difficult to find a discernible relationship between location and score for a single knot. The implication of this complexity is that gradient search methods which rely on the numerical computation of Jacobians and Hessians at every stage might struggle to converge on a good solution. This is exactly the type of complex optimization environment to which the GA is well suited [128, 129]. As seen in Figure

3.14, the GA is able to start from a random seed and then approach and ultimately find a viable solution quickly.

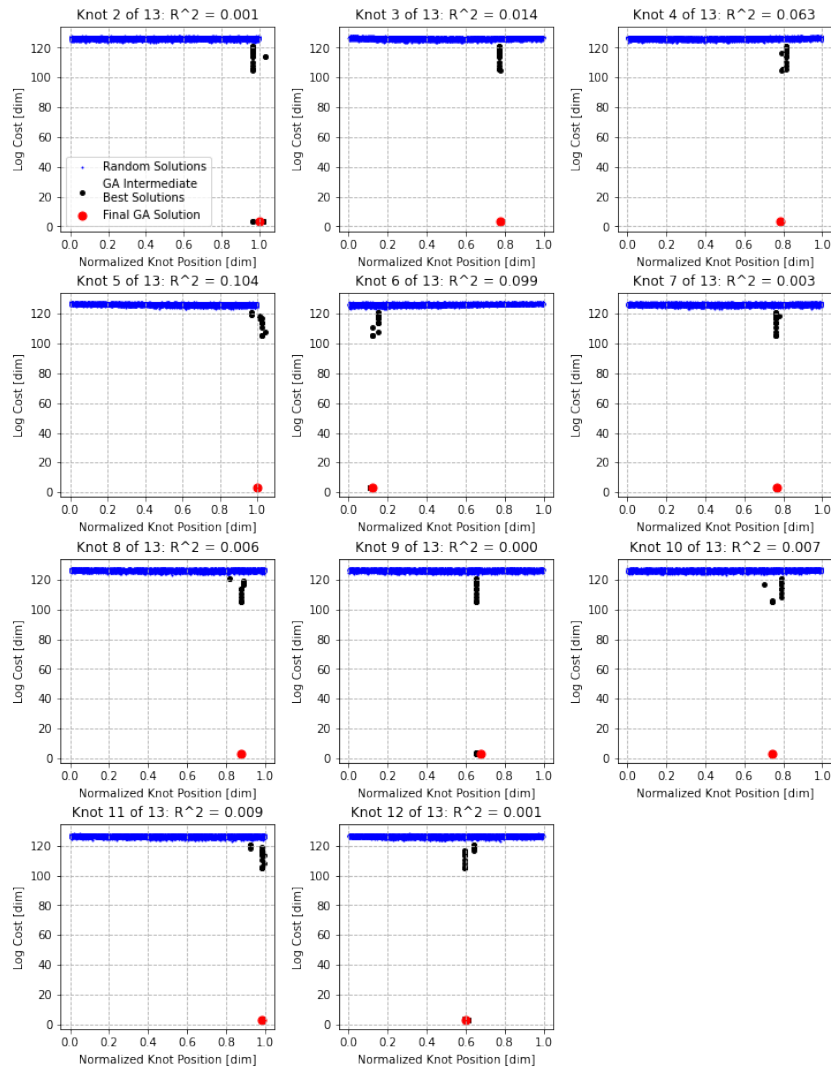


Figure 3.14: Progress of GA solution

For the example in Figure 3.14, the GA solver reached convergence ($1e-20$) at 126 iterations out of an allowed 500. The GA solver required only 9 iterations to find its first viable solution and then optimized in the viable space for the remaining 117 iterations until convergence. These results are typical for the problem and confirm that the GA is naturally well suited to the spline interpretation of the optimal Eco-Driving trace generation problem.

The optimal Eco-Driving trace generation problem is a complex optimization problem because of a combination of methodological factors. In order to reduce the dimensionality of the optimization space and allow for quick convergence on a solution, the trace is often generated using a PTO. The decision to use polynomial trajectories means that the shape of any spline segment is a function of the locations of all knots in the spline and not just the knots which terminate it. This nonlinearity interacts with the non-convex boundary conditions of the optimal Eco-Driving problem to create a complex optimization space which presents difficulty for gradient descent algorithms. These difficulties do not effect the GA and thus favor GA as a solver.

3.11 Conclusions

A great breadth of knowledge on the subject of autonomous Eco-Driving control has been generated by the research community in recent years. As the vehicular and infrastructural technology which enables vehicular autonomous control become ever more widespread, the opportunity to apply this knowledge in production vehicles becomes more realizable. A comprehensive, implementation oriented analysis was performed in order to compare the relative merits of several optimization methods found in literature. A survey of the literature was conducted and four representative optimization methods (two state dynamic programming, and trajectory optimization with IPOPT genetic algorithm, and particle swarm optimization) were implemented and refined for application in simulation with real-world infrastructure data. Numerical simulations were then conducted on these methods using three progressively less abstracted cost functions (l^2 norm of acceleration, road power, and calculated battery power) and each was evaluated relative to the others in terms of performance and run-time. From these simulations, the following conclusions were reached:

1. Minimizing the l^2 norm of acceleration is confirmed to provide EE improvements.
2. Speed sensitive cost functions that reflect vehicle and powertrain characteristics can yield improved EE results over the l^2 norm of acceleration for electric vehicles.

3. DP methods offer the highest potential for EE improvement (in the range of 7% to 15%) but are extremely computationally expensive compared to other methods requiring on the order of 100 to 1000 times as long to execute.
4. GA showed the most potential as a real-time method based on its relatively high performance (5% to 10% EE improvement) in EE optimization and its low computational cost.

Near-future ADAS systems are anticipated to include high performance in-vehicle computers and or embedded hardware which is capable of computing and executing Eco-Driving control. This development will enable the implementation of two-level optimal Eco-Driving control for CAVs. From the selected optimization approaches considered, the results suggest the use of a GA method with a RPC cost function as providing the best trade-off between achievable EE and computational overhead for optimal Eco-Driving trace generation for urban Eco-Driving BEVs.

3.12 Summary

The purpose of research directed towards RQ1 was to determine what energetic benefits could be attained through connected vehicle optimal control. The work in the previous chapter focused on Predictive Optimal Energy Management Strategies (POEMS) for Hybrid Electric Vehicles (HEVs). The work in this chapter focused on optimal Eco-Driving control for Electric Vehicles (EVs). In this chapter it was found that optimal Eco-Driving control can provide a realistic 5% to 10% increase in vehicular efficiency over a baseline control. the work in Chapters 2 and 3 in this dissertation comprehensively answer RQ1.

Chapter 4

Assessment of Factors in the Reduction of BEV operational Inconvenience

4.1 Preface

This chapter is derived from [164] which was primarily authored by this dissertation's author. The content of the paper addresses RQ2.T1, RQ2.T2, and RQ2.T3. RQ2 focused on understanding the relationship between vehicular design and Electric Vehicle Support Infrastructure (EVSE) infrastructure parameters on experienced inconvenience. Because of the physical realities of energy storage and charging, Battery Electric Vehicles (BEVs) require more charging time than Internal Combustion Vehicles (ICVs) do fueling time. Thus, a "gas-station" model of charging is likely unfeasible. However, Electric Vehicle (EV) charging can be conducted, in theory, in any location with access to electricity. Therefore, what charging options are available to BEV users will determine what level of inconvenience is experienced during charging. BEVs range may also play a role in determining operational inconvenience as lower ranges may constrain charging options and force more inconvenient charging events. Regardless, it is necessary to derive a quantitative metric for charging inconvenience and a method for calculating such metric from data in order to understand the aforementioned relationships.

4.2 Overview

As governments and the automotive industry push toward electrification, it becomes increasingly critical to address the broad set of factors influence individual car buying decisions. Evidence suggests that operational inconvenience or the perception thereof plays a large role in consumer decisions concerning BEVs. BEV ownership inconvenience and its causal factors have been relatively understudied, rendering efforts to mitigate the issues insufficiently informed. This

paper presents an empirical equation, derived using a novel data-based method, which relates operational inconvenience to a small number of housing and local EVSE infrastructure factors. The equation and method provided can be used to conduct quantitative analyses on the inconvenience impacts of current and proposed EVSE infrastructure. Ultimately such a quantitative approach is needed to understand and mitigate large inequities of BEV experience and adoption which might emerge from electrification.

4.3 Introduction

Policy makers and industry have recently set ambitious goals for BEV market penetration [4]. These targeted efforts will help accelerate the growth of the BEV market share. The success or failure of these initiatives will depend on millions of individual decisions on whether or not to purchase or lease a BEV. Although economic factors are important in individual car buying decisions, evidence suggests that consumers also weigh perceived operational inconvenience in their decision making process [29–31].

Concerns about BEV operational inconvenience are founded in several realities related to vehicular energizing (charging or fueling) namely BEV range and charging times [165]. BEV ranges are limited by the capabilities of modern batteries. Current state-of-the-art Lithium-Ion (Li-Ion) batteries have a specific energy of around 1000 kJ/kg [166] whereas gasoline has a specific energy of 457,200 kJ/kg. The result of this disparity is that even though BEVs are more efficient than ICVs they often have less range than similarly sized ICVs. Comparing midsize sedans, a 2022 Tesla 3 LR has a nominal range of 490 km and a curb weight of 1919 kg [167] while a 2022 Chevrolet Malibu has a nominal full-tank range of 915 km and a curb weight of 1422 kg [168]. Current BEV full-charge ranges are more than sufficient to meet daily driving requirements for most Americans [169], but their lesser range is perceived by consumers as an inconvenience.

The disparity in energizing times between BEVs and ICVs is also rooted in the fundamental characteristics of energizing. Gasoline contains 121.3 MJ per gallon [170]. At a fueling rate of 7 gallons per minute [171] an ICV is energizing at 14.15 MW. By comparison, modern DC

Fast Charging (DCFC) occurs at 80-350 kW or roughly 40 - 180 times slower than fueling. In combined driving conditions, the 2022 Tesla 3 LR uses roughly 5 times less energy per km than the 2022 Chevrolet Malibu [167, 168] but would still expect to add range 8 times slower. If one were to charge a BEV in the same manner as one fuels an ICV, by going to a dedicated station every time, then the BEV would be much more inconvenient to operate.

Historically, BEV operational inconvenience has not been studied in depth as most BEV owners charge primarily at home [32]. The recent development of public and private charging networks have made long distance BEV travel increasingly feasible [33]. However, as adoption of BEVs increases, and as BEVs penetrate non-luxury auto markets, the assumption that all BEV operators have access to overnight charging will become invalid, and the role of public infrastructure may become more important still.

The importance of public infrastructure for various potential BEV market segments has already been recognized and funding for rapid development of public BEV infrastructure has been a key component of many national and regional BEV readiness plans. [34]. However several key questions remain to be answered:

- What are the ultimate relative operational inconveniences for BEVs vs ICVs for those who can charge at home and those who cannot?
- What are the relative merits of different types of EVSE infrastructure in the reduction of BEV operational inconvenience?
- What level of EVSE infrastructure rollout, if any, is sufficient to achieve convenience parity for BEV operators?

In order to answer these questions, a method of evaluating energizing inconvenience was developed and is the subject of this paper. Novel aspects of this paper are as follows: This paper presents a novel, flexible, and data-based method for evaluating energizing inconvenience which allows for direct comparisons between different vehicles and different conditions of operation. This method utilizes longitudinal itinerary data and optimal energization scheduling in order to produce

least inconvenient energizing traces for vehicles following the itineraries. The objective function for the optimization is the novel metric Inconvenience Score (S_{IC}) which measures the distance-normalized sum of felt inconvenience for energizing events in an itinerary. The optimal energizing traces are influenced by vehicular and infrastructural parameters. Thus the results can be used to understand the relationships between vehicular and infrastructural parameters and operational inconvenience expressed as S_{IC} . Using the novel method, empirical equations relating S_{IC} to vehicular and infrastructural parameters are calculated using data from a proprietary, national, light-duty, longitudinal dataset. The empirical equations are generally applicable within the US and can be used to estimate felt inconvenience for light-duty BEVs and ICVs.

4.3.1 Quantifying Inconvenience

Quantifying the inconvenience experienced by users is a crucial step in the process of designing the BEV system to minimize inconvenience. In transportation literature, it is common to consider user inconvenience as a linear sum of separate factors which relate to time spent performing actions and to baseline inconveniences associated with performing certain actions. Examples of inconvenience being calculated as such a linear sum can be found in [172–177] which present a variety of linear sum cost functions. In [172], a train rescheduling algorithm is presented which calculates inconvenience as a weighted sum of time spent waiting, time spent in transit, and the number of transfers implicitly stating that the action of transferring trains has an inconvenience which is equivalent to a certain amount of waiting or transit time. A similar cost function for inconvenience can be found in [177] which also accounts for an equivalent inconvenience due to overcrowding of train cars. Some papers [174, 175] use cost functions which draw an equivalence between time and money in their cost functions. This allows for an implicit weighting of time-based inconvenience and cost of options. Researchers often represent inconvenience as being caused by actions happening outside of desired windows. [176] proposes a compound cost function where early arrivals at destinations are explicitly penalized, while [173] proposes a variety of

penalty functions which apply for deliveries that arrive either early or late compared to an expected delivery window.

A different approach sometimes taken is one which focuses on the users expectations as a source of inconvenience. In [178] time-based inconvenience is computed only for time spent in transit over an expected time in transit. An attempt was made in [179] to quantify the effects on perceived inconvenience due to expected waiting time of several factors including whether or not dynamic waiting times are displayed and found that displaying dynamic wait was most beneficial in reducing perceived inconvenience.

These two general approaches agree that inconvenience is fundamentally derived from delays and exertions. Any reduction in the underlying factors which cause inconvenience will almost certainly reduce perceived inconvenience. Thus for a high-sample-size study efforts are concentrated on modeling and quantifying the underlying factors that cause BEV inconvenience.

4.3.2 BEV Operational Inconvenience

The specific area of EV and Alternative Fuel Vehicle (AFV) operational inconvenience has been under-studied. Nevertheless several different approaches can be seen in literature. A fundamental difference between these methods is how they treat the issue of non-availability of home charging. Roughly 62% of Americans live in owner-occupied un-attached dwellings [180] leaving 38% who do not and, thus, are not well served by the "default" home charging model. Approaches to accounting for home charging availability or non-availability fall into three categories: assuming that only home charging will be available [181, 182], assuming that home charging will be available for all BEV operators but not sufficient to cover daily charging needs [183], and assuming that home charging will be available for some but not all BEV operators [184].

In [181, 182], a study was conducted using surveyed itineraries and assuming that charging could only occur at home. the conclusion reached was that BEVs with a range of 120 miles would be acceptable as one-to-one replacements for 90% of US vehicles under home-only charging and 60 miles of range would be sufficient for 90% of US households to own at least one BEV. In [183]

a dollar equivalence for time lost due to charging was used to determine the relative inconveniences of BEVs, AFVs, and ICVs using survey data and the locations of public EVSE infrastructure. The study found that significant inconvenience is encountered for daily itineraries of greater than 60 miles. In [184], a quantification of BEV inconvenience for users with limited charging options based on survey data, assumed EVSE infrastructure presence, and a charge scheduling heuristic is proposed. A key conclusion is that BEV operators may be able to charge their vehicles in the same amount of time as ICV operators would spend fueling or stopping for other purposes on a given long trip. The cited papers differ greatly in problem definition and methodology. What can be synthesized from the papers is that home charging is sufficient to complete a large portion of daily itineraries and that reliance on public EVSE infrastructure causes inconvenience for sufficiently long daily itineraries. It could be concluded, therefore, that complete reliance on public EVSE infrastructure would make all but the shortest daily itineraries inconvenient.

The different approaches seen in [181–184] reflect different assumptions regarding the nature of the problem. [181, 182] theorizes that BEV owners will predominantly charge at home and will not rely on public charging options to extend the range of their vehicles. [183] assumes that BEV owners will be forced to rely on public charging frequently. In [184] whether or not a BEV operator has access to home charging will determine how much that operator will rely on public charging. The papers studied place limits on BEV charging which are not reflective of the current reality or a likely future reality. Both opportunity charging at destinations and fast charging en-route are increasingly available [33, 185, 186]. In the literature some itineraries are labeled as infeasible for BEVs when these trips are increasingly feasible with BEVs due to newer DCFC infrastructure. A further limitation of the reviewed literature is the data used. The state of publicly available vehicle itinerary data is quite poor and generally comes in the form of survey data rather than longitudinal tracking data. Presumably, it is due to lacking data that researchers have opted for methods which either generate itineraries synthetically or use a series of assumptions to adapt their models to the limitations in the available datasets.

In response to the state of the field, this paper presents a method which builds on and advances previous work by computing BEV operational inconvenience accounting for the availability of home charging, the state of EVSE infrastructure, and BEV ranges in a manner which is directly comparable to ICV operation for the same set of big-data derived itineraries.

4.4 Data

The dataset used for this study was a proprietary long-term longitudinal dataset which tracked the movements of 2,177 vehicles across the continental US over the course of multiple years. The data was collected via an opt-in program which allowed the data collector to view CANbus data in real time. The raw data was processed into a longitudinal data format providing trip start and end locations, distances, and durations. Using this data the authors calculated dwell times for parking events and home locations for most of the vehicles based on location frequencies, dwell durations, and dwell times of day. The columns of the derived dataset are listed in Table 4.1

Table 4.1: Dataset Fields

Field	Description
Park Location	Lat-Lon coordinates of present dwell
Park Start Time	UTC code for start of dwell
Park End Time	UTC code for end of dwell
Is Home	Boolean for dwell location being at home or not being at home
Trip Distance	Distance traveled in the trip immediately prior to dwelling
Trip Time	Time in travel in the trip immediately prior to dwelling

The principle advantage of this dataset was the duration of the itineraries. Of the 2,177 itineraries in the dataset, 1,626 contained at least 1,000 entries. The distribution of itinerary lengths and mean driving distances are displayed in Figures 4.1 and 4.2.

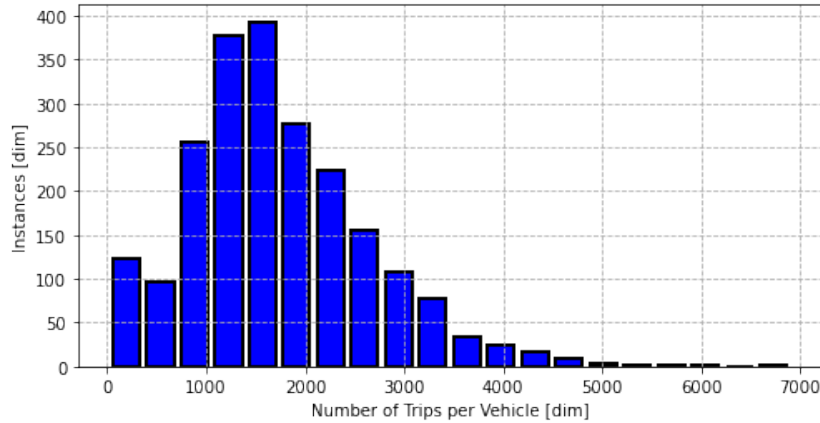


Figure 4.1: Distribution of Itinerary Lengths in the Dataset

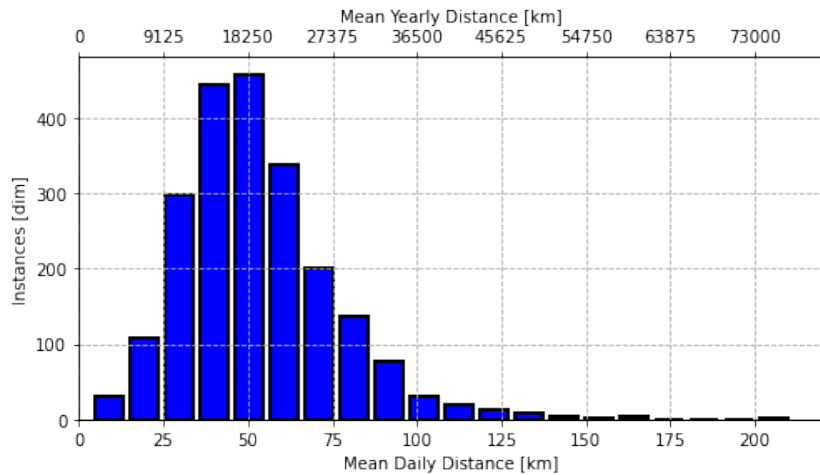


Figure 4.2: Distribution of Daily and Yearly Mean Driving Distances in the Dataset

The proprietary dataset used in this study had the advantage of being primarily intended for use as a longitudinal dataset and it compares favorably to publicly available datasets for that purpose. Two commonly used, publicly available alternatives are the 2005 Puget Sound Regional Council (PSRC) study available via National Renewable Energy Laboratory (NREL)’s

Transportation Secure Data Center (TSDC) and the 2009 or 2017 National Highway Transportation Survey (NHTS). The PSRC survey contains similar numbers of vehicle itineraries as this study's proprietary dataset but most PSRC itineraries contain missing entries which would have to be filled in order for the itineraries to be used. Other large datasets available from TSDC such as those used in [182] contain less data than the PSRC data and come with similar issues. The NHTS, collected most recently in 2017, provides a national dataset but is of limited use for longitudinal analysis as it is a manually filled survey for a single day of household activity. The proprietary dataset was, thus, the best alternative for use in this study.

On average, vehicles included in the dataset completed 1,445 trips per year for an average of 19,235.5 km traveled. For reference, the US Bureau of Transportation Statistics (BTS) calculated that the average American household completed 1,865 vehicle trips for 28,670.4 km based off of the 2017 NHTS [169]. Noting that the vehicles tracked in the proprietary dataset were not necessarily the only vehicle used by the households to which they belonged, these numbers are compatible with the available BTS data.

Although nominally a national dataset, the proprietary dataset showed a heavy bias towards large metropolitan areas in the south-western region of the continental US. Home locations were able to be estimated for 1,932 of the 2,177 vehicles in the dataset and these were located in a total of 127 counties. However, 30.1% of home locations were located in just Los Angeles County and San Diego County while the top ten most common counties accounted for 60.7% of home locations. The distribution of home locations is plotted in Figure 4.3.

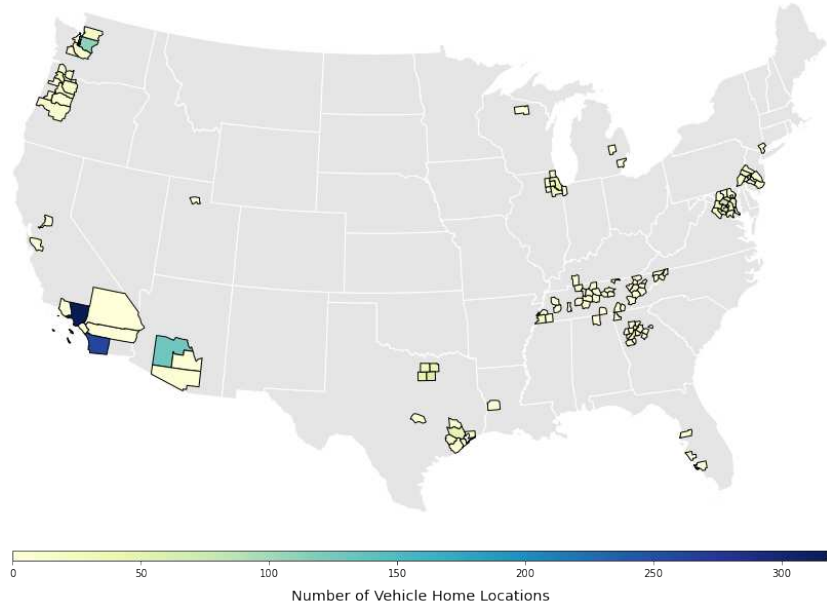


Figure 4.3: Home locations in dataset

Although the vehicles in the proprietary dataset were predominantly based in a small number of locations, the vehicles traveled considerably over the course of the tracking period and made frequent visits to a number of locations distant from their origins as plotted in Figure 4.4.

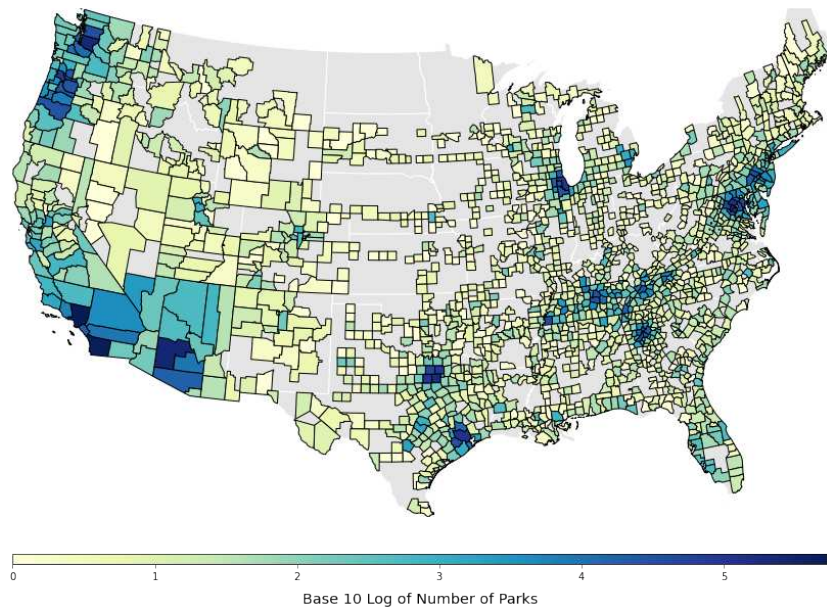


Figure 4.4: Parking event locations in dataset

4.5 Methods

The overall objective of this study was to understand what combinations of vehicular characteristics and charging infrastructure characteristics allow for BEVs to attain convenience parity with ICVs. In order to accomplish this a metric of inconvenience was created which could be evaluated for any vehicle and Dynamic Programming (DP) was used to find the optimal energizing strategy for any vehicle on a given itinerary defined in terms of trip lengths, dwell times, and location types. This allowed for the direct comparison of BEVs and ICVs traveling on the same itineraries and, thus, the direct comparison of inconvenience between the two.

4.5.1 Definition of Inconvenience

A fundamental insight in the study of vehicular operational inconvenience is that not all energizing events are the same. The authors contend that different types of energizing events inconvenience operators to vastly different degrees. The differences are rooted in the concept that energizing a vehicle is only inconvenient for the duration of time that it constrains an operator's actions. If one is able to energize a vehicle without having to add devoted energizing time to his or her daily itinerary then that person is not inconvenienced. If that same person has to spend significant time at locations that he or she would not otherwise visit in order to energize his or her vehicle then that person is inconvenienced. Thus charging at night and at home would be far less inconvenient than charging at a dedicated charging station during the day. Relative to inconvenience, charging events may be broken down into four categories as follows:

- Home energizing events: Energizing events which take place at the operator's home location. The operator's vehicle will normally dwell at home for long periods on a daily basis. Thus, home energizing events, regardless of duration, do not force the operator to devote time out of his or her itinerary to energizing.
- Work energizing events: Energizing events which take place at the operator's work location. The operator's vehicle will normally dwell at work for long periods on workdays. Thus,

work energizing events, regardless of duration, do not force the operator to devote time out of his or her itinerary to energizing.

- Destination energizing events: Energizing events which take place at long dwell destinations such as supermarkets, retail centers, gyms, etc. Because the operator would visit these locations regardless of whether or not he or she intended to energize a vehicle, these events do not force the operator to devote time out of his or her itinerary to energizing. Thus, destination energizing events only inconvenience the operator for the amount of time that he or she would need to spend paying for the energizing event.
- En-route energizing events: Energizing events which take place at a location which the operator visits specifically to energize a vehicle. Locations such as petroleum stations or centralized DCFC charging stations (Tesla Supercharger stations for example [187, 188]) may be located near amenities but operators will generally be constrained to stay within a small area adjacent to the station for the duration of the energizing event. Thus operators are inconvenienced for the duration of the event and payment process. An assumption is also made that operators will have to travel a non-negligible distance to the energizing station. Because operators are only traveling to the station to energize their vehicles the travel time is also considered to be devoted energizing time. Thus operators are also inconvenienced for the travel time required to get to and from the energizing station.

Because the different types of energizing events effect the operator differently it is important to define a metric of inconvenience which can account for all four. To this end the authors propose a flexible metric, Inconvenience Score (S_{IC}) defined as

$$S_{IC} = \frac{\sum_{k=0}^N [D_{E,k}M_{E,k} + D_{T,k}M_{T,k} + D_{P,k}M_{P,k}]}{\sum_{k=0}^N L_k} \quad (4.1)$$

for an itinerary of N trips where D_E is the duration of the energizing event, D_T is the duration of travel to get to the energizing location, D_P is the duration of the payment process, $M_{E,k}$, $M_{T,k}$, and $M_{P,k}$ are integer multipliers which respectively define whether or not to count the various durations

for trip k , and L_k is the length of trip k in kilometers. S_{IC} , thus, is the average dedicated energizing time per kilometer traveled in a given itinerary. The values of the multipliers based on the type of energizing event are shown in Table 4.2.

Table 4.2: Values of multipliers based on energizing event type

Energizing Event Type	M_E	M_T	M_P
Home	0	0	0
Work	0	0	0
Destination	0	0	1
En-route	1	1	1

So defined, S_{IC} is able to account for the differences between energizing event types and to account for differences in total travel distance between itineraries. The flexibility of the S_{IC} metric thus allows for the direct comparison of inconvenience between disparate itineraries.

4.5.2 Models

Vehicles

For evaluation purposes, a vehicle model was defined which simulates the amount of energy consumed by the vehicle on a given trip based on the trip length and mean speed. The vehicle model is defined by the parameters listed in Table 4.3.

Table 4.3: Vehicle Parameters

Parameter	Description
Energy Storage Capacity [kWh]	Maximum amount of energy that can be stored on vehicle [J]
City Consumption Rate [kJ/km]	Amount of energy consumed per unit distance [J/m] in urban driving conditions [less than 15.6 m/s]
Mixed Consumption Rate [kJ/km]	Amount of energy consumed per unit distance [J/m] in mixed urban and highway driving conditions [15.6 m/s – 29 m/s]
Highway Consumption Rate [kJ/km]	Amount of energy consumed per unit distance [J/m] in highway driving conditions [greater than 29 m/s]

The vehicle model is of a rather standard type used in longitudinal analysis. The efficiencies for the three speed ranges reflect vehicular efficiency in different driving conditions. In the absence of second-by-second speed data an assumption is made that if a trip’s average speed falls within a given range then that speed range will be most representative of the driving conditions of the trip. The energy storage parameter reflects the usable energy storage capacity of the vehicle. As batteries age usable storage capacity declines. This model also implicitly accounts for the effects of heating and cooling loads. On hot or cold days the auxiliary loads required to run the temperature control system for the vehicle will reduce the efficiency of the vehicle on an energy consumption per unit distance basis. Thus, one can account for battery degradation and significant auxiliary loads due to temperature control by changing the vehicle model parameters.

For this study two vehicles were used as representative models for BEVs and ICVs. These vehicles were based on the 2022 Tesla 3 LR and the 2022 Chevrolet Malibu. The Tesla 3 LR and

Chevrolet Malibu were chosen as they are roughly equivalent in size, shape, storage, and seating, as well as both being mid-tier models in their ranges.

The consumption data for the base vehicles is listed in Table 4.4.

Table 4.4: Base vehicle energy consumption rates

Vehicle	Parameter	Value
BEV	Energy Storage Capacity [kWh]	82
	City Consumption Rate [kJ/km]	385
	Mixed Consumption Rate [kJ/km]	479
	Highway Consumption Rate [kJ/km]	587
ICV	Energy Storage Capacity [kWh]	528
	City Consumption Rate [kJ/km]	2600
	Mixed Consumption Rate [kJ/km]	2356
	Highway Consumption Rate [kJ/km]	2094

The representative BEV and ICV models most closely represent the vehicles they are based on but the differences between the models are representative of the differences between BEVs and ICVs more generally. The important differences are the greater efficiency of the BEV model and the efficiency trends for each model. Where BEVs are more efficient in urban conditions, ICVs are more efficient on highways. The difference is because BEVs are able to recover energy when decelerating where ICVs are not. Data for vehicle energy consumption rates was attained from

[167, 168] and verified with data from [189] with the city consumption rate calculated from US06 drive cycles, the highway consumption rate calculated from HWFET drive cycles, and the mixed consumption rate calculated from FTP drive cycles.

BEV Charging

It was also necessary to define models for EVSE infrastructure. BEV charging rates were based on the Society of Automotive Engineers (SAE) J1772 standard [190] and information from [167]. The following assumptions were made about charging infrastructure:

1. If a home charger is available then it will be an AC Level 2 charger
2. If a destination charger is available it will be an AC Level 2 charger
3. All DC Level 2 (LVL 2) charging will be done at 12.1 kW which is the middle of the AC Level 2 range
4. All en-route charging will be done at dedicated DCFC stations with DC Level 1 or 2 chargers
5. At all times, all vehicles are within a certain travel time to the nearest DCFC station regardless of their location.

The infrastructure model assigns chargers to destinations based on the stated assumptions. The assignment of AC Level 2 chargers to home locations is based on a Boolean which determines if there will be chargers at home locations or not. The assignment of chargers to destinations is done by assigning chargers, randomly, to a certain percentage of the locations visited by the vehicles. Because this randomness can have an effect on inconvenience score for a configuration, all configurations are run multiple times and the inconvenience scores for the runs are averaged.

DC charging was modeled on the CC-CV curve model for lithium-ion batteries [191]. The energy added, as a function of time is

$$dSOE = \frac{P_{DC}}{C_B} t_{cc} + (1 - e^{(\lambda_C t_{cv})}) \quad (4.2)$$

$$P_{DC} = P_{AC} \eta \quad (4.3)$$

$$\lambda = \frac{P_{DC}}{0.2 C_B} \quad (4.4)$$

where $dSOE$ is the change in State of Energy (SOE) over the course of the charge event, P_{AC} is the nominal AC power level of the charge event, η is the efficiency of the conversion between AC and DC, P_{DC} is the DC power of the charge event, t_{cc} is the time spent in the constant current portion of the charge event, t_{cv} is the time spend in the constant voltage portion of the charge event, and C_B is the vehicle's battery capacity. This model defines a relationship wherein charging is linear below 80% SOE and inverse-exponential after as it approaches 100% SOE. For AC charging the model used was a pure linear charging model which cuts off at 100% SOE. These charging traces are illustrated in Figure 4.5.

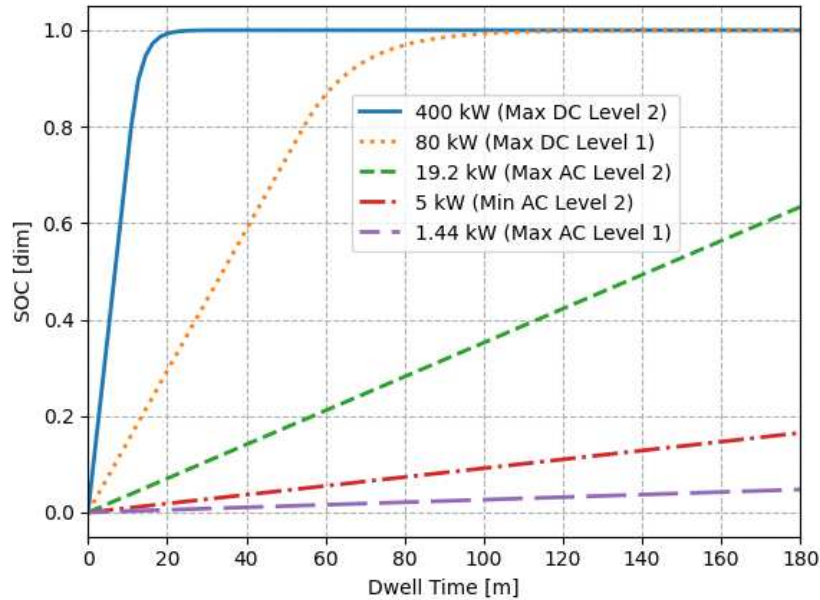


Figure 4.5: 3 hour SOE charging traces at various charging rates for a vehicle with an 80 kWh battery

ICV Fueling

ICV fueling events were treated as linear energization occurring at a rate of 7 gallons per minute [171]. Compared to charging, fueling times are relatively short and inconvenience is dominated by the time penalty for going out of one's way to get to the fueling station.

4.5.3 Optimal Charge Scheduling

Inconvenience will be effected by when and where a user chooses to charge. In order to evaluate all scenarios on equal footing, optimal charge scheduling was implemented. Optimal charge scheduling was conducted via Dynamic Programming (DP) [76, 100]. DP is a commonly used technique in optimal control which is guaranteed to find a globally optimal solution subject to the chosen discretization of the problem. The implementation used here is the "top-down" implementation [76] which includes an "optimization" step wherein an optimal control matrix is generated via backwards integration and an "evaluation" step wherein an optimal control trace is generated via forwards integration as diagrammed in Figure 4.6.

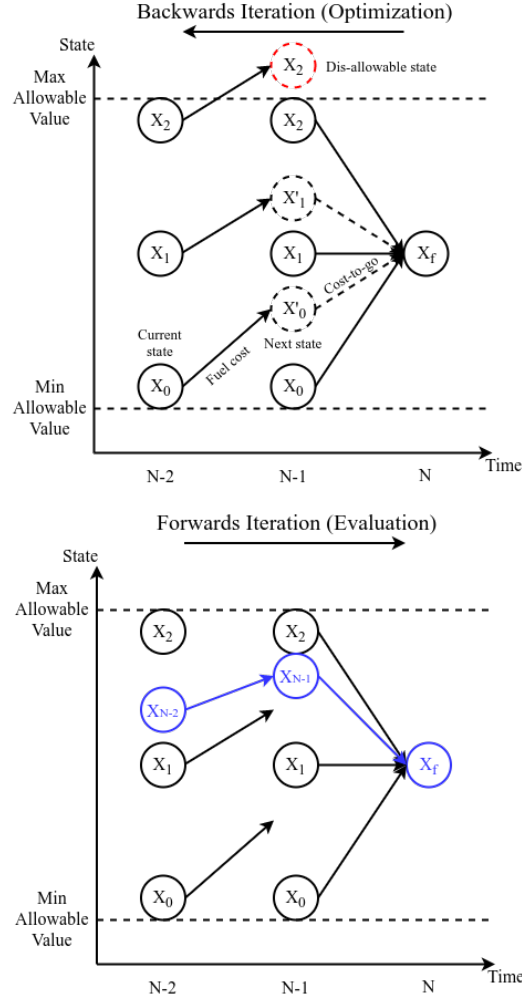


Figure 4.6: Top-down DP schematic

The goal of the optimization was to find an optimal charging control such that the inconvenience of the itinerary would be minimized. This goal can be stated as

$$\min_{\bar{U}} J(S_0, \bar{U}) \quad (4.5)$$

where

$$J(S_0, \bar{U}) = \Phi(S_N) + \sum_{k=1}^N \Psi(S_k, U_k) \quad (4.6)$$

s.t.

$$S_{k+1} = f(S_k, U_k), \quad k = 0, \dots, N - 1 \quad (4.7)$$

$$S_{min} \leq S(t) \leq S_{max} \quad (4.8)$$

where $\Psi(\bar{S}, \bar{U})$ is the running cost (inconvenience), $\Phi(\bar{S})$ is the final state cost, $\bar{S} = [SOE]$ is the state vector containing the vehicle SOE, \bar{U} is the control vector formulated as $\bar{U} = [D_{E,D}, D_{E,ER}]^T$ containing charging durations at destination $D_{E,D}$ and en-route $D_{E,ER}$ for BEVs or $\bar{U} = [D_{E,ER}]$ containing en-route fueling durations for ICVs, J is the cost for S and U , and S_{min} and S_{max} are lower and upper limits for the state vector and are constant in time. The overline indicates an array containing values at multiple discrete time intervals. The goal of the optimization is to find the optimal charging schedule (\bar{U}^*) such that J^* is equal to the global minimum value for J . J is the inconvenience score (S_{IC}) as defined in equation (4.1) which accounts for total dedicated energizing time.

The BEV model is a 1-state, 2-control model where the one state is the vehicle's SOE and the controls are destination charging and en-route charging. Destination charging is available to BEVs at locations where destination chargers are present which may include the BEV's home location. BEVs are assumed to charge for the duration of a dwell at a destination or until they have reached full charge. En-route charging is available to BEVs during every trip but requires the BEV operators to drive to a dedicated charging station which will cause them to deviate from their itineraries.

The ICV model is a 1-state, 1-control model where the one state is SOE which is the proportion of the fuel tank capacity which is fueled at any given moment and the control is en-route fueling. ICVs are not able to fuel at home or at destinations. En-route fueling is available to ICVs during every trip but requires the vehicle operators to drive to a dedicated fueling station which will cause them to deviate from their itineraries.

4.6 Results

Because the assignment of destination chargers is probabilistic, the results for a given BEV and set of infrastructure parameters may be different from run to run. Figure 4.7 demonstrates this by showing two simulation runs of 100 trips where all vehicle and infrastructure parameters are the same between the simulations. In both cases, the vehicle did not have access to home or work charging.

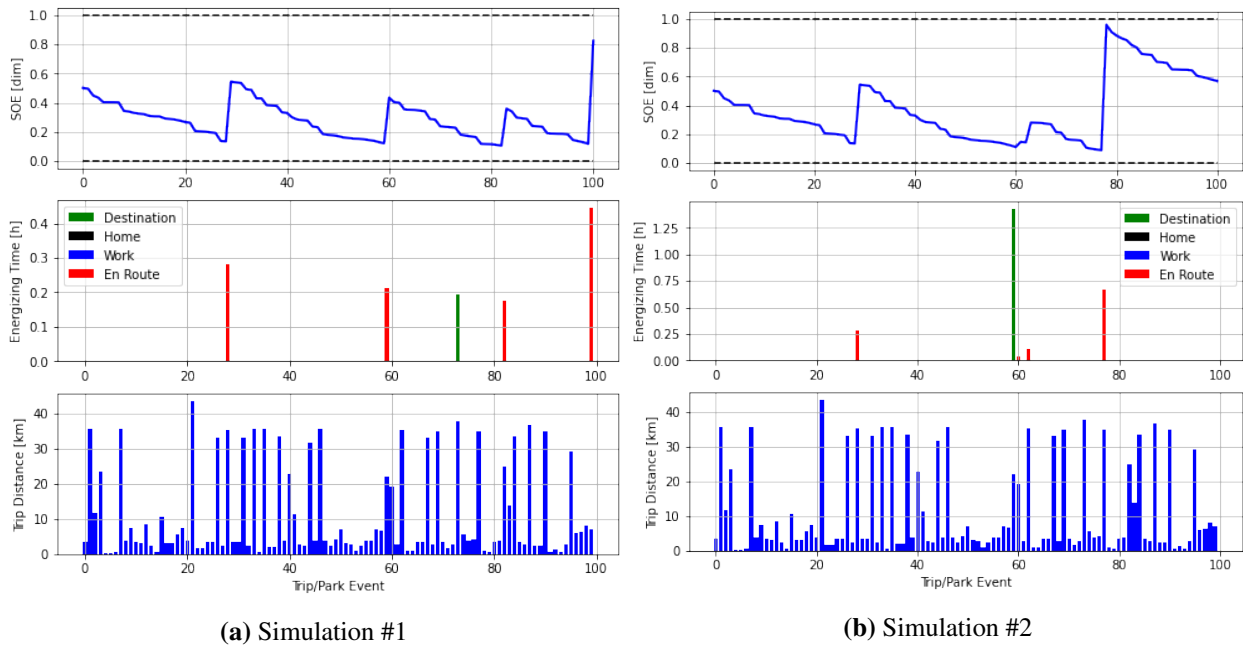


Figure 4.7: Optimal charging traces for BEVs with no home charging and identical vehicle and infrastructure parameters

Although all parameters were identical between the runs shown in Figure 4.7 the random assignment of chargers to destinations made the SOE traces visually different between the runs even if the S_{IC} values were within 10% of each-other.

Figure 4.8 illustrates a 100 trip trace for a BEV which is able to charge at home. The itinerary used in Figure 4.8 is the same as in Figure 4.7. The effects of being able to charge at home are visibly evident. Because home dwells are long and the operator does not suffer a payment or travel penalty associated with home charging events, these events tend to dominate.

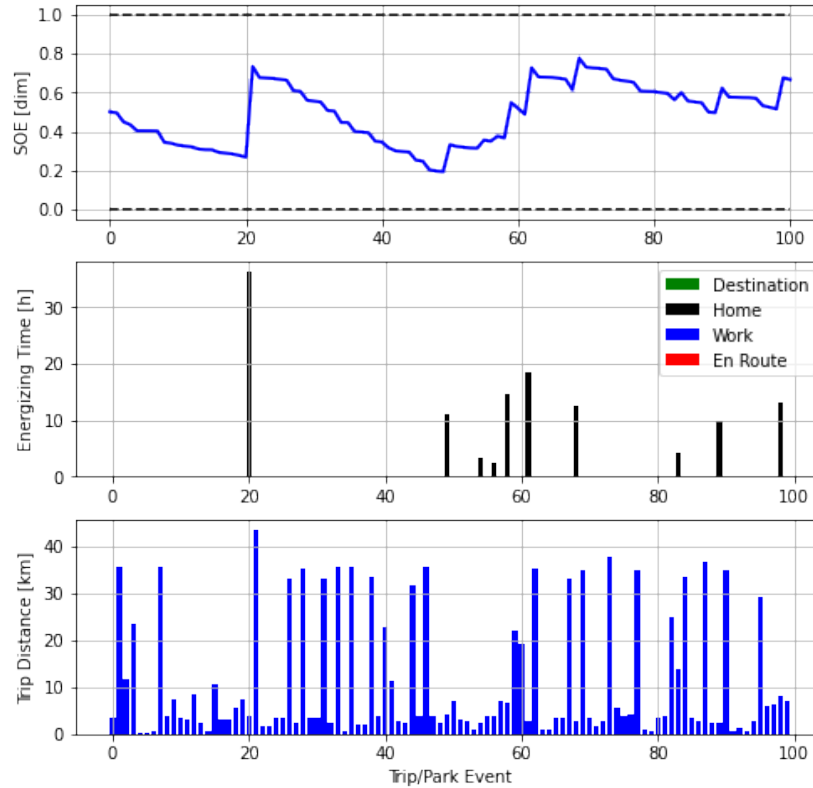


Figure 4.8: Optimal charging trace for BEV with home charging

The SOE traces presented are post-trip values. Those who can charge at home or during long dwells at destinations will be able to maintain acceptable SOE without needing to charge en-route in the course of normal operation but they will still need to do so for long trips. The pattern of frequent long duration and low rate charging events differs fundamentally from how ICV operators usually energize their vehicles and may even manifest a reduction in inconvenience compared to an ICV. For the purposes of this study ICVs may only charge en-route at a fueling station. An example of ICV operation is provided in Figure 4.9.

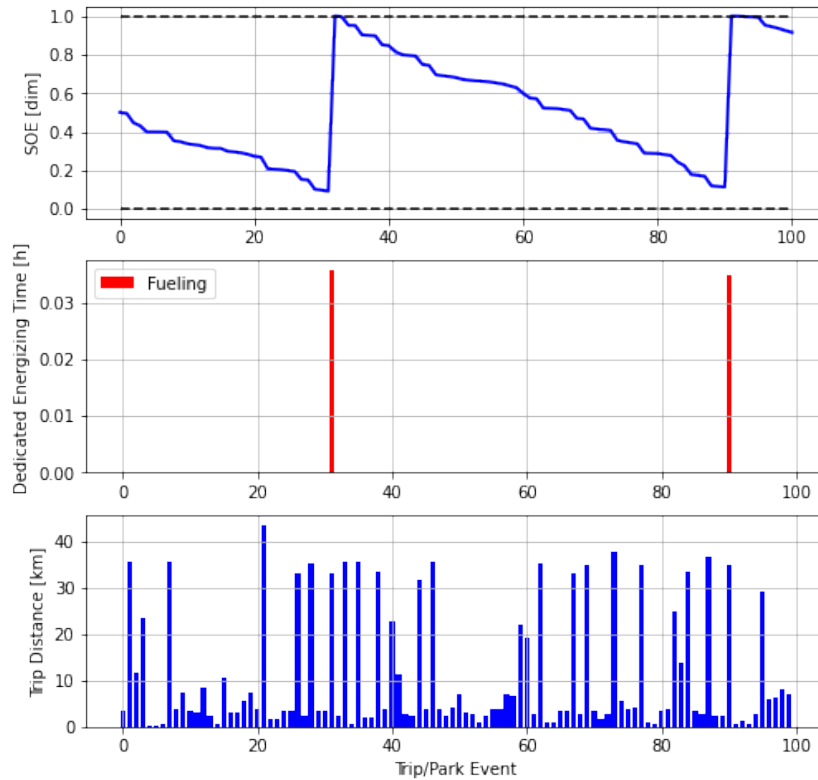


Figure 4.9: Optimal fueling trace for ICV

The typical ICV optimal fueling trace behavior is to let the SOE reduce until a safety margin is violated and then to completely refuel thus minimizing the number of fueling events. This type of charging behavior can be thought of as the "gas station" model. The type of behavior typical of optimal charging traces for BEVs where charging during dwells at home, work, or other destinations is most common can be thought of as the "dwell charging" model. The psychological effects of range anxiety are not addressed in this study but it is worth noting that BEV operators who follow the gas station model of charging may suffer from additional range anxiety in addition to whatever inconvenience they experience.

4.6.1 Experiment and Regression Analysis

EV Inconvenience Analysis

Having derived a model for energizing inconvenience an experiment was run considering several vehicle and EVSE infrastructure parameters. The purpose of the experiment was to create regressed empirical equations relating vehicular and infrastructural parameters to inconvenience. The empirical equations can be used to evaluate expected inconvenience for individuals or groups based on their experimental parameter values. The experiment was a full-factorial design on the parameters listed in Table 4.5.

Table 4.5: Experiment Parameters and Levels

Parameter	Levels	Unit
Home Charging (HC)	[False, True]	Boolean
Work Charging (WC)	[False, True]	Boolean
Battery Capacity (BC)	[40, 80, 120]	kWh
Destination Charger Likelihood (DCL)	[0, 7.5, 15]	%
En-Route Charging Rate (ERCR)	[50, 150, 250]	kW
En-Route Charging Penalty (ERCP)	[15, 30, 45]	min

The rationale for these levels was to capture the realistic range of values for each parameter in the present and near future. The range of battery capacities was based on the values of usable battery capacity found in [192]. The range for ERCR was based on ranges identified in [167, 193]. It would be quite difficult to find a true range of values for DCL or ERCP but these values

were estimated by comparing the numbers of different types of chargers present at different types of locations identified in [193] with statistics about numbers and geographical distributions of petroleum fueling stations found in [171].

The electric vehicle models used in the experiment were those described in Table 4.4. For each of the 324 experimental cases, inconvenience scores were generated for all 1,626 vehicles with itineraries of at least 1000 trips. Each case was simulated 3 times and the mean inconvenience score was used as the result for the case. A linear regression was then performed on all min-max normalized terms and interactions. Minimums and maximum values for all terms can be found in Table 4.5. The output (S_{IC}) was not normalized. Significant results for this regression, including the terms of the empirical equation, are presented in Tables 4.6, 4.7, and 4.8.

Table 4.6: Model summary

R	R-Squared	Adjusted R-Squared	Std. Error
0.986	0.972	0.965	0.000

Table 4.7: ANOVA

Category	Sum of Squares	DOF	Mean Squares
Model	1.521	63	0.024
Error	0.044	260	0.000
Total	1.565	323	0.005
F		$P(> F)$	
143.798		$2.256 \exp(-170)$	

Table 4.8: Significant terms in empirical equation ($\alpha = 0.01$)

Coefficient	Value	t-value	p-value
Intercept	0.242	26.910	0.000
HC	-0.186	-14.637	0.000
WC	-0.154	-12.110	0.000
BC	-0.056	-4.032	0.000
DCL	-0.092	-6.606	0.000
ERCR	-0.136	-9.785	0.000
ERCP	0.146	10.493	0.000
HC:WC	0.129	7.182	0.000
HC:DCL	0.073	3.725	0.000
WC:DCL	0.060	3.062	0.002
WC:ERCP	-0.089	-4.519	0.000
HC:ERCP	-0.109	-5.523	0.000
HC:ERCR	0.111	5.617	0.000
WC:ERCR	0.093	4.719	0.000
BC:ERCP	-0.081	-3.744	0.000
DCL:ERCR	0.063	2.904	0.004
HC:WC:ERCR	-0.079	-2.817	0.005
HC:WC:ERCP	0.075	2.678	0.008

The significant coefficients from the regression are also shown visually in Figure 4.10.

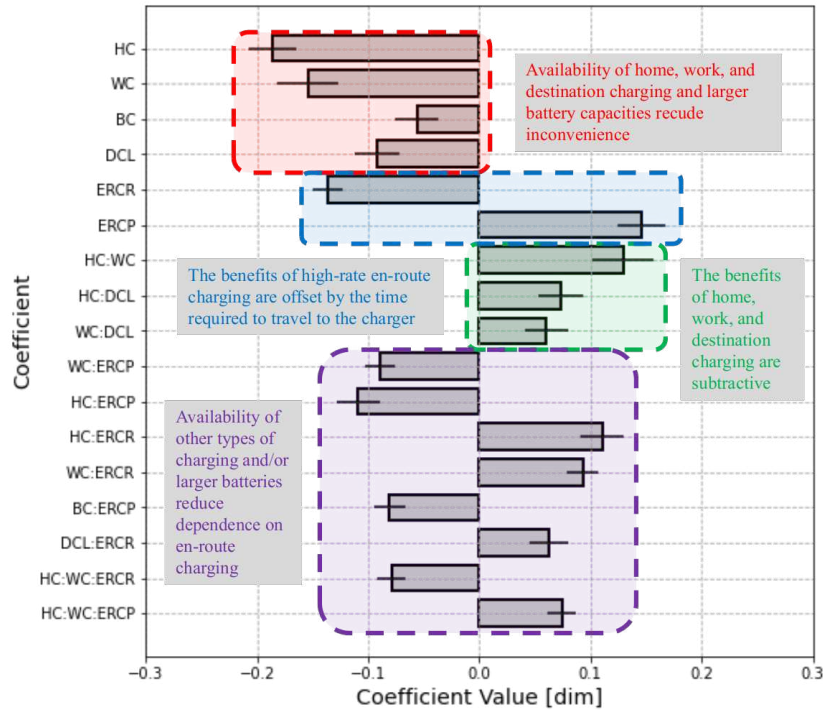


Figure 4.10: Significant ($\alpha = 0.01$) terms of empirical equation and standard error

The regression was performed with normalized regressor values in order to remove the impact of the scales of the regressors. Thus normalized, it is possible to make a comparative analysis of the importance of the parameters and their interactions. Of the parameters BC, HC, WC, DCL and ERCR were shown to contribute to decreasing inconvenience while ERCP was shown to contribute to decreasing inconvenience. A few key findings can be taken from the regression analysis. The variables HC and WC (home and work charging availability) play a major role in decreasing inconvenience as does DCL (the percentage of regular destinations where a charger might be available) but the interactions between the terms are positive. Home, work, and destination charging fill the same role in charging schedules. More charging availability at long dwell locations will not increase the need for charging and, as such, a saturation effect is seen. Generally the regression analysis indicates that those factors which contribute to lowering inconvenience work to mitigate the impacts of one-another in reducing inconvenience while also reducing the effects of ERCP in increasing inconvenience.

ICV Inconvenience Analysis

For ICVs, inconvenience derives from the need to refuel en-route. ICV operators, like BEV operators, will live at varying distances from fueling stations and ICVs, like BEVs, will have different energy capacities. A full-factorial designed experiment was run for ICVs on the previously mentioned parameters. The parameter levels for the ICV experiment are listed in Table 4.9.

Table 4.9: Experiment Parameters and Levels

Parameter	Levels	Unit
Fuel Tank Capacity (FTC)	[264, 528, 792]	kWh
Fueling Time Penalty (FTP)	[10, 15, 20]	min

The levels for FTC were set based on the capacity of the base ICV model seen in Table 4.4 $\pm 50\%$ and the levels for FTP were based on information from [171].

The experiment was conducted similarly to the BEV experiment with each case being evaluated using all 1,626 vehicles with itineraries of at least 1000 trips. Significant results for the ICV regression analysis, including the terms of the empirical equation, are presented in Tables 4.10, 4.11, and 4.12.

Table 4.10: Model Summary

R	R-Squared	Adjusted R-Squared	Std. Error
0.973	0.946	0.892	0.008

Table 4.11: ANOVA

Category	Sum of Squares	DOF	Mean Squares
Model	0.002	3	0.000
Error	0.000	5	0.000
total	0.002	8	0.000
<i>F</i>		<i>P(> F)</i>	
29.204		0.001	

Table 4.12: Significant terms in empirical equation

Coefficient	Beta	t-value	p-value
Intercept	0.035	8.519	0.000
FTC	-0.020	-3.084	0.027
FTP	0.032	4.980	0.004

4.7 Discussion

The results of the regression analysis point to the overwhelming importance of home and work charging availability in determining the inconvenience experienced by BEV operators. Also shown to be very important were the infrastructure parameters DCL and ERCP. It should be noted that the effects of investing in destination and en-route charging infrastructure simultaneously were shown to be subtractive i.e. the impact of one reduces the impact of the other. Investment policies which seek to increase DCL by creating an ubiquity of low rate chargers are projected to be more effective than those which seek to promote high rate charging stations unless high rate charging stations become very common.

The empirical equations derived in this study can be used to project the experience of individuals who may be considering purchasing a BEV. Infrastructure and housing parameters for three example localities which are presented in Table 4.13.

Table 4.13: Parameters for example localities

Locality	DCL	ERCR	ERCP	FTP
Small Town	0%	50	45	20
Suburb	5%	150	25	15
Major City	10%	250	15	10

The presented scenarios reflect an assumption that public charging infrastructure tends to be more prevalent in highly urbanized locations and that high volume residences also tend to be more common in highly urbanized locations. Everyone in a given locality will have access to the same public charging infrastructure but those who live in single unit residences and, more importantly, those who own their homes are more likely to be able to install charging stations at home. Projected operational inconvenience for the vehicle models from Table 4.4 and the localities listed in Table 4.13 are shown in Table 4.14.

Table 4.14: S_{IC} [min/km] for ICV and BEV with and without home charging in example localities

Locality	ICV	BEV			
		Home Charging	Work Charging	Both	Neither
Small Town	0.047	0.053	0.085	0.031	0.214
Suburb	0.036	0.047	0.076	0.029	0.188
Major City	0.025	0.042	0.067	0.028	0.164

For the given example localities three clear trends emerge: (1) Those EV operators who can charge at home, work, or both experience similar levels of inconvenience between the ICV and BEV but those who cannot charge at either can expect large increases in inconvenience, (2) those in highly urbanized localities experience less operational inconvenience than those in suburban or semi-rural localities, and (3) with home charging, BEV operational inconvenience can approach and surpass parity with ICV operational inconvenience. These trends underlie two forms of inequity in relation to BEV operation - economic and geographical. BEV ownership or usage will remain a much more desirable alternative for middle class to wealthy urbanites and suburbanites as long as home charging remains such an important determinant of BEV operational experience. If public EVSE infrastructure investment comes disproportionately into economically advantaged communities then the inequity of experience will grow and an inequity in BEV adoption may follow.

4.8 Conclusions

As governments around the world attempt to reduce the climate impact of their transportation sectors while maintaining personal mobility for their citizens they will increasingly turn to the promotion of BEVs. While BEV technology has advanced significantly in recent years and is projected to continue to do so, BEVs will continue to be significantly slower to energize than ICVs for the foreseeable future. As a result of the energizing rate limitations inherent to BEVs, patterns of energizing behavior which allow for energizing to happen while the operator is otherwise occupied such as charging at home, at work, or at destinations are necessary in order for individuals to achieve convenience parity. Important specific conclusions from this study are:

- At present, BEV operational inconvenience is greatly different for those who can and cannot charge at home.
- BEV operational inconvenience for who can charge at home, work, or both approaches and even surpasses parity with ICV operational inconvenience for the same itineraries.

- For those who cannot charge at home, a ubiquity of AC Level 2 chargers at common destinations or easy access to DCFC charging stations can help to reduce the inconvenience disparity between BEVs and ICVs.

The state of public EVSE infrastructure will define the experience of BEV operators unable to charge at home or work. This dependence on public charging means that governments will play a major role in the ultimate course of BEV adoption. EVSE infrastructure investment must be implemented in a thoughtful and balanced manner or massive economic and geospatial inequities of BEV experience and adoption will emerge. Failure to equitably distribute EVSE investment will fundamentally limit the BEV market to those confident of the availability of home charging.

4.9 Summary

The purpose of research directed towards RQ2 was to understand the relationship between vehicular design and EVSE infrastructure parameters and BEV operational inconvenience. In this chapter the research question was answered via the use of a data-driven optimal charging simulation. The results of the research outlined in this chapter showed the importance of charging availability during long dwells in reducing inconvenience. The takeaway is that the availability of home charging is very important in determining BEV operational inconvenience and that public charging availability will have to substantially improved in order to close the gap.

Chapter 5

A Geo-Spatial Method for Calculating BEV

Charging Inconvenience using Publicly Available Data

5.1 Preface

This chapter is derived from [194, 195] which were primarily authored by this dissertation's author. The content of the paper addresses RQ2.T4. RQ2 focused on understanding the relationship between vehicular design and Electric Vehicle Support Infrastructure (EVSE) infrastructure parameters on experienced inconvenience. The research described in this chapter is an extension of Chapter 4. In Chapter 4 an empirical formula relating said parameters to inconvenience was developed and it is applied on a geo-spatial basis in this chapter using publicly available data in a scalable manner. This metric can be used to directly evaluate Battery Electric Vehicle (BEV) operational inconvenience in relation to geography and demography.

5.2 Overview

As governments and the automotive industry push towards electrification, it becomes increasingly critical to address the factors which influence individual car buying decisions. Evidence suggests that operational inconvenience or the perception thereof plays a large role in consumer decisions concerning BEVs. BEV ownership inconvenience and its causal factors have been relatively understudied, rendering efforts to mitigate the issues insufficiently informed. This paper presents a method of producing an empirical equation which relates operational inconvenience to a small number of housing and local EVSE infrastructure factors. The paper then further provides a method of applying the equation in a geo-spatial context allowing for the evaluation of the effects of policies in a geographical manner. this method enables future

quantitative analyses concerning investment in EVSE infrastructure to be directly sensitive to BEV operational inconvenience due to charging.

5.3 Introduction

Americans rely on personal vehicles for much of their personal transportation [196] and light-duty vehicles are responsible for 57% of greenhouse-gas emissions [197] in the US. While changes in consumer behavior and land use can have major effects on emissions these changes are inherently long term processes [198–200]. A more direct alternative is to promote vehicle electrification. Recently, US policy makers and automotive industry have announced ambitious goals for promoting the sales of BEVs for personal transport [4] . Currently BEVs and Electric Vehicles (EVs) in general make up only a small share of new car sales and this percentage actually declined slightly from 2020 to 2021 [3]. Current and near future sales figures will have a lengthy impact on transportation emissions due to the long and lengthening life-cycle of modern cars [201, 202]. Each new Internal Combustion Vehicle (ICV) sold can be expected to contribute 4.6 metric tons of CO₂ per year [203] for the 12.1 years that it will be operated [202]. By contrast, the ultimate operating emissions for a BEV are determined by the energy mix of the power grid it draws from and may change over the course of the vehicle’s service life. In the last 30 years, emissions from power generation have significantly declined and should continue to do so [197]. Thus, it is very important to push for increasing electrification of personal transportation.

Each customer will evaluate the choice between purchasing a new EV or a new ICV based on different criteria. However, research suggests that a significant factor is perceived inconvenience due to charging [29–31]. EV charging adds range at a much lower rate than ICV fueling even at the highest charging rates currently available [204]. This reality will effect EV users unevenly. Those who drive longer daily distances or have worse access to charging should be more adversely effected. In order for to achieve a dominant market share in the US, they must be an attractive proposition for most of the market. A previous study by the authors [164] revealed a serious inequity of experience between EV users based on the availability of home charging. Home

Table 5.1: Total US population in housing units by density and tenure per 2021 American Community Survey (ACS) table B25033 [205]

Tenure	Type	Population	Percentage
Owned	All	221,165,400	68.23%
	Single	200,376,221	61.82%
	2 to 4	3,964,225	1.22%
	5 or more	4,895,043	1.51%
	Mobile home	11,744,205	3.62%
	Boat, RV, van, etc.	185,706	0.06%
Rented	All	102,967,486	31.77%
	Single	41,717,468	12.87%
	2 to 4	17,434,968	5.38%
	5 or more	38,890,889	12.00%
	Mobile home	4,806,065	1.48%
	Boat, RV, van, etc.	118,096	0.04%

charging will not be available to everyone and the likelihood of charging being available will be a function of residence type and tenure. Logically, homeowners will have a greater degree of freedom in installing EVSE than renters. Also those in lower density structures will have more freedom to install EVSE than those in more dense structures. Distributions of residence type and tenure for Americans are listed in Table 5.1.

About 62% of Americans live in single-unit owner-occupied dwellings while residents of owner-occupied dwellings of all types make up roughly 68%. It is reasonable to assume that a sizable percentage of Americans will not have access to home charging for a variety of reasons. Work charging may also be beneficial in the reduction of inconvenience but as of 2021, just fewer than 10,000 workplace EVSE ports existed in the US [206]. It is, at least, worth considering a future where many potential EV users will have to rely on public EVSE infrastructure.

A common model for BEV charging is the "Charging Pyramid" model as shown in Figure 5.1. In essence, the Charging Pyramid model states that the frequency of charge events will be inversely proportional to the rate at which the events occur. Explicitly, the Charging Pyramid model views home and work charging as fundamental as evidenced by their presence at the base of the pyramid.

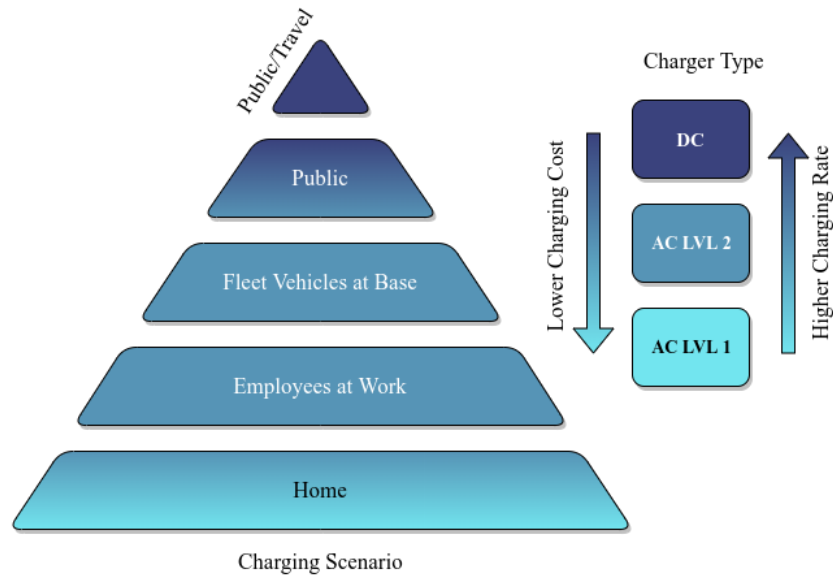


Figure 5.1: Charging activity pyramid. Modified composite of original graphic by T. Bohn, Argonne National Laboratory. From [207]

It is intuitive to see that the Charging Pyramid model breaks down if home and/or work charging is not available. If owning a BEV is a major inconvenience for those unable to charge at home then there will be a limit to market penetration, especially in poorer and more densely populated areas. In order to avoid such a constraint, public EVSE infrastructure roll-out must be handled in a careful manner informed by quantitative metrics of inconvenience. In [164], the authors defined a metric (S_{IC}) of operational inconvenience due to charging/fueling which could be applied to vehicles of any powertrain configuration. The principle behind this metric was that charging or fueling a vehicle is only inconvenient for the duration of time that the user must directly spend in the process. When charging at a centralized high-rate charging station, the user is inconvenienced for the duration of time required to travel to the station and the time required to charge. When charging at a destination that the user would travel to regardless (gym, retail, entertainment), the user is only inconvenienced for the time required to pay for the charging event. When charging at home the user is only inconvenienced for the time required to plug the vehicle in. Based on assumptions about vehicle and EVSE infrastructure parameters, a minimum value for S_{IC} can be computed for any given multi-day itinerary. A particular advantage that S_{IC} holds over

previously defined metrics of operational inconvenience [181–184] is that it is primarily focused on infrastructure parameters and can be readily estimated in a geo-spatial context.

Geo-spatial analysis is a very important tool in understanding inequities which derive primarily from different levels of access to goods and services. Geo-spatial analysis has been used extensively in social sciences to identify many different inequities such as in access to healthy food [207] and healthcare [208, 209] which lead to differentials in health and life expectancy. As part of its EVI-X suite [210], National Renewable Energy Laboratory (NREL) has developed a geo-spatial EV equity tool EVI-Equity [211]. EVI-Equity allows for a census-block-group level analysis of ev adoption rates, availability of EVSE infrastructure, and demographic information. Integration of S_{IC} into such a geo-spatial analysis would allow for the direct quantification of inequity of experience along geographical and demographic lines and for the informed evaluation of potential new EVSE infrastructure investment. In this paper, an empirical formula for the S_{IC} metric is derived and the formula is applied on a census-tract level using only publicly available data and a case study concerning the Denver Colorado urbanized area is presented.

5.4 BEV Operational Inconvenience

5.4.1 Definition of Inconvenience Score

In a previous paper [164], the authors proposed a metric (S_{IC}) which reflects this understanding of inconvenience. A BEV operator is only inconvenienced by charging their vehicle if they must devote time to doing so in which they are unable to, or have a limited ability to, perform other activities. For example, if a BEV owner parks at home and immediately begins charging his or her car then the amount of time dedicated to charging is only the time required to plug the car in and to un-plug it later. The inconvenience is minimal regardless of the duration of the charging event. Conversely, if one charges at a public charging station then he or she must remain at that location for the duration of the charge and is inconvenienced for the entire duration of the charge as well as the time required to travel to and back from the station. Relative to inconvenience, charging events may be broken down into four categories as follows:

- Home charging events: Charging events which take place at the operator's home location. The operator's vehicle will normally dwell at home for long periods on a daily basis. Thus, home charging events, regardless of duration, do not force the operator to devote time out of his or her itinerary to charging.
- Work charging events: Charging events which take place at the operator's work location. The operator's vehicle will normally dwell at work for long periods on workdays. Thus, work charging events, regardless of duration, do not force the operator to devote time out of his or her itinerary to charging.
- Destination charging events: Charging events which take place at long dwell destinations such as supermarkets, retail centers, gyms, etc. Because the operator would visit these locations regardless of whether or not he or she intended to energize a vehicle, these events do not force the operator to devote time out of his or her itinerary to charging. Thus, destination charging events only inconvenience the operator for the amount of time that he or she would need to spend paying for the charging event.
- En-route charging events: Charging events which take place at a location which the operator visits specifically to energize a vehicle. Locations such as petroleum stations or centralized DC Fast Charging (DCFC) charging stations may be located near amenities but operators will generally be constrained to stay within a small area adjacent to the station for the duration of the charging event. Thus operators are inconvenienced for the duration of the event and payment process. An assumption is also made that operators will have to travel a non-negligible distance to the charging station. Because operators are only traveling to the station to energize their vehicles the travel time is also considered to be devoted charging time. Thus operators are also inconvenienced for the travel time required to get to and from the charging station.

Because the different types of charging events effect the operator differently it is important to define a metric of inconvenience which can account for all four. To this end the authors propose a flexible metric, Inconvenience Score (S_{IC}) defined as

$$S_{IC} = \frac{\sum_{k=0}^N [D_{E,k}M_{E,k} + D_{T,k}M_{T,k} + D_{P,k}M_{P,k}]}{\sum_{k=0}^N L_k} \quad (5.1)$$

for an itinerary of N trips where D_E is the duration of the charging event, D_T is the duration of travel to get to the charging location, D_P is the duration of the payment process, $M_{E,k}$, $M_{T,k}$, and $M_{P,k}$ are integer multipliers which respectively define whether or not to count the various durations for trip k , and L_k is the length of trip k in kilometers. S_{IC} , thus, is the average dedicated charging time per kilometer traveled in a given itinerary. The values of the multipliers based on the type of charging event are shown in Table 5.2.

Table 5.2: Values of multipliers based on charging event type

Energizing Event Type	M_E	M_T	M_P
Home	0	0	0
Work	0	0	0
Destination	0	0	1
En-route	1	1	1

So defined, S_{IC} is able to account for the differences between charging event types and to account for differences in total travel distance between itineraries. The flexibility of the S_{IC} metric thus allows for the direct comparison of inconvenience between disparate itineraries.

5.4.2 Itinerary Data

Itinerary data for this study was based on the 2017 National Highway Transportation Survey (NHTS) [212]. The decision to use NHTS data was taken due to the scope and information content of the survey when compared to other publicly available data-sets.

The NHTS is a comprehensive non-commercial travel survey conducted by the US FHA which serves as an authoritative source on travel behavior in the US. The most recent NHTS was conducted in 2017. The NHTS collects, by survey, travel activities for selected households for a single day. The surveyed households are located in all 50 US states and the District of Columbia. Data collected includes demographic data for the household as well as travel itineraries for each person and vehicle within the household. The publicly available version of the 2017 NHTS contains single day itinerary data for 117,222 households containing 219,194 persons and 153,351 vehicles. Because the daily itinerary distances for vehicles in the 2017 NHTS are more varied than trip counts, the decision was made to scale by distance in this paper.

The format of the NHTS is not ideal for use in longitudinal analysis due to the single day itineraries. Using NHTS data for longitudinal analysis requires one to derive long term itineraries from single day itineraries. Additionally because NHTS offers neither precise home locations nor precise destination locations, it is not possible to construct Household Activity Pattern Problems (HAPPs) [213] as was done in [183] using California Household Travel Survey (CHTS) data. However, NHTS data does enable more demographic selection than any other comparable study and thus enables the most specific results to be attained. In order to use NHTS data for long term itineraries, the single day itineraries were simply tiled for a given number of repetitions.

5.5 Calculating Inconvenience Score

For any given itinerary, operators will experience different levels of inconvenience based on how they choose to schedule charging events. The authors contend that the fundamental inconvenience for a given itinerary is the minimum inconvenience for said itinerary. In order to calculate the minimum inconvenience for a given itinerary optimal charge scheduling was used.

Optimal charge scheduling was conducted via Dynamic Programming (DP) [bellman1956, 76]. DP is a commonly used technique in optimal control which is guaranteed to find a globally optimal solution subject to the chosen discretization of the problem.

The goal of the optimization was

$$\min_{\bar{U}} J(S_0, \bar{U}) \quad (5.2)$$

where

$$J(S_0, \bar{U}) = \Phi(S_N) + \sum_{k=1}^N \Psi(S_k, U_k) \quad (5.3)$$

s.t.

$$S_{k+1} = f(S_k, U_k), \quad k = 0, \dots, N-1 \quad (5.4)$$

$$S_{min} \leq S(t) \leq S_{max} \quad (5.5)$$

where $\Psi(\bar{S}, \bar{U})$ is the running cost (charging inconvenience), $\Phi(\bar{S})$ is the final state cost, $\bar{S} = [SOC]$ is the state vector containing the battery State of Charge (SOC) for the vehicle, \bar{U} is the control vector formulated as $\bar{U} = [D_D, D_{ER}]^T$ containing durations of opportunity charging events at destinations C_D and durations of en-route charging events at centralized high-rate charging stations C_{ER} , J is the cost for S and U , and S_{min} and S_{max} are lower and upper limits for the state vector and are constant in time. The overline indicates an array containing values at multiple discrete time intervals. The goal of the optimization is to find the optimal charging schedule (\bar{U}^*) such that J^* is equal to the global minimum value for J . J is the inconvenience score (S_{IC}) as defined in equation (5.1) which accounts for total dedicated charging time.

5.6 Models

5.6.1 Vehicle Model

For evaluation purposes, a vehicle model was defined which simulates the amount of energy consumed by the vehicle on a given trip based on the trip length and mean speed. The vehicle model is defined by the parameters listed in Table 5.3.

Table 5.3: Vehicle Parameters

Parameter	Description
Energy Storage Capacity [kWh]	Maximum amount of energy that can be stored on vehicle [J]
City Consumption Rate [kJ/km]	Amount of energy consumed per unit distance [J/m] in urban driving conditions [less than 15.6 m/s]
Mixed Consumption Rate [kJ/km]	Amount of energy consumed per unit distance [J/m] in mixed urban and highway driving conditions [15.6 m/s – 29 m/s]
Highway Consumption Rate [kJ/km]	Amount of energy consumed per unit distance [J/m] in highway driving conditions [greater than 29 m/s]

For this study the 2021 Tesla 3 LR was chosen as the baseline vehicle. The consumption data for the 2021 Tesla 3 LR is listed in Table 5.4.

Table 5.4: Base vehicle energy consumption rates

Parameter	Value
Energy Storage Capacity [kWh]	82
City Consumption Rate [kJ/km]	385.2
Mixed Consumption Rate [kJ/km]	478.8
Highway Consumption Rate [kJ/km]	586.8

This is, necessarily, an approximate measure. Data for vehicle energy consumption rates was attained from [167, 168] and verified with data from [189] with the city consumption rate calculated from US06 drive cycles, the highway consumption rate calculated from HWFET drive cycles, and the mixed consumption rate calculated from FTP drive cycles.

5.6.2 Infrastructure Model

It was also necessary to define models for EVSE infrastructure. BEV charging rates were based on the Society of Automotive Engineers (SAE) J1772 standard [190] and information from [167]. The following assumptions were made about charging infrastructure:

1. If a home charger is available then it will be an AC Level 2 charger
2. If a destination charger is available it will be an AC Level 2 charger
3. All DC Level 2 (LVL 2) charging will be done at 12.1 kW which is the middle of the AC Level 2 range
4. All en-route charging will be done at dedicated DCFC stations with DC Level 1 or 2 chargers
5. At all times, all vehicles are within a certain travel time to the nearest DCFC station regardless of their location.

The infrastructure model assigns chargers to destinations based on the stated assumptions. The assignment of AC Level 2 chargers to home locations is based on a Boolean which determines if there will be chargers at home locations or not. The assignment of chargers to destinations is done by assigning chargers, randomly, to a certain percentage of the locations visited by the vehicles. Because this randomness can have an effect on inconvenience score for a configuration, all configurations are run multiple times and the inconvenience scores for the runs are averaged. DC charging was modeled on the CC-CV curve model for lithium-ion batteries [191]. The energy added, as a function of time is

$$dSOE = \frac{P_{DC}}{C_B} t_{cc} + (1 - e^{(\lambda_C t_{cv})}) \quad (5.6)$$

$$P_{DC} = P_{AC} \eta \quad (5.7)$$

$$\lambda = \frac{P_{DC}}{0.2 C_B} \quad (5.8)$$

where $dSOE$ is the change in State of Energy (SOE) over the course of the charge event, P_{AC} is the nominal AC power level of the charge event, η is the efficiency of the conversion between AC and DC, P_{DC} is the DC power of the charge event, t_{cc} is the time spent in the constant current portion of the charge event, t_{cv} is the time spend in the constant voltage portion of the charge event, and C_B is the vehicle's battery capacity. This model defines a relationship wherein charging is linear below 80% SOE and inverse-exponential after as it approaches 100% SOE. For AC charging the model used was a pure linear charging model which cuts off at 100% SOE.

5.7 Individual Trace Results

Because the assignment of destination chargers is probabilistic, the results for a given BEV and set of infrastructure parameters may be different from run to run. Figure 5.2 demonstrates this by showing three simulation runs of 7 tiled day long itineraries where all vehicle and infrastructure parameters are the same between the simulations.

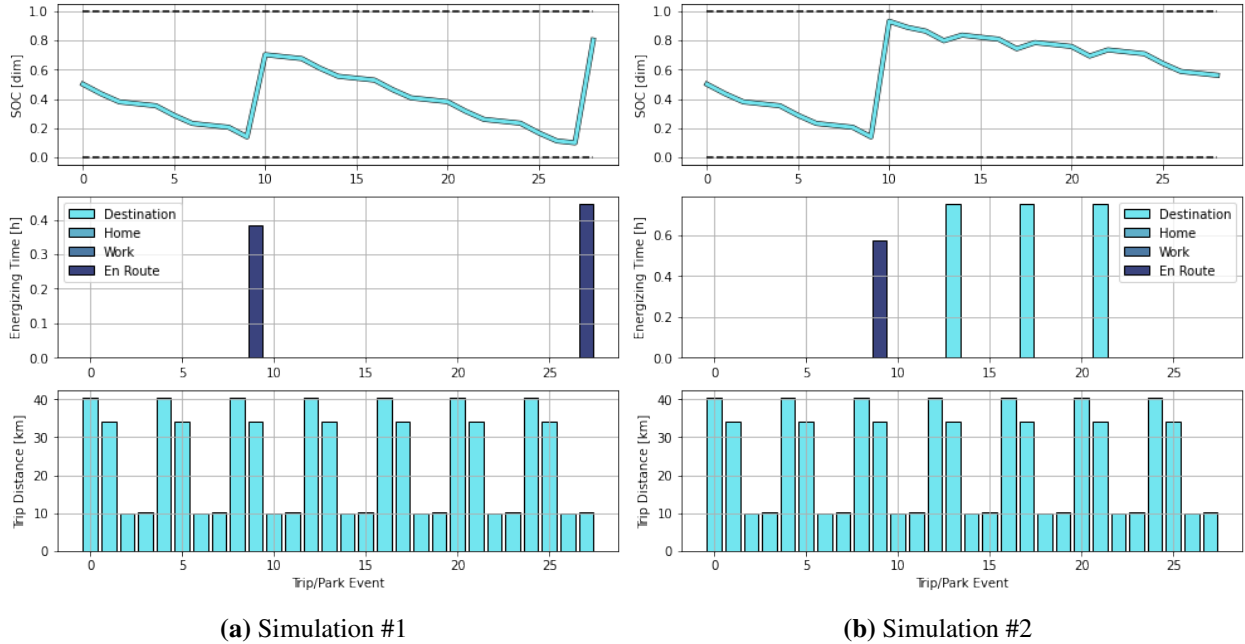


Figure 5.2: Simulation traces for a BEV (vehicle #118,211) with no home or work charging and identical parameters

In Figure 5.2 the vehicle, in all cases, was neither able to charge at home nor at work. The effects of being able to charge at home or work are visually apparent. Because home and work dwells are long and the operator does not suffer a payment or travel penalty associated with home or work charging events, these events tend to dominate. Example 7 day traces with home and work charging are shown in Figure 5.3.

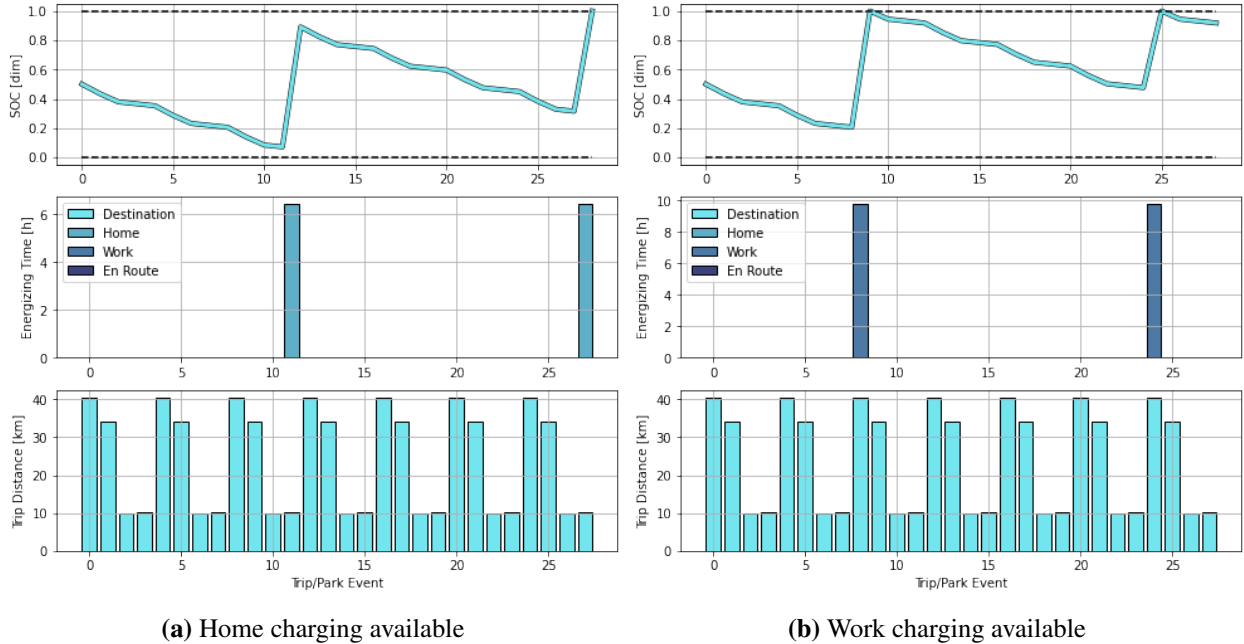


Figure 5.3: Simulation traces for a BEV (vehicle #118,211) with home or work charging available and identical parameters

Vehicle #118,211, as shown in Figures 5.2 and 5.3, had a typical commuter itinerary which was dominated by two long daily trips. For this type of itinerary charging at home and work is particularly important as the vehicle uses a significant amount of its range over a given day. Having the ability to charge at work allows for a much smaller reliance on public charging but the operator will still have to occasionally charge at a destination or DC charging station.

5.8 Inconvenience Formulae

Having derived a model for energizing inconvenience an experiment was run concerning several vehicle and EVSE infrastructure parameters. The purpose of this experiment was to derive an empirical formula for Inconvenience Score based on vehicular and infrastructural parameters. The experiment was a full-factorial design on the parameters listed in Table 5.5.

Table 5.5: Experiment Parameters and Levels

Parameter	Levels	Unit
Home Charging availability (HC)	[0, 1]	dim
Work Charging availability (WC)	[0, 1]	dim
Battery Capacity (BC)	[40, 80, 120]	kWh
Destination Charging Likelihood (DCL)	[0, 4.5, 15]	%
En-Route Charging Rate (ERCR)	[50, 150, 250]	kW
En-Route Charging Penalty (ERCP)	[0, 25, 50]	min

The rationale for these levels was to capture the realistic range of values for each parameter in the present and near future. The range of battery capacities was based on the values of usable battery capacity found in [192]. The range for En-Route Charging Rate (ERCR) was based on ranges identified in [33, 167, 185, 186, 193]. It would be quite difficult to find a true range of values for Destination Charger Likelihood (DCL) or En-Route Charging Penalty (ERCP) but these values were estimated by comparing the numbers of different types of chargers present at different types of locations identified in [193] with statistics about numbers and geographical distributions of petroleum fueling stations found in [171]. The ranges of values used for DCL and ERCP were also in line with calculated values for the Denver Colorado urbanized area as discussed later.

The electric vehicle model used for energy consumption was the Tesla 3 LR model described in Tables 5.3 and 5.4 with Battery Capacity (BC) being the only parameter modified during the

experiment. For each of the 324 experimental cases, inconvenience scores were generated for all 61,039 itineraries from vehicles in the 2017 NHTS containing more than 3 trips. A linear regression was then performed on all min-max normalized terms and interactions. Significant results for this regression ($\alpha = 0.05$) are presented in Tables 5.6, 5.7, and 5.8.

Table 5.6: Model Summary

R	R-Squared	Adjusted R-Squared	Std. Error
0.991	0.982	0.978	0.000

Table 5.7: ANOVA

Category	Sum of Squares	DOF	Mean Squares
Model	10.100	63	0.160
Error	0.181	260	0.001
total	10.281	323	0.032
<i>F</i> Statistic		<i>P</i> (> <i>F</i>)	
290.509		3.504exp(-200)	

Table 5.8: Significant Coefficients

Coefficient	Value	t-value	p-value
Intercept	0.204	24.257	0.000
HC	-0.191	-16.096	0.000
WC	-0.080	-6.750	0.000
DCL	-0.065	-4.968	0.000
ERCR	-0.103	-7.892	0.000
ERCP	0.461	35.389	0.000
HC:WC	0.076	4.500	0.000
HC:DCL	0.063	3.402	0.001
HC:ERCR	0.096	5.206	0.000
WC:ERCR	0.052	2.808	0.005
HC:ERCP	-0.431	-23.432	0.000
WC:ERCP	-0.166	-9.009	0.000
BC:ERCP	-0.113	-5.602	0.000
DCL:ERCP	-0.163	-8.069	0.000
HC:WC:ERCP	0.154	5.935	0.000
HC:BC:ERCP	0.093	3.278	0.001
HC:DCL:ERCP	0.156	5.477	0.000

The significant coefficients from the regression are also shown visually in Figure 5.4.

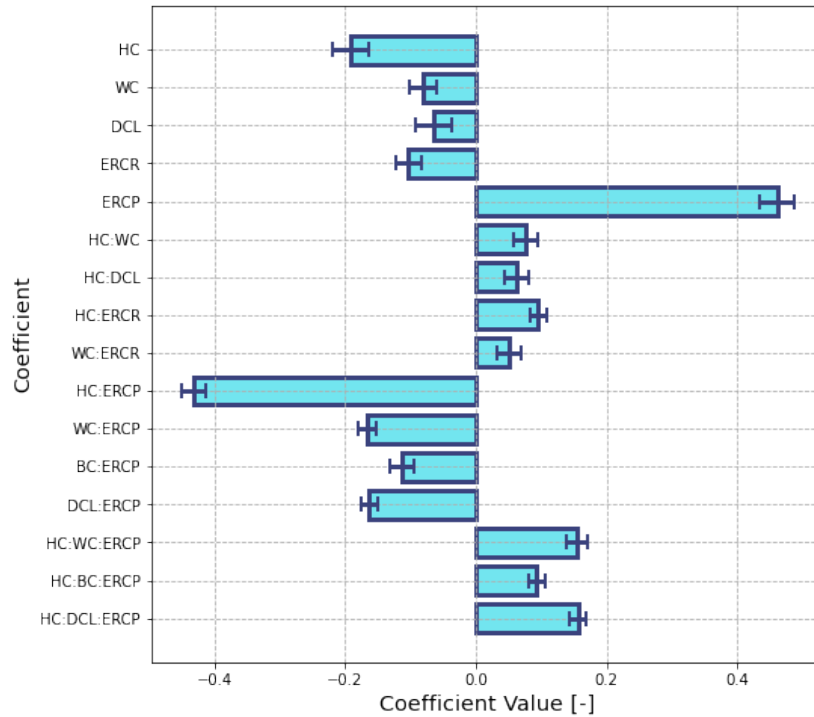


Figure 5.4: Significant Regression Coefficients and Error Bars

The regression was performed with normalized regressor values in order to remove the impact of the scales of the regressors. Thus normalized, it is possible to make a comparative analysis of the importance of the parameters and their interactions. Of the parameters BC, Home Charging (HC), DCL and ERCR were shown to contribute to decreasing inconvenience while ERCP was shown to contribute to decreasing inconvenience. Of the parameters, the most important for reducing inconvenience was HC. As discussed previously, BEV operators who are able to charge at home rarely need to charge anywhere else to complete their daily driving. The dominance of home charging is further borne out in the primary interaction terms where all interactions with HC strongly counteract the impacts of the primary terms. It is also worth noting that, while the rate of high-rate charging matters in reducing inconvenience, the penalty for having to travel to a fast charging center is quite large and thus, for many BEV operators, traveling to a fast charging station will not be an attractive option.

One advantage of using NHTS data for itinerary analysis is the degree to which the data can be down-selected to increase specificity. In order to increase the relevance of the empirical formula for the Denver CO case study, the same experiment was run for only Colorado itineraries and for only Denver Metropolitan Statistical Area (MSA) itineraries. The differences in values for the significant terms from these itinerary subsets and from the national set were minor. A comparison between the values of the significant parameters of the empirical equations from the mentioned itinerary subsets is provided in Figure 5.5.

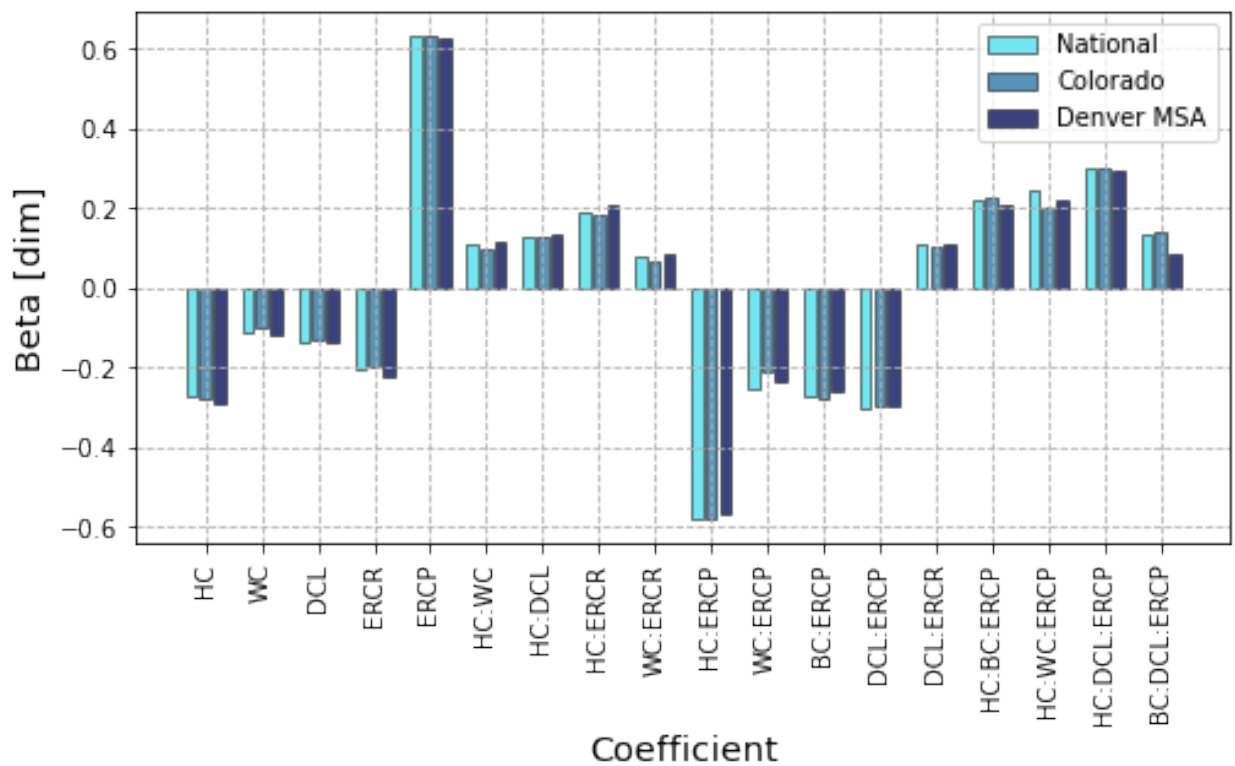


Figure 5.5: Significant Regression Coefficients and Error Bars for national, Colorado, and Denver MSA itinerary subsets

5.9 Geographical Calculation

One promising application for the Inconvenience Score is that it can be directly used to evaluate expected inconvenience on a geographical basis. Using any desired subset of NHTS data, an empirical formula for inconvenience based on the parameters in table 5.5 can be derived. Values

for the coefficients can be calculated for a given geographical area using publicly available data and from this an Inconvenience Score can be assigned to the area. This geographical analysis allows for the visualization of location based inequity of experience due to BEV charging inconvenience and for the direct evaluation of proposed future EVSE infrastructure in terms of its effects on BEV charging inconvenience. In this section, the methods for computing Inconvenience Score on a geo-spatial basis are presented using the Denver Colorado urban area as an example.

5.9.1 Geographies

Demographic data used in this study taken form the 2019 ACS on a census tract level. The 2019 ACS is the most recent complete version of the survey. In this paper, the authors defined the area of interest as the urbanized area surrounding Denver Colorado. This area contained all census tracts with centroids within 25 km from the center of the city as plotted in Figure 5.6.

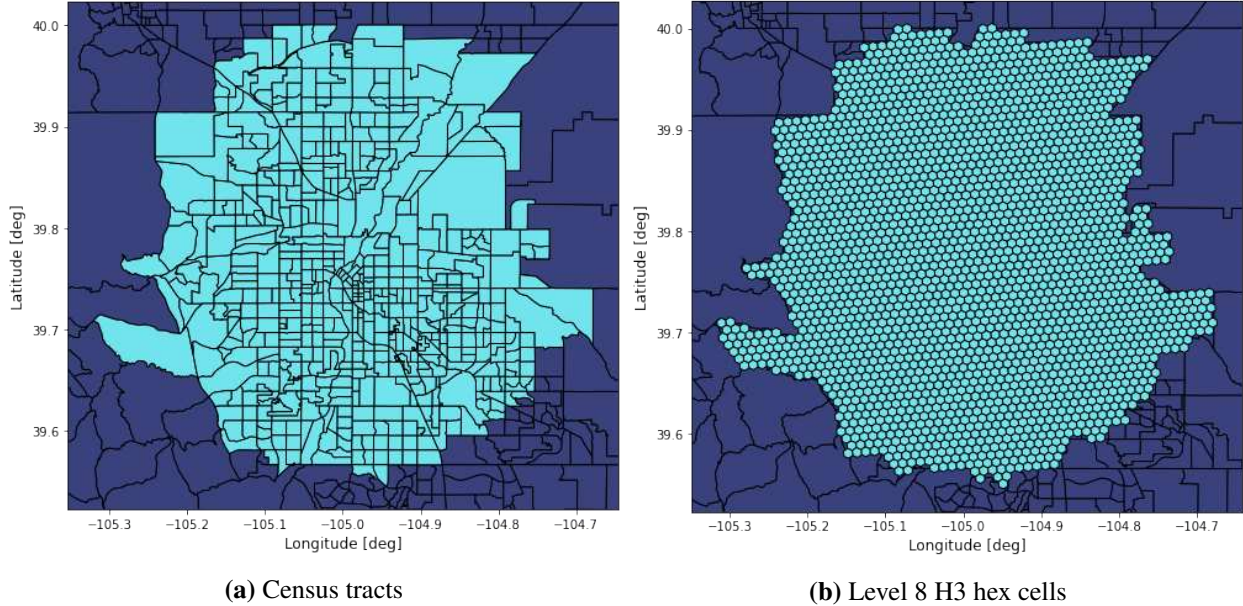


Figure 5.6: Geometries in Denver Colorado urbanized area

Census geometries are designed to reflect roughly equal units of population and, thus, have vastly different areas and irregular geometries. Because (S_{IC}) calculation relies on geometric distances and uses geometry centroids for seeding a regular geometric division scheme was sought.

For this level 8 H3 hex cells [214] were used. The use of level 8 H3 hex cells increased the number of geometries in the area of interest from 561 to 2,254. The average size of the H3 hex cells was 795.7 km² with a standard deviation of 1.3 km². The mean area of the hex cells was smaller than the average and median areas of the census tracts. A comparison of the distribution of areas of the census tracts with the mean area of the hex cells is provided in Figure 5.7.

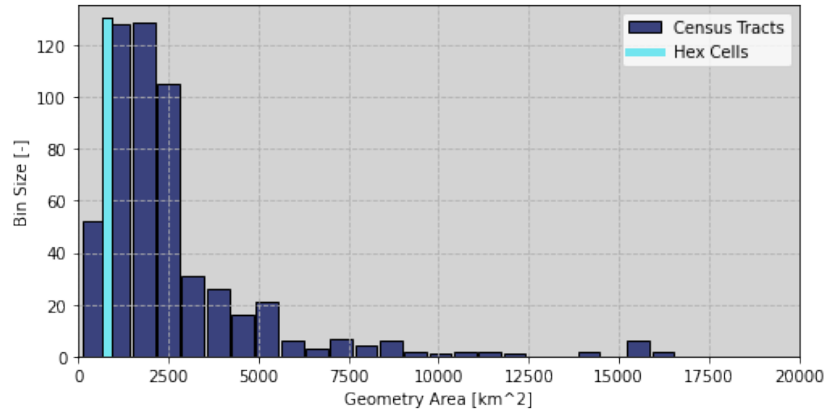


Figure 5.7: Distribution of census tract areas compared to mean level 8 H3 hex cell area for Denver Colorado urbanized area

5.9.2 Locations of EVSE Infrastructure

The locations of existing chargers were pulled from NREL’s Alternative Fuels Data Center (ADFC) [215]. The data provided by ADFC lists the locations of publicly available as well as private chargers along with the charger category (AC level 1, AC level 2, DC) and other information. ADFC data does not distinguish between DC level 1 and 2 nor does it provide specific charger max rates. For this study only publicly available AC level 2 and DC chargers were considered. Maps of the locations of level 2 and DC chargers in the Denver Colorado urbanized area are provided in Figure 5.8.

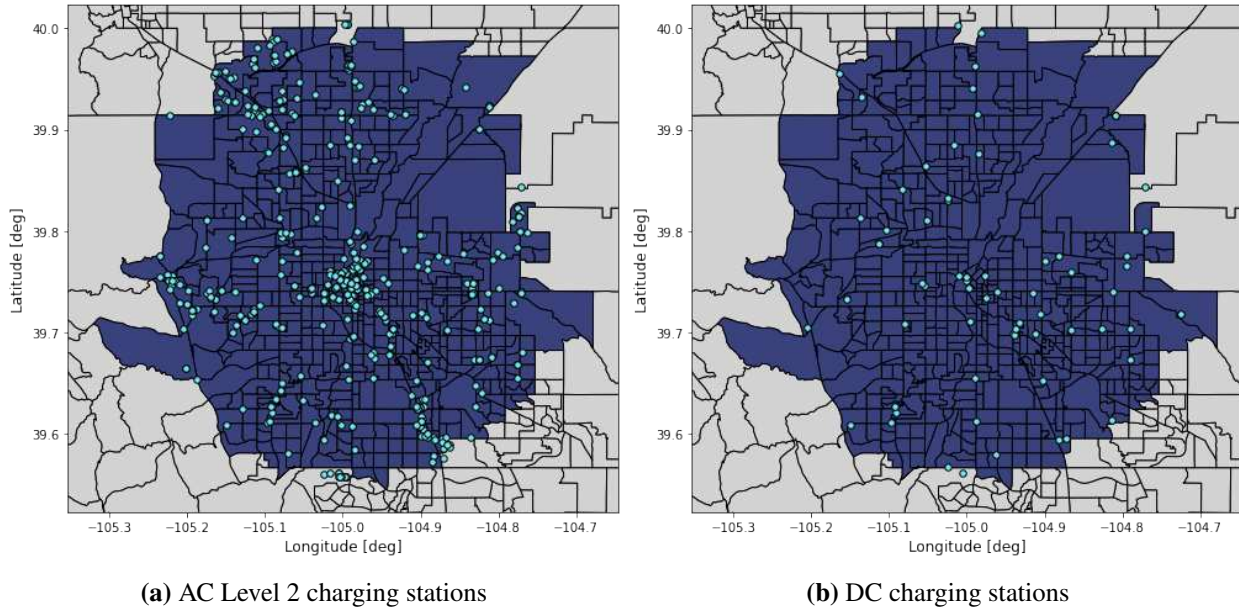


Figure 5.8: Locations of charging stations in Denver Colorado urbanized area

5.9.3 Geographic Computation of DCL

DCL is defined as the likelihood of finding an AC Level 2 charger at or close to a given destination. Thus, to compute DCL requires knowledge of the locations of all likely destinations for a given person or geographical area. There are a huge number of possible destinations that a person could visit in a given area. The authors propose that the only destinations that are relevant are popular long-dwell locations. The locations of popular long-dwell locations can be pulled from various mapping services such as OSM [216], Google Maps [217], Bing Maps [218, 219], and others. The authors chose to use Bing Maps due to a combination of factors including the ease-of-use of the API, the quality of documentation, and pricing factors.

Using Bing Maps API, it is possible to pull the 25 most relevant destinations of a given category for a 5 kilometer area around a given point. The categories selected were the "Shop" category which includes the locations of major retailers, the "EatDrink" category which includes the locations of bars, restaurants, and grocery stores, and the "SeeDo" category which includes the locations of entertainment venues and local attractions. For a given geometry, up to 75 popular, long-dwell destinations could be pulled based on the location of the centroid. Because the radii

of the hex cells were less than 5 km there was large overlap ion popular long-dwell locations between cells. The locations of the destinations can then be compared to the locations of AC Level 2 charging stations. Those within a given distance (in this case 50 m) are considered to have a nearby charger. For a given census block the value for DCL is the ratio of destinations with nearby chargers to total destinations. Values of DCL for hex cells in the area of interest are presented in Figure 5.9. The distribution of values of DCL for hex cells in the area of interest are presented in Figure 5.10

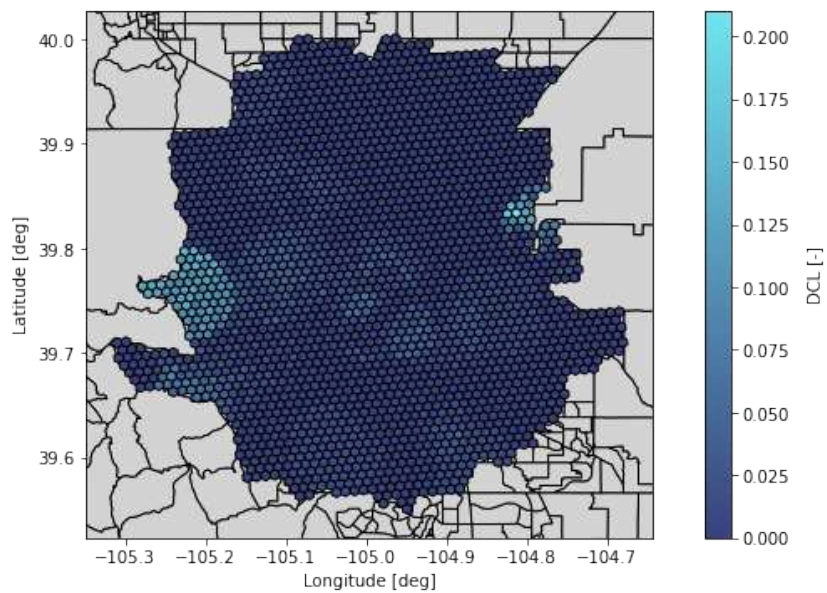


Figure 5.9: DCL for hex cells in Denver Colorado urbanized area

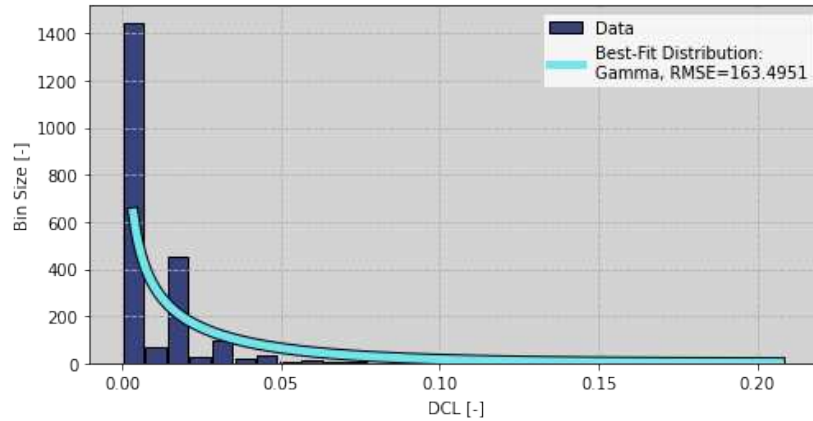


Figure 5.10: DCL distribution for hex cells in Denver Colorado urbanized area

5.9.4 Geographic Computation of ERCP

ERCP is the round-trip travel time, in minutes, to the nearest DC charging station. For a geometry this can be approximated by calculating the time required to travel from the geometry centroid to the nearest DC charging station. To calculate the expected travel time from a given block centroid to the nearest DC charging station the authors used Mapbox’s routing engine [220]. Values of ERCP for hex cells in the area of interest are presented in Figure 5.11. The distribution of values of DCL for hex cells in the area of interest are presented in Figure 5.12

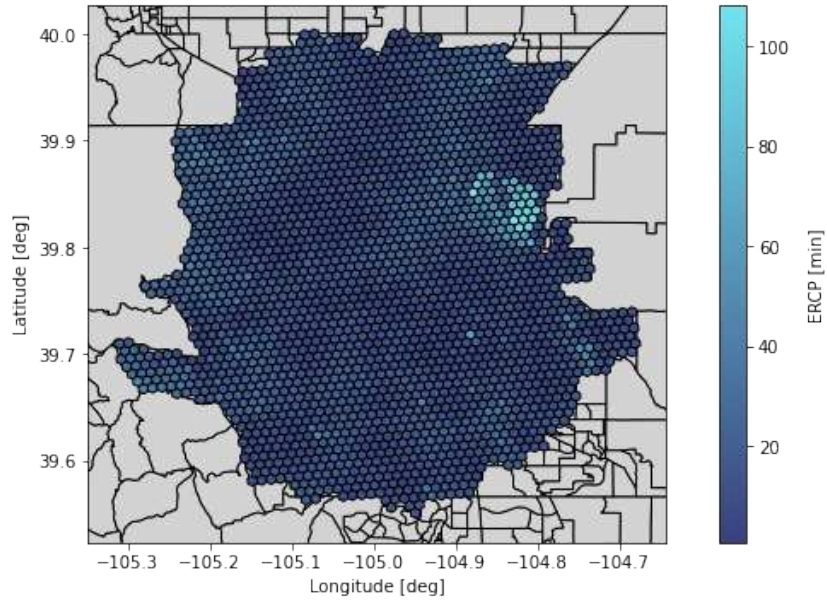


Figure 5.11: ERCP for hex cells in Denver Colorado urbanized area

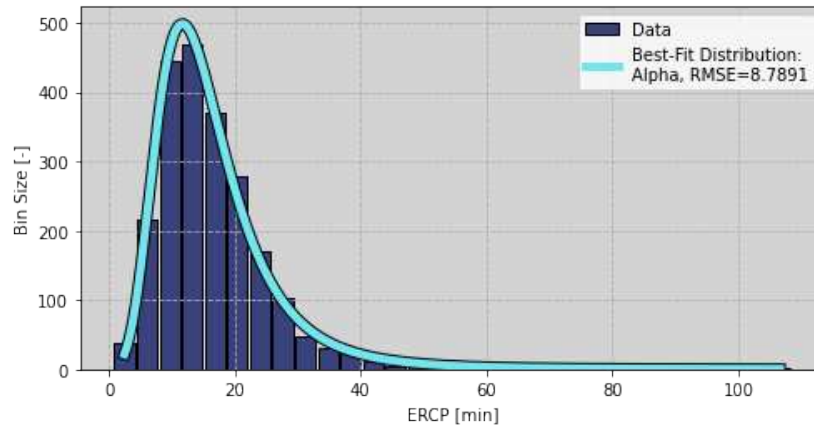


Figure 5.12: ERCP distribution for hex cells in Denver Colorado urbanized area

5.9.5 Geographic Computation of HC

Finally, the ability of BEV users to charge at home can be estimated on a census tract level using housing type and tenure data. For this data from ACS table B25033 5 year estimates (summarized on a national scale in Table 5.1) was used. Residence type and tenure patterns for the Denver Colorado urbanized area are shown in Figure 5.13.

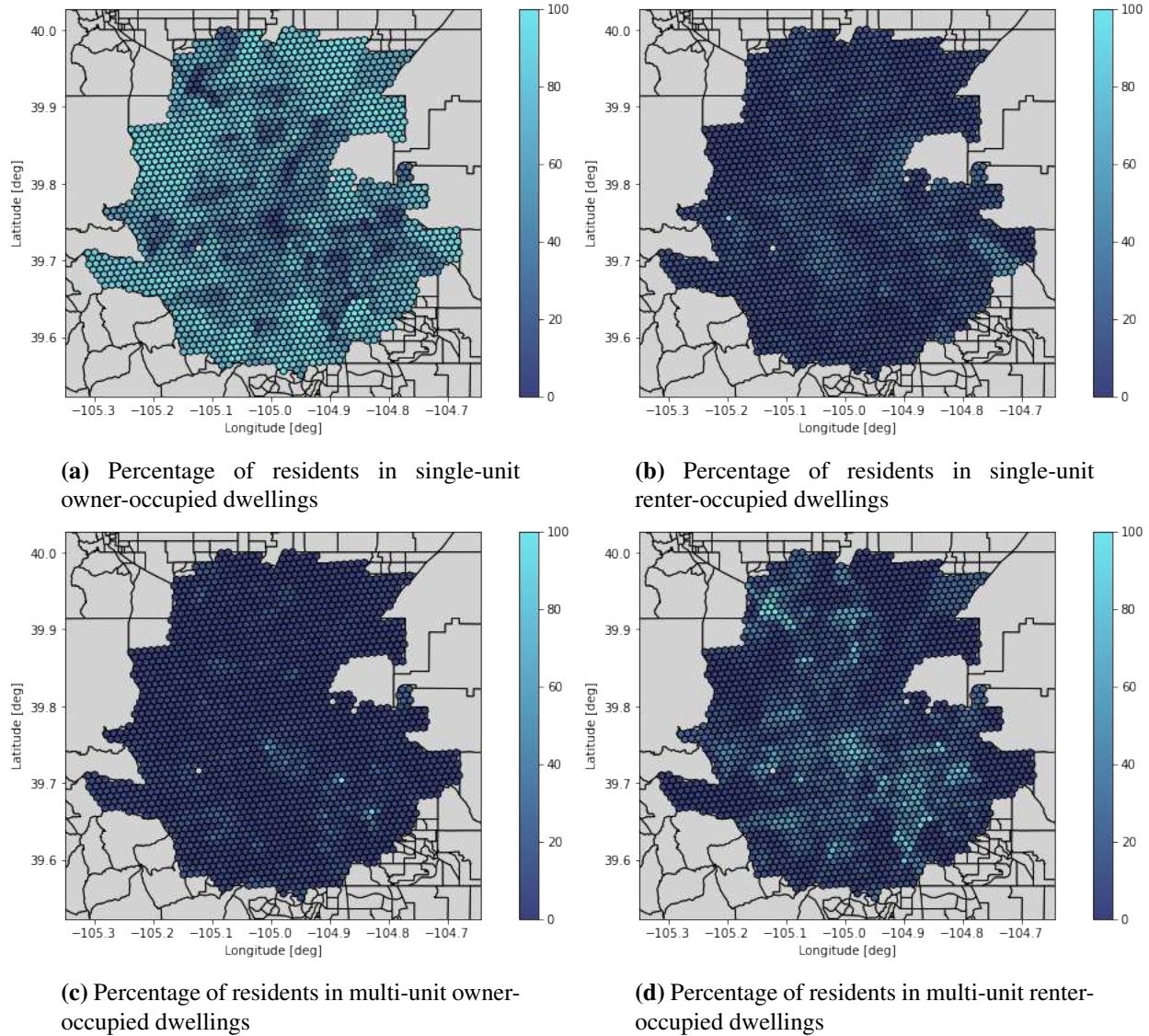


Figure 5.13: Census tract level residence type and tenure patterns

Residential patterns in the Denver Colorado urbanized area heavily favor single-unit owner-occupied and multi-unit renter-occupied dwellings. It is impossible to know precisely which residents have access to or could have a access to a home charger. NREL conducted a study [221] which surveyed residents of various structure types and tenures on access to charging. [221] broke respondents down into 5 scenarios based on access to electricity at their parking location, whether or not access could be readily added, access would be available with modified charging behavior. The scenarios were as follows:

1. Existing discounted electrical access: respondents had access to electricity at their parking locations with specific discounted EV charging pricing plans.
2. Existing electrical access: respondents had access to electricity at their parking locations.
3. Existing electrical access with parking behavior modification: respondents had the ability to access electricity at parking locations which they do not currently use but could use.
4. Enhanced electrical access: respondents had the reasonable ability to add electrical access at their parking locations.
5. Enhanced electrical access with parking behavior modification: respondents had the reasonable ability to add electrical access to parking locations which they do not currently use but could use.

The authors chose scenario 4 as the most realistic surrogate for home charging access. Also considered were scenarios 1 and 5. Scenarios 1 and 5 serve as upper and lower bounds on home charging access. In the remainder of this paper scenarios 1, 4, and 5 will be referred to as the exclusive, realistic, and inclusive scenarios. The selected scenarios are detailed in Table 5.9.

Table 5.9: Estimations for home charging availability

Residence Category	Portion of Residents	Exclusive	Realistic	Inclusive
Single Owned	0.602	0.168	0.614	0.852
Single Rented	0.035	0.089	0.387	0.600
2 to 4 Owned	0.007	0.100	0.360	0.480
2 to 4 Rented	0.154	0.020	0.210	0.260
5+ Owned	0.028	0.100	0.360	0.480
5+ Rented	0.010	0.043	0.197	0.253

Using geo-spatial housing type and tenure data from the ACS and the scenarios from Table 5.9, geo-spatial HC can be calculated. HC for H3 hex cells in the Denver Colorado urbanized area for all HC assumption sets are shown in Figure 5.14. Probability Distribution Functions (PDFs) for HC by assumption set are displayed in Figure 5.15.

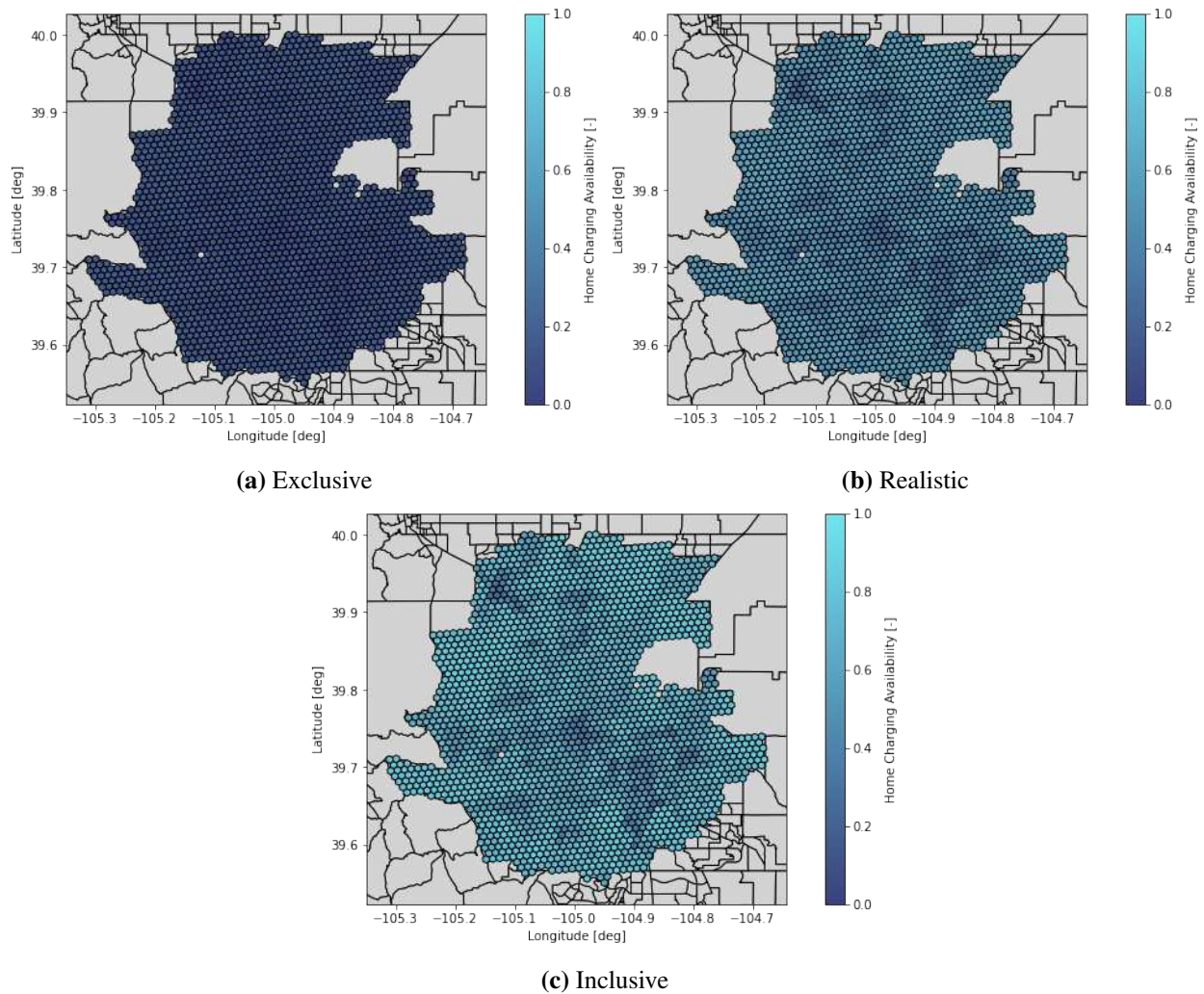


Figure 5.14: HC for H3 hex cells in Denver Colorado urbanized area

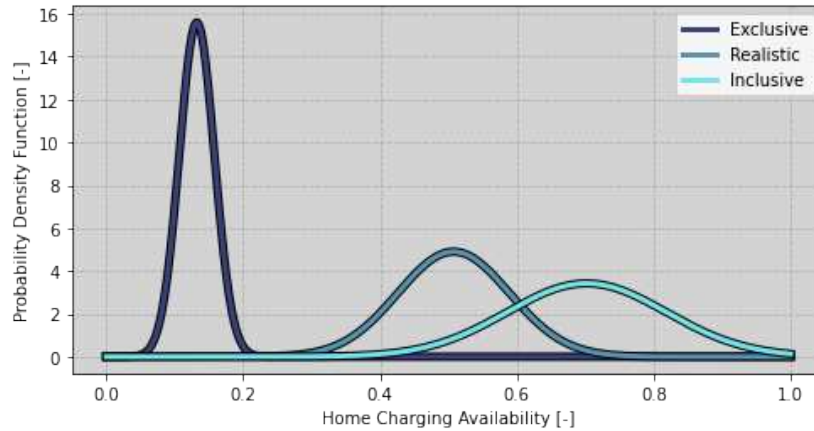


Figure 5.15: HC PDF comparison for H3 hex cells in Denver Colorado urbanized area

5.9.6 Assumed Values

Relevant data was not available to the authors for setting values for BC, Work Charging (WC), and ERCR on a geometric basis. Constants were used for all three parameters for all geometries. The value used for BC was 80 kWh and represented a mid-range BEV usable battery capacity [192]. The value used for WC was 0.1. There is very little recent data on the availability of workplace charging in the US so this number was based loosely off of [206]. The value used for ERCR was 80 kW which is the upper end of DC level 1 charging rates [190].

5.10 Results

As seen in Figure 5.4, HC is majorly important in determining operator experience both on its own and in its interactions with other factors. The HC scenarios taken from [221] are used to model the range of possibilities for access to home charging based on housing type and tenure. Based on housing type and tenure data from the ACS, home charging availability can be computed on a geo-spatial basis. Combined with computed values for DCL and ERCP and assumed values for other factors S_{IC} can be computed for geometries. S_{IC} for H3 hex cells in the Denver Colorado urbanized area for all HC assumption sets are shown in Figure 5.16.

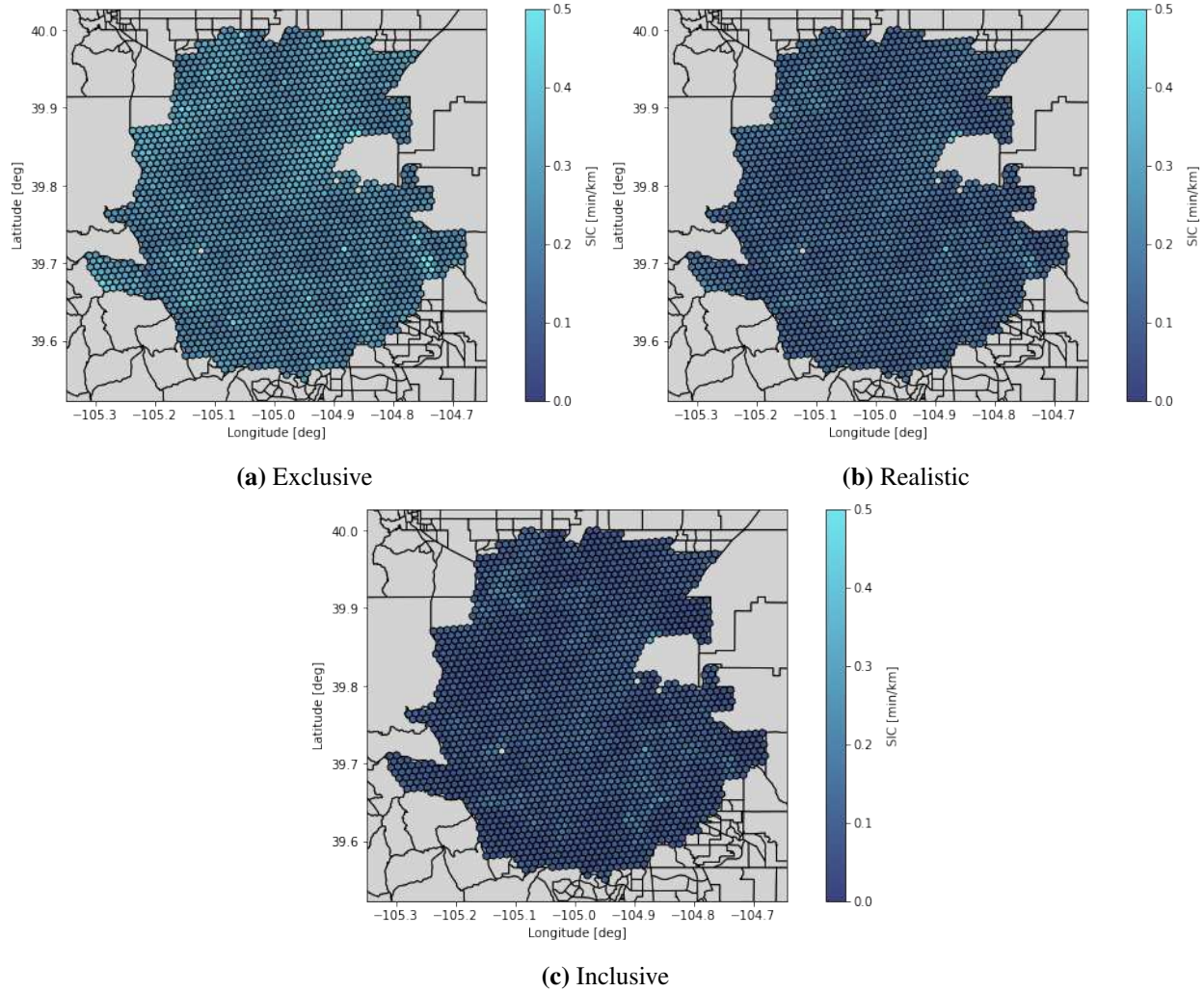


Figure 5.16: S_{IC} for H3 hex cells in Denver Colorado urbanized area

The different assumption sets for HC produce visibly different results which underline the importance of HC. For the exclusive assumption set wherein home charging is rare S_{IC} is high across the board and the distribution is dominated by availability of public charging. Because public charging is more plentiful in more densely populated areas these areas are seen as the most convenient for BEV operation. For the realistic and inclusive assumption sets home charging is far more common for all categories but still biased towards lower density housing and home ownership. Thus, for the realistic assumption sets, S_{IC} drops across the board but it drops most in the lower housing density areas. Based on assumptions about home charging availability the

direction of geo-spatial inconvenience inequity with respect to housing density may flip entirely. The effect on the PDFs of S_{IC} of HC assumption set is displayed in Figure 5.17.

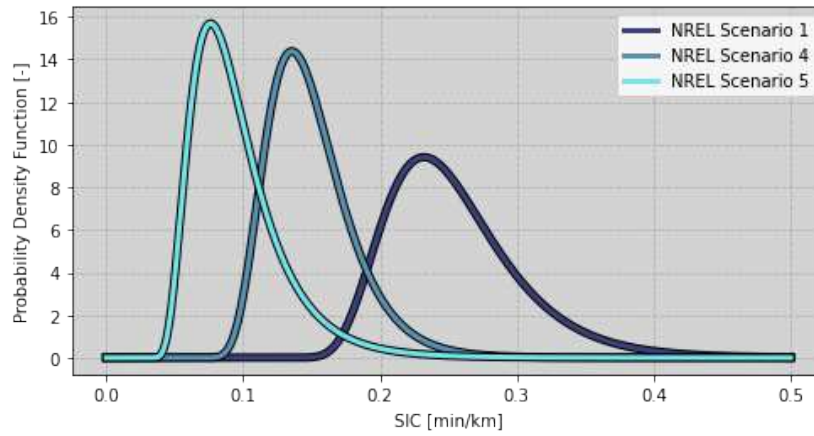


Figure 5.17: S_{IC} PDF comparison for H3 hex cells in Denver Colorado urbanized area

The differences between the distributions are significant at greater than 99% confidence. All distributions display a slight positive skew while the more inclusive distributions show decreasing kurtosis. Put together, the distribution characteristics indicate that a minimum level of inconvenience is to be expected no matter what and that the majority of residents within a greater urbanized area will have experiences which approach this value. Also indicated is that residents of under-served areas will have negative experiences which are more atypical than the positive experiences enjoyed in well-served areas.

5.11 Discussion

Results of this study showed the importance of long-dwell charging in determining BEV operational inconvenience. Because long-dwell charging can be most reliably conducted at home or workplaces the availability of chargers at these locations will make BEV operation far more convenient. However, the criticality of home and workplace charger availability should not be overstated. Public charging can play a large role in determining experience as well. In this study three home charging availability scenarios were considered based on [221]. The scenarios

included exclusive and inclusive scenarios meant to represent boundary cases and a realistic scenario meant as a best guess as to the actual conditions experienced. It is notable that the differences in home charging availability between the studies are larger than the differences in S_{IC} . The impacts of public charging infrastructure help to moderate the differences in home charging availability. This is in line with the charging pyramid model as discussed in 5.3. With the public charging infrastructure currently present in the Denver Colorado urbanized area it is still much more inconvenient to operate a BEV without reliable home charging. The results suggest that investment in public charging may help to reduce the inequities which manifests in the long tails in Figure 5.15 while investment in private charging will help most to reduce the mean and lower bound of S_{IC} .

S_{IC} as a metric of optimization for charging infrastructure is valuable because it tells a different story than other demographic measures. The most basic measure of EV charging inequity would be to compare the locations of chargers to demographic factors for given geometries. This is the approach taken by [211]. However, this method makes an implicit assumption that proximity to chargers will meaningfully correlate with experience. One major flaw with this method is that data on public chargers is far more complete than private chargers. Because of the importance of private chargers in determining experience the proximity method leads to an incomplete picture. The novelty of S_{IC} is demonstrated by comparing S_{IC} to other important demographic metrics. In Figure 5.18 population, percentage of single unit dwelling residents, median annual income, and percentage minority residents are plotted for hex cells in the Denver Colorado urbanized area where data is available.

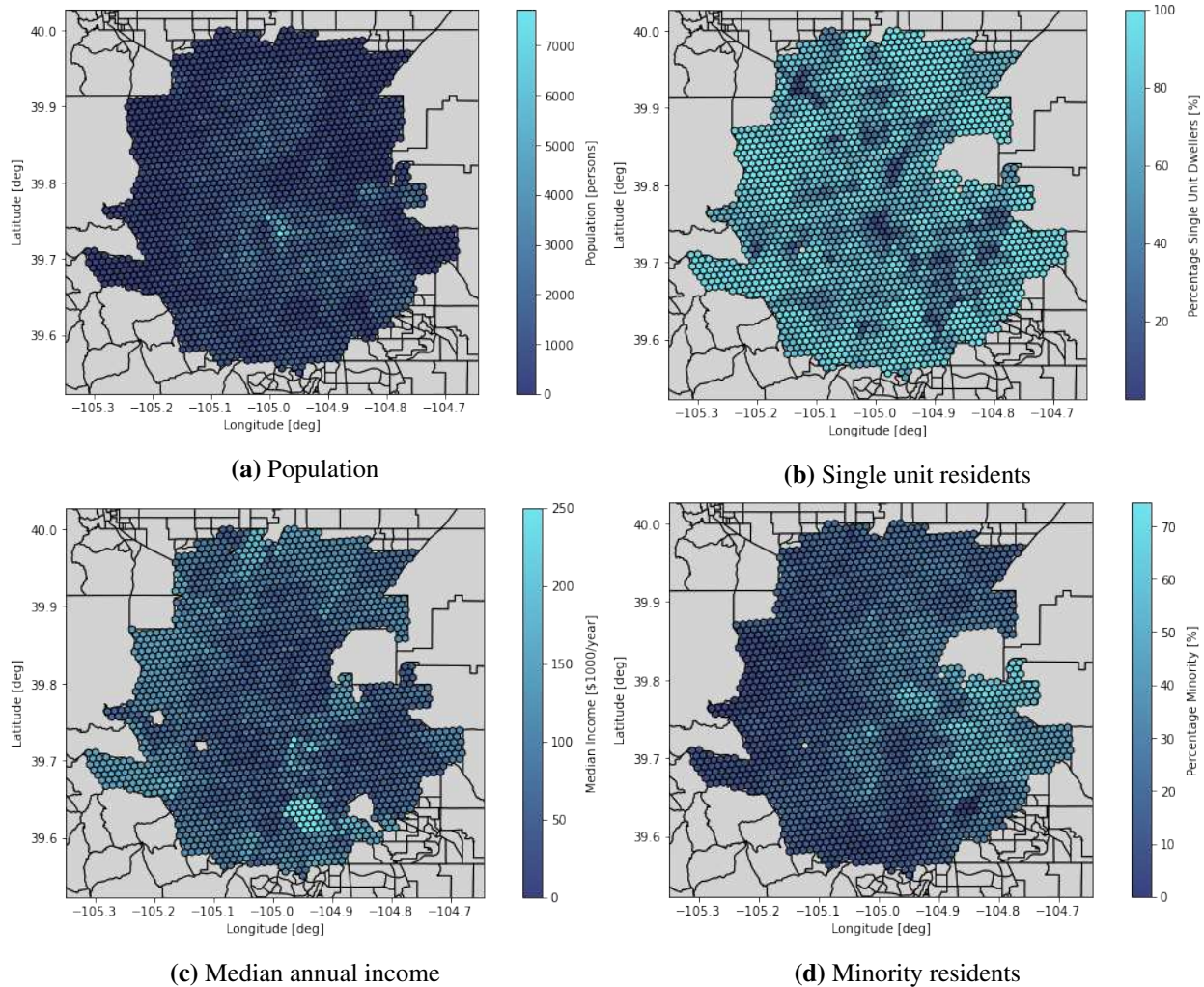


Figure 5.18: Demographic data for H3 hex cells in Denver Colorado urbanized area

As might be expected, there are relationships present between the plotted data. As must be the case, higher population hex cells also have lower percentages of single unit dwelling residents. Unfortunately it is also the case that an inverse relationship exists between percentage minority residents and median income. Neither of these relationships are particularly strong and neither tell a complete story. Rather relationships between the mentioned demographic factors are the result of long-term and complex processes which have resulted in much local variance; one does not reliably predict any other and none are redundant. That S_{IC} is also unique is supported by Figure 5.19.

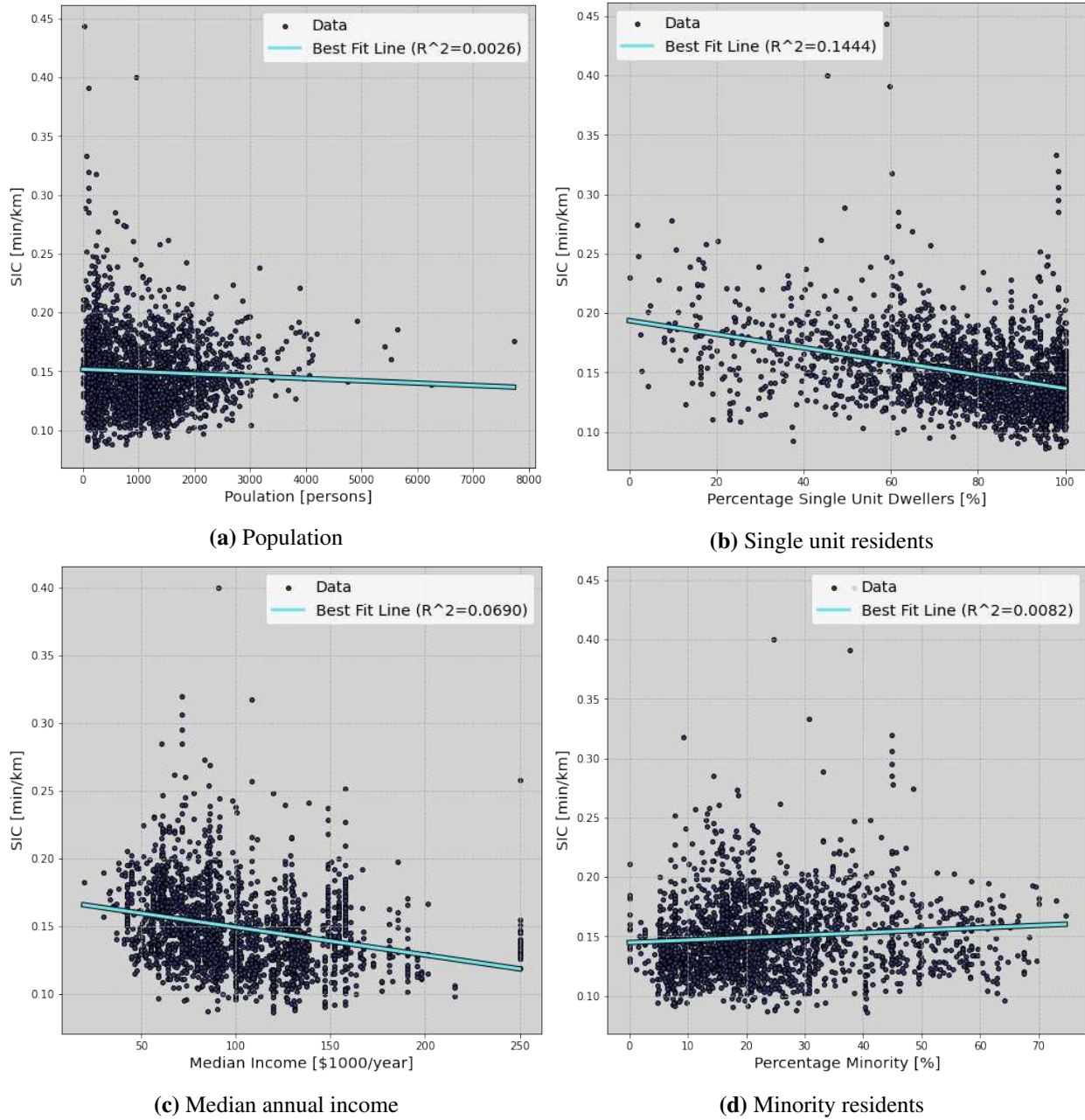


Figure 5.19: Demographic data for H3 hex cells in Denver Colorado urbanized area

The plots in Figure 5.19 show that no strong correlation exists between S_{IC} and any of the selected demographic factors. Nor does S_{IC} correlate strongly with simple measures of distance to chargers as evidenced by the comparatively minor coefficients for DCL and ERCP. The strongest

correlation exists between S_{IC} and percentage single unit dwelling residents and this may be explained by the direct use of the latter in computing the former.

5.12 Conclusions

The success or failure for the green transition in the US transportation sector will be decided by millions of individual decisions. Governments have the ability to influence these decisions through the application of personal and corporate incentives. An effective strategy can only be formulated if informed by the right metrics. In this study, the authors' previously developed metric S_{IC} is applied on a geo-spatial basis using publicly available data. An example of this application is conducted for the Denver Colorado urbanized area which is a representative large US metropolitan area. The results of this study show that BEV operational inconvenience, and thus user experience, due to charging times is effected significantly and in different ways by public and private charging. Where private charging such as at homes or workplaces serves to lower the lower bound and mean inconvenience due to charging. Public charging serves primarily to reduce inequity of experience thus making BEVs more feasible to those with limited private charging options. Also shown is the uniqueness and novelty of the S_{IC} metric as applied on a geo-spatial basis which provides a more complete picture than simple charger proximity based metrics. The S_{IC} metric provides planners with a direct approach to evaluating the impacts of proposed EVSE infrastructure investments in terms of their impact on BEV experience, equity, and ultimate adoption potential.

5.13 Summary

The purpose of research directed towards RQ2 was to understand the relationship between vehicular design and EVSE infrastructure parameters and BEV operational inconvenience. Having derived an empirical relationship between the factors and inconvenience in Chapter 4, this equation was applied in a geo-spatial context in this chapter. Using this equation, inequities can be shown geographically and compared to demographic factors. Using Denver Colorado as a case study it

is apparent that BEV inequity of experience is multi-causal not well predicted by socio-economic factors.

Chapter 6

Class 8 BEV Tractor Economic Modeling

6.1 Preface

This chapter is based on work that has not yet been prepared for publication. Data from this analysis was provided by EPRI. The content of the paper addresses RQ3. RQ3 sought to identify areas where class 8 Battery Electric Vehicle (BEV) tractors could be competitive with Internal Combustion Vehicle (ICV) equivalents. In order to accomplish this, Total Cost of Ownership (TCO) models were built for class 8 BEV and ICV tractors. A large operational difference between the two is the requirement to charge BEVs. The dynamics of BEV range and charging mean that, while low rate charging during dwells is desirable, high rate charging may be necessary to complete long itineraries. The degree to which a truck is required to utilize fast charging will have a substantial effect on operating costs both due to charging costs and due to driver time lost to charging. The BEV TCO model used in this analysis improves on previous studies by accounting for this dynamic with a data based modeling and simulation method. The TCO models are used to identify market niches wherein BEVs are and will become competitive thus answering RQ3. Finally a sensitivity analysis is performed on model parameters in order to understand how evolution in constituent factors may effect results.

6.2 Introduction

The US economy relies on a fleet of nearly 40 million commercial trucks which move more than 70% of the nation's freight tonnage [35] and are responsible for 17.2% of US GHG emissions [36]. About 4 million of these trucks are class 8 tractors [37] which haul the most freight per vehicle and have the highest energy consumption rates. In order to mitigate the environmental impact of the transportation sector, government and industry have pushed for increasing vehicle electrification [34]. As a general rule, costs and difficulties associated with electric powertrains scale with energy

and power requirements. For Light Duty (LD) vehicles, BEVs have already achieved and exceeded TCO parity with equivalent ICVs [222, 223]. The economics are less favorable for delivery vans but still feasible [43]. Although Medium Duty / Heavy Duty (MD/HD) BEVs are currently on the market, they are generally more expensive than ICV equivalents without the benefit of subsidies and credits [224].

The issue comes down to fundamental characteristics of Lithium-Ion (Li-Ion) batteries [165]. Current state-of-the-art Li-Ion batteries have a specific energy of around 1000 kJ/kg [166]. Diesel fuel has a specific energy of 45.6 MJ/kg. The result of this disparity is that even though BEVs are more efficient than ICVs they often have less range than equivalent ICVs. In order to increase BEV range more battery must be added but doing so either increases overall weight or reduces payload capacity. The apparent trade-off between range and payload capacity is sometimes referred to as the "electric vehicle conundrum" within the trucking industry [225].

The second disadvantage BEVs experience is in relation to energizing times. Diesel contains 136.6 MJ per gallon [170]. At a fueling rate of 7 gallons per minute [171] a diesel ICV is energizing at 15.94 MW. By comparison, modern DC Fast Charging (DCFC) occurs at 80-400 kW [190] for LD with some early commercialization of charging rates up to 1 MW for MD/HD vehicles [226]. Charging at higher rates is more expensive [227] and leads to higher battery cell degradation [228]. Slow charging rates are an issue because charging a BEV counts as work time for truck drivers if conducted outside of the mandatory 30 minute driving break [229]. Should a BEV need to travel for a longer daily distance than its full-charge range, significant driving time may be lost to charging.

The economic disadvantages inherent to MD/HD BEVs are important because adoption of BEVs in the MD/HD market will likely be driven principally by economic factors. In order to drive adoption of BEVs in the MD/HD market, MD/HD BEVs must be developed to be economically competitive with MD/HD ICVs in a number of market segments. The market segment which will be most effected by the scaling of costs is class 8 tractors. Class 8 tractors are, however, both economically vital and relatively environmentally costly making electrification relatively

impactful. In this study, the economic viability of class 8 BEV tractors is quantified and, based on the results of the study, implications for the future of the US transportation industry are discussed.

6.3 Literature Review

6.3.1 HD BEV TCO

Considerable effort has been expended into identifying markets in which BEVs can currently and in the future compete with ICVs. Strong evidence exists that TCO parity has already been achieved for many LD vehicles [222]. TCO parity is harder to achieve in the MD/HD market. MD/HD vehicles have higher energy consumption rates and, on average, higher range requirements [37] than LD vehicles. Thus MD/HD vehicles require greater energy storage and higher charging rates. The greater energetic requirements of heavier duty vehicles disadvantage BEVs in three related ways. First, the specific energy of modern Li-Ion Electric Vehicle (EV) batteries is much lower than that of liquid hydrocarbon fuels [230, 231] meaning that for equal range vehicles the BEV will be heavier. The added weight of BEVs somewhat reduces the efficiency advantage that electric powertrains hold over internal combustion powertrains. Added vehicular weight will also lead to reduced payload capacity for commercial BEVs. Second, current Electric Vehicle Support Infrastructure (EVSE) cannot charge EV batteries at rates comparable to the equivalent energizing rate of ICV fueling. Charging at higher rates is less efficient [232], requires more expensive vehicular and supply equipment [233], and places higher requirements on the electricity grid [234]. For this reason, the most common pattern for BEV usage is to charge at low rates while the vehicle is at rest [32]. Finally, BEV battery packs are difficult and expensive to manufacture. Assessments of the current per-unit-energy price of EV battery packs vary considerably by the source [235–240] with even higher uncertainty for future prices. BEV manufacturing costs are driven by battery pack prices. [42] assesses that the powertrain for an ICV class 8 sleeper tractor (engine and transmission) costs \$40,600 while an equivalent BEV powertrain (motor and single-speed transmission) costs \$18,400. However the battery pack for the equivalent BEV is assessed to cost \$382,200.

6.3.2 Battery Pricing

Because battery prices are so high, any TCO analysis will be sensitive to assumptions about battery price [38–40, 42]. This is a particular issue because battery price is an uncertain parameter, even in the present. There is a large corpus of literature on battery pack prices for LD vehicles. There are two general approaches which can be used independently or in combination. The first approach is the "bottom-up" approach which attempts to estimate future EV battery pack prices from projected component prices. Examples of bottom-up approaches to estimation are [236, 237] and Argonne National Lab (ANL)'s BaTPaC model [241]. Published in 2017, [236] provides a comprehensive review of studies published between 2007 and 2015 on the subject of EV battery pack costs. The survey found large disagreement and uncertainty among the reviewed studies. A general trend from [236] is that estimates drop from the \$600 to \$1,000 per kWh range in 2010 to \$400-\$800 per kWh in 2015 to \$200-\$400 in 2020 and beyond. The values from [236] are consistent with BaTPaC. Per [241], estimated prices for Li-Ion EV battery packs fell from roughly \$1,000 per kWh in 2008, down to \$400 per kWh in 2012, and to less than \$200 per kWh in 2022. [236] also conducted a Subject Matter Expert (SME) survey in which the SMEs were asked to fill in values for battery pack component prices. The results suggested a higher range of \$300-\$500 per kWh. The disagreement between market assessments and component-based cost models may be caused by SMEs over-costing certain components or may be the result of EV battery pack manufacturers or their suppliers experiencing the significant per-unit cost benefits of large scale production. The effects of production scale on manufacturing costs for modern EV batteries were investigated in [237]. Findings suggest that costs decrease exponentially with scale until about 5 GWh production then linearly after.

The second approach is a "top-down" approach which projects future battery pack prices based on data using a learning curve model [242–244]. Learning curve models, on their own, are insufficient to deal with the complexities of the battery production process. Reference [235] compared several top-down models and found that these models often resulted in battery prices

falling below projected materials costs by 2030. To remedy this issue [235] proposed a 2 stage learning curve model wherein the initial and mature stages of production are treated separately.

The broad agreement in the literature is that EV battery pack prices are set by a combination of materials acquisition and manufacturing costs. As demand for EV batteries increases, supply of raw materials is not expected to keep pace [235] which should result in rising raw material prices. Increasing demand should also lead to lower manufacturing costs due to innovation and economy-of-scale effects. Eventually, thus, EV battery pack prices should approach raw materials prices. How fast battery pack prices approach materials prices and what those prices will be at that time is contingent on the pace of EV adoption and general battery demand. Based on historical prices, it seems that the period of exponential decreases in Li-Ion battery pack prices has already occurred and reductions in price for Li-Ion battery packs will be incremental in the future. In the context of the literature, US Department of Energy (DOE) targets of \$80-\$100 per kWh for EV batteries [245] seem achievable in the medium term future for LD EVs. It is also possible that targets will be exceeded with advanced battery chemistries [235, 243, 246] but the functionality of these chemistries and the infrastructure investment required to enter large scale production will be a challenge [238–240].

6.4 Baseline TCO Model

The baseline TCO model used was based on National Renewable Energy Laboratory (NREL)'s TEMPO [38–40] model. TEMPO is a common and comprehensive model for projecting TCO for vehicles of various types, classes, and powertrains in the near through long term future. TEMPO's model largely uses data from Autonomie [247] which is collected and managed by ANL. The model is oriented towards light-duty BEVs and there is reason to think that some of the model's scaling assumptions are invalid for heavier vehicles. Nevertheless, TEMPO is a good comparison point and CSU's model was built with a similar structure and validated against it. In this section the basic structure of the CSU model is outlined with TEMPO assumptions and the CSU model outputs are validated against TEMPO.

In order to evaluate the economic competitiveness of vehicles in a scalable manner, the metric chosen was TCO which is the net present value of the vehicle’s total cash flows over its term of use. The cash flows considered in this analysis are listed below. An assumption is made that all vehicle purchases are financed. Cash flows in CSU’s TCO model are listed in Table 6.1.

Table 6.1: TCO Model Cash Flows

Cash Flow	Description
Vehicle	The cost of purchasing the vehicle with financing with the salvage value subtracted
Energy	The recurring costs of energizing the vehicle
Insurance	The recurring costs of insuring the vehicle
Maintenance	The recurring costs of maintaining the vehicle
Taxes and Fees	The recurring costs of taxes and fees on the vehicle.
Payload	The equivalent cost of lost payload capacity due to vehicle technology
Labor	The recurring costs of salaries and benefits for drivers and other personnel
Capacity	The equivalent cost of the payload capacity lost due to added tractor weight
Time Loss	The equivalent cost of the driving time lost due to en-route charging for BEVs (Not included in TEMPO)

With the exception of the Time Loss cash flow, which will be defined in Section 6.5, the cash flows used in CSU’s model were the same as those used in TEMPO. The Net Present Value (NPV) of the cash flows is calculated as in (6.1) with an assumed constant discount rate

$$NPV = \frac{CF_t}{(1+d)^t} \quad (6.1)$$

where CF_t is the cash flow in a given time period t and d is the discount rate. TCO is calculated as in (6.2)

$$TCO = \sum_{CF} NPV(CF) \quad (6.2)$$

where \overline{CF} is the set of cash flows. The methods of calculating the cash flows found in CSU's baseline model are described in the following subsections.

6.4.1 Vehicle Cash Flow

The Vehicle cash flow contains the net values of the vehicle purchase price, financing cost, and salvage value. The purchase price of the vehicle is based on the prices of the vehicle's components and a retail markup. The salvage value of a vehicle is based on both distance driven and calendar depreciation. The pricing models used for the subsystems are taken from Autonomie and [248–250]. All costs are assumed to scale with power or energy storage linearly. The vehicle cash flow is sufficiently different for ICVs and BEVs to merit independent explanations.

ICV Vehicle Cash Flow

ICV component costs are fairly straightforward. Based on data from previously mentioned sources, ICV component costs are listed in Table 6.2.

Table 6.2: ICV component costs

Component	Cost Formula	Source
Glider	\$82,200	[247, 248, 251]
Engine	\$47.50 per kW	[249, 250]
Exhaust System	\$20 per kW	[248]
Transmission	\$21.50 per kW	[248]
Fuel Tank	\$6 per kWh	[248]

An assumed retail markup of 50% [38] is applied to the summed component costs. Financing is modeled as a standard fixed-payment lease with a term of 63 months, a down-payment of 12% and an interest rate of 4% [38]. The salvage value for ICVs is modeled as a function of age and distance driven as shown in (6.3)

$$S_a = C(.9071)^a(.9990)^m \quad (6.3)$$

where S_a is the salvage value of the vehicle in year a , C is the initial purchase price of the vehicle, and m is the distance driven in units of 1000 miles. In other words, a class 8 sleeper cab ICV is expected to retain 90.71% of its value every year and 99.9% of its value every 1000 miles (1609 km) driven. The baseline assumption is that a new truck will be used for 10 years and travel 870,000 miles (1,399,830 km) in that time frame. Table 6.3 lists the vehicle cash flow components for a sleeper cab class 8 tractor with 5000 kWh fuel storage capability and a 212 kW engine [141].

Table 6.3: ICV Vehicle cash flow components (2020 USD)

Component	Description	Cost
Vehicle Component Costs	Sum of costs of individual components	\$97,821
Retail Markup	Difference between component costs and retail price	\$48,911
Financing	Difference between NPV of loan and retail price	\$9,895
Salvage	Value that the vehicle can be sold for at any given time	\$20,574
Total	Total NPV of the cash flow	\$136,053

BEV Vehicle Cash Flow

For BEVs the components are broken down into the major areas of glider, battery, motor, inverter, and auxiliary systems. The major auxiliary systems on a BEV are the transmission, charger, and DCDC converter. There are very few class 8 BEVs currently on the market and, as such, it is difficult to model the costs of components due to lack of data and the effects of low volume production. The major driver of cost for BEVs is the battery. TEMPO uses Autonomie modeling for the cost of batteries per unit capacity. Autonomie modeling of battery prices does not distinguish between vehicle classes and LD prices are used for MD/HD vehicles. Autonomie posits high and low technological progress scenarios for battery pack pricing. [41]. These scenarios are visualized in Figures 6.1 and 6.2.

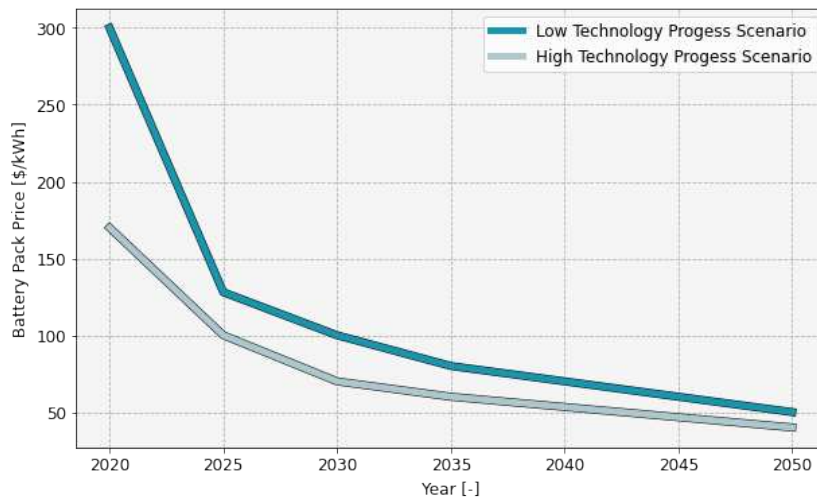


Figure 6.1: Battery pack cost scenarios

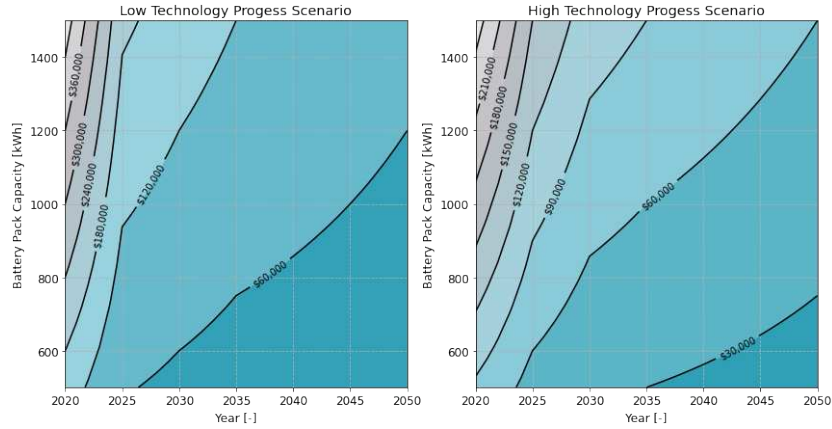


Figure 6.2: Battery pack cost scenario contours

Battery pack mass is also an important economic factor given that increased mass will mean lower efficiency when empty and lower maximum payload capacity. In this respect, cell specific energy is the driving factor and may play a large role in determining the economic viability of MD/HD BEVs. The cell specific energy projection is shown in Figure 6.3.

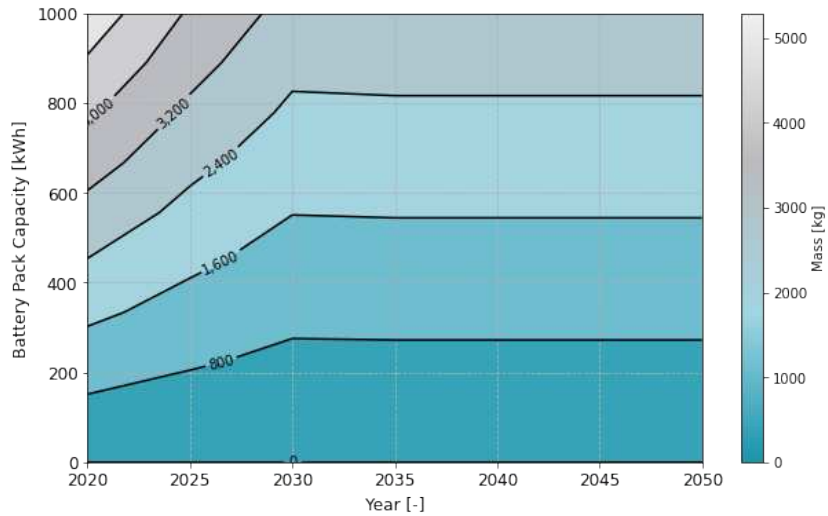


Figure 6.3: Battery pack mass by capacity and year of manufacture

The motor, inverter, and auxiliary costs are modeled to scale with power. The models are based on Autonomie data and are presented in Figure 6.4.

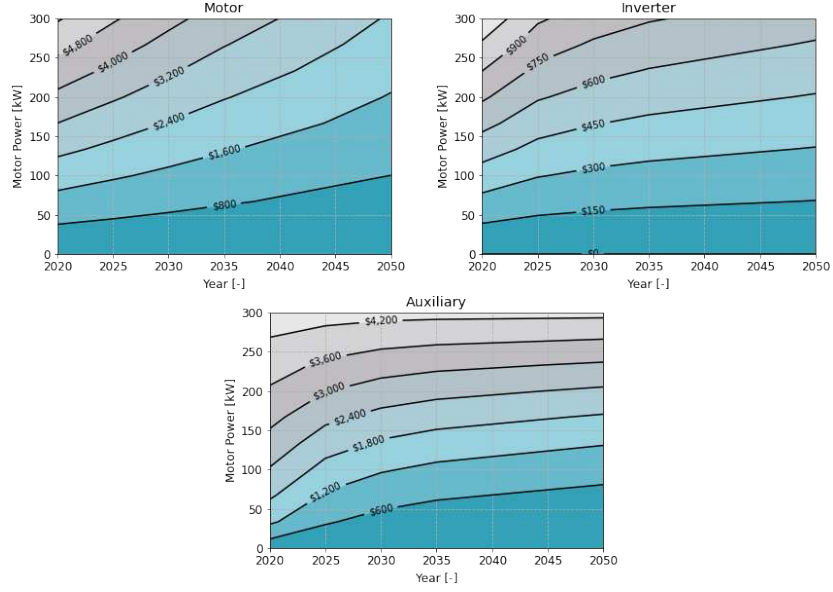


Figure 6.4: Motor, inverter, and auxiliary systems cost by capacity and year of manufacture

The purchase price for the BEV model is computed by summing the vehicle costs, applying the retail markup, and subtracting the salvage value at the end of the term-of-use. Because class 8 BEV production is currently very low volume, the markup is initially higher than that for equivalent ICVs. The markup is estimated using a learning curve formula starting at 70% in 2020 and reducing to 50% in 2050. For BEVs salvage value is computed separately for the battery pack and for the rest of the vehicle. This accounts for the different aging curves for the battery cells and for the mechanical components of the vehicle. As with the ICV model, the depreciation of the non-battery components of the vehicle is modeled using (6.3). The battery pack depreciation is modeled as in [252]. The formula for battery pack depreciation is

$$V_{salvage} = (1 - K_r - K_u)(1 - K_h Y)(V_{new})(1 + M) \quad (6.4)$$

Where V_{new} and $V_{salvage}$ are the battery pack value initially and at salvage respectively, K_r is the refurbishment cost factor valued at 15%, K_u is the used product discount factor valued at 15%, K_h is the battery health factor valued at 3% per year, Y is the age of the vehicle, and M is the

retail markup valued at 50%. Table 6.4 shows the vehicle cash flow components for a class 8 BEV sleeper tractor with 800 km of nominal range.

Table 6.4: BEV Vehicle cash flow components (2020 USD)

Component	Description	Cost
Vehicle Component Costs	Sum of costs of individual components	\$586,908
Retail Markup	Difference between component costs and retail price	\$410,835
Financing	Difference between NPV of loan and retail price	\$67,286
Salvage	Value that the vehicle can be sold for at any given time	\$119,705
Total	Total NPV of the cash flow	\$945,324

6.4.2 Energy Cash Flow

The energy cash flow constitutes the periodic expenditure on energy required to complete the vehicles workload. The amount of energy expended in a given year is a function of the vehicle, yearly driving distance, and driving conditions. TEMPO uses operating data from the 2002 (most recent) Vehicle Inventory and Use Survey (VIUS) [37]. The distribution of miles driven by load range from VIUS is displayed in Figure 6.5.

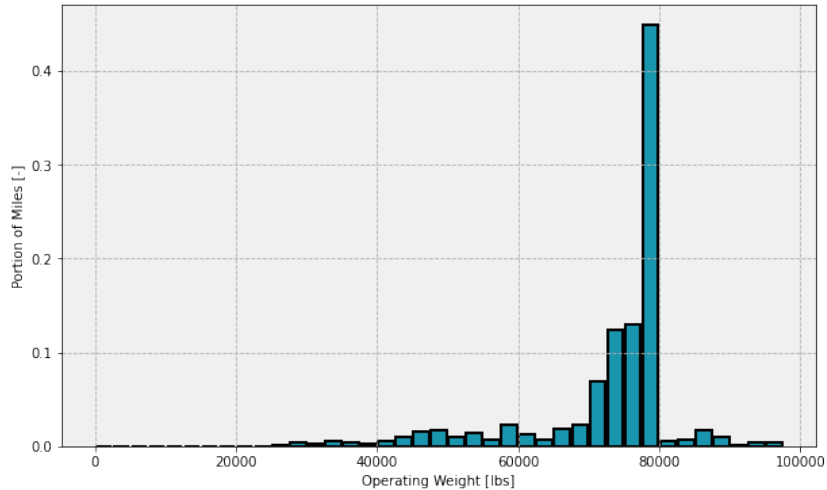


Figure 6.5: Distribution of miles driven by load for class 8 sleeper tractors (2002 VIUS)

The weighted average of load by miles driven in VIUS was 73,446 lbs (33,314.5 kg) for class 8 sleeper tractors. The efficiencies and ranges in Table 6.5 were calculated using the mileage-weighted average load.

Table 6.5: Class 8 sleeper tractor loaded fuel economy and range from TEMPO

Powertrain	Fuel Economy [mpgde] 2020	Fuel Economy [mpgde] 2025 Low	Fuel Economy [mpgde] 2025 High
ICV	6.66	7.17	8.27
BEV	11.59	12.60	14.67

The distribution of class 8 sleeper tractor Vehicle Miles Traveled (VMT) from the 2002 VIUS is shown in Figure 6.6. Per VIUS, class 8 sleeper trucks drive roughly 75,500 miles per year on average. VIUS includes a large group of trucks with extremely low VMTs, if this group are dropped the average annual VMT moves up to roughly 87,000 miles. The 87,000 mile figure was used for calculations.

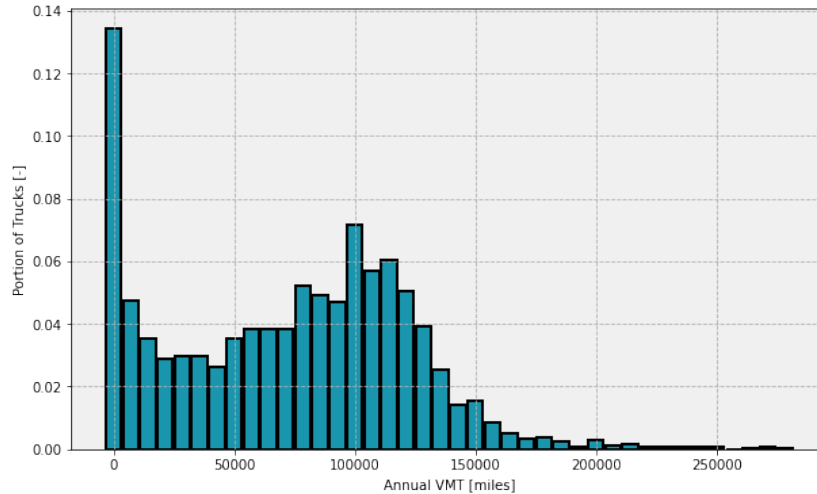


Figure 6.6: Distribution of annual VMT for class 8 sleeper tractors (2002 VIUS)

The final component of the Energy cash flow is energy pricing. The TEMPO value for the price of diesel is \$3.08 per gallon in 2020 USD. The TEMPO value for the price of electricity for charging purposes is \$0.123 per kWh or \$4.76 per diesel gallon equivalent in 2020 USD.

6.4.3 Insurance Cash Flow

Based on data from [38, 253] insurance is assessed at \$0.065 per mile driven for freight trucks in 2020 USD.

6.4.4 Maintenance Cash Flow

Maintenance cost data is taken from Autonomie. Maintenance is modeled as a function of vehicle age but not production year. The cost of maintenance should increase as the vehicle ages and parts degrade. Correspondingly, spare parts should become more expensive as vehicles age. Because of the relative simplicity of BEVs compared to ICVs, maintenance costs are lower for BEVs. In the TEMPO model BEVs and ICVs utilize the same maintenance cost vs. time relationship with a constant multiplier of 0.6 being applied for BEVs [38]. The per km cost of maintenance for both powertrain types is shown in Figure 6.7.

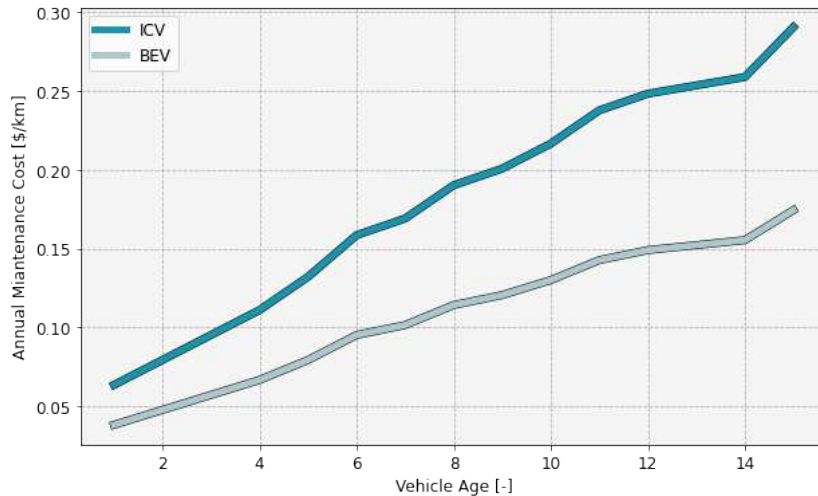


Figure 6.7: Maintenance cost per km driven for class 8 sleeper tractors

6.4.5 Taxes and Fees Cash Flow

Based on data from [38, 253] taxes and fees are assessed at \$0.065 per mile driven for ICV freight trucks in 2020 USD.

6.4.6 Labor Cash Flow

Based on data from [38, 253] labor is assessed at \$0.79 per mile driven for freight trucks in 2019 USD.

6.4.7 Payload Cash Flow

The maximum total weight that a vehicle can operate at is set by Department of Transportation (DOT) regulations. For class 8 trucks, the maximum operating weight is 80,000 lbs (36,287.36 kg). BEVs are allowed an extra 2,000 lb (907.184 kg) [38]. Because of the maximum total vehicle weight limit, extra tractor weight means lower payload capacity. It is important to account for payload capacity loss due to tractor weight because BEVs are significantly heavier than equivalent ICVs due to battery pack weight. Two assumptions are made about the type of fleet operators considered in this study. First, the fleet operators are assumed to be Less Than Truckload (LTL) operators meaning that the individual parcels transported weigh much less than the truck payload

capacity. Thus LTL operators have the flexibility to assign packages to trucks such that all packages can be transported, all trucks are mostly filled, and no truck is over limit. Second, it is assumed that the fleets are of sufficient size that a reduction in per-truck capacity on a given route can be made up by sending more trucks on that route without inordinately effecting shipping costs.

With the previously stated assumptions, the value of lost payload capacity for a given truck can be computed by calculating the percentage of an identical truck that would be required in order to move the lost payload. The first step to computing the lost payload capacity cost is to compute the Lost Payload Capacity Portion (LPCP). The equation for the LPCP (6.5) is

$$LPCP = \frac{P_L}{G - W_T} \quad (6.5)$$

where P_L is the payload capacity lost, G is the Gross Vehicle Weight Rating (GVWR) of the vehicle, and W_T is the weight of the tractor. P_L is calculated as in (6.6)

$$P_L = \int_{G-\Delta W}^G P(W) dW \quad (6.6)$$

where ΔW is the additional weight of the tractor over a baseline tractor, W is the total loaded weight of the vehicle and $P(W)$ is the probability of the truck operating at W . For the baseline tractor weight TEMPO uses an equivalent range diesel tractor. The distribution of miles driven within weight ranges is provided in Figure 6.5 and the CDF of the distribution is shown in Figure 6.8.

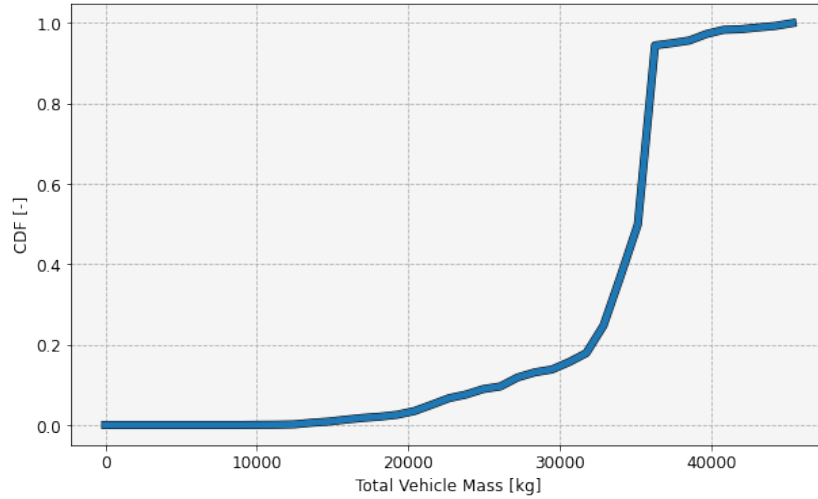


Figure 6.8: CDF of miles driven by load for class 8 sleeper tractors (2002 VIUS)

The NPV of the Payload cash flow can be computed by multiplying the sum of the NPVs of the other cash flows by the LPCP. The NPV of the Payload cash flow by battery capacity and model year is displayed in Figure 6.9. The value of the Payload cash flow is expected to become insignificant in the 2030s due to battery specific energy increases.

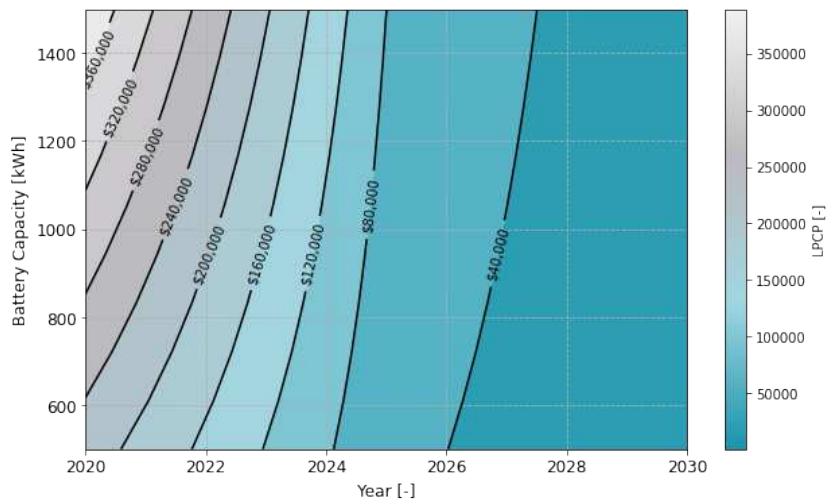


Figure 6.9: NPV of Payload cash flow by battery capacity and model year

6.4.8 Summary

CSU’s TCO model for class 8 sleeper tractors produces results which are very similar to TEMPO results when using TEMPO assumptions. Figure 6.10 displays the assessed TCO for 800 km nominal range, model year 2025 ICV and BEV class 8 sleeper tractors. All trucks were assumed to be bought new in 2025, used for 10 years, and then sold, while driving 87,000 miles (139,983 km) per year.

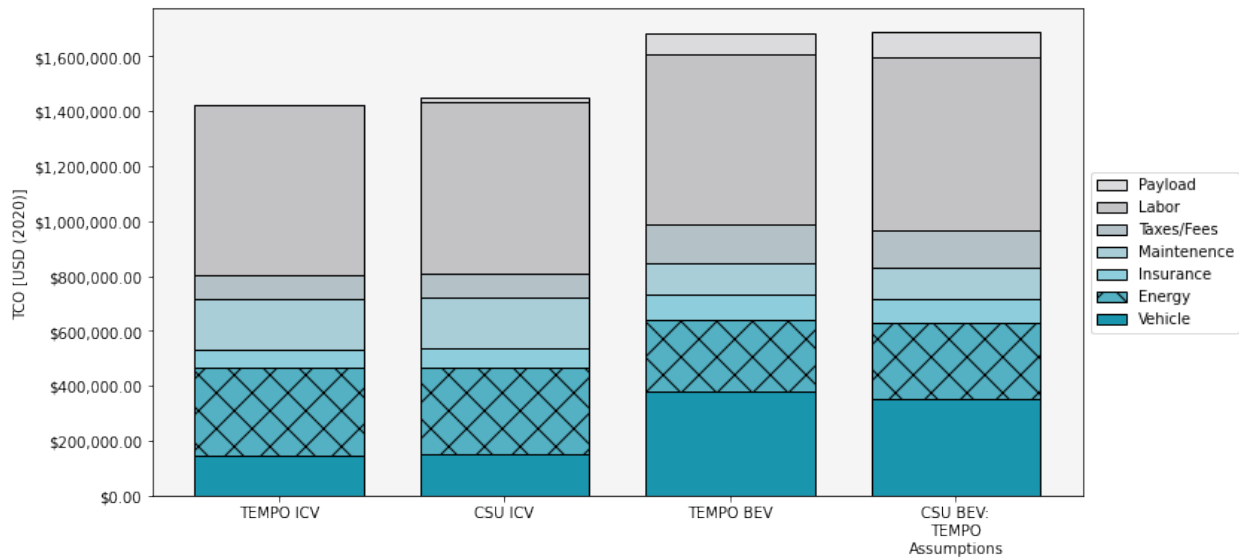


Figure 6.10: TCO for ICV and BEV model year 2025 class 8 sleeper tractors from TEMPO and CSU model with TEMPO assumptions

A minor difference between TEMPO and CSU’s model is in how the payload cost is evaluated. TEMPO uses the payload capacity of an ICV truck as the baseline for computing payload cost. CSU uses a constant value of one third of class 8 GVWR. Thus the CSU model shows the ICV as having a small payload cost while TEMPO shows no payload cost for the same vehicle. The decision to compute the payload cost against a constant value was made because the weights of class 8 ICV tractors with the same nominal range can differ [248]. Because TEMPO’s 800 km nominal range ICV tractor weighs more than the constant weight used by CSU, the CSU model shows slightly higher payload costs.

6.5 Modified TCO Model

In the previous section, a TCO model which mimics TEMPO [38–40] was defined. This model used TEMPO assumptions and arrived at results which very closely matched TEMPO results. In this section that model will be modified to reflect certain complexities not represented in TEMPO's modeling. The structure of the modified model will be identical to that of the baseline model with some cash flows modified and the addition of the Time Loss cash flow. The modified and added cash flows are defined in the following subsections.

6.5.1 Modified Vehicle Cash Flow

TEMPO's model for battery pricing through time is based on projections for LD vehicles. LD vehicle manufacturers enjoy economies of scale not seen in the MD/HD market, especially in the class 8 segment. The scale of LD vehicle production allows Original Equipment Manufacturers (OEMs) to negotiate low prices with battery suppliers and to lower the per-unit cost of manufacturing battery packs. Currently MD/HD BEV production is very low scale and might remain so in the future.

Based on data and arguments from [224, 235, 236] and consultation with an electric MD/HD OEM, Lightning e-Motors [254], three scenarios for EV battery pack pricing per kWh were developed. These scenarios, labeled "optimistic", "baseline", and "pessimistic" are displayed in Figures 6.11 and 6.12. All three CSU developed scenarios project EV battery pack prices higher than either Autonomie projection through to 2050. The CSU Pessimistic scenario projects that improvements to EV battery pack manufacturing will not be sufficient to offset increased commodity costs when EV batteries reach maturity. CSU's Baseline and Optimistic scenarios project that improvements to EV battery pack manufacturing will be sufficient offset increased commodity costs when EV batteries reach maturity but assume different rates of learning and different start points.

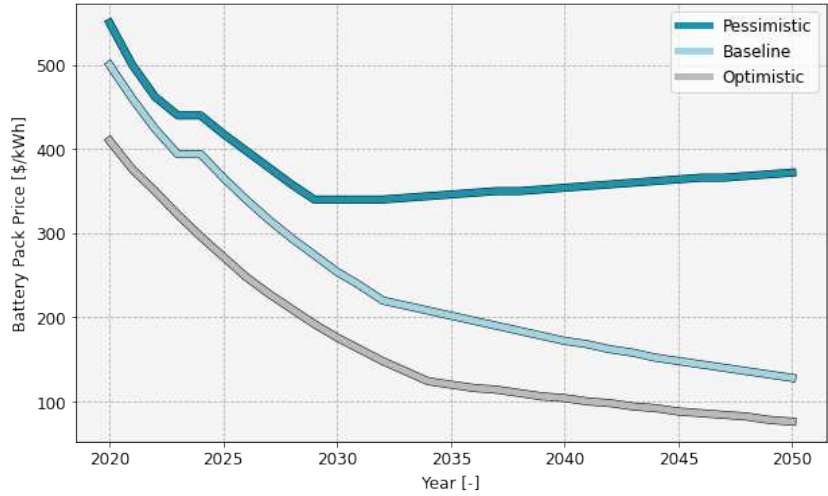


Figure 6.11: CSU battery pack cost scenarios

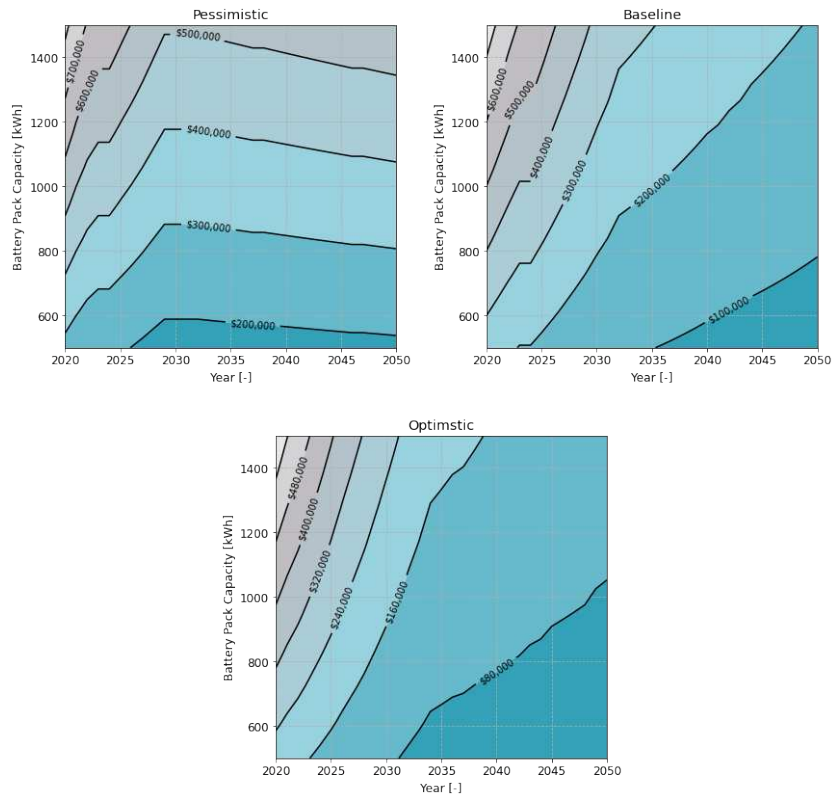


Figure 6.12: CSU battery pack cost scenario contours

Battery pack cost was the only difference between CSU's and TEMPO's Vehicle cash flow model. Nevertheless, battery pack prices play a large role in determining overall BEV TCO and, thus, the difference is important.

6.5.2 Modified Energy Cash Flow

Another major difference between CSU's model set and TEMPO is in how energy prices are modeled. TEMPO uses constant values for energy pricing regardless of time and location. However, fuel and electricity prices are volatile and depend on region. Electricity prices may also depend on power and energy consumption, time-of-day, and season among other factors. As seen in Figure 6.10, the Energy cash flow is behind only Labor and Vehicle in magnitude and is highly driven by energy prices.

Diesel Prices

US diesel prices are set on a global market and have historically been volatile subject to economic and political factors. The average US diesel price per gallon since 1995 [255] is shown in Figure 6.13.

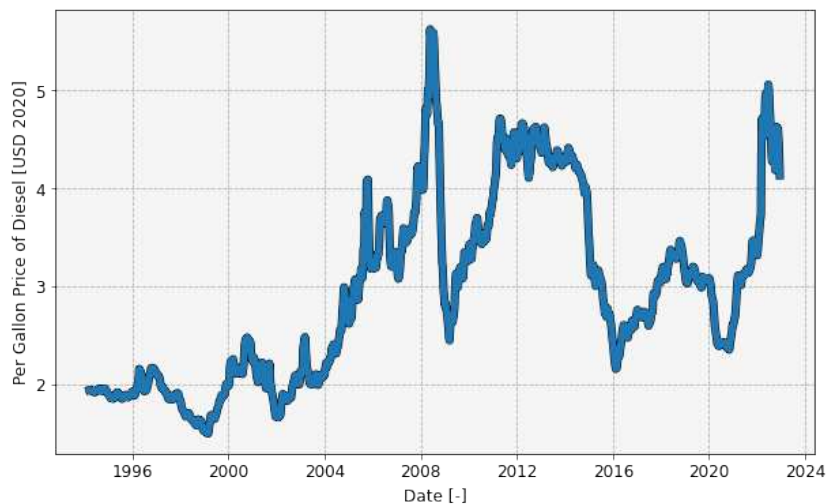


Figure 6.13: Historical diesel prices in 2020 USD

Commodity prices, especially in the energy sector, are hard to predict. The effects of market shocks such as the 2008 financial crisis and the Coronavirus pandemic are seen clearly in the historical diesel prices. The effects of economic globalization can be seen in the post-2000 prices with their higher mean and greater volatility. The price used in [38] was reasonable when it was published but is not reflective of greater trends in diesel price in the 21st century. CSU elected to use price data dating back 15 years to establish a range for prices. The mean price for a gallon of diesel in the previous 15 years was \$3.54 with a standard deviation of \$0.79 both in constant 2020 USD. The mentioned values are used in this analysis.

Electricity Prices

Electricity prices are, like fuel prices, set by market forces. However, while fuel prices are set daily based on short term futures contracts, electric utilities often offer yearly contracts with the cost of uncertainty built in. Thus, the volatility in the price of electricity has historically been lower. The yearly average US commercial electricity price per kWh since 1995 [256, 257] is shown in Figure 6.14.

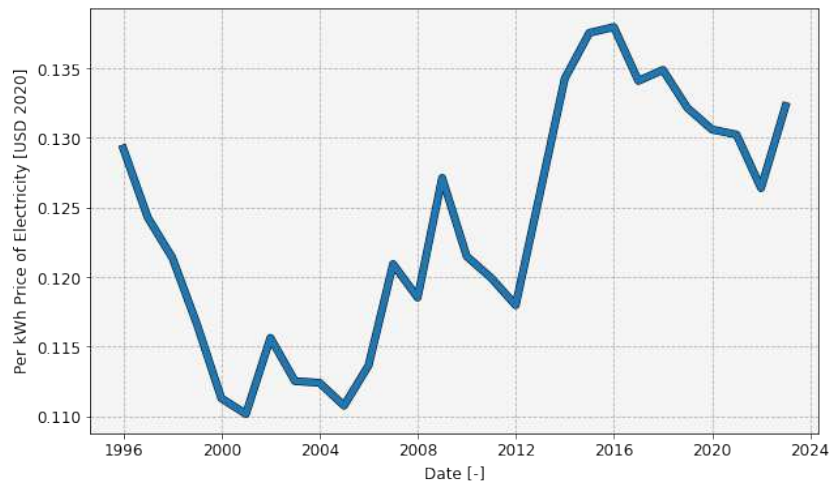


Figure 6.14: Historical commercial electricity prices in 2020 USD

In the last 15 years (2008-2023) the average US residential electricity price per kWh was \$0.1295 with a standard deviation of \$0.006 both in constant 2020 USD. The relatively small

constant dollar fluctuations seen in the historical residential electricity pricing data imply that future prices will also remain relatively stable.

Regional and TOU Pricing

The price of electricity is dependent on many factors including location, time of year, time of day, power requirement, plan type, and customer type (residential, commercial, industrial). Utility companies have to pay for and maintain the equipment required to meet their maximum power and energy delivery demands regardless of how often these capabilities are actually required. Thus, utilities offer Time of Use (TOU) tariffs which incentivise customers to spread demand out throughout the day and use less energy during times of year when more is required for heating or air conditioning. A general structure of a TOU tariff consists of an energy charge, a power charge, and a customer charge. The energy charge is a function of the total energy used during a billing cycle. The power charge is a function of the peak metered power used during a billing cycle. Peak power is measured as the amount of energy used during a meter cycle which are, often, 15 to 30 minutes in duration. The power charge is meant to pass on the cost of higher power delivery equipment to the customers who require it rather than to all customers. The customer charge covers the costs of metering equipment and labor. One can estimate the cost of a unit of energy with a TOU tariff as in (6.7)

$$C(E) = \left(R_E(M, T) + \frac{R_P(M, T) + R_C}{D_M} \right) E \quad (6.7)$$

where $C(E)$ is the cost of a unit of energy, R_E , R_P , and R_C are the energy, power, and customer charges respectively, M is the month, T is the time-of-day, and D_M is the duration of the month in seconds.

Electricity pricing plans used in this study were taken from [258] which compiled details of commercial and industrial TOU tariffs throughout the US in 2015. The rates from [258] were adjusted to 2020 USD. Figure 6.15 displays TOU tariffs in North Dakota, California, Massachusetts, and Alabama.

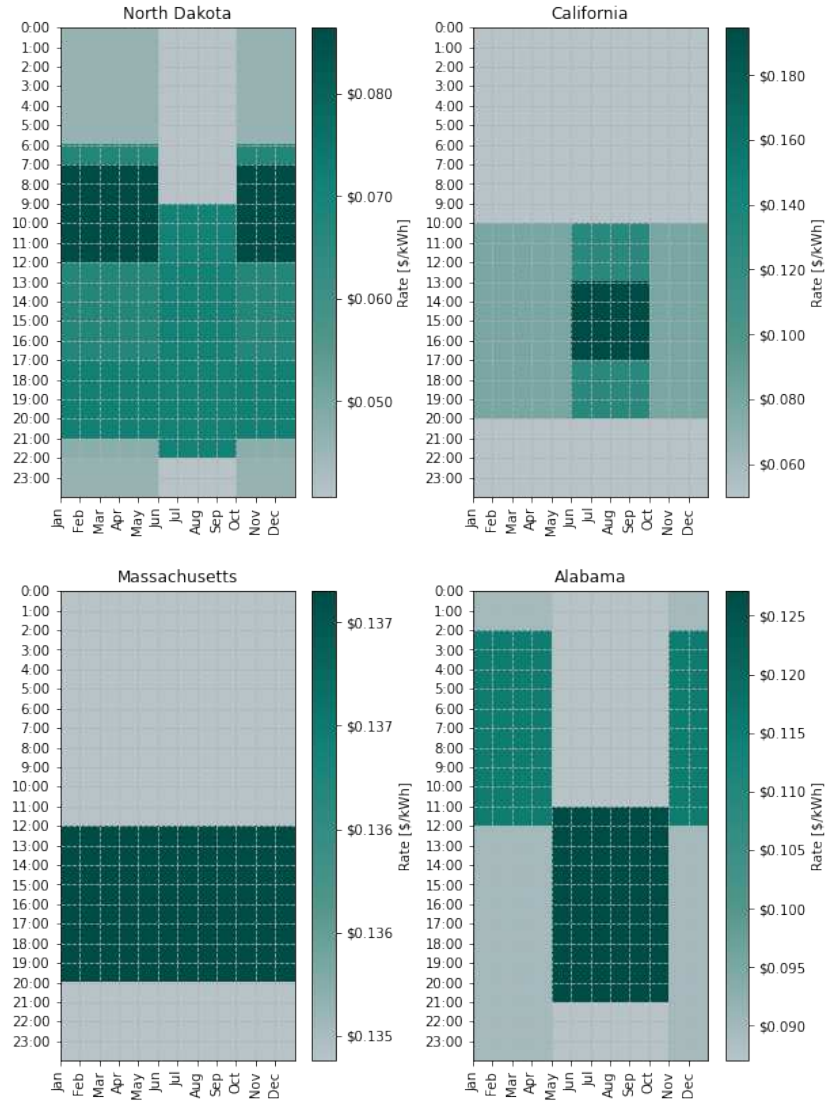


Figure 6.15: TOU tariffs in 4 US states

The selected states are from four different climatic and sociopolitical regions within the US and serve to demonstrate how local conditions effect TOU pricing. In literature, the heuristic that EVs should charge at night to save money is generally accepted. It is notable that this would be a bad strategy in southern states during the summer when residential air conditioning demand is high during evening hours. The strategy will also be of relatively little value in Massachusetts where the price of electricity is only marginally effected by time-of-day.

CSU’s model assigns electricity prices by location, month, and time-of-day. The data from [258] was used to produce temporal pricing for geometries throughout the US defined by level 3 H3 Hex cells [214]. The average, standard deviation, minimum, and maximum electricity prices for each geometrically defined model in the continental US are shown in Figure 6.16.

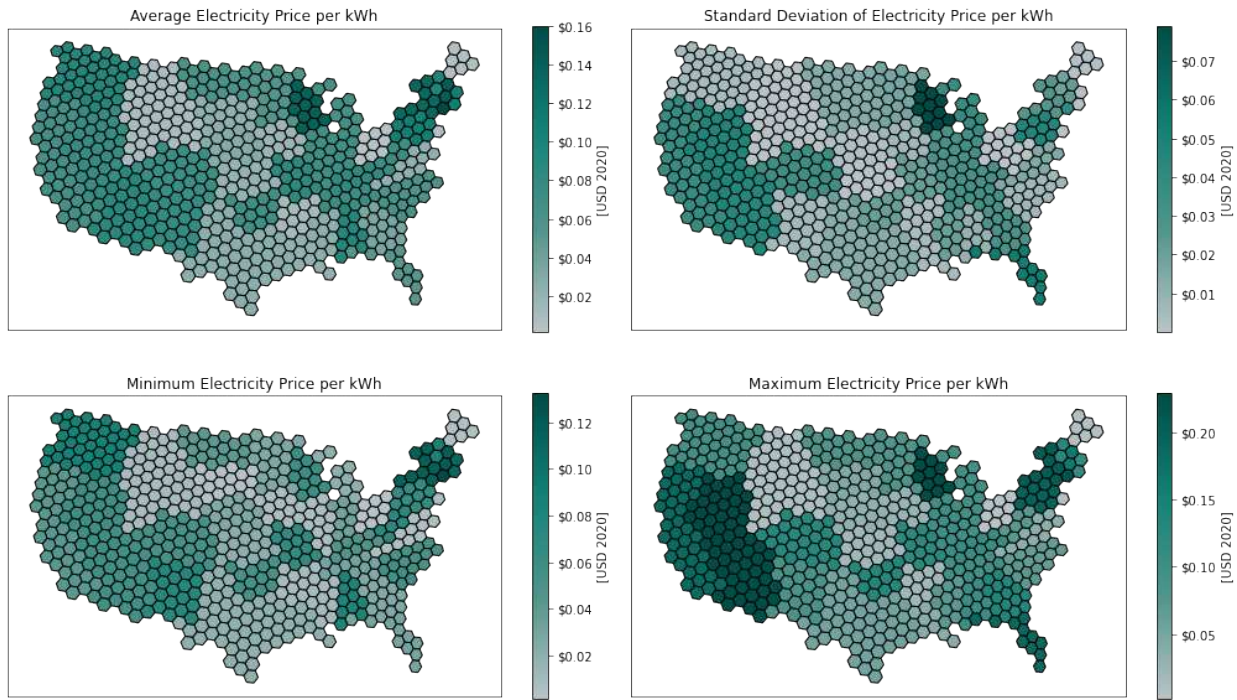


Figure 6.16: Electricity pricing in continental US by level 3 H3 Hex cell

Optimal Charge Scheduling

In order to minimize electricity expenses subject to a TOU tariff, optimal charge scheduling can be employed. The aim of optimal charge scheduling is to minimize the cost of charging for a vehicle over a given itinerary. In this case the cost is simply the dollar value of the cost of charging the vehicle. Vehicles have the ability to charge while parked at depot or at a charging station while en-route to a destination. Optimal charge scheduling was conducted via Dynamic Programming (DP) [76, 100]. The goal of the optimization was to find an optimal charging control such that the charging cost of the itinerary would be minimized. This goal can be stated as

$$\min_{\bar{U}} J(S_0, \bar{U}) \quad (6.8)$$

where

$$J(S_0, \bar{U}) = \Phi(S_N) + \sum_{k=1}^N \Psi(S_k, U_k) \quad (6.9)$$

s.t.

$$S_{k+1} = f(S_k, U_k), \quad k = 0, \dots, N-1 \quad (6.10)$$

$$S_{min} \leq S(t) \leq S_{max} \quad (6.11)$$

where $\Psi(\bar{S}, \bar{U})$ is the running cost (inconvenience), $\Phi(\bar{S})$ is the final state cost, $\bar{S} = [SOE]$ is the state vector containing the vehicle State of Energy (SOE), \bar{U} is the control vector formulated as $\bar{U} = [D_{E,D}, D_{E,ER}]^T$ containing charging durations at depot $D_{E,D}$ and en-route $D_{E,ER}$ for BEVs or $\bar{U} = [D_{E,ER}]$ containing en-route fueling durations for ICVs, J is the cost for S and U , and S_{min} and S_{max} are lower and upper limits for the state vector and are constant in time. The overline indicates an array containing values at multiple discrete time intervals. The goal of the optimization is to find the optimal charging schedule (\bar{U}^*) such that J^* is equal to the global minimum value for J . J is the cost of charging for the itinerary.

Optimal charge scheduling model is 1-state, 2-control where the one state is the vehicle's SOE and the controls are depot charging and en-route charging. Depot charging is available to BEVs at depot locations. En-route charging is assumed to be available to BEVs every trip. For depot charges, it is assumed that time is not of the essence and thus charging should take place at the lowest rate possible in order to maximize efficiency and minimize power cost. Conversely, en-route charges are assumed to occur at the maximum possible rate. The reasoning for this is that time spent energizing a vehicle is considered working time for commercial drivers if it exceeds 30

minutes [229]. Driving time lost to energizing is expensive and reduces the effective capacity of the fleet. Thus it is assumed that en-route refueling time will need to be minimized.

The itineraries used to evaluate electricity costs for BEVs are from INRIX and provided to CSU by Electric Power Research Institute (EPRI). These itineraries are from tracked Heavy Duty (HD) vehicles and include trip origin and destination, time, and distance information. Each itinerary is for one day only and the locations are snap-to-node anonymized to make it impossible to track vehicles over multiple days. The INRIX data provides a well distributed and representative snapshot of HD travel in the US as discussed in Appendix B.

In order to enable optimal operation, long trips and dwells are broken up into smaller chunks thus allowing for more precise cost function evaluations and controls. An example optimal charging schedule is shown in Figure 6.17.

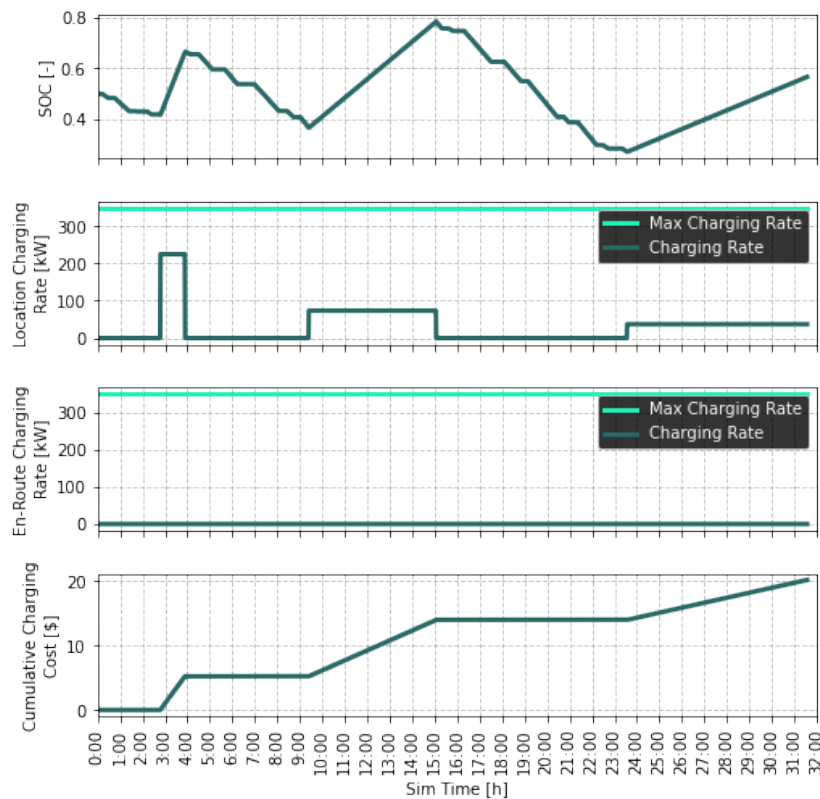


Figure 6.17: Optimal charge schedule for an INRIX HD itinerary with a long range battery

The vehicle in Figure 6.17 is incentivized to charge in the morning and evening when at depot and only incentivized to charge en-route late in the day in order to return to its required end-of-day SOE. Generally, vehicles will only charge en-route when they are unable to complete a trip or need to energize quickly to meet the end-of-day SOE condition. The vehicle in Figure 6.17 has a 1,000 kWh battery pack which gave it 800+ km of range. The vehicle in Figure 6.18 traveled the same itinerary as the previous vehicle but has a 300 kWh battery pack. As a result it has charge en-route more often leading to a higher cumulative charging cost. Critically, the longer range vehicle spends no time en-route charging while the shorter range vehicle loses almost two hours of driving time to en-route charging. The shorter range vehicle will have a lower purchase price and more cargo capacity but in order to operate on this itinerary the fleet would have to be nearly 25% larger.

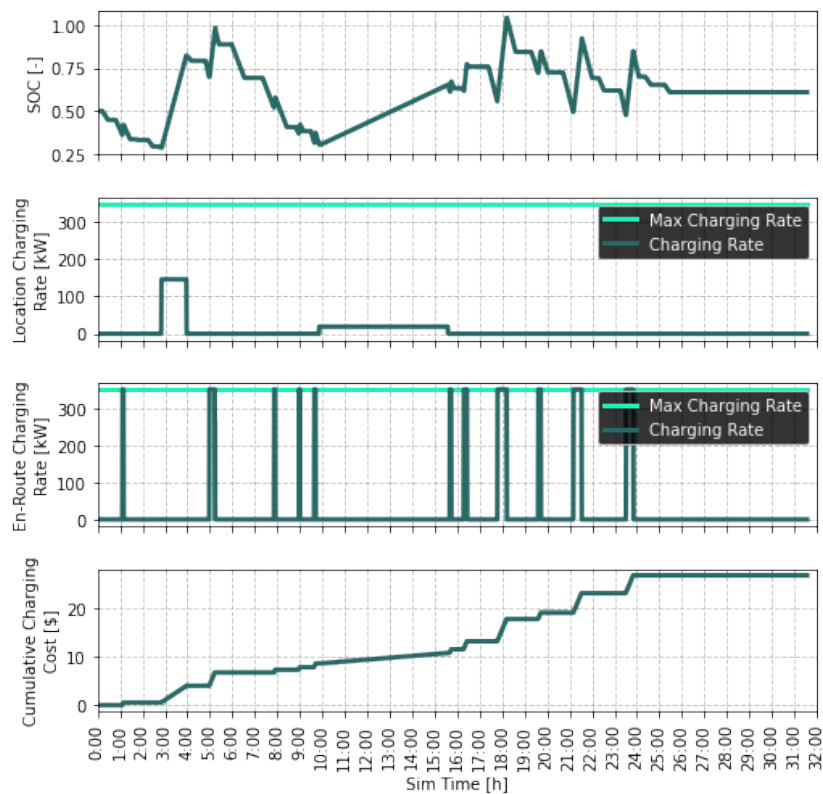


Figure 6.18: Optimal charge schedule for an INRIX HD itinerary with a short range battery

The amount that a class 8 truck operator pays for electricity is generally proportional to how often the truck needs to be charged en-route. A heuristic that is often, but not always, beneficial is

to match a truck’s capability with its workload such that all charging can be done when the truck is parked at depot. Larger vehicles both consume more energy per unit distance and, generally, are tasked with longer itineraries, thus making the capability matching more restrictive.

Using INRIX itineraries, geographic and temporal electricity pricing, and optimal charge scheduling, simulations were run for trucks with battery capacities ranging from 500 kWh to 1500 kWh. The maximum en-route charging rate used in simulation was 350 kW. The average prices paid for electricity vs. battery capacity and daily driving distance are shown in Figure 6.19.

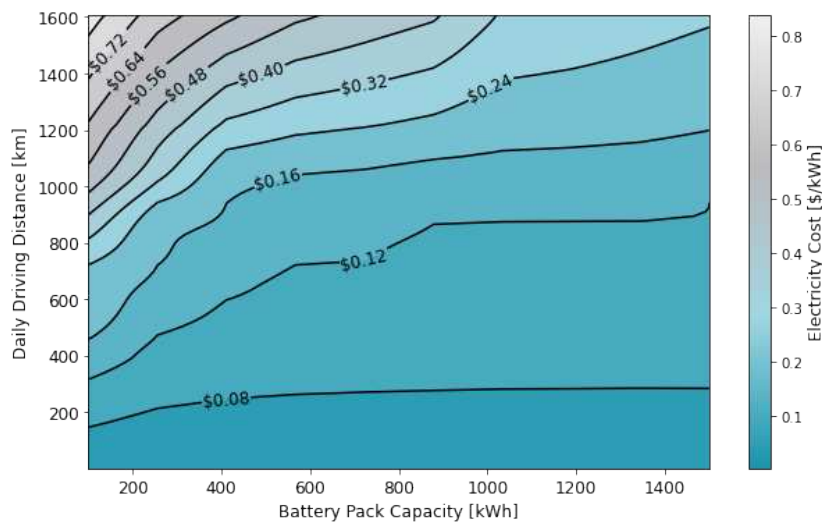


Figure 6.19: Price paid per kWh by battery pack size and daily driving distance for class 8 BEV tractor

Average electricity price is driven by en-route charging. Because en-route charging occurs at high rates and lower efficiencies it requires more energy per unit range added. En-route charging also often occurs during mid-peak and on-peak periods. For lower daily driving distances, BEVs can pay considerably less for electricity than the national average rate. This advantage erodes once the nominal range of the vehicle is approached due to the requirement to charge en-route. For itineraries which exceed the vehicle range threshold, electricity prices can start to rise quickly. Per the 2002 VIUS, the average annual VMT for a class 8 sleeper cab tractor is 87,000 miles (193,983 km). If an average truck works 6 days per week then the average daily driving distance for class 8

sleeper cab tractors is 278.5 miles (448.7 km) at which distance, electricity is still cheaper than the national average for most battery pack sizes.

6.5.3 Time Loss Cash Flow

Per US DOT regulations [229], drivers of property-carrying vehicles can drive 11 hours after a 10 hour off-duty period. Drivers may distribute their 11 hours of driving over 14 consecutive hours between 10 hour rest periods but will still be incentivized to minimize the total hours and start the off-duty period as soon as possible. After driving for 8 cumulative hours a mandatory 30 minute break must be taken. Charging may occur without incurring time penalties during the mandatory 30 minute break. Thus the Lost Time Portion (LTP) is calculated as in (6.12)

$$LTP = \max \left[\frac{T_{C,ER} - T_B}{T_D}, 0 \right] \quad (6.12)$$

where $T_{C,ER}$ is the time spent charging en-route, T_B is the duration of the mandatory break, and T_D is the cumulative driving time allowed between rest periods. The value of time spent en-route charging is computed by multiplying the LTP by the TCO.

Using INRIX itineraries, geographic and temporal electricity pricing, and optimal charge scheduling, simulations were run for trucks with battery capacities ranging from 500 kWh to 1500 kWh. The maximum en-route charging rate used in simulation was 350 kW. The average daily time spent en-route charging vs. battery capacity and daily driving distance is shown in Figure 6.20.

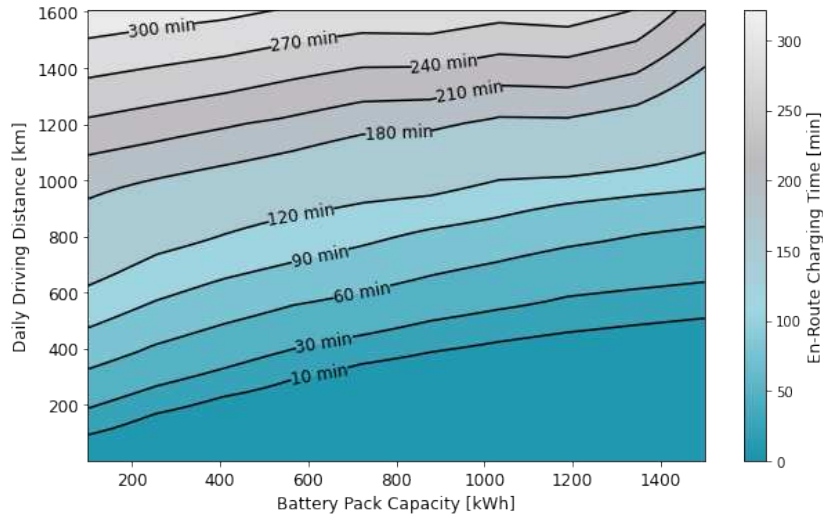


Figure 6.20: Time spent en-route charging per day by battery pack size and daily driving distance for class 8 BEV tractor

6.5.4 Summary

The CSU model differs from the TEMPO model in three key areas: battery pricing, energy pricing, and the valuation of driving time lost due to en-route charging. The differences result in modifications to the Vehicle and Energy cash flows and the addition of the Time Loss cash flow. The results generated using the modified TCO model are presented in Figure 6.21

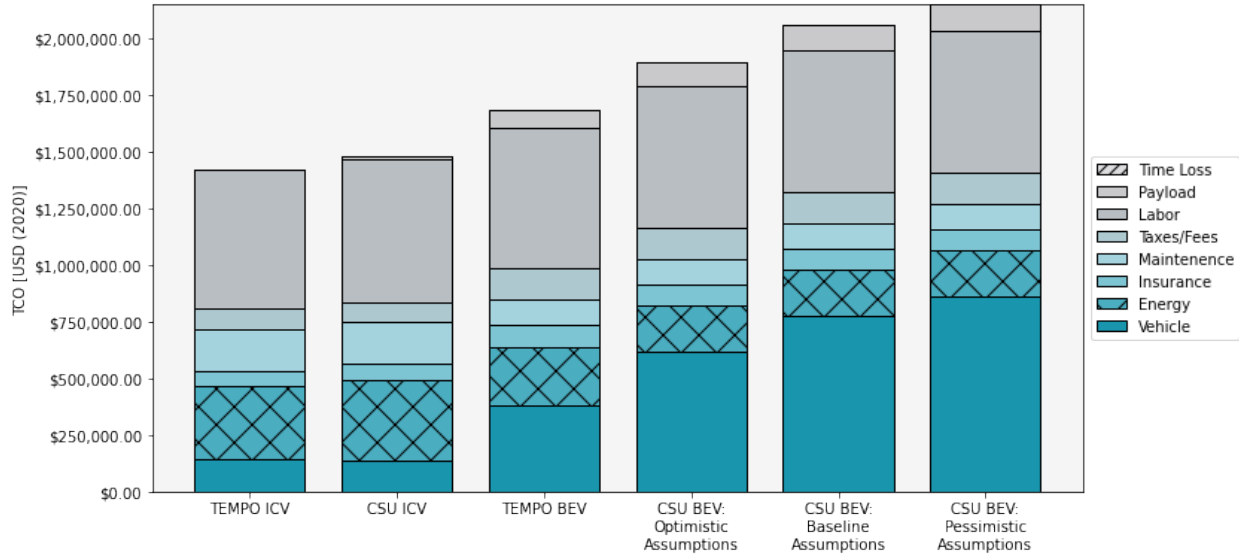


Figure 6.21: TCO for ICV and BEV model year 2025 class 8 sleeper tractors from TEMPO and CSU models with realistic costs of electricity and cost of en-route charging and average annual VMT

The effects of the changes to the Vehicle and Energy cash flows are apparent in Figure 6.21. TEMPO predicts that the purchase price for a class 8 BEV tractor with 800 km of range will have a greater purchase price than an equivalent ICV in 2025 but this disparity still greater with CSU’s assumptions. Conventional wisdom in the LTL industry is that purchase price is a small component of TCO. For class 8 ICV tractors the Vehicle cash flow is around 10% of the TCO. However, using CSU’s assumptions for battery pack pricing, the Vehicle cash flow is between 30% and 40% of the TCO for BEVs. The increased purchase price means that insurance rates, taxes, and the equivalent value of lost payload and driving time will be higher as well. The changes to the Energy cash flow manifest as higher fuel costs for ICVs and lower electricity costs for BEVs. The lower electricity costs are due to optimal charge scheduling. The results show a non-negligible improvement of roughly 20% on the TEMPO value resulting from optimal charge scheduling. The values for the Time Loss cash flow were all zero in Figure 6.21. This is because the average daily driving range from VIUS (448.7 km) results in below national average electricity prices and less than 30 minutes of en-route charging time for the BEV model with its 1,470 kWh battery pack. If this daily driving distance is doubled then the cost of electricity per kWh will increase and the time required for en-

route charging will cross the 30 minute threshold. The results with doubled daily driving distances are shown in Figure 6.22.

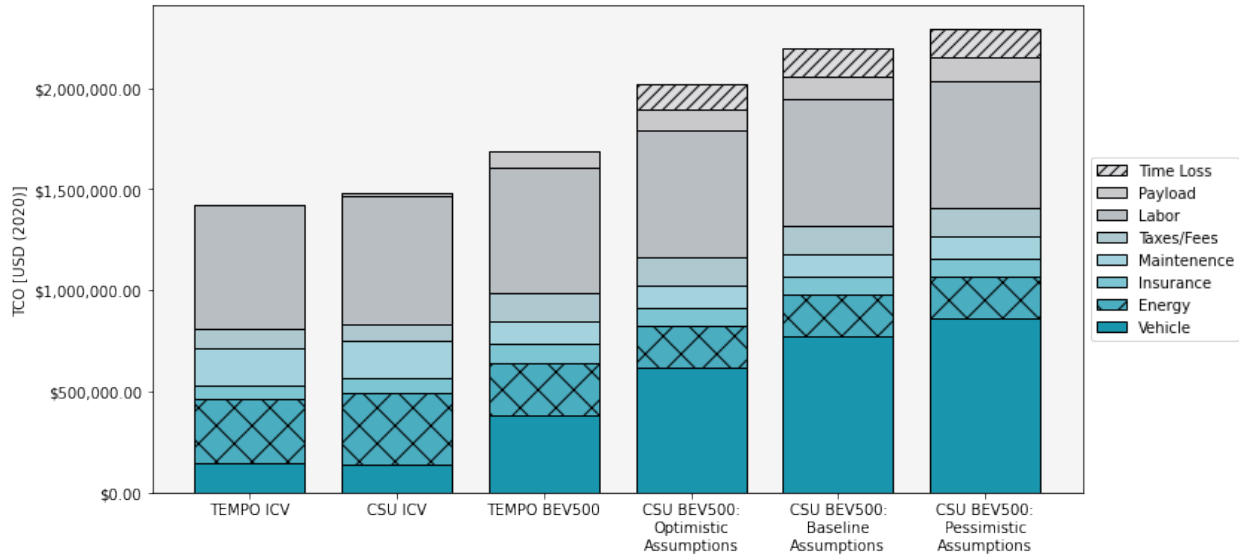


Figure 6.22: TCO for ICV and BEV model year 2025 class 8 sleeper tractors from TEMPO and CSU models with realistic costs of electricity and cost of en-route charging and double average annual VMT

In the longer daily driving scenario the equivalent cost of en-route charging becomes non-negligible and even eclipses that of capacity lost due to battery pack mass. It is also notable that the comparative disadvantage of BEVs to ICVs diminishes as operating costs make up a larger portion of the TCO.

6.6 Results

6.6.1 Model Results

Having built a comprehensive and data-based model for class 8 BEV and ICV tractor TCO it is possible to evaluate the economic competitiveness between the two powertrain types. The relative cost of a BEV and equivalent ICV will depend on many factors such as the nominal range of the trucks, the driving distance requirements, the prices and densities of battery cells, the price

of diesel, and other factors. Class 8 BEV tractor TCO as a function of model year, battery pack capacity, and daily driving distance with CSU baseline assumptions is shown in Figure 6.23.

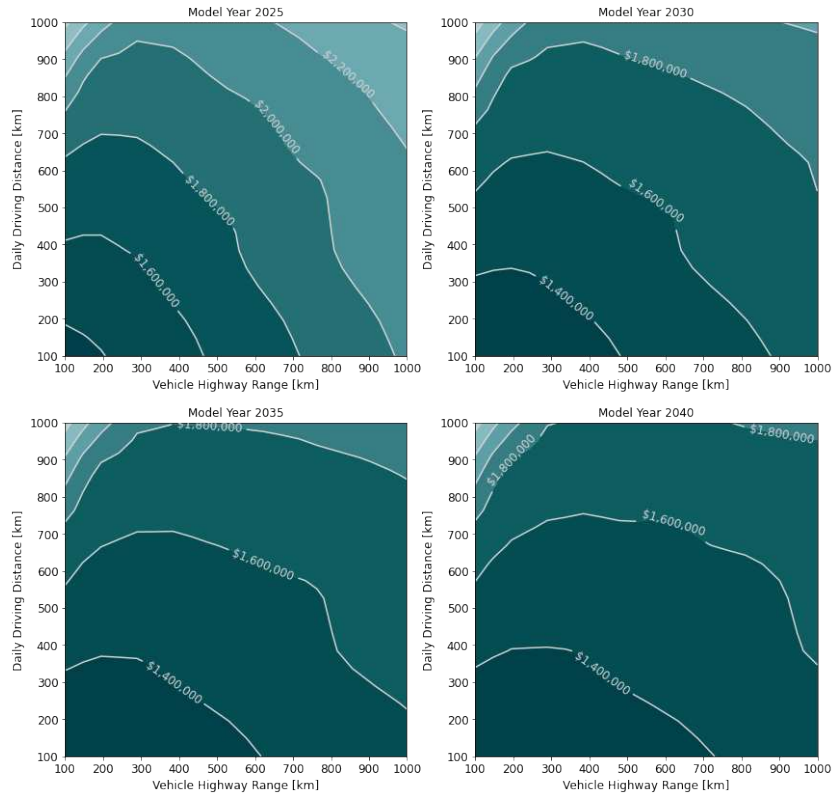


Figure 6.23: Projected TCO for class 8 BEV tractors by model year, battery pack capacity, and daily driving distance with CSU baseline assumptions

Class 8 BEV tractor TCO as a percentage of equivalent range ICV TCO as a function of model year, battery pack capacity, and daily driving distance with CSU baseline assumptions is displayed in Figure 6.24.

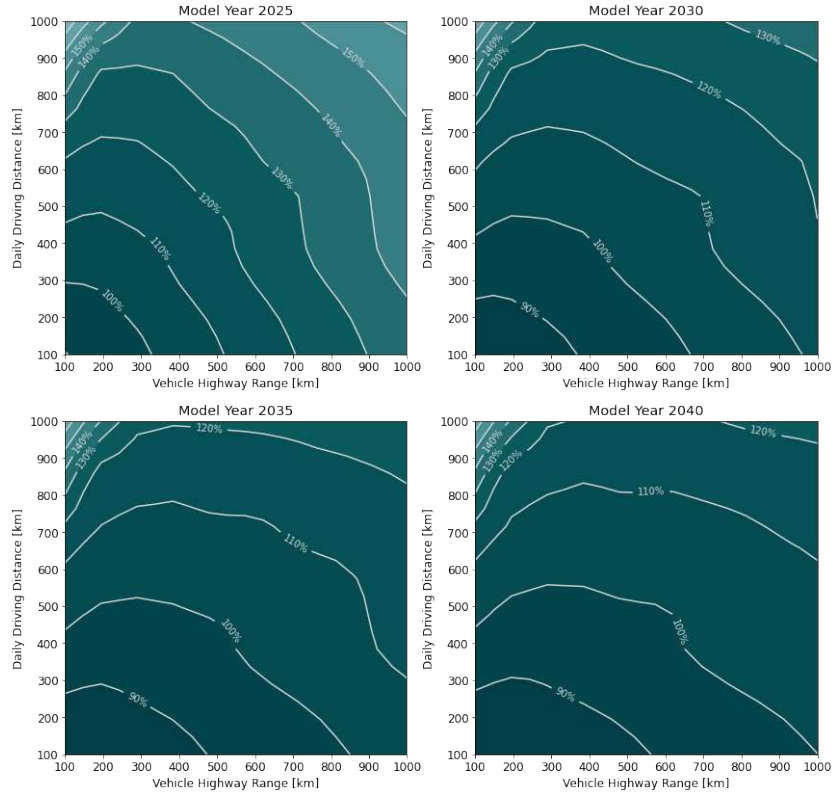


Figure 6.24: Projected TCO for class 8 BEV tractors as a percentage of equivalent ICV TCO by model year, battery pack capacity, and daily driving distance with CSU baseline assumptions

The area below the 100% contour represents the area of projected cost savings for class 8 BEV tractors. The results presented in Figure 6.24 reveal two salient trends. First, in general, the peak daily distance point of all contour lines occurs where the vehicle nominal range is less than the daily distance. Second, the size of battery packs which can be economically competitive increases faster than the daily driving range for which BEVs can be economically competitive. These trends indicate that the cost of increasing battery pack size more than offsets the increased costs of performing a moderate amount of en-route charging and that the costs of en-route charging rise quickly and form an artificial ceiling on BEV competitiveness.

As might be expected, different assumptions about the evolution of battery cell price and specific energy produce substantially different results. Class 8 BEV tractor TCO as a percentage of equivalent range ICV TCO as a function of model year, battery pack capacity, and daily driving distance with CSU optimistic assumptions is displayed in Figure 6.25.

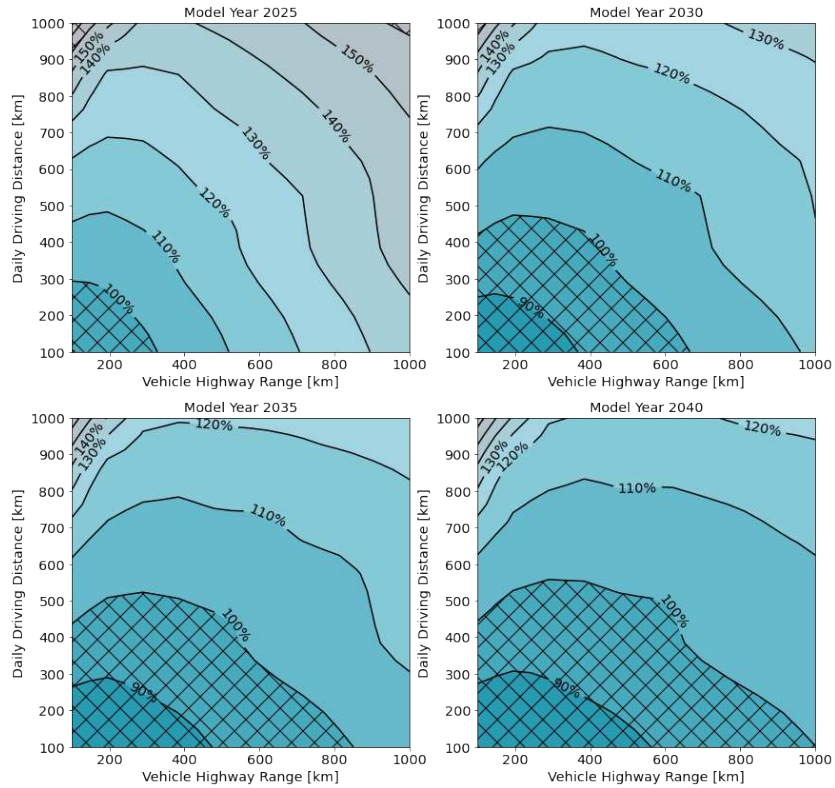


Figure 6.25: Projected TCO for class 8 BEV tractors as a percentage of equivalent ICV TCO by model year, battery pack capacity, and daily driving distance with CSU optimistic assumptions

Although the optimistic assumption set results in a larger area of economic competitiveness for all model years shown, the previously mentioned trends hold true. A useful metric for evaluating the change in class 8 BEV tractor competitiveness over time is the maximum competitive distance-matched vehicle range. The maximum competitive distance-matched vehicle range is here defined as the nominal range of the largest range BEV for which operating a daily driving distance equal to the vehicle’s nominal range is economically competitive with a ICV of the same range. In other words, the range where the diagonal from bottom-left to top-right intersects with the 100% contour on an economic competitiveness plot such as those in Figures 6.24 and 6.25. The maximum competitive distance-matched vehicle range for class 8 BEV tractors using CSU’s model and assumptions vs. model year is presented in Figure 6.26.

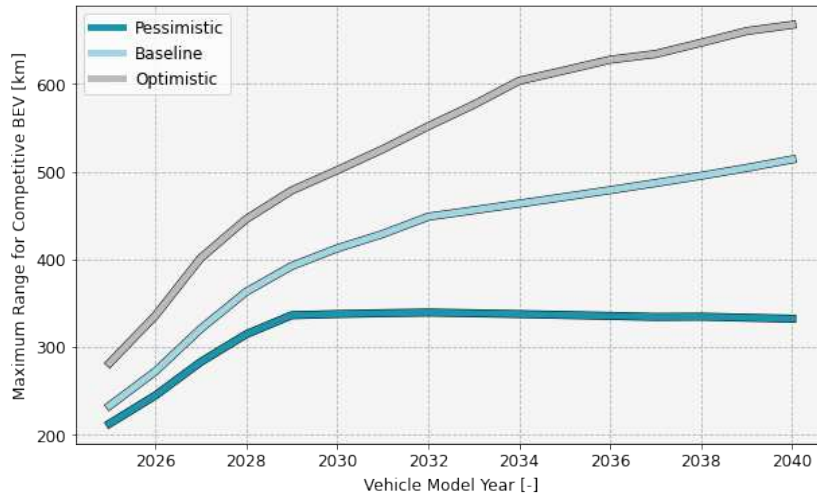


Figure 6.26: Projected maximum competitive distance-matched vehicle range for class 8 BEV tractors by model year using CSU’s battery pack price projections

With CSU’s baseline battery pack price projection, class 8 BEV tractors with a nominal range of 300 miles (483 km) will become competitive in the mid 2030s. Using CSU’s optimistic battery pack price projection, class 8 BEV tractors with a nominal range of 400 miles (644 km) will become competitive in the same time frame. Using CSU’s pessimistic battery pack price projection, the competitive nominal range for class 8 BEV tractors is projected to peak just above 210 miles (338 km). This indicates that the future of class 8 BEV tractors lies in the shorter haul segments of the LTL model (day cabs rather than sleeper cabs). These results are sensitive to fuel prices. Increasing the price of diesel fuel by just \$1.00 per gallon to \$4.54 per gallon (in line with recent prices) radically increases the maximum competitive distance-matched ranges as seen in Figure 6.27

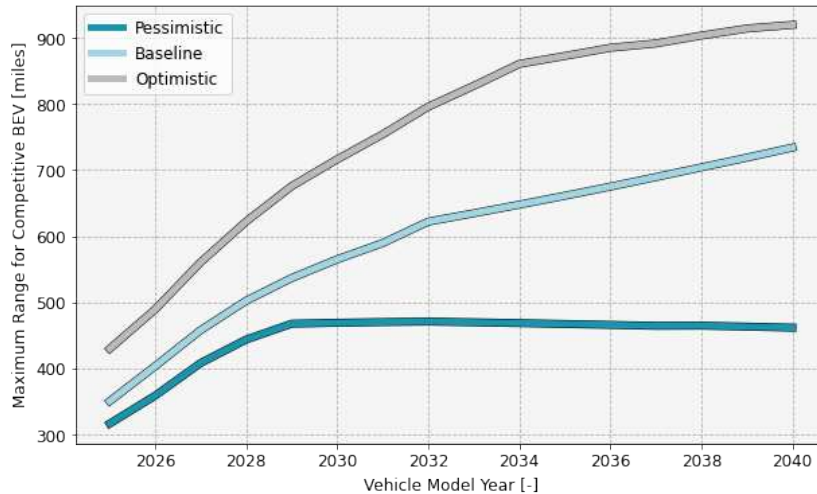


Figure 6.27: Projected maximum competitive distance-matched vehicle range for class 8 BEV tractors by model year using CSU’s battery pack price projections with increased diesel price

As seen in Figures 6.24 and 6.25 the economics between ICVs and BEVs are rather sensitive. Many more BEVs come in within 110% of the equivalent ICV price than come within 100% and this trend intensifies with time. Thus, it is worth evaluating the contingency of the results.

6.6.2 Sensitivity Analysis

The TCO model described in this study is based on projections of future component pricing and physical properties as well as a set of assumptions about vehicle operation. It is not possible to assess the accuracy of any set of projections or assumptions in the present. Nevertheless, it is important to understand how these assumptions may effect the outcomes. Thus, a sensitivity analysis was carried out on the parameters listed in Table 6.6.

Table 6.6: Parameters in sensitivity analysis

Parameter	Description	Values
Yearly Distance (YD)	Representative yearly distance driven [km]	[79,000, 140,000, 193,000]
Daily Distance (DD)	Representative daily distance driven [km]	[400, 800, 1200] (Matched to Vehicle Nominal Range (VNR))
VNR	Vehicle nominal range [km]	[400, 800, 1200] (250, 500, and 750 miles)
Number of Years of Ownership (NYO)	Length of term of ownership [years]	[5, 10, 15]
Age at Purchase (AP)	Vehicle age at purchase [years]	[0, 5]
Diesel Price Multiplier (DPM)	Diesel price multiplier [-]	[0.64, 1, 1.44] (95% confidence interval)
EVSE Premium (EVSEP)	EVSE premium for charging BEVs [\$/kWh]	[.05, .1, .15]
Payload Exemption (PE)	Payload exemption for BEVs [kg]	[0, 907, 1814]
Battery Pack Pricing (BPP)	Battery pack pricing [\$/kWh]	[100, 235, 370] (Based on CSU battery pack pricing scenarios in the 2030s)
Model Year (MY)	Vehicle model year [-]	[2030, 2035, 2040]

The ranges chosen were meant to reflect realistic ranges for the parameters for the years studied (2030-2040). The range for YD was chosen based off of the VMT distribution from VIUS. The values for VNR were for the 250, 500, and 750 mile nominal range market segments and the values for DD were set to match these. The values for NYO and AP were set to reflect the range of outcomes for large LTL fleets. The values for DPM were taken from historical data and reflect the edges and center of the 95% confidence interval of the continuous distribution. No similar multiplier was applied to the electricity price due to the tightness of the observed historical distribution. Boundaries for EVSEP were taken from [38, 224]. Values for PE were taken from

[38]. Values for BPP were based on CSU’s battery pricing assumptions in the time period defined by MY.

Having defined the ranges, a full-factorial designed experiment was conducted using CSU’s TCO model. The regression was done using normalized regressors. Significant terms from the regression analysis for ICV normalized TCO, BEV normalized TCO, and relative TCO (BEV/ICV) and are found in Figure 6.28. Model information for the regression analyses can be found in Appendix A.

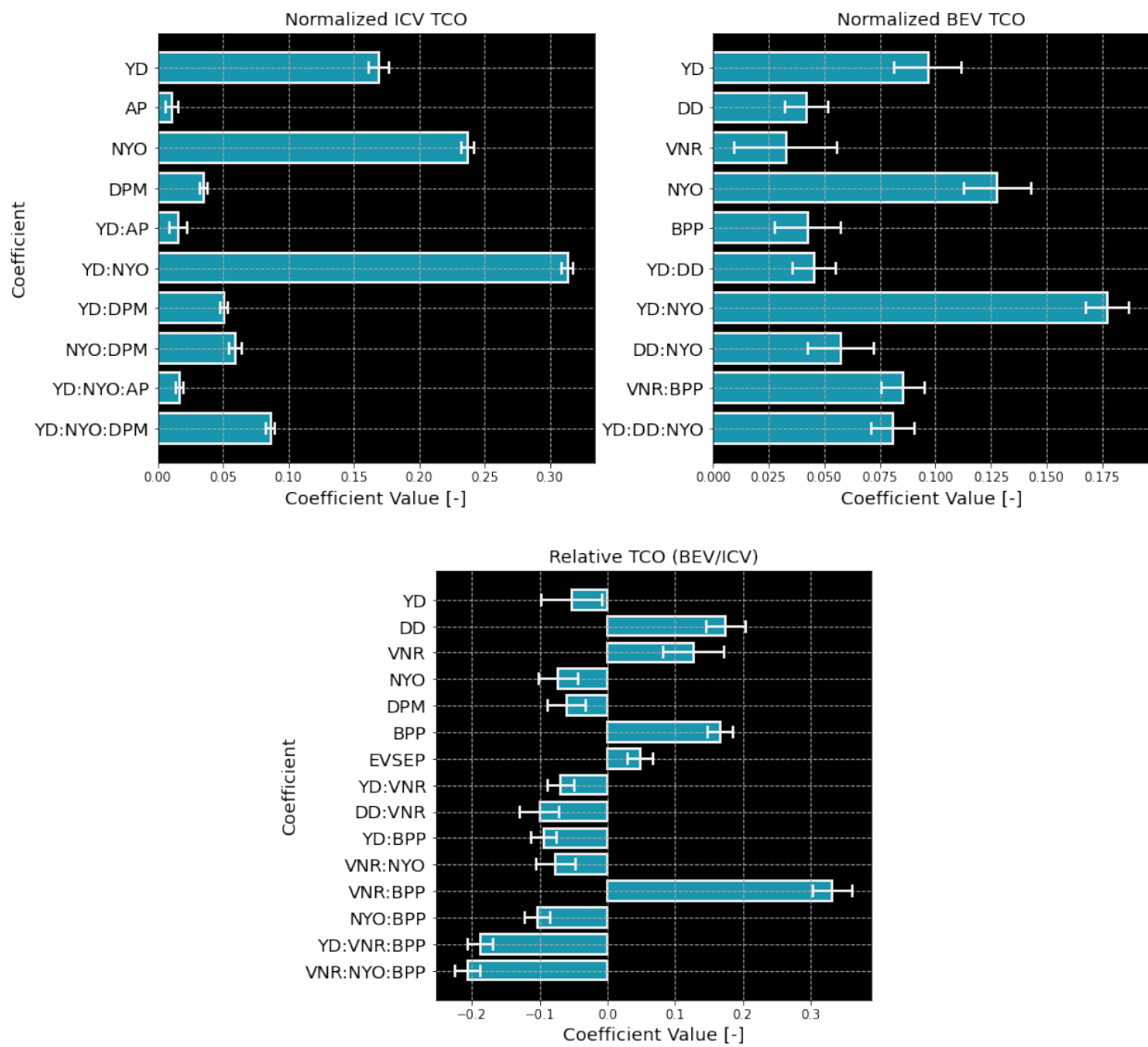


Figure 6.28: Significant coefficients ($\alpha = 0.05$) from normalized TCO regression

The TCO for a class 8 ICV tractor is dominated by term-of-use factors such as yearly distance driven and number of years of ownership. Because maintenance costs increase with age, buying newer ICVs is a better deal even with higher purchase prices. The cost of fuel is also significant in determining TCO. For BEVs, the term-of-use parameters are still the most important in determining TCO but factors such as daily driving distance, nominal range, and battery pack pricing are more important in determining TCO than their ICV equivalents. The relative results show that the term-of-use factors tend to favor BEVs as the operating costs come to dominate and offset the purchase price differential. However, the equivalence is still driven by battery pack size and pricing. Larger battery packs are more expensive and this is difficult to overcome.

The cost of operation can also be assessed on a per-unit-distance basis using the metric Levelized Cost of Driving (LCOD) which is the TCO divided by total distance driven. Significant terms from the regression analysis for ICV LCOD, BEV LCOD, and relative LCOD (BEV/ICV) and are found in Figure 6.29.

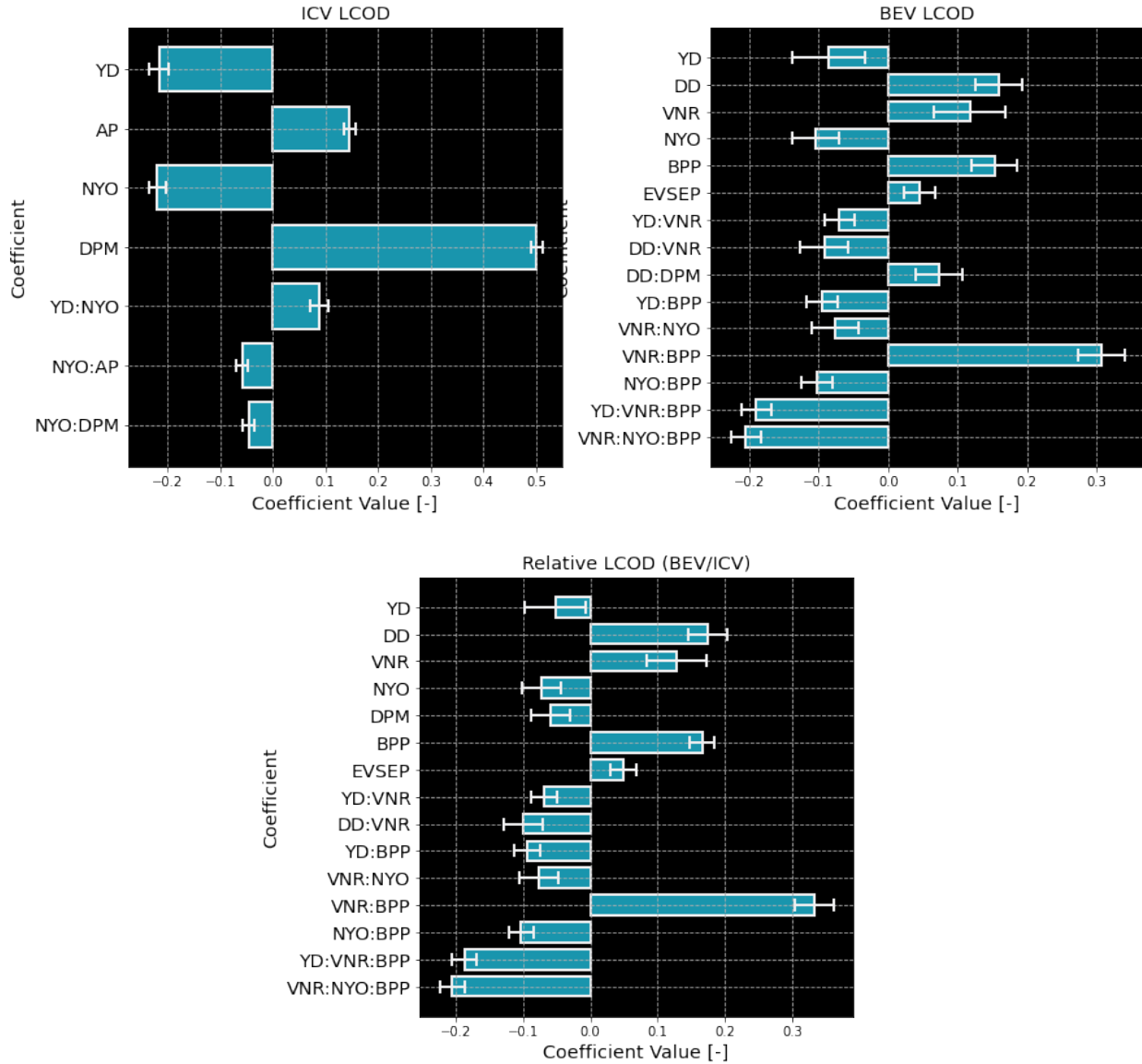


Figure 6.29: Significant coefficients ($\alpha = 0.05$) from LCOD regression

The LCOD results lead to the same conclusions as the TCO results for the relative economics. However, it is worth noting that term-of-use factors reduce LCOD.

6.7 Discussion

The main area in which the model used in this study improves on previous models in the literature is in how charging is handled. In the literature electricity pricing is often handled with

a flat rate. If range is accounted for this takes the form of declaring certain itineraries infeasible. However, DC fast charging allows for substantial range to be added in relatively short periods of time. The presence of fast charging stations allow for electric vehicles to travel further than their nominal ranges without needing multi-hour dwells. Commercial drivers in the US are required to take one 30 minute break during each driving day and important charging can occur during this time period. Fast charging will, however, be more expensive than low rate charging. In order to account for this dynamic, the CSU TCO model uses an electricity pricing model which is sensitive to rate and TOU considerations. The CSU TCO model also accounts for time lost due to en-route charging with the Time Loss cash flow. As has been shown in Sections 6.5 and 6.6, BEV purchase price and TCO are heavily driven by battery pack price which is, itself, proportional to range. An interesting question is whether fleets would be better served by vehicles with large batteries which mostly charge at low rates or by vehicles with lower ranges that have to charge en-route more often. For model year 2025 trucks the trade-off favors shorter range vehicles as shown in Figures 6.30 and 6.31.

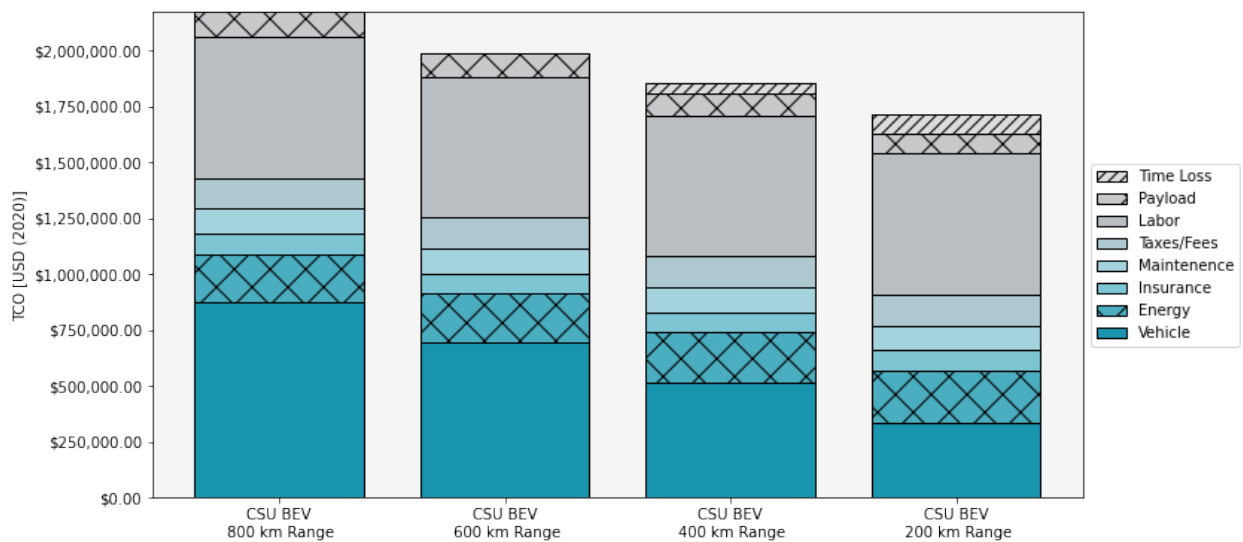


Figure 6.30: TCO comparison for model year 2025 class 8 BEV tractors with various ranges and 500 km daily driving requirements

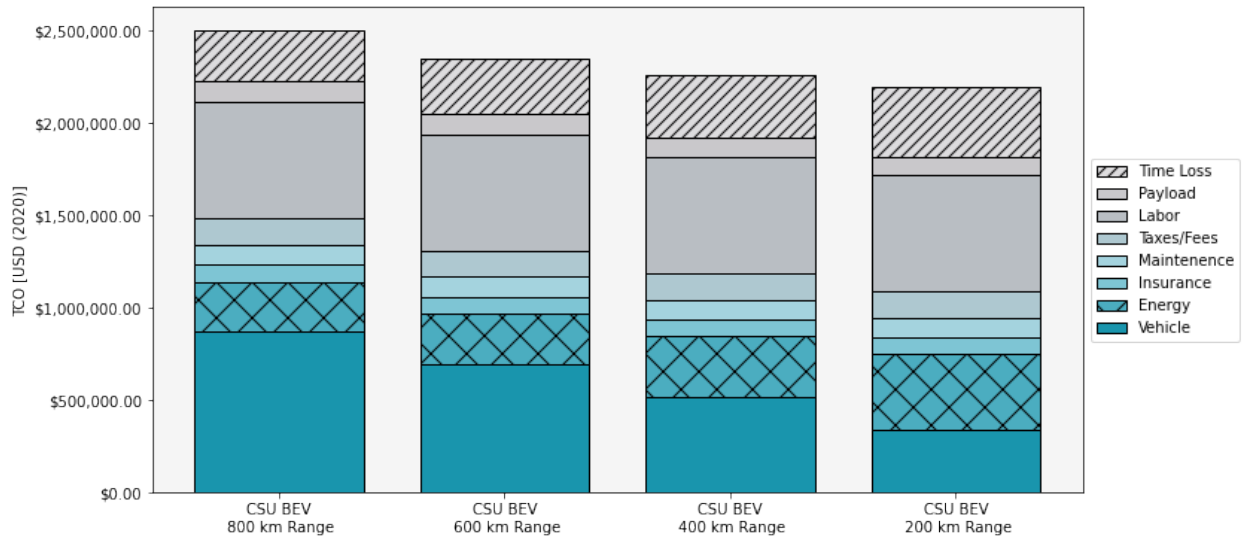


Figure 6.31: TCO comparison for model year 2025 class 8 BEV tractors with various ranges and 1000 km daily driving requirements

Because of the relatively high battery prices expected for 2025, the higher purchase prices of the longer range trucks are enough to offset the increased operation expenses that low range trucks experience. Notably, the savings seen for lower range vehicles with a 500 km daily driving requirement are much reduced with a 1000 km daily driving requirement. A 200 km range truck has a roughly 300 kWh battery. In this study the highest charging rate available was 350 kW. With such rates available the 200 km range truck would need to perform a series of roughly 40 minute charging events throughout the day to travel any long distance. In this study, the effects of C-rate on battery health were not considered but one can assume that the 200 km range truck will need a battery replacement sooner than the longer range trucks. Nevertheless, batteries are projected to be expensive enough in 2025 that the shorter range vehicles still prevail. The situation in 2035 is projected to be far more ambiguous as presented in Figure 6.32.

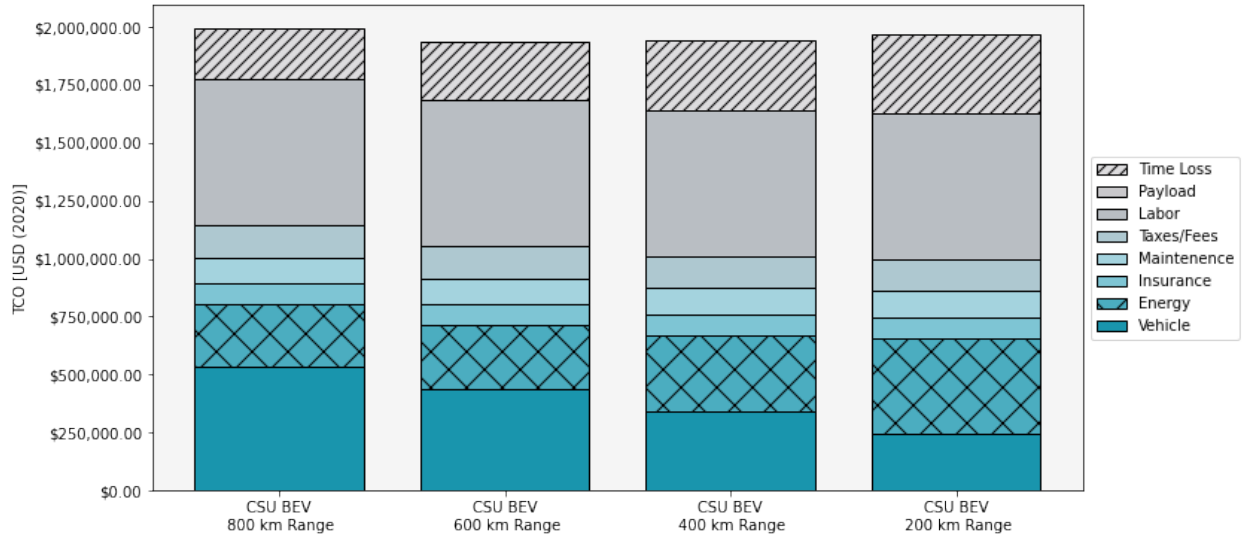


Figure 6.32: TCO comparison for model year 2035 class 8 BEV tractors with various ranges and 1000 km daily driving requirements

Because of the projected drop in battery prices by 2035, the differences in operational costs between the vehicles are enough to offset the purchase price differences. The economics of class 8 BEV tractors are, as shown in this study, highly contingent and fundamentally different to that of class 8 ICV tractors. Where conventional trucking economics are dominated by operational expenses, the battery costs of class 8 BEV tractors mean that purchase prices may be high enough to comprise 30% to 50% of TCO. The effect of this is that truck range must be matched well to required range; if a BEV truck has more battery capacity than needed then it will be a bad investment. Generally, purchasing trucks with slightly lower ranges than range requirements will be less damaging than purchasing trucks with slightly higher ranges than requirements assuming that high-rate chargers are available. An implication is that OEMs may want to offer vehicles with a wide variety of ranges or with the ability to add or remove battery capacity easily.

A commonly cited concern with respect to HD BEVs is the payload capacity loss that will result from the battery weight. While BEVs will be heavier than equivalent ICVs in the near-term future, this capacity loss is not as extreme of an issue as it might seem for LTL carriers. In the LTL industry where loads are dictated more by packing and logistical considerations, trucks rarely

travel at GVWR capacity. Most of the time, LTL trucks operate several tons under GVWR. The additional mass of the battery will mean that trucks operate closer to GVWR and, thus, get worse equivalent fuel economy. However, as most of the driving done by the trucks will be on highways, the additional mass has a minimal effect on efficiency. The decrease in per-truck payload and equivalent fuel economy were shown to amount to 5% of TCO in 2025 and to nearly vanish by 2035 as battery specific energy increases.

6.8 Conclusions

Class 8 trucks are a critical segment of the transportation sector in the US and other areas of the world; in many respects, the modern global economy could not function without them. Customers and suppliers of physical goods are linked by a complex multi-modal freight transportation system that is built around the standardized shipping container. One constant within the freight transportation system is the inverse relationship between overall vehicle weight and per-unit-weight shipping costs (air-freight excepted). For very long distances marine and rail transport are the most sensible options but these have limited reach. Rail operations rely on the presence of expensive infrastructure and marine operations rely on geography and infrastructure. Linking US ports and rail-heads to distribution centers or customers is a fleet of 4 million class 8 tractors.

Class 8 tractors represent the most difficult to electrify transportation application. The economics of BEVs are effected by energy and power requirements as well as economies of scale. Class 8 tractors have enormous energy and power requirements and are inherently low volume items compared to LD vehicles. In order to achieve a green transportation future the emissions from class 8 trucks will have to be mitigated and there are several paths to accomplishing this. The first path is to replace existing class 8 ICV tractors with BEVs. The second path is to change the model for fleet operators towards a more storage oriented model with less capable trucks operating shorter hauls. The third is to build out rail infrastructure in order to reduce the need for long haul truck transportation. changes to vehicular technology such as advanced battery chemistries,

battery swapping, through-the-road charging among others may effect the relative viability of the paths towards electrification.

Results from this study indicate that the economics for BEVs will become favorable for shorter haul class 8 BEV tractors in the medium term future (throughout the 2030s). BEVs are cheaper to operate than equivalent ICV due to simplicity of maintenance and drastically lower fuel costs. Lower nominal range class 8 BEV tractors will still be more expensive at purchase than equivalent ICVs but this effect reduces with reduced battery size. Matching a BEV's daily driving requirements to its full-charge range will minimize the costs of en-route charging and push the balance in favor of BEVs. Increases in diesel fuel prices will also substantially increase the economic competitiveness of BEVs. However, it is unlikely that BEVs will capture the long-haul sleeper cab market segment in the foreseeable future. The results of this study indicate that changes to the multi-modal freight transportation system will have to be made in order to accommodate class 8 tractor electrification.

In this study a data-based model for the TCO of class 8 BEV tractors was developed. This model differs from previous models in the manner by which it deals with charging. The developed model uses real class 8 tractor itineraries from data and real geographic TOU electricity pricing plans to inform an optimal charge scheduling algorithm for simulation. Using the optimal charging simulation, a better understanding of the electricity prices really paid by fleet operators is ascertained as well as an understanding of how much driving time will be lost to en-route charging if necessary. The developed model also uses battery pack pricing obtained from a real MD/HD BEV OEM which better reflects likely prices which will be paid for class 8 tractor batteries than LD battery pack pricing data. The developed model showed that in the medium-term future (2030s) lower range class 8 BEV tractors will become economically competitive with equivalent range ICV tractors. Results indicate that BEVs may gain a substantial footing in the day-cab market segment without the assistance of subsidies or increased fuel taxes. The economics of class 8 trucks are heavily impacted by fuel costs and even small increases in fuel prices radically increase the competitiveness of ICV tractors. Ultimately, BEV tractors are unlikely to become competitive

in the long-haul market segments in the foreseeable future without substantial changes to vehicle design such as battery swapping or through-the-road charging. In order to achieve a green future in the long-haul market, changes to the multi-modal freight transportation framework are likely necessary.

6.9 Summary

In this chapter RQ3 was answered. Using data based modeling and simulation to inform an economic analysis, areas of competitiveness for class 8 BEV tractors were identified in the LTL market. The economic competitiveness of class 8 BEV tractors compared to their ICV equivalents was related to design and operational parameters and the model sensitivity to said parameters was investigated.

Chapter 7

Conclusion

7.1 Summary

Underpinning every advanced economy is a highly productive transportation sector. The transportation sector is what enables nearly all transactions and associated economic activity to occur. Modern market economies have created standards of living that are simultaneously quite atypical in the scope of human history and often taken for granted. Powering advanced economies and the transportation sectors upon which they rest is a mix of energy sources which includes and is often dominated by fossil fuel combustion which has well documented negative effects on human health and global environmental conditions. In order to preserve the elevated standard of living which we now enjoy for future generations advanced economies and, in particular, their transportation sectors will have to find ways to de-carbonize.

Because transportation relies on a mix of vehicles it is natural to seek solutions in novel vehicular technology. In recent times the two largest paradigm shifting trends in vehicular technology have been electrification and connected autonomy. Electrification is important as it both reduces vehicular energy consumption on a per-unit-distance basis and decouples energy generation from locomotion. Electric Vehicle (EV) and Internal Combustion Vehicle (ICV) powertrain technology have reached states of high maturity and in present forms EV powertrains enjoy large advantages in efficiency and cost-of-maintenance being fundamentally simpler machines. The main drawback to EVs is the battery which is costly, difficult to manufacture, requires scarce materials, and degrades at a quicker rate than the rest of the vehicle. The most important benefit that EVs provide is the opportunity to achieve lower emissions per-unit-distance over a vehicle term-of-use. Because power generation and locomotion are decoupled for EVs the composition of the local energy generation mix will directly impact the environmental impact of the EV. This should be seen as a massive positive as the pace of de-carbonization in

the energy sector has been rapid in developed countries in recent decades. Vehicular efficiency is also effected by the manner in which the vehicle is operated. Vehicular connected autonomy has the potential to create large efficiency improvements on a vehicle and fleet level. As vehicle on-board computing power increases and Vehicle to Everything (V2X) communications infrastructure rollout accelerates the potential for large increases in efficiency are rapidly attainable - a software update away.

The combination of electrification and autonomy can result in large reductions in vehicular emissions on a per-unit-distance basis. The first research question answered in this dissertation investigated this potential from two different angles. Firstly, optimal energy management strategies were investigated for Hybrid Electric Vehicles (HEVs) and, second, optimal Eco-Driving strategies were investigated for Battery Electric Vehicles (BEVs). Both of these topics are the subject of extensive literature which, nevertheless, contained important gaps towards commercialization. In the first case, the mathematical basis of HEV powertrain optimization has been well known for decades but the optimization relies on knowledge of future vehicle velocity. As a practical control strategy, Predictive Optimal Energy Management Strategies (POEMS) for HEVs only became feasible in recent years with advancements in Machine Learning (ML) which enable high-fidelity vehicle velocity prediction. An important research gap existed as to what ML methods were able to produce sufficiently accurate predictions, what data was necessary, and what ultimate efficiencies could be attained. In Chapter 2, this gap was comprehensively addressed. A representative real-world Connected Autonomous Vehicle (CAV) dataset was collected. This dataset was used in a study on various ML techniques with different subsets of the collected data. It was discovered that sufficiently accurate predictions of vehicle velocity could be made using Long Short-Term Memory (LSTM) Deep Neural Networks (DNNs) and that only data available to non-connected vehicles was necessary. Efficiency benefits were found to be in the 10% to 15% range over baseline torque-filling control. Optimal Eco-Driving control has also been extensively studied in more recent times. Autonomous Eco-Driving control is currently feasible with level 2 autonomous vehicles becoming the norm in the US. To date, autonomous longitudinal control has followed

rules-based controls which primarily serve to avoid collision risk but can be tuned to provide energetic benefits. There is also evidence that the predictability of autonomous longitudinal control contributes to traffic calming. When rules-based control is used to achieve energetic benefits it comes at the cost of reducing average speed. Optimal control can be employed to produce greater energetic gains without the time loss. The literature to date on optimal Eco-Driving control is scattered and no comprehensive comparative assessment of methods could be found in order to guide future development and deployment. This research gap was addressed by the study described in Chapter 3 which surveyed the literature and applied common methods using consistent and realistic constraints derived from real-world data. The analysis found that the constraints of the problem introduce much complexity which hampers gradient descent solvers. However, results suggested that trajectory optimization is possible within run-times which are feasible for real-time control. The potential improvements in energy consumption for BEVs are in the range of 10% to 15%. Both types of optimal control are a software update away for modern EVs and could result in massive cumulative energy savings in the near term future.

However efficient EVs are, their impact will be minimal should they remain a low percentage of the vehicle fleet. Chapters 4, 5, and 6 deal with BEV adoption driving factors in multiple sectors. For Light Duty (LD) vehicles, although economics are a factor, consumers also value convenience. BEVs are at a disadvantage relative to ICVs due to their relatively short ranges and long energizing times. Because of the long charging times inherent to modern BEVs a "gas-station" charging behavior model is infeasible. Rather, charging is best accomplished at low rates at home and work. This state of affairs can result in massive inequities of experience and adoption between those able to charge at home and work. The majority of residents of single unit dwellings and the majority of home owners will be able to charge at home with little modification to their homes or parking behavior. The story is different for multi-unit residence dwellers who are, also, dominantly renters. Those with limited ability to charge at home will have to rely more on public charging infrastructure. Questions arise as to how to best design BEVs and deploy Electric Vehicle Support Infrastructure (EVSE) infrastructure to minimize inequity and maximize adoption. In

Chapter 4 a novel metric is introduced which relates inconvenience due to dedicated energizing time to vehicular design parameters. This metric can be computed for individual vehicles based on itineraries and information about available EVSE infrastructure. Results from a designed experiment are used to compute coefficients of an empirical equation which can be generally applied. This equation implies that those with access to home charging will make little use of public infrastructure as all daily charging needs can be taken care of during long home dwells. Also implied by the results is that a plurality of low rate chargers at common destination such as supermarkets, malls, and gyms will be more beneficial to BEV operators for daily travel than clustered high rate charging stations. In chapter 5 the empirical equation is applied on a geo-spatial basis in order to visualize inconvenience and resulting inequities. This study revealed that BEV charging creates notable spatial inequities due to differences in home charging availability and that these are somewhat mitigated by public charging infrastructure. The results showed that expected inconvenience is not well predicted by demographic factors such as income, race, unit type and tenure, or population density. This is due to the fact that inconvenience is caused by many factors. The inconvenience metric introduced in this dissertation will allow policy makers, urban planners, and interest groups to directly evaluate the effects of EVSE infrastructure in a manner which is more insightful than merely computing distances to and densities of chargers. This work will lead to a greater understanding of inconvenience in the scientific and policy communities and thus help to more efficiently promote LD BEV adoption.

While the vast majority of road vehicles in the US are LD personal transportation vehicles, roughly one quarter of road vehicle emissions come from Medium Duty / Heavy Duty (MD/HD) vehicles. The delivery of goods in the US relies on a huge fleet of commercial vehicles ranging from delivery vans all the way up to semi-trucks. Because these vehicles are large and operate at higher intensity than LD vehicles, the environmental impact of each commercial delivery vehicle is relatively high. Electrification presents unique issues in heavier BEVs due to battery pack mass and cost. Logically, the most difficult to electrify sector of the market to electrify will be class 8 tractors. For large delivery fleets, vehicle purchasing decisions will be dominated by Total Cost

of Ownership (TCO) which accounts for purchase price and operating costs. Although purchase prices are higher for BEVs than equivalent ICVs operating costs are lower, specifically in the areas of energy and maintenance. Predictable technological progress will also play a role in determining the economic competitiveness of BEVs in the future. In chapter 6 a comprehensive TCO model for class 8 tractors for Less Than Truckload (LTL) fleets is presented. This model is verified against state-of-the-art modeling with simplified assumptions. The model improves on the state-of-the-art with a detailed simulation and data-driven approach to computing charging times and prices. The result is projections of economic competitiveness between class 8 BEV and ICV tractors in the near and medium term future and a sensitivity analysis on model parameters. The results shown that much of the day-cab (shorter-range) class 8 LTL market can be captured by BEVs in the 2030s but the sleeper-cab market is unlikely to see much adoption. An instructive finding is that BEV economic competitiveness is strongly effected by the degree to which the vehicle range is matched with its range requirements. Because adding range means adding battery capacity, TCO for class 8 BEVs scales with range and having more range than necessary can render a truck too expensive to justify. The implication is that class 8 BEV tractor manufacturers should offer a range of battery sizes for the same chassis and possibly make battery packs modular in order that range is made flexible for a given chassis. It is also noteworthy that the ratio of diesel price to electricity pricing has a large impact on economic competitiveness. With recent fluctuations and overall increases in fuel prices, the economics of Heavy Duty (HD) BEVs may be more favorable in the future than is currently thought.

It is widely accepted that a green transition in the transportation sector is needed in order for environmental goals to be met. In general this is approached via separate research thrusts with these being research into vehicular technology, infrastructure development, and consumer behavior. These directions of research are carried out by subject matter experts and are valuable contributions in their own right. However, the reality is that technology, infrastructure, and consumer behavior are interrelated. It is the responsibility of the systems engineering community to connect knowledge created in dissimilar fields to answer important overarching questions. The

question of how to best enable a green transition in the transportation sector is such a question. Relationships between vehicular technology, infrastructure, and consumer behavior can only be fully understood through simulation and modeling. In this dissertation important research gaps relating the mentioned fields to each other were addressed using rigorous data-driven simulation and modeling techniques. Insightful answers to questions arising from the research gaps were provided, and the body of knowledge was meaningfully expanded.

7.2 Research Contributions

Specific research contributions from this dissertation are:

1. This research has developed a set of computational experiments that illustrate the trade-offs among real-time-capable predictive optimal control algorithms for vehicle dynamic control of electric and hybrid electric vehicles. Results of these experiments quantify both the costs and benefits of each of the major families of optimal infrastructure-enabled Eco-Driving algorithms in literature, but also defined novel strategies for highly efficient Eco-Driving techniques that result in 95% of optimal fuel economy.
2. This research has developed a novel and quantitative method for computing time-based inconvenience associated with battery electric vehicle operation. This method uses survey data and principles of optimal control in order to compute minimal energizing times required for a given vehicle and itinerary. This is the first method of computing vehicle and itinerary based operational inconvenience in a manner which is both sensitive to supply infrastructure and powertrain agnostic.
3. This research has developed computational experiments to identify the relative importance of vehicular and infrastructural factors in determining battery electric vehicle operational inconvenience. The results of these experiments point to the importance of low-rate long-dwell charging opportunities in reducing charging inconvenience for battery electric vehicle

users. The results indicate a large inequity of experience between those who are able to charge at home and those who are not.

4. This research has applied the novel vehicle operational inconvenience metric on a geo-spatial basis. Results showed that the inconvenience metric developed in this research provided novel insight into spatial inequity of experience not available from current demographic and location based methods. Results also showed that public charging infrastructure deployment, as is, does not redress the inequity caused by differential access to home charging.
5. A novel simulation and data-based model for assessing the total cost of ownership of class 8 semi-tractors with combustion and electric powertrains was developed. This model uses principles of optimal control in order to simulate dynamic charging behavior for electric vehicles. This model represents a significant improvement over current state-of-the-art models in assessing the actual initial and operating costs for heavy duty battery electric vehicles.
6. This research has developed computational experiments that identify the relative importance of vehicular and infrastructural factors in determining heavy duty battery electric vehicle economic competitiveness in the present and future. Results of these experiments indicate that longer terms of operation and shorter ranges favor heavy duty electric vehicles over conventional equivalents.

7.3 Future Work

Investigation of Effects of Boundaries of Optimal Eco-Driving control

The boundaries which define the optimal Eco-Driving problem in position (defined by traffic signals and lead vehicles) provide significant complexity. The complexity arises from the facts real-time capable optimal Eco-Driving methods rely on the computation of optimal polynomial trajectories and because the boundaries are inherently non-convex. The benefits of optimal control over baseline (rules-based) control vary depending on the exact composition of the boundary

functions. Understanding the precise relation between boundary shape and value of optimality will provide more nuance into the understanding of the benefits of optimal control. Future work will include further parameterization of the boundary functions and a study into the relationship between said parameters and the value of optimal control.

Specific Vehicle and Infrastructure Inconvenience Computation

The focus of the inconvenience research presented was to produce metrics which could be easily computed and broadly applied. For this reason the data used was survey data which is location agnostic. Because of the location agnostic data, supply infrastructure was modeled based on assumptions about availability. When applied geo-spatially the metric was computed using a pre-defined empirical equation. Another approach would be to use specific vehicle and supply equipment data. Vehicle itineraries with location or approximate locations can be attained even if access is limited. Using actual vehicle and supply equipment locations and routing algorithms, specific inconvenience scores can be computed. It is worth investigating how different the results obtained by specific analysis would be from those obtained via existing analysis. If the specific results are substantially different then scalable methods of assessment should be developed.

Effects of Capability Sensitive Vehicle Routing and Warehousing on MD/HD Fleet BEV Economic Competitiveness

In this research, the economic competitiveness of MD/HD Fleet BEVs was evaluated using routes taken from data collected for conventional vehicles. The main limitations of BEVs in comparison to conventional vehicles are range and energizing time. There is no reason to assume that BEVs will be operated in the same manner as conventional vehicles currently are. Fleets will adjust operations to the capabilities of the vehicles at their disposal. This might mean different routing schemes, different depot locations and sizes, or more unconventional solutions such as battery swapping. How these changes may impact the economics of MD/HD fleet BEVs is a topic worth studying in detail.

References

- [1] *Other Air Pollution from Transportation*. <https://www.epa.gov/transportation-air-pollution-and-climate-change/smog-soot-and-other-air-pollution-transportation>. 2015. (Visited on 10/06/2021).
- [2] *CO2 Emissions from Fuel Combustion 2019*. 2019, p. 514. DOI: <https://doi.org/10.1787/2a701673-en>. (Visited on 01/21/2023).
- [3] *EV Sales*. 2022. URL: <https://evadoption.com/ev-sales/> (visited on 06/05/2022).
- [4] David Person and Jeff Mason. *Biden seeks to make half of new U.S. Auto Fleet Electric by 2030*. <https://www.reuters.com/business/autos-transportation/biden-set-target-50-evs-by-2030>. 2021. (Visited on 02/16/2022).
- [5] *Fact sheet: Biden-Harris Administration proposes new standards for National Electric Vehicle Charging Network*. <https://www.whitehouse.gov/briefing-room/statements-releases/2022/06/09/>. 2022. (Visited on 08/06/2022).
- [6] Benjamin Loeb and Kara M. Kockelman. “Fleet performance and cost evaluation of a shared autonomous electric vehicle (SAEV) fleet: A case study for Austin, Texas”. In: *Transportation Research Part A: Policy and Practice* 121 (2019), pp. 374–385. ISSN: 0965-8564. DOI: <https://doi.org/10.1016/j.tra.2019.01.025>.
- [7] Riccardo Iacobucci, Benjamin McLellan, and Tetsuo Tezuka. “Modeling shared autonomous electric vehicles: Potential for transport and power grid integration”. In: *Energy* 158 (2018), pp. 148–163. ISSN: 0360-5442. DOI: <https://doi.org/10.1016/j.energy.2018.06.024>.
- [8] Reza Vosooghi et al. “Shared autonomous electric vehicle service performance: Assessing the impact of charging infrastructure”. In: *Transportation Research Part D: Transport and Environment* 81 (2020), p. 102283. ISSN: 1361-9209. DOI: <https://doi.org/10.1016/j.trd.2020.102283>.

- [9] Yugong Luo, Tao Chen, and Keqiang Li. “Multi-objective decoupling algorithm for active distance control of intelligent hybrid electric vehicle”. In: *Mech. Syst. Signal Process.* 64-65 (2015), pp. 29–45. DOI: <https://doi.org/10.1016/j.ymsp.2015.02.025>.
- [10] Yugong Luo et al. “Intelligent Hybrid Electric Vehicle ACC With Coordinated Control of Tracking Ability, Fuel Economy, and Ride Comfort”. In: *IEEE Trans. Intell. Transp. Syst.* 16.4 (2015), pp. 2303–2308. DOI: <https://doi.org/10.1109/TITS.2014.2387356>.
- [11] Qian Wang and Beshah Ayalew. “A Probabilistic Framework for Tracking the Formation and Evolution of Multi-Vehicle Groups in Public Traffic in the Presence of Observation Uncertainties”. In: *IEEE Trans. Intell. Transp. Syst.* 19.2 (2018), pp. 560–571. DOI: <https://doi.org/10.1109/TITS.2017.2750073>.
- [12] Chan-Chiao Lin et al. “Energy management strategy for a parallel hybrid electric truck”. In: *Proceedings of the 2001 American Control Conference. (Cat. No.01CH37148)*. Vol. 4. 2001, 2878–2883 vol.4. DOI: <https://doi.org/10.1109/ACC.2001.946337>.
- [13] David Baker, Zachary Asher, and Thomas Bradley. “Investigation of Vehicle Speed Prediction from Neural Network Fit of Real World Driving Data for Improved Engine On/Off Control of the EcoCAR3 Hybrid Camaro”. In: *SAE Technical Paper Series* (2017). DOI: <https://doi.org/10.4271/2017-01-1262>.
- [14] David A. Trinko, Zachary D. Asher, and Thomas H. Bradley. “Application of pre-computed acceleration event control to improve fuel economy in Hybrid Electric Vehicles”. In: *SAE Technical Paper Series* (2018). DOI: <https://doi.org/10.4271/2018-01-0997>.
- [15] Zachary D. Asher et al. “Real-Time Implementation of Optimal Energy Management in Hybrid Electric Vehicles: Globally Optimal Control of Acceleration Events”. In: *Journal of Dynamic Systems, Measurement, and Control* 142.8 (2020). DOI: <https://doi.org/10.1115/1.4046477>.

- [16] Frank A. Bender, Martin Kaszynski, and Oliver Sawodny. “Drive Cycle Prediction and Energy Management Optimization for Hybrid Hydraulic Vehicles”. In: *IEEE Trans. Veh. Technol.* 62.8 (2013), pp. 3581–3592. DOI: <https://doi.org/10.1109/TVT.2013.2259645>.
- [17] Teresa Donateo, Damiano Pacella, and Domenico Laforgia. “Development of an Energy Management Strategy for Plug-in Series Hybrid Electric Vehicle Based on the Prediction of the Future Driving Cycles by ICT Technologies and Optimized Maps”. In: *SAE Technical Paper Series* (2011). DOI: <https://doi.org/10.4271/2011-01-0892>.
- [18] Chao Sun et al. “Dynamic Traffic Feedback Data Enabled Energy Management in Plug-in Hybrid Electric Vehicles”. In: *IEEE Trans. Control Syst. Technol.* 23.3 (2015), pp. 1075–1086. DOI: <https://doi.org/10.1109/TCST.2014.2361294>.
- [19] Chao Sun et al. “Velocity Predictors for Predictive Energy Management in Hybrid Electric Vehicles”. In: *IEEE Trans. Control Syst. Technol.* 23.3 (2015), pp. 1197–1204. DOI: <https://doi.org/10.1109/TCST.2014.2359176>.
- [20] Qiuming Gong, Yaoyu Li, and Zhong-Ren Peng. “Power management of plug-in hybrid electric vehicles using neural network based trip modeling”. In: *2009 American Control Conference* (2009), pp. 4601–4606. DOI: <https://doi.org/10.1109/ACC.2009.5160623>.
- [21] Amir Rezaei and Jeffrey B Burl. “Prediction of Vehicle Velocity for Model Predictive Control”. In: *IFAC-PapersOnLine* 48.15 (2015), pp. 257–262. DOI: <https://doi.org/10.1016/j.ifacol.2015.10.037>.
- [22] Qiuming Gong, Yaoyu Li, and Zhong-Ren Peng. “Trip-Based Optimal Power Management of Plug-in Hybrid Electric Vehicles”. In: *IEEE Trans. Veh. Technol.* 57.6 (2008), pp. 3393–3401. DOI: <https://doi.org/10.1109/TVT.2008.921622>.
- [23] Mohd Azrin Mohd Zulkefli et al. “Hybrid powertrain optimization with trajectory prediction based on inter-vehicle-communication and vehicle-infrastructure-integration”. In: *Transp. Res. Part C: Emerg. Technol.* 45 (2014), pp. 41–63. DOI: <https://doi.org/10.1016/j.trc.2014.04.011>.

- [24] Tushar D Gaikwad et al. “Vehicle Velocity Prediction and Energy Management Strategy Part 2: Integration of Machine Learning Vehicle Velocity Prediction with Optimal Energy Management to Improve Fuel Economy”. In: *SAE Technical Paper* (2019). DOI: <https://doi.org/10.4271/2019-01-1212>.
- [25] Zachary D. Asher et al. “Identification and Review of the Research Gaps Preventing a Realization of Optimal Energy Management Strategies in Vehicles”. In: *SAE International Journal of Alternative Powertrains* 8.2 (2019). DOI: <https://doi.org/10.4271/08-08-02-0009>.
- [26] S. Javanmardi et al. “Driving style modelling for eco-driving applications”. In: *IFAC-PapersOnLine* 50.1 (2017), 13866–13871. DOI: <https://doi.org/10.1016/j.ifacol.2017.08.2233>.
- [27] Yiik-Diew Wong Sze-Hwee Ho and Victor Wei-Chung Chang. “What can eco-driving do for sustainable road transport? Perspectives from a city (Singapore) eco-driving programme”. In: *Sustainable Cities and Society* 14.- (2015), pp. 82–88. DOI: <https://doi.org/10.1016/j.scs.2014.08.002>.
- [28] Farhang Motallebi Araghi et al. *Machine Learning and Optimization Techniques for Automotive Cyber-Physical Systems*. (To Appear). Springer Nature, 2022. Chap. Identifying and Assessing Research Gaps for Energy Efficient Control of Electrified Autonomous Vehicle Eco-driving.
- [29] Yeongmin Kwon, Sanghoon Son, and Kitae Jang. “User satisfaction with battery electric vehicles in South Korea”. In: *Transportation Research Part D: Transport and Environment* 82 (2020), p. 102306. ISSN: 1361-9209. DOI: <https://doi.org/10.1016/j.trd.2020.102306>.
- [30] Iana Vassileva and Javier Campillo. “Adoption barriers for electric vehicles: Experiences from early adopters in Sweden”. In: *Energy* 120 (2017), pp. 632–641. ISSN: 0360-5442. DOI: <https://doi.org/10.1016/j.energy.2016.11.119>.

- [31] Myriam Neaimeh et al. “Analysing the usage and evidencing the importance of fast chargers for the adoption of battery electric vehicles”. In: *Energy Policy* 108 (2017), pp. 474–486. ISSN: 0301-4215. DOI: <https://doi.org/10.1016/j.enpol.2017.06.033>.
- [32] Jamie Dunckley and Gil Tal. “Plug-In Electric Vehicle Multi-State Market and Charging Survey”. In: *EPRI* (2016). URL: <https://www.epri.com/research/products/000000003002007495> (visited on 01/30/2023).
- [33] *EV Charging Statistics*. 2022. URL: <https://evadoption.com/ev-charging-stations-statistics/> (visited on 01/20/2022).
- [34] *President Biden, USDOT and USDOE announce \$5 billion over five years for national EV charging network, made possible by bipartisan infrastructure law*. URL: <https://highways.dot.gov/newsroom/president-biden-usdot-and-usdoe> (visited on 05/09/2022).
- [35] Bob Costello. *Economics and Industry Data*. <https://www.trucking.org/economics-and-industry-data>. 2023. (Visited on 03/19/2023).
- [36] EPA. “Inventory of U.S. Greenhouse Gas Emissions and Sinks: 1990-2021”. In: *U.S. Environmental Protection Agency, EPA 430-R-23-002* (2023). URL: <https://www.epa.gov/ghgemissions/inventory-us-greenhouse-gas-emissions-and-sinks-1990-2021> (visited on 02/01/2023).
- [37] *Vehicle Inventory and Use Survey (VIUS)*. <https://doi.org/10.21949/1506070>. (Visited on 01/01/2023).
- [38] Andrew Burnham et al. “Comprehensive Total Cost of Ownership Quantification for Vehicles with Different Size Classes and Powertrains”. In: *National Renewable Energy Laboratory* (Apr. 2021). DOI: <https://doi.org/10.2172/1780970>.
- [39] Matteo Muratori. “Exploring the Future of Mobility, Transportation Energy and Mobility Pathway Options (TEMPO) Model”. In: *National Renewable Energy Laboratory* (Oct. 2020). DOI: <https://doi.org/10.2172/1780970>.

- [40] Matteo Muratori et al. “Future integrated mobility-energy systems: A modeling perspective”. In: *Renewable and Sustainable Energy Reviews* 119 (2020), p. 109541. ISSN: 1364-0321. DOI: <https://doi.org/10.1016/j.rser.2019.109541>.
- [41] Ehsan Sabri Islam et al. “A Detailed Vehicle Modeling & Simulation Study Quantifying Energy Consumption and Cost Reduction of Advanced Vehicle Technologies Through 2050”. In: *Energy Systems Division, Argonne National Laboratory* (Oct. 2021). <https://publications.anl.gov/anlpubs/2021/10/171713.pdf>.
- [42] Ram Vijayagopal and Aymeric Rousseau. “Electric Truck Economic Feasibility Analysis”. In: *World Electric Vehicle Journal* 12.2 (2021). ISSN: 2032-6653. DOI: <https://doi.org/10.3390/wevj12020075>.
- [43] Kate Forrest et al. “Estimating the technical feasibility of fuel cell and battery electric vehicles for the medium and heavy duty sectors in California”. In: *Applied Energy* 276 (2020), p. 115439. ISSN: 0306-2619. DOI: <https://doi.org/10.1016/j.apenergy.2020.115439>.
- [44] Tessa T. Taefi, Sebastian Stütz, and Andreas Fink. “Assessing the cost-optimal mileage of medium-duty electric vehicles with a numeric simulation approach”. In: *Transportation Research Part D: Transport and Environment* 56 (2017), pp. 271–285. ISSN: 1361-9209. DOI: <https://doi.org/10.1016/j.trd.2017.08.015>.
- [45] Martina Wikström, Lisa Hansson, and Per Alvfors. “An End has a Start – Investigating the Usage of Electric Vehicles in Commercial Fleets”. In: *Energy Procedia* 75 (2015), pp. 1932–1937. ISSN: 1876-6102. DOI: <https://doi.org/10.1016/j.egypro.2015.07.223>.
- [46] “21st Century Truck Partnership Research Blueprint”. In: *Vehicle Technologies Office* (2019). URL: <https://www.energy.gov/eere/vehicles/articles/21st-century-truck-partnership-research-blueprint> (visited on 11/20/2022).
- [47] Aaron Rabinowitz et al. “Development and evaluation of Velocity Predictive Optimal Energy Management Strategies in intelligent and connected Hybrid Electric Vehicles”. In: *Energies* 14.18 (2021), p. 5713. DOI: <https://doi.org/10.3390/en14185713>.

- [48] Tushar Gaikwad et al. “Vehicle Velocity Prediction Using Artificial Neural Network and Effect of Real World Signals on Prediction Window”. In: *SAE Technical Paper* (2020). DOI: <https://doi.org/10.4271/2020-01-0729>.
- [49] World Health Organization. *World Health Statistics 2016: Monitoring Health for the SDGs Sustainable Development Goals*. en. World Health Organization, 2016. URL: <https://apps.who.int/iris/handle/10665/206498> (visited on 09/15/2021).
- [50] A E Atabani et al. “A review on global fuel economy standards, labels and technologies in the transportation sector”. In: *Renewable Sustainable Energy Rev.* 15.9 (2011), pp. 4586–4610. DOI: <https://doi.org/10.1016/j.rser.2011.07.092>.
- [51] Clara Marina Martinez et al. “Energy Management in Plug-in Hybrid Electric Vehicles: Recent Progress and a Connected Vehicles Perspective”. In: *IEEE Trans. Veh. Technol.* 66.6 (2017), pp. 4534–4549. DOI: <https://doi.org/10.1109/TVT.2016.2582721>.
- [52] Stephan Uebel et al. “Optimal Energy Management and Velocity Control of Hybrid Electric Vehicles”. In: *IEEE Trans. Veh. Technol.* 67.1 (2018), pp. 327–337. DOI: <https://doi.org/10.1109/TVT.2017.2727680>.
- [53] Lorenzo Serrao, Simona Onori, and Giorgio Rizzoni. “ECMS as a realization of Pontryagin’s minimum principle for HEV control”. In: *2009 American Control Conference*. 2009, pp. 3964–3969. DOI: <https://doi.org/10.1109/ACC.2009.5160628>.
- [54] Jinglai Wu et al. “An Optimized Real-Time Energy Management Strategy for the Power-Split Hybrid Electric Vehicles”. In: *IEEE Transactions on Control Systems Technology* 27.3 (2019), pp. 1194–1202. DOI: <https://doi.org/10.1109/TCST.2018.2796551>.
- [55] Cong Liang et al. “Coordinated control strategy for mode transition of dm-phev based on mld”. In: *Nonlinear Dynamics* 103.1 (2021), 809–832. DOI: <https://doi.org/10.1007/s11071-020-06126-z>.
- [56] Jordan A. Tunnell et al. “Towards Improving Vehicle Fuel Economy with ADAS”. In: *SAE Technical Paper Series* (2018). DOI: <https://doi.org/10.4271/2018-01-0593>.

- [57] Qiuming Gong, Yaoyu Li, and Zhong-Ren Peng. “Trip-Based Optimal Power Management of Plug-in Hybrid Electric Vehicles”. In: *IEEE Transactions on Vehicular Technology* 57.6 (2008), 3393–3401. DOI: <https://doi.org/10.1109/tvt.2008.921622>.
- [58] Zachary D Asher et al. “Enabling Prediction for Optimal Fuel Economy Vehicle Control”. In: *SAE Technical Paper* (2018). DOI: <https://doi.org/10.4271/2018-01-1015>.
- [59] David Baker, Zachary D. Asher, and Thomas Bradley. “V2V Communication Based Real-World Velocity Predictions for Improved HEV Fuel Economy”. In: *SAE Technical Paper Series* (2018). DOI: <https://doi.org/10.4271/2018-01-1000>.
- [60] Xuewei Qi et al. “Deep reinforcement learning enabled self-learning control for energy efficient driving”. In: *Transportation Research Part C: Emerging Technologies* 99 (2019), 67–81. DOI: <https://doi.org/10.1016/j.trc.2018.12.018>.
- [61] Kuan Liu et al. “Vehicle Velocity Prediction and Energy Management Strategy Part 1: Deterministic and Stochastic Vehicle Velocity Prediction Using Machine Learning”. In: *SAE Technical Paper* (2019). DOI: <https://doi.org/10.4271/2019-01-1051>.
- [62] Aaron I Rabinowitz et al. “Infrastructure Data Streams for Automotive Machine Learning Algorithms Research”. In: *SAE Technical Paper* (2020). DOI: <https://doi.org/10.4271/2020-01-0736>.
- [63] Andrew A Frank. *Control method and apparatus for internal combustion engine electric hybrid vehicles*. U.S. Patent 6054844, Apr. 2000. URL: <https://patents.justia.com/patent/6054844>.
- [64] Mohammad Reza Amini et al. “Experimental validation of eco-driving and eco-heating strategies for connected and automated hevs”. In: *SAE Technical Paper Series* (2021). DOI: <https://doi.org/10.4271/2021-01-0435>.
- [65] Xun Gong et al. “Real-time integrated power and thermal management of connected hevs based on hierarchical model predictive control”. In: *IEEE/ASME Transactions on Mechatronics* 26.3 (2021), 1271–1282. DOI: <https://doi.org/10.1109/tmech.2021.3070330>.

- [66] Hao Wang et al. “Eco-Cooling control strategy for Automotive Air-Conditioning System: Design and experimental validation”. In: *IEEE Transactions on Control Systems Technology* (2020), 1–12. DOI: <https://doi.org/10.1109/tcst.2020.3038746>.
- [67] *Dedicated Short Range Communications (DSRC) Message Set Dictionary*. URL: https://www.sae.org/standards/content/j2735_200911/ (visited on 06/14/2021).
- [68] *Taxonomy and Definitions for Terms Related to Driving Automation Systems for On-Road Motor Vehicles*. URL: https://www.sae.org/standards/content/j3016_202104/ (visited on 06/15/2022).
- [69] Ryosuke Okuda, Yuki Kajiwara, and Kazuaki Terashima. “A survey of technical trend of ADAS and autonomous driving”. In: *Proceedings of Technical Program - 2014 International Symposium on VLSI Technology, Systems and Application (VLSI-TSA)* (2014), pp. 1–4. DOI: <https://doi.org/10.1109/VLSI-TSA.2014.6839646>.
- [70] Christine Gschwendtner, Simon R. Sinsel, and Annegret Stephan. “Vehicle-to-X (V2X) implementation: An overview of predominate trial configurations and technical, social and regulatory challenges”. In: *Renewable and Sustainable Energy Reviews* 145 (2021), p. 110977. ISSN: 1364-0321. DOI: <https://doi.org/10.1016/j.rser.2021.110977>.
- [71] Cristian Musardo et al. “A-ECMS: An Adaptive Algorithm for Hybrid Electric Vehicle Energy Management”. In: *European Journal of Control* 11.4 (2005), pp. 509–524. ISSN: 0947-3580. DOI: <https://doi.org/10.3166/ejc.11.509-524>.
- [72] Chao Sun, Hongwen He, and Fengchun Sun. “The Role of Velocity Forecasting in Adaptive-ECMS for Hybrid Electric Vehicles”. In: *Energy Procedia* 75 (2015), 1907–1912. DOI: <https://doi.org/10.1016/j.egypro.2015.07.181>.
- [73] Zachary D. Asher, David A. Baker, and Thomas H. Bradley. “Prediction Error Applied to Hybrid Electric Vehicle Optimal Fuel Economy”. In: *IEEE Transactions on Control Systems Technology* 26.6 (2018), pp. 2121–2134. DOI: <https://doi.org/10.1109/TCST.2017.2747502>.

- [74] Weijing Shi et al. “Algorithm and hardware implementation for visual perception system in autonomous vehicle: A survey”. In: *Integration* 59 (2017), pp. 148–156. ISSN: 0167-9260. DOI: <https://doi.org/10.1016/j.vlsi.2017.07.007>.
- [75] Simona Onori, Lorenzo Serrao, and Giorgio Rizzoni. *Hybrid Electric Vehicles: Energy Management Strategies*. Springer, London, 2016. DOI: <https://doi.org/10.1007/978-1-4471-6781-5>.
- [76] Donald E. Kirk. *Optimal control theory: An introduction*. Prentice-Hall, 1970.
- [77] Mike Huang, Shengqi Zhang, and Yushi Shibaïke. “Real-time Long Horizon Model Predictive Control of a Plug-in Hybrid Vehicle Power-Split Utilizing Trip Preview”. In: *2019 JSAE/SAE Powertrains, Fuels and Lubricants* (2019). ISSN: 0148-7191. DOI: <https://doi.org/10.4271/2019-01-2341>.
- [78] Richard T. Meyer et al. “Hybrid Model Predictive Power Management of A Fuel Cell-Battery Vehicle”. In: *Asian Journal of Control* 15.2 (2013), pp. 363–379. DOI: <https://doi.org/10.1002/asjc.553>.
- [79] Namwook Kim, Aymeric Rousseau, and Eric Rask. “Autonomie Model Validation with Test Data for 2010 Toyota Prius”. In: *SAE Technical Paper Series* (2012). DOI: <https://doi.org/10.4271/2012-01-1040>.
- [80] *Downloadable Dynamometer Database: Argonne National Laboratory*. URL: <https://www.anl.gov/es/downloadable-dynamometer-database> (visited on 01/05/2021).
- [81] Sepp Hochreiter and Jurgen Schmidhuber. “Long short-term memory”. en. In: *Neural Comput.* 9.8 (1997), pp. 1735–1780. DOI: <http://dx.doi.org/10.1162/neco.1997.9.8.1735>.
- [82] Chiou-Jye Huang and Ping-Huan Kuo. “A Deep CNN-LSTM Model for Particulate Matter (PM_{2.5}) Forecasting in Smart Cities”. In: *Sensors* 18.7 (2018). ISSN: 1424-8220. DOI: <https://doi.org/10.3390/s18072220>.
- [83] Aaron I Rabinowitz et al. “Real Time Implementation Comparison of Urban Eco-Driving Controls”. In: *IEEE Transactions on Control Systems Technology* (2023). (To Appear).

- [84] Ernani F. Choma et al. “Health benefits of decreases in on-road transportation emissions in the United States from 2008 to 2017”. In: *Proceedings of the National Academy of Sciences* 118.51 (2021). DOI: <https://doi.org/10.1073/pnas.2107402118>.
- [85] David L. Greene, Charles B. Sims, and Matteo Muratori. “Two trillion gallons: Fuel savings from fuel economy improvements to US light-duty vehicles, 1975–2018”. In: *Energy Policy* 142 (2020), p. 111517. DOI: <https://doi.org/10.1016/j.enpol.2020.111517>.
- [86] Charles Andrew Miller. “Fifty Years of EPA Science for Air Quality Management and Control”. In: *Environmental Management* 67.6 (2021), 1017–1028. DOI: <https://doi.org/10.1007/s00267-021-01468-9>.
- [87] Peter Slowik and Nic Lutsey. URL: https://theicct.org/wp-content/uploads/2021/06/Transition_EV_US_Cities_20180724.pdf (visited on 05/07/2022).
- [88] Lucas Spangher et al. “Quantifying the impact of U.S. Electric Vehicle Sales on light-duty vehicle fleet CO₂ emissions using a novel agent-based simulation”. In: *Transportation Research Part D: Transport and Environment* 72 (2019), 358–377. DOI: <https://doi.org/10.1016/j.trd.2019.05.004>.
- [89] A. S. M. Bakibillah, M. A. S. Kamal, and C. P. Tan. “Sustainable Eco-driving Strategy at Signalized Intersections from Driving Data”. In: *2020 59th Annual Conference of the Society of Instrument and Control Engineers of Japan (SICE)*. 2020, pp. 165–170. DOI: <https://doi.org/10.23919/SICE48898.2020.9240463>.
- [90] Arne Kesting et al. “Adaptive cruise control design for active congestion avoidance”. In: *Transportation Research Part C: Emerging Technologies* 16.6 (2008), pp. 668–683. ISSN: 0968-090X. DOI: <https://doi.org/10.1016/j.trc.2007.12.004>.
- [91] Martin Treiber, Ansgar Hennecke, and Dirk Helbing. “Congested traffic states in empirical observations and microscopic simulations”. In: *Physical Review E* 62.2 (2000), 1805–1824. ISSN: 1095-3787. DOI: <https://doi.org/10.1016/j.trc.2007.12.004>.

- [92] Chaoru Lu et al. “An Ecological Adaptive Cruise Control for Mixed Traffic and Its Stabilization Effect”. In: *IEEE Access* 7 (2019), pp. 81246–81256. DOI: <https://doi.org/10.1109/ACCESS.2019.2923741>.
- [93] Qi Xin et al. “Predictive intelligent driver model for eco-driving using upcoming traffic signal information”. In: *Physica A: Statistical Mechanics and its Applications* 508 (2018), pp. 806–823. ISSN: 0378-4371. DOI: <https://doi.org/10.1016/j.physa.2018.05.138>.
- [94] Mofan Zhou, Xiaobo Qu, and Sheng Jin. “On the Impact of Cooperative Autonomous Vehicles in Improving Freeway Merging: A Modified Intelligent Driver Model-Based Approach”. In: *IEEE Transactions on Intelligent Transportation Systems* 18.6 (2017), pp. 1422–1428. DOI: <https://doi.org/10.1109/TITS.2016.2606492>.
- [95] Zhipeng Li et al. “Stability analysis of an extended intelligent driver model and its simulations under open boundary condition”. In: *Physica A: Statistical Mechanics and its Applications* 419 (2015), pp. 526–536. ISSN: 0378-4371. DOI: <https://doi.org/10.1016/j.physa.2014.10.063>.
- [96] Hesham Rakha and Raj Kishore Kamalanathsharma. “Eco-driving at signalized intersections using V2I communication”. In: *2011 14th International IEEE Conference on Intelligent Transportation Systems (ITSC)*. 2011, pp. 341–346. DOI: <https://doi.org/10.1109/ITSC.2011.6083084>.
- [97] Zifei Nie and Hooman Farzaneh. “Role of Model Predictive Control for Enhancing Eco-Driving of Electric Vehicles in Urban Transport System of Japan”. In: *Sustainability* 13.16 (2021). ISSN: 2071-1050. DOI: <https://doi.org/10.3390/su13169173>.
- [98] Wenqing Chen et al. “Platoon-Based Speed Control Algorithm for Ecodriving at Signalized Intersection”. In: *Transportation Research Record* 2489.1 (2015), pp. 29–38. DOI: <https://doi.org/10.3141/2489-04>.

- [99] Chaoru Lu and Arvid Aakre. “A new adaptive cruise control strategy and its stabilization effect on traffic flow”. In: *European Transport Research Review* 10 (June 2018). DOI: <https://doi.org/10.1186/s12544-018-0321-9>.
- [100] R Bellman. “Dynamic Programming and Lagrange Multipliers”. In: *National Acad Sciences* 42.10 (1956), pp. 767–769. DOI: <https://doi.org/10.1073/pnas.42.10.767>.
- [101] Masafumi Miyatake, Motoi Kuriyama, and Yuzuru Takeda. “Theoretical study on eco-driving technique for an Electric Vehicle considering traffic signals”. In: *2011 IEEE Ninth International Conference on Power Electronics and Drive Systems*. 2011, pp. 733–738. DOI: <https://doi.org/10.1109/PEDS.2011.6147334>.
- [102] Motoi Kuriyama, Sou Yamamoto, and Masafumi Miyatake. “Theoretical study on eco-driving technique for an electric vehicle with Dynamic Programming”. In: *Journal of international Conference on Electrical Machines and Systems* 1.1 (2012), 114–120. DOI: <https://doi.org/10.11142/jicems.2012.1.1.114>.
- [103] Erik Hellström et al. “Look-ahead control for heavy trucks to minimize trip time and fuel consumption”. In: *Control Engineering Practice* 17.2 (2009), pp. 245–254. ISSN: 0967-0661. DOI: <https://doi.org/10.1016/j.conengprac.2008.07.005>.
- [104] D. Maamria et al. “On the use of Dynamic Programming in eco-driving cycle computation for electric vehicles”. In: *2016 IEEE Conference on Control Applications (CCA)* (2016), pp. 1288–1293. DOI: <https://doi.org/10.1109/CCA.2016.7587984>.
- [105] D. Maamria et al. “Optimal eco-driving for conventional vehicles: Simulation and experiment”. In: *IFAC-PapersOnLine* 50.1 (2017). 20th IFAC World Congress, pp. 12557–12562. ISSN: 2405-8963. DOI: <https://doi.org/10.1016/j.ifacol.2017.08.2195>.
- [106] Shreshta Rajakumar Deshpande et al. “Real-Time Ecodriving Control in Electrified Connected and Autonomous Vehicles Using Approximate Dynamic Programming”. In: *Journal of Dynamic Systems, Measurement, and Control* 144.1 (Jan. 2022). 011111. ISSN: 0022-0434. DOI: <https://doi.org/10.1115/1.4053292>.

- [107] Shobhit Gupta et al. “A Computationally Efficient Algorithm for Perturbed Dynamic Programs (A-PDP)”. In: *IEEE Control Systems Letters* 7 (2023), pp. 847–852. DOI: <https://doi.org/10.1109/LCSYS.2022.3227910>.
- [108] Ardalan Vahidi and Antonio Sciarretta. “Energy saving potentials of connected and automated vehicles”. In: *Transportation Research Part C: Emerging Technologies* 95 (2018), pp. 822–843. ISSN: 0968-090X. DOI: <https://doi.org/10.1016/j.trc.2018.09.001>.
- [109] Thomas Stanger and Luigi del Re. “A model predictive Cooperative Adaptive Cruise Control approach”. In: *2013 American Control Conference*. 2013, pp. 1374–1379. DOI: <https://doi.org/10.1109/ACC.2013.6580028>.
- [110] Shaobing Xu and Huei Peng. “Design and Comparison of Fuel-Saving Speed Planning Algorithms for Automated Vehicles”. In: *IEEE Access* 6 (2018), pp. 9070–9080. DOI: <https://doi.org/10.1109/ACCESS.2018.2805883>.
- [111] Ben Groelke et al. “A Comparative Assessment of Economic Model Predictive Control Strategies for Fuel Economy Optimization of Heavy-Duty Trucks”. In: *2018 Annual American Control Conference (ACC)*. 2018, pp. 834–839. DOI: <https://doi.org/10.23919/ACC.2018.8431050>.
- [112] Sangjae Bae et al. “Real-time ecological velocity planning for plug-in hybrid vehicles with partial communication to traffic lights”. In: *2019 IEEE 58th Conference on Decision and Control (CDC)* (2019). DOI: <https://doi.org/10.1109/cdc40024.2019.9030166>.
- [113] Chao Sun et al. “Optimal eco-driving control of connected and autonomous vehicles through signalized intersections”. In: *IEEE Internet of Things Journal* 7.5 (2020), 3759–3773. DOI: <https://doi.org/10.1109/jiot.2020.2968120>.
- [114] Sangjae Bae et al. “Design and implementation of ecological adaptive cruise control for autonomous driving with communication to traffic lights”. In: *2019 American Control Conference (ACC)* (2019). DOI: <https://doi.org/10.23919/acc.2019.8814905>.

- [115] Heeyun Lee, Namwook Kim, and Suk Won Cha. “Model-Based Reinforcement Learning for Eco-Driving Control of Electric Vehicles”. In: *IEEE Access* 8 (2020), pp. 202886–202896. DOI: <https://doi.org/10.1109/ACCESS.2020.3036719>.
- [116] Shai Shalev-Shwartz, Shaked Shammah, and Amnon Shashua. *Safe, Multi-Agent, Reinforcement Learning for Autonomous Driving*. 2016. URL: <https://arxiv.org/abs/1610.03295>.
- [117] Meixin Zhu et al. “Safe, efficient, and comfortable velocity control based on reinforcement learning for autonomous driving”. In: *Transportation Research Part C: Emerging Technologies* 117 (2020), p. 102662. ISSN: 0968-090X. DOI: <https://doi.org/10.1016/j.trc.2020.102662>.
- [118] Diego Pardo et al. “Evaluating direct transcription and nonlinear optimization methods for robot motion planning”. In: *IEEE Robotics and Automation Letters* 1.2 (2016), pp. 946–953. DOI: <https://doi.org/10.1109/LRA.2016.2527062>.
- [119] Ahad Hamednia et al. “Computationally efficient algorithm for eco-driving over long look-ahead horizons”. In: *IEEE Transactions on Intelligent Transportation Systems* (2021), 1–15. DOI: <https://doi.org/10.1109/tits.2021.3058418>.
- [120] Z. Khalik et al. “Vehicle Energy Management with ecodriving: A sequential quadratic programming approach with dual decomposition”. In: *2018 Annual American Control Conference (ACC)* (2018). DOI: <https://doi.org/10.23919/acc.2018.8431544>.
- [121] G. P. Padilla, S. Weiland, and M. C. Donkers. “A global optimal solution to the eco-driving problem”. In: *IEEE Control Systems Letters* 2.4 (2018), 599–604. DOI: <https://doi.org/10.1109/lcsys.2018.2846182>.
- [122] Laura V. Pérez and Elvio A. Pilotta. “Optimal power split in a hybrid electric vehicle using direct transcription of an optimal control problem”. In: *Mathematics and Computers in Simulation* 79.6 (2009). Applied and Computational Mathematics Selected Papers of the

- Sixth Pan American Workshop July 23-28, 2006, Huatulco-Oaxaca, Mexico, pp. 1959–1970. ISSN: 0378-4754. DOI: <https://doi.org/10.1016/j.matcom.2007.03.006>.
- [123] Yara Hazem Mahmoud et al. “Autonomous Eco-Driving with Traffic Light and Lead Vehicle Constraints: An Application of Best Constrained Interpolation”. In: *IFAC-PapersOnLine* 10.10 (2021), pp. 45–50. DOI: <https://doi.org/10.1016/j.ifacol.2021.10.139>.
- [124] Asen L. Dontchev and Ilya Kolmanovsky. “State constraints in the linear regulator problem: A case study”. In: *Proceedings of 1994 33rd IEEE Conference on Decision and Control* (1995). DOI: <https://doi.org/10.1109/cdc.1994.410935>.
- [125] Asen L. Dontchev and Ilya Kolmanovsky. “Best interpolation in a strip II: Reduction to unconstrained convex optimization”. In: *Computational Optimization and Applications* 5.3 (1996), 233–251. DOI: <https://doi.org/10.1007/bf00248266>.
- [126] R. Eberhart and J. Kennedy. “A new optimizer using particle swarm theory”. In: *MHS'95. Proceedings of the Sixth International Symposium on Micro Machine and Human Science*. 1995, pp. 39–43. DOI: <https://doi.org/10.1109/MHS.1995.494215>.
- [127] Alan Turing. “Computing machinery and intelligence (1950)”. In: *The Essential Turing* (2004). DOI: <https://doi.org/10.1093/oso/9780198250791.003.0017>.
- [128] Alex Fraser and Donald Burnell. *Population Genetics: Computer models in Genetics*. McGraw-Hill, 1970. DOI: <https://doi.org/10.1126/science.172.3979.147.a>.
- [129] Jack L. Crosby. *Computer simulation in genetics*. Wiley London, New York, 1973, xiii, 477 p. ISBN: 0471188808. URL: <https://nla.gov.au/nla.cat-vn428632>.
- [130] Wonang Jang, Daeseong Jong, and Dohoon Lee. “Methodology to improve driving habits by optimizing the in-vehicle data extracted from OBDII using genetic algorithm”. In: *2016 International Conference on Big Data and Smart Computing (BigComp)*. 2016, pp. 313–316. DOI: <https://doi.org/10.1109/BIGCOMP.2016.7425936>.

- [131] Jinjian Li, Mahjoub Dridi, and Abdellah El-Moudni. “A cooperative traffic control for the vehicles in the intersection based on the Genetic Algorithm”. In: *2016 4th IEEE International Colloquium on Information Science and Technology (CiSt)*. 2016, pp. 627–632. DOI: <https://doi.org/10.1109/CIST.2016.7804962>.
- [132] Subramaniam Saravana Sankar et al. “Optimal Eco-Driving Cycles for Conventional Vehicles Using a Genetic Algorithm”. In: *Energies* 13.17 (2020). ISSN: 1996-1073. DOI: <https://doi.org/10.3390/en13174362>.
- [133] Mukesh Gautam et al. “A GA-based Approach to Eco-driving of Electric Vehicles Considering Regenerative Braking”. In: *2021 IEEE Conference on Technologies for Sustainability (SusTech)* (2021), pp. 1–6. DOI: 10.1109/SusTech51236.2021.9467457.
- [134] Sina Torabi, Mauro Bellone, and Mattias Wahde. “Energy minimization for an electric bus using a genetic algorithm”. In: *European Transport Research Review* 12 (2020), pp. 1–8. DOI: <https://doi.org/10.1186/s12544-019-0393-1>.
- [135] Sofiene Kachroudi, Mathieu Grossard, and Neil Abroug. “Predictive Driving Guidance of Full Electric Vehicles Using Particle Swarm Optimization”. In: *IEEE Transactions on Vehicular Technology* 61.9 (2012), pp. 3909–3919. DOI: <https://doi.org/10.1109/TVT.2012.2212735>.
- [136] Adrián Fernández-Rodríguez, Antonio Fernández-Cardador, and Asunción P. Cucala. “Real time eco-driving of high speed trains by simulation-based dynamic multi-objective optimization”. In: *Simulation Modelling Practice and Theory* 84 (2018), pp. 50–68. ISSN: 1569-190X. DOI: <https://doi.org/10.1016/j.simpat.2018.01.006>.
- [137] Vito Calderaro et al. “Deterministic vs heuristic algorithms for eco-driving application in metro network”. In: *2015 International Conference on Electrical Systems for Aircraft, Railway, Ship Propulsion and Road Vehicles (ESARS)*. 2015, pp. 1–6. DOI: <https://doi.org/10.1109/ESARS.2015.7101502>.

- [138] Bing Liu and Abdelkader El Kamel. “V2X-Based Decentralized Cooperative Adaptive Cruise Control in the Vicinity of Intersections”. In: *IEEE Transactions on Intelligent Transportation Systems* 17.3 (2016), pp. 644–658. DOI: <https://doi.org/10.1109/TITS.2015.2486140>.
- [139] Mark Campbell et al. “Autonomous driving in urban environments: approaches, lessons and challenges”. en. In: *Philos. Trans. A Math. Phys. Eng. Sci.* 368.1928 (2010), pp. 4649–4672. DOI: <https://doi.org/10.1098/rsta.2010.0110>.
- [140] *IIHS announcement on AEB*. 2017. URL: <https://www.nhtsa.gov/press-releases/nhtsa-iihs-announcement-aeb> (visited on 08/14/2021).
- [141] Aaron Brooker et al. “FASTSim: A model to estimate vehicle efficiency, cost and performance”. In: *SAE Technical Paper Series* (2015). DOI: <https://doi.org/10.4271/2015-01-0973>.
- [142] Francesco Viti et al. “Speed and acceleration distributions at a traffic signal analyzed from microscopic real and simulated data”. In: *2008 11th International IEEE Conference on Intelligent Transportation Systems*. 2008, pp. 651–656. DOI: <https://doi.org/10.1109/ITSC.2008.4732552>.
- [143] Rui Liu et al. “Statistical characteristics of driver acceleration behaviour and its probability model”. In: *Proceedings of the Institution of Mechanical Engineers, Part D: Journal of Automobile Engineering* 236.2-3 (2021), 395–406. DOI: <https://doi.org/10.1177/09544070211018039>.
- [144] Wouter J. Schakel, Victor L. Knoop, and Bart van Arem. “Integrated Lane change model with relaxation and synchronization”. In: *Transportation Research Record: Journal of the Transportation Research Board* 2316.1 (2012), 47–57. DOI: <https://doi.org/10.3141/2316-06>.

- [145] Martin Treiber and Dirk Helbing. “Microsimulations of freeway traffic including control measures”. In: *Auto* 49.11 (2001), p. 478. DOI: <https://doi.org/10.1524/auto.2001.49.11.478>.
- [146] Christian Thiemann, Martin Treiber, and Arne Kesting. “Estimating acceleration and Lane-changing dynamics from Next Generation simulation trajectory data”. In: *Transportation Research Record: Journal of the Transportation Research Board* 2088.1 (2008), 90–101. DOI: <https://doi.org/10.3141/2088-10>.
- [147] Bharatkumar Hegde et al. “Real-World Driving Features for Identifying Intelligent Driver Model Parameters”. In: *SAE WCX Digital Summit* (2021). ISSN: 0148-7191. DOI: <https://doi.org/10.4271/2021-01-0436>.
- [148] Niket Prakash et al. “Assessing fuel economy from Automated Driving: Influence of preview and velocity constraints”. In: *Volume 2: Mechatronics; Mechatronics and Controls in Advanced Manufacturing; Modeling and Control of Automotive Systems and Combustion Engines; Modeling and Validation; Motion and Vibration Control Applications; Multi-Agent and Networked Systems; Path Planning and Motion Control; Robot Manipulators; Sensors and Actuators; Tracking Control Systems; Uncertain Systems and Robustness; Unmanned, Ground and Surface Robotics; Vehicle Dynamic Controls; Vehicle Dynamics and Traffic Control* (2016). DOI: <https://doi.org/10.1115/dscc2016-9780>.
- [149] Niket Prakash et al. “Use of the hypothetical lead (HL) vehicle trace: A new method for evaluating fuel consumption in automated driving”. In: *2016 American Control Conference (ACC)* (2016). DOI: <https://doi.org/10.1109/acc.2016.7525453>.
- [150] Shima Nazari et al. “On the effectiveness of hybridization paired with eco-driving”. In: *2019 American Control Conference (ACC)* (2019). DOI: <https://doi.org/10.23919/acc.2019.8814975>.

- [151] *Road Load Measurement and Dynamometer Simulation Using Cooldown Techniques*. URL: https://saemobilus.sae.org/content/J1263_201003 (visited on 06/14/2021).
- [152] Jinwoo Seok et al. “Energy-efficient control approach for automated hev and bev with short-horizon preview information”. In: *Dynamic Systems and Control Conference* (2018). DOI: <https://doi.org/10.1115/DSCC2018-8980>.
- [153] John T. Betts. “Survey of Numerical Methods for Trajectory Optimization”. In: *Journal of Guidance, Control, and Dynamics* 21.2 (1998), pp. 193–207. DOI: <https://doi.org/10.2514/2.4231>.
- [154] Jorge Nocedal and Stephen J Wright. *Numerical Optimization*. 2nd ed. Springer, 2013. DOI: <https://doi.org/10.1007/978-0-387-40065-5>.
- [155] Daniel Ronald Herber et al. “Advances in combined architecture, plant, and Control Design”. PhD thesis, 90–135.
- [156] Andreas Wächter and Lorenz T. Biegler. “On the implementation of an interior-point filter line-search algorithm for large-scale nonlinear programming”. In: *Mathematical Programming* 106.1 (2005), 25–57. DOI: <https://doi.org/10.1007/s10107-004-0559-y>.
- [157] Seung-Jean Kim et al. “An interior-point method for large-scale ℓ_1 -regularized least squares”. In: *IEEE Journal of Selected Topics in Signal Processing* 1.4 (2007), 606–617. DOI: <https://doi.org/10.1109/jstsp.2007.910971>.
- [158] Chad Baker et al. “Future Automotive Systems Technology Simulator (fastsim) validation report - 2021”. In: *National Renewable Energy Laboratory* (2021). DOI: <https://doi.org/10.2172/1828851>.
- [159] *2015 Kia Soul ev - specifications*. URL: <https://www.evspecifications.com/en/model/f45094> (visited on 05/17/2022).
- [160] Xing Cai, Hans Petter Langtangen, and Halvard Moe. “On the performance of the Python programming language for serial and Parallel Scientific Computations”. In: *Scientific Programming* 13.1 (2005), 31–56. DOI: <https://doi.org/10.1155/2005/619804>.

- [161] Giancarlo Zaccone. *Python Parallel Programming Cookbook*. Packt Publishing Limited, 2015. URL: <https://github.com/PacktPublishing/Python-Parallel-Programming-Cookbook-Second-Edition>.
- [162] Alexandru Constantin Serban, Erik Poll, and Joost Visser. “A Standard Driven Software Architecture for Fully Autonomous Vehicles”. In: *2018 IEEE International Conference on Software Architecture Companion (ICSA-C)*. 2018, pp. 120–127. DOI: <https://doi.org/10.1109/ICSA-C.2018.00040>.
- [163] Chao Sun et al. “An integrated software environment for powertrain feasibility assessment using optimization and optimal control”. In: *Asian Journal of Control, Special Issue on New Trends in Automotive Powertrain Systems* 8.3 (2006), pp. 199–209. DOI: <https://doi.org/10.1111/j.1934-6093.2006.tb00271.x>.
- [164] Aaron I. Rabinowitz et al. “Assessment of Factors in the Reduction of BEV Operational Inconvenience”. In: *IEEE Access* 11 (2023), pp. 30486–30497. DOI: <https://doi.org/10.1109/ACCESS.2023.3255103>.
- [165] Mohd Khalid et al. “A comprehensive review on advanced charging topologies and methodologies for electric vehicle battery”. In: *Journal of Energy Storage* 53 (2022), p. 105084. ISSN: 2352-152X. DOI: <https://doi.org/10.1016/j.est.2022.105084>.
- [166] *Lithium-Ion Battery*. 2020. URL: <https://www.cei.washington.edu/education/science-of-solar/battery-technology> (visited on 01/20/2022).
- [167] EV-Database. *Tesla Model 3 long range dual motor*. 2021. URL: <https://ev-database.org/car/1525/Tesla-Model-3-Long-Range-Dual-Motor> (visited on 01/20/2022).
- [168] Cars.com. *2022 Chevrolet Malibu Specs, Trims & Colors*. 2022. URL: <https://www.cars.com/research/chevrolet-malibu-2022/specs/> (visited on 07/08/2021).
- [169] *Average annual PMT, VMT person trips and trip length by Trip Purpose*. URL: <https://www.bts.gov/content/average-annual-pmt-vmt-person-trips-and-trip-length-trip-purpose> (visited on 07/08/2021).

- [170] *Fuel conversion factors to gasoline gallon equivalents*. URL: <https://epact.energy.gov/fuel-conversion-factors> (visited on 02/01/2023).
- [171] API. *Consumer Resources*. 2023. URL: <https://www.api.org/oil-and-natural-gas/consumer-information/consumer-resources/> (visited on 02/01/2023).
- [172] Keisuke Sato, Kei Tamura, and Norio Tomii. “A MIP-based timetable rescheduling formulation and algorithm minimizing further inconvenience to passengers”. In: *Journal of Rail Transport Planning and Management* 3.3 (2013), 38–53. DOI: <https://doi.org/10.1016/j.jrtpm.2013.10.007>.
- [173] Kjetil Fagerholt. “Ship scheduling with soft time windows: An optimisation based approach”. In: *European Journal of Operational Research* 131.3 (2001), pp. 559–571. ISSN: 0377-2217. DOI: [https://doi.org/10.1016/S0377-2217\(00\)00098-9](https://doi.org/10.1016/S0377-2217(00)00098-9).
- [174] Jean-Francois Cordeaa et al. “Minimizing User Inconvenience and Operational Costs in a Dial-a-Flight Problem for Air Safaris”. In: *Chaire Logistique* (2021). DOI: <https://chairelogistique.hec.ca/wp-content/uploads/2021/12/DAFP.pdf>.
- [175] Xiao-Bing Hu and Ezequiel Di Paolo. “An efficient genetic algorithm with uniform crossover for air traffic control”. In: *Computers & Operations Research* 36.1 (2009). Part Special Issue: Operations Research Approaches for Disaster Recovery Planning, pp. 245–259. ISSN: 0305-0548. DOI: <https://doi.org/10.1016/j.cor.2007.09.005>.
- [176] Qian Sun et al. “Optimizing Multi-Terminal Customized Bus Service With Mixed Fleet”. In: *IEEE Access* 8 (2020), pp. 156456–156469. DOI: <https://doi.org/10.1109/ACCESS.2020.3018883>.
- [177] Kazumasa Kumazawa, Kosuke Hara, and Takafumi Koseki. “A Novel Train Rescheduling Algorithm for Correcting Disrupted Train Operations in a Dense Urban Environment”. In: *WIT Transactions on the Built Environment* 103 (2008), pp. 565–574. DOI: <https://doi.org/10.2495/CR080551>.

- [178] S. Murata and C.J. Goodman. “Optimally regulating disturbed metro traffic with passenger inconvenience in mind”. In: *1998 International Conference on Developments in Mass Transit Systems Conf. Publ. No. 453*. 1998, pp. 86–91. DOI: <https://doi.org/10.1049/cp:19980102>.
- [179] Kari Edison Watkins et al. “Where Is My Bus? Impact of mobile real-time information on the perceived and actual wait time of transit riders”. In: *Transportation Research Part A: Policy and Practice* 45.8 (2011), pp. 839–848. ISSN: 0965-8564. DOI: <https://doi.org/10.1016/j.tra.2011.06.010>.
- [180] *Homeownership rate in the United States*. 2022. URL: <https://fred.stlouisfed.org/series/RHORUSQ156N> (visited on 08/07/2022).
- [181] Michael A. Tamor and Miloš Milačić. “Electric vehicles in multi-vehicle households”. In: *Transportation Research Part C: Emerging Technologies* 56 (2015), 52–60. DOI: <https://doi.org/10.1016/j.trc.2015.02.023>.
- [182] Michael A. Tamor et al. “Rapid estimation of electric vehicle acceptance using a general description of driving patterns”. In: *Transportation Research Part C: Emerging Technologies* 51 (2015), 136–148. DOI: <https://doi.org/10.1016/j.trc.2014.10.010>.
- [183] Jee Eun Kang and Will W. Recker. “Measuring the inconvenience of operating an alternative fuel vehicle”. In: *Transportation Research Part D: Transport and Environment* 27 (2014), 30–40. DOI: <https://doi.org/10.1016/j.trd.2013.12.003>.
- [184] James Dixon et al. “On the ease of being green: An investigation of the inconvenience of Electric Vehicle Charging”. In: *Applied Energy* 258 (2020), p. 114090. DOI: <https://doi.org/10.1016/j.apenergy.2019.114090>.
- [185] Eric Wood, Jeremy S. Neubauer, and Evan Burton. “Quantifying the Effect of Fast Charger Deployments on Electric Vehicle Utility and Travel Patterns via Advanced Simulation”. In: *SAE 2015 World Congress & Exhibition*. SAE International, 2015. DOI: <https://doi.org/10.4271/2015-01-1687>.

- [186] Yutaka Motoaki. “Location-Allocation of Electric Vehicle Fast Chargers—Research and Practice”. In: *World Electric Vehicle Journal* 10.1 (2019). ISSN: 2032-6653. DOI: <https://doi.org/10.3390/wevj10010012>.
- [187] *Supercharger | Tesla Other Europe*. URL: https://www.tesla.com/en_eu/supercharger (visited on 03/16/2022).
- [188] *Tesla Superchargers in United States*. URL: <https://www.tesla.com/findus/list/superchargers/United%20States> (visited on 03/16/2022).
- [189] EPA. *Data on Cars used for Testing Fuel Economy*. 2023. URL: <https://www.epa.gov/compliance-and-fuel-economy-data/data-cars-used-testing-fuel-economy> (visited on 02/01/2023).
- [190] *J1772: SAE Electric Vehicle and Plug in Hybrid Electric Vehicle Conductive Charge Coupler*. URL: https://www.sae.org/standards/content/j1772_201710/ (visited on 01/30/2023).
- [191] Francesco Marra et al. “Demand profile study of battery electric vehicle under different charging options”. In: *2012 IEEE Power and Energy Society General Meeting* (2012), pp. 1–7. DOI: <https://doi.org/10.1109/PESGM.2012.6345063>.
- [192] EV-Database. *Useable battery capacity of full electric vehicles*. 2023. URL: <https://ev-database.org/cheatsheet/useable-battery-capacity-electric-car> (visited on 01/20/2022).
- [193] David Trinko et al. “Combining ad hoc text mining and descriptive analytics to investigate public EV charging prices in the United States”. In: *Energies* 14.17 (2021), p. 5240. DOI: <https://doi.org/10.3390/en14175240>.
- [194] Aaron I Rabinowitz et al. “A Geo-Spatial Method for Calculating BEV Charging Inconvenience using Publicly Available Data”. In: *INCOSE IS23* (2023). (To Appear).
- [195] Aaron I Rabinowitz et al. “Geo-Spatial Measurement of BEV Charging Inconvenience and Implications for BEV Equity”. In: *IEEE Transactions on Intelligent Transportation Systems* (2023). (To Appear).

- [196] Stacey C Davis and Robert G Boundy. “Transportation Energy Data Book”. In: *Oak Ridge National Laboratory* (2022). URL: <https://tedb.ornl.gov/>.
- [197] *Inventory of U.S. Greenhouse Gas Emissions and Sinks: 1990-2020*. URL: <https://www.epa.gov/ghgemissions/inventory-us-greenhouse-gas-emissions-and-sinks-1990-2020> (visited on 02/01/2023).
- [198] Giulio Mattioli et al. “The political economy of car dependence: A systems of provision approach”. In: *Energy Research & Social Science* 66 (2020), p. 101486. ISSN: 2214-6296. DOI: <https://doi.org/10.1016/j.erss.2020.101486>.
- [199] Ralph Buehler. “Determinants of transport mode choice: a comparison of Germany and the USA”. In: *Journal of Transport Geography* 19.4 (2011), pp. 644–657. ISSN: 0966-6923. DOI: <https://doi.org/10.1016/j.jtrangeo.2010.07.005>.
- [200] Pedram Saeidizand, Koos Fransen, and Kobe Boussauw. “Revisiting car dependency: A worldwide analysis of car travel in global metropolitan areas”. In: *Cities* 120 (2022), p. 103467. ISSN: 0264-2751. DOI: <https://doi.org/10.1016/j.cities.2021.103467>.
- [201] S Lu. “Vehicle Survivability and Travel Mileage Schedules”. In: *NHTSA’s National Center for Statistics and Analysis* (2006). URL: <https://crashstats.nhtsa.dot.gov/Api/Public/ViewPublication/809952>.
- [202] *Average age of automobiles and trucks in operation in the United States*. URL: <https://www.bts.gov/content/average-age-automobiles-and-trucks-operation-united-states> (visited on 07/08/2021).
- [203] *Greenhouse Gas Emissions from a Typical Passenger Vehicle*. URL: <https://www.epa.gov/greenvehicles/greenhouse-gas-emissions-typical-passenger-vehicle> (visited on 02/01/2023).
- [204] *Electric Vehicle Charging Speeds*. 2022. URL: <https://www.transportation.gov/rural/ev/toolkit/ev-basics/charging-speeds> (visited on 07/08/2021).

- [205] United States Census Bureau. *TOTAL POPULATION IN OCCUPIED HOUSING UNITS BY TENURE BY UNITS IN STRUCTURE*. U.S. Census Bureau's American Community Survey Office. <https://data.census.gov/table?q=single+unit&d=ACS+1-Year+Estimates+Detailed+Tables&tid=ACSDT1Y2021.B25033>. 2021. (Visited on 11/05/2022).
- [206] Abby Brown, Alexis Schayowitz, and Emily Klotz. "Electric Vehicle Charging Infrastructure Trends from the Alternative Fueling Station Locator: First Quarter 2021". In: *National Renewable Energy Laboratory* (2021). URL: <https://www.nrel.gov/docs/fy21osti/80684.pdf>.
- [207] Margaret Smith and Jonathan Castellano. "Costs Associated With Non-Residential Electric Vehicle Supply Equipment". In: *U.S. Department of Energy* (2015). https://afdc.energy.gov/files/u/publication/evse_cost_report_2015.pdf.
- [208] Cheng Jin et al. "Spatial inequity in access to healthcare facilities at a county level in a developing country: A case study of deqing county, zhejiang, China". In: *International Journal for Equity in Health* 14.1 (2015). DOI: <https://doi.org/10.1186/s12939-015-0195-6>.
- [209] Melissa E. Cyr et al. "Access to Specialty Healthcare in urban versus rural US populations: A systematic literature review - BMC health services research". In: *BioMed Central* (2019). DOI: <https://doi.org/10.1186/s12913-019-4815-5>.
- [210] *Evi-X modeling suite of Electric Vehicle Charging Infrastructure Analysis Tools*. URL: <https://www.nrel.gov/transportation/evi-x.html> (visited on 03/16/2022).
- [211] Dong-Yeon Lee. *EVI Equity*. URL: <https://www.nrel.gov/transportation/evi-equity.html> (visited on 03/01/2022).
- [212] FHA. *2017 National Household Travel Survey*. 2017. URL: <https://nhts.ornl.gov/> (visited on 01/31/2022).

- [213] Will W. Recker. “The household activity pattern problem: General formulation and solution”. In: *Transportation Research Part B: Methodological* 29.1 (1995), pp. 61–77. ISSN: 0191-2615. DOI: [https://doi.org/10.1016/0191-2615\(94\)00023-S](https://doi.org/10.1016/0191-2615(94)00023-S).
- [214] *H3: Hexagonal hierarchical geospatial indexing system*. URL: <https://h3geo.org/> (visited on 01/12/2022).
- [215] AFDC. *EERE: Alternative fuels data center home page*. 2023. URL: <https://afdc.energy.gov/> (visited on 01/12/2022).
- [216] OpenStreetMap. *API*. 2023. URL: <https://wiki.openstreetmap.org/wiki/API> (visited on 05/11/2021).
- [217] Google. *Maps JavaScript API*. 2023. URL: <https://developers.google.com/maps/documentation/javascript> (visited on 05/09/2022).
- [218] Microsoft. *Technical documentation*. 2023. URL: <https://learn.microsoft.com/en-us/docs/> (visited on 05/09/2022).
- [219] Microsoft. *Bing maps API: Free trial, explore features, talk to specialists*. 2022. URL: <https://www.microsoft.com/en-us/maps/choose-your-bing-maps-api> (visited on 05/09/2022).
- [220] Mapbox. *Maps and location for developers*. 2023. URL: <https://www.mapbox.com/> (visited on 01/12/2022).
- [221] Ge Yanbo et al. “There’s No Place Like Home: Residential Parking, Electrical Access, and Implications for the Future of Electric Vehicle Charging Infrastructure”. In: *National Renewable Energy Laboratory NREL/TP-5400-81065* (2021). <https://www.nrel.gov/docs/fy22osti/81065.pdf>.
- [222] Chris Harto. “Electric Vehicle Ownership Costs: Today’s Electric Vehicles Offer Big Savings for Consumers”. In: *Consumer Reports* (). <https://advocacy.consumerreports.org/wp-content/uploads/2020/10/EV-Ownership-Cost-Final-Report-1.pdf>.

- [223] Adrian König et al. “An Overview of Parameter and Cost for Battery Electric Vehicles”. In: *World Electric Vehicle Journal* 12.1 (2021). ISSN: 2032-6653. DOI: <https://doi.org/10.3390/wevj12010021>.
- [224] David Trinko et al. “Transportation and electricity systems integration via electric vehicle charging-as-a-service: A review of techno-economic and societal benefits”. In: *Renewable and Sustainable Energy Reviews* 175 (2023), p. 113180. ISSN: 1364-0321. DOI: <https://doi.org/10.1016/j.rser.2023.113180>.
- [225] Jeffrey Short, Alexandra Shirk, and Alexa Pupillo. “Charging Infrastructure Challenges for the U.S. Electric Vehicle Fleet”. In: *ATRI* (Dec. 2022). URL: <https://truckingresearch.org/2022/12/charging-infrastructure-challenges-for-the-u-s-electric-vehicle-fleet/>.
- [226] R. S. K. Moorthy et al. “Megawatt Scale Charging System Architecture”. In: *2022 IEEE Energy Conversion Congress and Exposition (ECCE)*. 2022, pp. 1–8. DOI: <https://doi.org/10.1109/ECCE50734.2022.9947403>.
- [227] David Trinko et al. “Combining Ad Hoc Text Mining and Descriptive Analytics to Investigate Public EV Charging Prices in the United States”. In: *Energies* 14.17 (2021). ISSN: 1996-1073. DOI: <https://doi.org/10.3390/en14175240>.
- [228] Samuel Pelletier et al. “Battery degradation and behaviour for electric vehicles: Review and numerical analyses of several models”. In: *Transportation Research Part B: Methodological* 103 (2017). Green Urban Transportation, pp. 158–187. ISSN: 0191-2615. DOI: <https://doi.org/10.1016/j.trb.2017.01.020>.
- [229] *Summary of Hours of Service Regulations*. URL: <https://www.fmcsa.dot.gov/regulations/hours-service/summary-hours-service-regulations> (visited on 03/05/2023).
- [230] Carlo Cunanan et al. “A Review of Heavy-Duty Vehicle Powertrain Technologies: Diesel Engine Vehicles, Battery Electric Vehicles, and Hydrogen Fuel Cell Electric Vehicles”. In: *Clean Technologies* 3.2 (2021), pp. 474–489. ISSN: 2571-8797. DOI: <https://doi.org/10.3390/cleantechnol3020028>.

- [231] Gautam Kalghatgi. “Is it really the end of internal combustion engines and petroleum in transport?” In: *Applied Energy* 225 (2018), pp. 965–974. ISSN: 0306-2619. DOI: <https://doi.org/10.1016/j.apenergy.2018.05.076>.
- [232] Anna Tomaszewska et al. “Lithium-ion battery fast charging: A review”. In: *eTransportation* 1 (2019), p. 100011. ISSN: 2590-1168. DOI: <https://doi.org/10.1016/j.etrans.2019.100011>.
- [233] Brennan Borlaug et al. “Levelized Cost of Charging Electric Vehicles in the United States”. In: *Joule* 4.7 (2020), pp. 1470–1485. ISSN: 2542-4351. DOI: <https://doi.org/10.1016/j.joule.2020.05.013>.
- [234] Tisura Gamage, Gil Tal, and Alan T. Jenn. “The costs and challenges of installing corridor DC Fast Chargers in California”. In: *Case Studies on Transport Policy* 11 (2023), p. 100969. ISSN: 2213-624X. DOI: <https://doi.org/10.1016/j.cstp.2023.100969>.
- [235] I-Yun Lisa Hsieh et al. “Learning only buys you so much: Practical limits on battery price reduction”. In: *Applied Energy* 239 (2019), pp. 218–224. ISSN: 0306-2619. DOI: <https://doi.org/10.1016/j.apenergy.2019.01.138>.
- [236] Apurba Sakti et al. “Consistency and robustness of forecasting for emerging technologies: The case of Li-ion batteries for electric vehicles”. In: *Energy Policy* 106 (2017), pp. 415–426. ISSN: 0301-4215. DOI: <https://doi.org/10.1016/j.enpol.2017.03.063>.
- [237] Marc Wentker, Matthew Greenwood, and Jens Leker. “A Bottom-Up Approach to Lithium-Ion Battery Cost Modeling with a Focus on Cathode Active Materials”. In: *Energies* 12.3 (2019). ISSN: 1996-1073. DOI: <https://doi.org/10.3390/en12030504>.
- [238] Lukas Mauler et al. “Battery cost forecasting: a review of methods and results with an outlook to 2050”. In: *Energy Environ. Sci.* 14 (9 2021), pp. 4712–4739. DOI: <https://doi.org/10.1039/D1EE01530C>.

- [239] F. Duffner et al. “Battery cost modeling: A review and directions for future research”. In: *Renewable and Sustainable Energy Reviews* 127 (2020), p. 109872. ISSN: 1364-0321. DOI: <https://doi.org/10.1016/j.rser.2020.109872>.
- [240] F. Duffner et al. “Post-lithium-ion battery cell production and its compatibility with lithium-ion cell production infrastructure”. In: *Nature Energy* 6 (2021), pp. 123–134. DOI: <https://doi.org/10.1038/s41560-020-00748-8>.
- [241] Shabbir Ahmed et al. “BaTPaC Model Developemnt”. In: *2016 DOE Vehicle Technologies Office Annual Merit Review and Peer Evaluation Meeting* (June 2016). URL: <https://www.anl.gov/cse/batpac-model-software>.
- [242] Bjorn Nykvist and Mans Nilsson. “Rapidly falling costs of battery packs for electric vehicles”. In: *Nature Climate Change* 5 (Mar. 2015). <https://www.nature.com/articles/nclimate2564>, pp. 329–332.
- [243] O. Schmidt et al. “The future cost of electrical energy storage based on experience rates”. In: *Nature Energy* 2.17110 (July 2017). <https://doi.org/10.1038/nenergy.2017.110>.
- [244] N Kittner, F Lill, and D M Kammen. “Energy storage deployment and innovation for the clean energy transition”. In: *Nature Energy* 2.17125 (July 2017). <https://doi.org/10.1038/nenergy.2017.125>.
- [245] Steven Boyd. “Batteries and Electrification R&D”. In: *2020 DOE Vehicle Technologies Office Program Review* (June 2020). <https://www.energy.gov/node/4523480>.
- [246] P A Nelson et al. “Modeling the Performance and Cost of Lithium-Ion Batteries for Electric-Drive Vehicles”. In: *DOE Vehicle Technologies Office* (Dec. 2012). <https://publications.anl.gov/anlpubs/2015/05/75574.pdf>.
- [247] *Autonomie Vehicle System Simulation Tool*. URL: <https://www.anl.gov/taps/autonomie-vehicle-system-simulation-tool> (visited on 04/09/2021).

- [248] Marissa Moultak, Nic Lustey, and Hall Dale. “Transitioning to Zero-Emission Heavy-Duty Freight Vehicles”. In: *The International Council on Clean Transportation* (Sept. 2017). <https://theicct.org/publication/transitioning-to-zero-emission-heavy-duty-freight-vehicles/>.
- [249] S Gilleon, M Penev, and C Hunter. “Powertrain Performance and Total Cost of Ownership Analysis for Class 8 Yard Tractors and Refuse Trucks.” In: *National Renewable Energy Laboratory. NREL/TP-5400-83968* (2022). <https://www.nrel.gov/docs/fy23osti/83968.pdf>.
- [250] C Hunter et al. “Spatial and Temporal Analysis of the Total Cost of Ownership for Class 8 Tractors and Class 4 Parcel Delivery Trucks.” In: *National Renewable Energy Laboratory. NREL/TP-5400-71796* (2021). <https://www.nrel.gov/docs/fy21osti/71796.pdf>.
- [251] E Den Boer et al. “Zero emission trucks. An overview of state-of-the-art technologies and their potential.” In: *CE Delft* (July 2013). http://www.theicct.org/sites/default/files/publications/CE_Delft_4841_Zero_emissions_trucks_Def.pdf.
- [252] J Neubauer and A Pesaran. “NREL’s PHEV/EV Li-ion Battery Secondary-Use Project”. In: *Advanced Automotive Batteries Conference (AABC) 2010* (Oct. 2010). <https://www.nrel.gov/docs/fy10osti/48042.pdf>.
- [253] Dan Murray and Seth Glidewell. “An Analysis of the Operational Costs of Trucking: 2019 Update.” In: *American Transportation Research Institute (ATRI)* (Nov. 2019). <https://truckingresearch.org/wp-content/uploads/2019/11/ATRI-Operational-Costs-of-Trucking-2019-1.pdf>.
- [254] *Lightning Electric Zero Emission Transit Cargo Van*. URL: <https://lightningemotors.com/lightningelectric-ford-transit-cargo/> (visited on 11/09/2022).
- [255] *Gasoline and Diesel Fuel Update*. URL: <https://www.eia.gov/petroleum/gasdiesel> (visited on 02/01/2023).

- [256] *Table 5.3. Average Price of Electricity to Ultimate Customers: Total by End-Use Sector, 2013 - February 2023 (Cents per Kilowatthour)*. https://www.eia.gov/electricity/monthly/epm_table_grapher.php?t=epmt_5_03. (Visited on 03/08/2023).
- [257] *Table 8.10 Average Retail Prices of Electricity, 1960-2011 Cents per Kilowatthour, Including Taxes*. <https://www.eia.gov/totalenergy/data/annual/showtext.php?t=ptb0810>. (Visited on 03/08/2023).
- [258] Yong Wang and Lin Li. “Time-of-use electricity pricing for industrial customers: A survey of U.S. utilities”. In: *Applied Energy* 149 (2015), pp. 89–103. ISSN: 0306-2619. DOI: <https://doi.org/10.1016/j.apenergy.2015.03.118>.
- [259] Matthew R. Graham, Mark J. Kutzbach, and Brian McKenzie. “Design Comparison of LODES and ACS Commuting Data Products”. In: *Center for Economic Studies, U.S. Census Bureau* 14-38 (2014). URL: <https://ideas.repec.org/p/cen/wpaper/14-38.html>.

Appendix A

Regression Results

A.1 Normalized TCO for Class 8 ICV Tractors

Table A.1: ICV Normalized TCO model summary

R	R-Squared	Adjusted R-Squared	Std. Error
1.000	1.000	1	0.000

Table A.2: ICV Normalized TCO ANOVA

Category	Sum of Squares	DOF	Mean Squares
Model	2593.358	1023	2.535
Error	0.844	38342	0.000
Total	2594.202	39365	0.066
<i>F</i>		<i>P(> F)</i>	
115188.994		0.000	

Table A.3: ICV Normalized TCO significant terms in empirical equation ($\alpha = 0.05$)

Coefficient	Value	t-value	p-value
YD	0.169	53.975	0.000
AP	0.011	3.698	0.000
NYO	0.237	74.647	0.000
DPM	0.035	10.859	0.000
YD:AP	0.016	3.632	0.000
YD:NYO	0.314	64.694	0.000
YD:DPM	0.051	10.261	0.000
NYO:DPM	0.060	11.930	0.000
YD:NYO:AP	0.017	2.462	0.014
YD:NYO:DPM	0.086	11.272	0.000

A.2 Normalized TCO for Class 8 BEV Tractors

Table A.4: BEV Normalized TCO model summary

R	R-Squared	Adjusted R-Squared	Std. Error
0.997	0.994	1	0.000

Table A.5: BEV Normalized TCO ANOVA

Category	Sum of Squares	DOF	Mean Squares
Model	1304.862	1023	1.276
Error	7.909	38342	0.000
Total	1312.771	39365	0.033
<i>F</i>		<i>P(> F)</i>	
6183.853		0.000	

Table A.6: BEV Normalized TCO Significant terms in empirical equation ($\alpha = 0.05$)

Coefficient	Value	t-value	p-value
YD	0.097	10.092	0.000
DD	0.042	4.318	0.000
VNR	0.033	3.367	0.001
NYO	0.128	13.153	0.000
BPP	0.043	4.391	0.000
YD:DD	0.046	3.065	0.002
YD:NYO	0.177	11.932	0.000
DD:NYO	0.057	3.815	0.000
VNR:BPP	0.086	5.678	0.000
YD:DD:NYO	0.081	3.515	0.000

A.3 Relative TCO for Class 8 BEV and ICV Tractors

Table A.7: Relative TCO model summary

R	R-Squared	Adjusted R-Squared	Std. Error
0.979	0.958	0.957	0.000

Table A.8: Relative TCO ANOVA

Category	Sum of Squares	DOF	Mean Squares
Model	4638.937	1023	4.535
Error	204.711	38342	0.005
Total	4843.648	39365	0.123
<i>F</i>		<i>P(> F)</i>	
849.330		0.000	

Table A.9: Relative TCO Significant terms in empirical equation ($\alpha = 0.05$)

Coefficient	Value	t-value	p-value
Intercept	1.141	35.740	0.000
YD	-0.137	-2.810	0.005
DD	0.459	9.286	0.000
VNR	0.335	6.781	0.000
NYO	-0.192	-3.881	0.000
DPM	-0.157	-3.119	0.002
BPP	0.437	8.830	0.000
EVSEP	0.128	2.592	0.010
YD:VNR	-0.181	-2.395	0.017
DD:VNR	-0.263	-3.429	0.001
YD:BPP	-0.247	-3.270	0.001
VNR:NYO	-0.200	-2.609	0.009
VNR:BPP	0.874	11.409	0.000
NYO:BPP	-0.271	-3.533	0.000
YD:VNR:BPP	-0.494	-4.224	0.000
VNR:NYO:BPP	-0.542	-4.565	0.000

Appendix B

INRIX Data Weighting

Itinerary data for MD/HD vehicles was provided to CSU from INRIX. This data was collected from MD/HD trucks in the US in 2019. The following is an outline of the process by which geo-spatial weights were computed for the data.

INRIX vehicles represent some percentage of total US MD/HD traffic but the extent of coverage is not necessarily flat nationally. Thus a set of weights are computed for geographical regions in the US. The geographical regions were level 3 H3 Hex cells [214]. The weighting is done against transportation jobs in geographic areas. Information on the location of transportation jobs can be found using the US Census Bureau's LODS WAC data [259]. The WAC data breaks down jobs in a given locality by industry classification. Transportation jobs are identified by NAICS classifications 48/49. Currently 5 year WAC data is available most recently for 2019. WAC data is associated with US Census GEOIDs. Census geometries are irregular and widely varying in area. In order to facilitate easier analysis, WAC data is converted to H3 Hex cells using area interpolation.

The weighting is done using tracked nightly counts using INRIX data. INRIX vehicles do not necessarily keep constant device IDs. Rather, at least some of the time, the data are carefully anonymized in order to keep users from tracking vehicles over multiple days. This is done by a daily re-setting of the device ID and by employing a "snap-to-node" scheme with recorded locations. Because of the snap-to-node scheme, multiple vehicles are recorded as having parked in the same exact (to precision) location simultaneously making tracking impossible. While vehicle tracking may be impossible, a daily count for a given area is possible to produce using a "conservation of vehicles" approach. The conservation of vehicles approach is outlined below:

1. For a given geometry (g) on a given day (n) a number of vehicles (m) are estimated to exist in geometry g at the start of day n (initially 0)

2. The number of devices recorded starting day n in geometry g (m_s) is counted
3. The number of devices recorded ending day n in geometry g (m_e) is counted
4. If $m_s > m_e$ the geometry g lost vehicles on day n so m is reduced by the difference: $m \geq 0$ must be met so if the difference is greater than m then new vehicle are tracked and added to the number tracked
5. At the end of each day, the count is taken in all geometries and this is the reported number
6. Tracked vehicles are weighted against WAC data using Iterative Proportional Fitting with N dimensions (IPFN).

Total tracked vehicles as a function of day is shown in Figure B.1 and average tracked vehicles for each geometry is shown in Figure B.2.

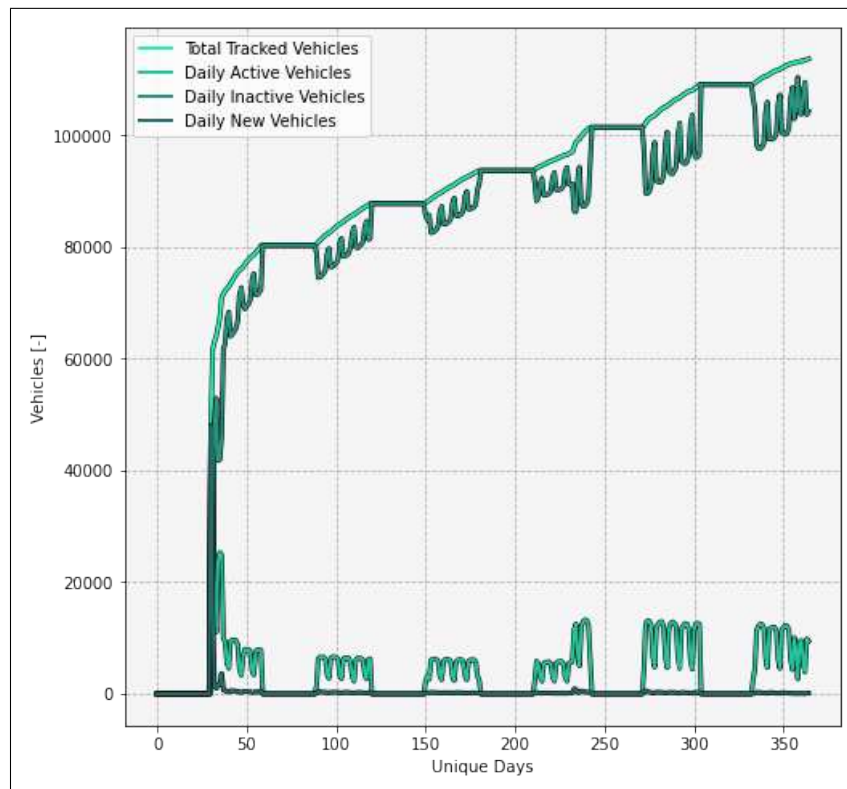


Figure B.1: Total tracked vehicles in INRIX data by day

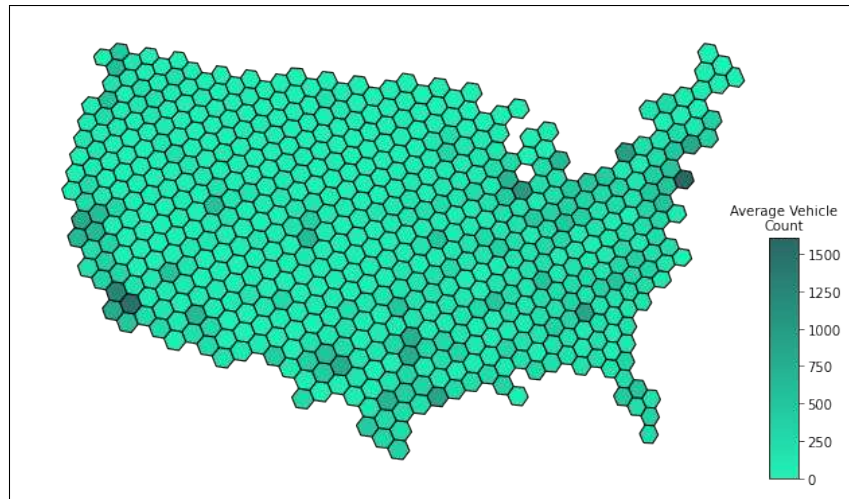


Figure B.2: Average tracked vehicles in INRIX data by geometry

Having found the density of vehicles for the H3 Hex cells, the INRIX data could be weighted against LODES WAC data using IPFN. The densities of transportation jobs from LODES WAC by geometry is shown in Figure B.3. the ultimate geographic weights are shown in Figure B.4 and a comparison of the weighted and un-weighted densities is shown in Figure B.5

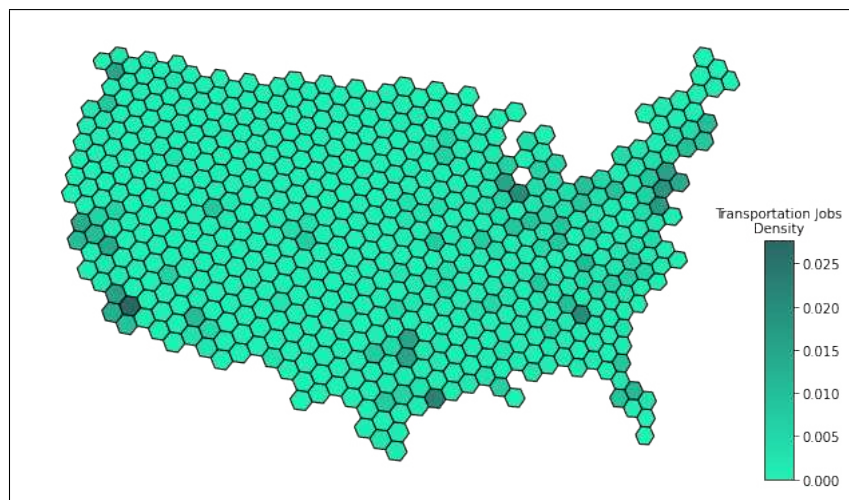


Figure B.3: Transportation job densities by geometry from LODES WAC (NAICS 48/49)

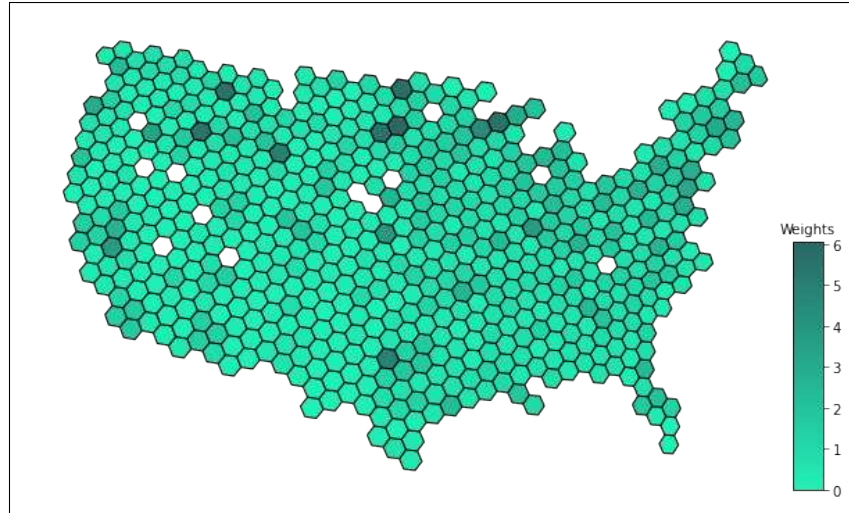


Figure B.4: INRIX data geo-spatial weights

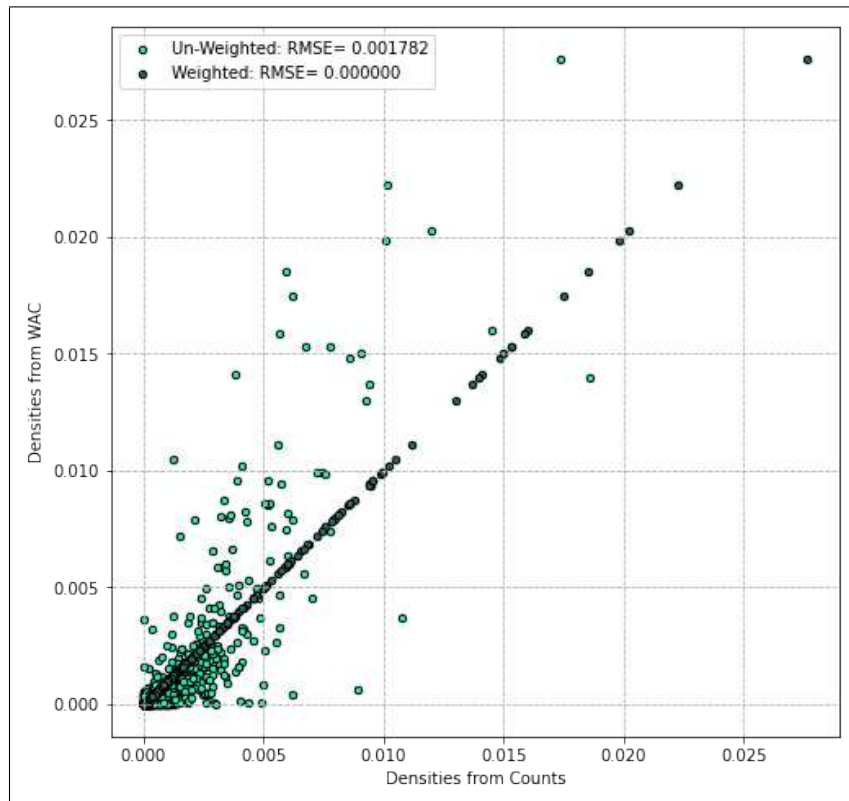


Figure B.5: Comparison between weighted and un-weighted INRIX geo-spatial densities

The relative flatness of the weighting implied that the INRIX data was well distributed in all but the most sparsely populated regions.

List of Abbreviations

2SDP 2 State Dynamic Programming. 68, 70, 75, 77, 82

ACS American Community Survey. xi, 125, 142, 147, 150, 151

ADAS Advanced Driver Assistance System. 3, 16, 19, 21, 22, 39, 45, 58, 90

ADFC Alternative Fuels Data Center. 143

ADP Approximate Dynamic Programming. 52, 77

AFV Alternative Fuel Vehicle. 95, 96

AI Artificial Intelligence. 15, 18, 27

AL2N Acceleration L^2 Norm. 65, 66, 68, 75, 78, 81

ANL Argonne National Lab. 162, 163

ANN Artificial Neural Network. 16, 17, 23, 25, 38, 45

AP Age at Purchase. 197

BC Battery Capacity. 114, 117, 137, 140, 151

BEV Battery Electric Vehicle. ii, viii, x, xi, xiii–xv, 2, 5–7, 9–12, 47, 48, 90–97, 101, 104–106, 110–113, 118–127, 133–136, 140, 142, 147, 151–154, 157–161, 163–165, 167–173, 176, 177, 179, 184, 185, 187, 189–199, 201–206, 208–211, 214

BPC Battery Power Cost. 66, 68, 75, 83

BPP Battery Pack Pricing. 197, 198

BTS Bureau of Transportation Statistics. 99

C_D Coefficient of Drag. 72

CRR Coefficient of Rolling Resistance. 72

CAV Connected Autonomous Vehicle. ii, x, 1–4, 8, 9, 14, 16, 20–22, 25, 27, 40, 47, 49, 58, 83, 90, 208

CHTS California Household Travel Survey. 130

CV-MPC Constant Velocity Model Predictive Control. x, 15, 18, 35–38, 42–45

CVT Continuously Variable Transmission. 34

D³ Downloadable Dynamometer Database. 71, 72

DCFC DC Fast Charging. 5, 10, 92, 96, 102, 106, 122, 128, 133, 160

DCL Destination Charger Likelihood. xiii, 114, 117, 119, 120, 137, 140, 144–146, 151, 156

DCO Discretized Control Optimization. 50, 51, 56, 61

DD Daily Distance. 197

DNN Deep Neural Network. x, xii, 38–41, 45, 46, 208

DOE Department of Energy. 163

DOT Department of Transportation. 173, 188

DP Dynamic Programming. x, xii, xiii, 3, 6, 15, 16, 18, 27–29, 32, 33, 35–37, 42–45, 48, 50–56, 61, 68, 75, 77, 78, 82, 90, 108, 109, 131, 183

DPM Diesel Price Multiplier. 197

DT Direct Transcription. 69

EDC Eco-Driving Control. 4

EE Energy Economy. x, xii, 4, 47, 48, 52, 63, 66, 73–78, 81–84, 89, 90

EPA Environmental Protection Agency. xii, 48, 67

EPRI Electric Power Research Institute. 185

ERCp En-Route Charging Penalty. xiii, 114, 117, 119, 120, 137, 140, 146, 147, 151, 156

ERCR En-Route Charging Rate. 114, 117, 120, 137, 140, 151

EV Electric Vehicle. ii, 1, 6, 8, 9, 90, 91, 95, 114, 121, 124, 149, 154, 161–163, 177, 182, 207, 209

EVSE Electric Vehicle Support Infrastructure. viii, 1, 6, 11, 91–93, 96, 97, 106, 114, 121–127, 133, 136, 142, 143, 157, 161, 197, 209, 210

EVSEP EVSE Premium. 197

FASTSim Future Automotive Systems Technology Simulator. x, 48, 63, 66, 71, 72, 75

FC-DP Full Cycle Dynamic Programming. xii, 15, 18, 32, 33, 35–37, 42, 45

FE Fuel Economy. vi, x, xii, 15–20, 27, 32, 34, 35, 37, 42–45

FTC Fuel Tank Capacity. 118

FTP Fuling Time Penalty. 118, 120

GA Genetic Algorithm. xii, 48, 54, 55, 61, 70, 71, 83, 85–90

GHG Green-House Gas. 1, 48

GVWR Gross Vehicle Weight Rating. 174, 176, 204

HAPP Household Activity Pattern Problem. 130

HC Home Charging. xiii, 114, 117, 140, 150–153

HD Heavy Duty. ii, xiv, 6, 7, 12, 185, 186, 203, 211

HEV Hybrid Electric Vehicle. 2, 3, 8, 9, 14, 16–18, 27, 29, 34, 45, 46, 90, 208

HIL Hardware In Loop. 52

I2V Infrastructure to Vehicle. 15

ICE Internal Combustion Engine. 48

ICV Internal Combustion Vehicle. ii, x, xi, xiii, xiv, 1, 5, 7, 9, 11, 12, 91–94, 96, 97, 101, 104, 105, 108, 110, 112, 113, 118, 120–122, 124, 159–161, 165, 166, 169, 171–173, 176, 184, 190–194, 196, 198, 199, 203–207, 209, 211

IDM Intelligent Driver Model. x, 51, 56, 59, 61, 63, 75, 77, 81

IOL Ideal Operating Line. xii, 19, 20, 31

IPFN Iterative Proportional Fitting with N dimensions. 252, 253

IPOPT Interior-Point Optimization. 53, 61, 69, 70, 83, 86, 89

LCOD Levelized Cost of Driving. xiv, 199, 200

LD Light Duty. 1, 6, 7, 12, 160–163, 167, 177, 204, 205, 209, 210

Li-Ion Lithium-Ion. 7, 92, 160–163

LPCP Lost Payload Capacity Portion. 174, 175

LSTM Long Short-Term Memory. x, xii, 17, 25–27, 38–41, 43, 45, 46, 208

LTL Less Than Truckload. ii, 6, 7, 173, 174, 190, 195, 197, 203, 204, 206, 211

LTP Lost Time Portion. 188

LVL 2 DC Level 2. 5, 10, 106, 133

MAE Mean Absolute Error. xii, 26, 40, 41, 43–45

MAP Positions of Subsequent Traffic Lights. 58

MD Medium Duty. 2

MD/HD Medium Duty / Heavy Duty. 11, 160, 161, 167, 168, 177, 205, 210, 214, 251

ML Machine Learning. 15, 16, 23, 25, 45, 208

MPC Model Predictive Control. xii, 3, 15, 16, 18, 32, 33, 43, 45, 61

MSA Metropolitan Statistical Area. xiii, 141

MY Model Year. 197, 198

NHTS National Highway Transportation Survey. 99, 130, 138, 141

NHTSA National Highway Traffic Safety Administration. 57

NPV Net Present Value. xiv, 164, 166, 170, 175

NREL National Renewable Energy Laboratory. 11, 98, 127, 143, 148, 163

NYO Number of Years of Ownership. 197

OEM Original Equipment Manufacturer. 1, 5, 12, 48, 177, 203, 205

OEMS Optimal Energy Management Strategies. 8, 9

PCHIP Piecewise Cubic Hermitic Interpolation Polynomial. 70

PDF Probability Distribution Function. 150, 153

PE Payload Exemption. 197

PHEV Plug-in Hybrid Electric Vehicle. 3, 16, 45

POEMS Predictive Optimal Energy Management Strategies. vi, xii, 9, 14–20, 22, 27, 45, 46, 90,

PP-MPC Perfect Prediction Model Predictive Control. x, 15, 18, 35–37, 42, 43, 45

PSO Particle Swarm Optimization. 54, 55, 61, 71, 83, 85, 86

PSRC Puget Sound Regional Council. 98, 99

PTO Polynomial Trajectory Optimization. 50, 53–56, 61, 82–86, 89

RBED Rules-Based Eco-Driving. 50, 51, 56, 61

RL Reinforcement Learning. 51, 53, 56

RNN Recurrent Neural Network. 38

RP-MPC Real Prediction Model Predictive Control. 15, 42–45

RPC Road Power Cost. 65, 66, 68, 75, 83, 90

SAE Society of Automotive Engineers. 57, 106, 133

SGA Spline Genetic Algorithm. 70, 71, 77, 83, 86

SLSQP Sequential Least Squares Programming. 53, 69

SME Subject Matter Expert. 162

SNLP Spline Non-Linear Programming. 70, 75, 83

SOC State of Charge. 18, 29, 30, 32, 34–36, 45, 72, 131

SOE State of Energy. xiii, 107, 110–113, 134, 184, 186

SPAT Signal Phase and Timing. 58, 60

SPSO Spline Particle Swarm Optimization. 71, 77, 83

TCO Total Cost of Ownership. ii, xi, xiv, xv, 7, 11, 159–165, 176, 177, 179, 188–194, 196, 198–205, 210, 211

TOU Time of Use. xiv, 181–183, 201, 205

TSDC Transportation Secure Data Center. 99

V2I Vehicle to Infrastructure. 52, 57, 58

V2X Vehicle to Everything. 3, 19, 45, 208

VIUS Vehicle Inventory and Use Survey. xiii, xiv, 170–172, 175, 187, 190, 197

VMT Vehicle Miles Traveled. xiv, 171, 172, 187, 190, 191, 197

VNR Vehicle Nominal Range. 197

VP-OEMS Velocity Prediction enabled Optimal Energy Management Strategies. 3

WC Work Charging. 114, 117, 151

YD Yearly Distance. 197